VOLUME 87 NO. SM4
AUGUST 1961
PART 1

JOURNAL of the

Soil Mechanics and Foundations Division

PROCEEDINGS OF THE

AMERICAN SOCIETY OF CIVIL ENGINEERS

BASIC REQUIREMENTS FOR MANUSCRIPTS

Original papers and discussions of current papers should be submitted to the Manager of Technical Publications, ASCE. Authors should indicate the technical division to which the paper is referred. The final date on which a discussion should reach the Society is given as a footnote with each paper. Those who are planning to submit material will expedite the review and publication procedures by complying with the following basic requirements:

1. Titles must have a length not exceeding 50 characters and spaces.

2. A summary of approximately 50 words must accompany the paper, a 300-word synopsis must precede it, and a set of conclusions must end it.

3. The manuscript (an original ribbon copy and two duplicate copies) should be double-spaced on one side of 8½-inch by 11-inch paper. Three copies of all illustrations, tables, etc., must be included.

4. The author's full name, Society membership grade, and footnote reference stating present employment must appear on the first page of the paper.

5. Mathematics are recomposed from the copy that is submitted. Because of this, it is necessary that letters be drawn carefully, and that special symbols be properly identified. The letter symbols used should be defined where they first appear, in the illustrations or in the text, and arranged alphabetically in an Appendix.

6. Tables should be typed (an original ribbon copy and two duplicate copies) on one side of 8½-inch by 11-inch paper. Specific illustrations and explanation must be made in the text for each table.

7. Illustrations must be drawn in black ink on one side of 8½-inch by 11-inch paper. Because illustrations will be reproduced with a width of between 3-inches and 4½-inches, the lettering must be large enough to be legible at this width. Photographs should be submitted as glossy prints. Explanations and descriptions must be made within the text for each illustration.

8. The desirable average length of a paper is about 12,000 words and the absolute maximum is 18,000 words. As an approximation, each full page of typed text, table, or illustration is the equivalent of 300 words.

9. Technical papers intended for publication must be written in the third person.

10. The author should distinguish between a list of "Reading References" and a "Bibliography," which would encompass the subject of his paper.

This Journal is published bi-monthly by the American Society of Civil Engineers. Publication office is at 2500 South State Street, Ann Arbor, Michigan. Editorial and General Offices are at 33 West 39 Street, New York 18, New York. $4.00 of a member's dues are applied as a subscription to this Journal. Second-class postage paid at Ann Arbor, Michigan.

The index for 1959 was published as ASCE Publication 1960-10 (list price $2.00); indexes for previous years are also available.

Vol. 87 No. SM 4

Journal of the

SOIL MECHANICS AND FOUNDATIONS DIVISION

Proceedings of the American Society of Civil Engineers

CONTENTS

August, 1961

Papers

(over)

Note.—Part 2 of this Journal is the 1961-30 Newsletter of the Soil Mechanics and Foundations Division.

The three preceding issues of this Journal are dated February 1961, April 1961, and June 1961.

DISCUSSION

Journal of the
SOIL MECHANICS AND FOUNDATIONS DIVISION
Proceedings of the American Society of Civil Engineers

FOUNDATION STABILITY FOR A SUBMARINE LIQUID SULPHUR PIPELINE

By Basil W. Wilson,[1] F. ASCE

SYNOPSIS

This paper examines the vertical and lateral stability of a 7-mile long hot sulphur pipeline, entrenched in the sediments between Grand Isle, Louisiana, and the offshore sulphur mine in the Gulf of Mexico. Hot water under pressure in a jacket pipe maintains fluid sulphur flow in an inner line at an average temperature of 300°F. These hot lines are insulated within an outer casing pipe. Under normal operation, the expansive tendencies of the hot lines are blocked by end anchorages, prescribed for this purpose; the lesser tendency to expansion of the casing pipe is similarly prevented. The resulting compression in the composite pipeline could involve buckling and critical exposure of the pipeline in the absence of adequate soil support. The adequacy of this support and the nature of the thermal stresses in the pipeline are subjects of enquiry, having regard to the special nature of the foundation. The latter involves fine sands and silts over 50% of the pipeline length and very soft cohesive sediment over the remainder. It is shown that the pipeline will be stable against buckling, but may suffer limited subsidence from thermal osmosis in the clay and convection currents in the sand. Apart from this, the pipeline will probably sink below trench level in a pocket of very weak sediment at two-thirds the distance from the shore. It should stabilize, however, without suffering unduly severe strain from the sag. A finding of the study is that initial prestressing of the casing pipe during the laying operation will be foiled, very likely, by the resistance forces of the sediments; from this it is

Note.—Discussion open until January 1, 1962. To extend the closing date one month, a written request must be filed with the Executive Secretary, ASCE. This paper is part of the copyrighted Journal of the Soil Mechanics and Foundations Division, Proceedings of the American Society of Civil Engineers, Vol. 87, No. SM 4, August, 1961.

[1] Prof., Engrg. Oceanography and Meteorology, Agric. and Mech. College of Texas, College Sta., Tex.

concluded that soil resistance also renders unnecessary the use of costly anchorages for needless control of pipeline expansions.

NATURE OF THE PROBLEM

The decision in 1956 to mine the large sulphur deposits discovered in 1949 offshore from Grand Isle, La., in the Gulf of Mexico, led to the design of an over-water Frasch extraction plant, unique in being located seven miles from shore in water of 44 ft depth.[2] Recovery here of liquid sulphur at a temperature of some 300°F posed problems of transport in a sometimes

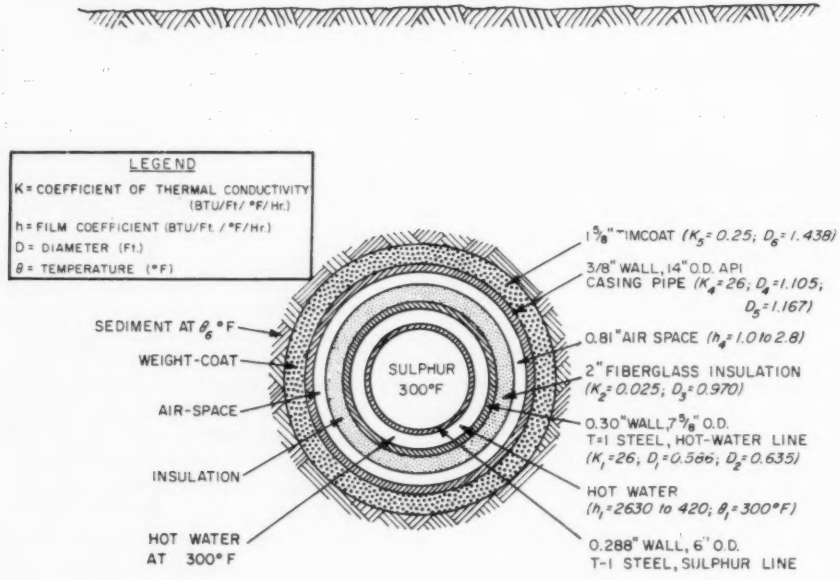

FIG. 1.—SCHEMATIC REPRESENTATION OF CROSS-SECTION OF PIPELINE SHOWING SIZES, MATERIALS, AND HEAT CONDUCTIVITIES

hostile environment that, it was decided, could best be overcome with an underwater hot-sulphur pipeline from the offshore structures to the Grand Isle base.[2,3,4] But design[3] and construction[4] of this pipeline presented problems concerning the foundation for which there were no immediate answers.

2 "The Grand Isle Mine; Freeport Sulphur Company's Offshore Venture," by C. O. Lee, Z. W. Bartlett, and R. Feierabend, Soc. of Mineral Engrs., AIME, Reprint No. 59H97, November, 1958.

3 "The Grand Isle Sulphur Mine Heating Plant and Underwater Sulphur Line Design," by C. M. Cockrell, ASME, paper no. 59-A-183, August, 1959.

4 "Construction Features of a Seven Mile Hot Sulphur Line under the Gulf of Mexico," by E. J. McNamara, Proceedings, ASCE, Vol. 86, April, 1960, p. 47.

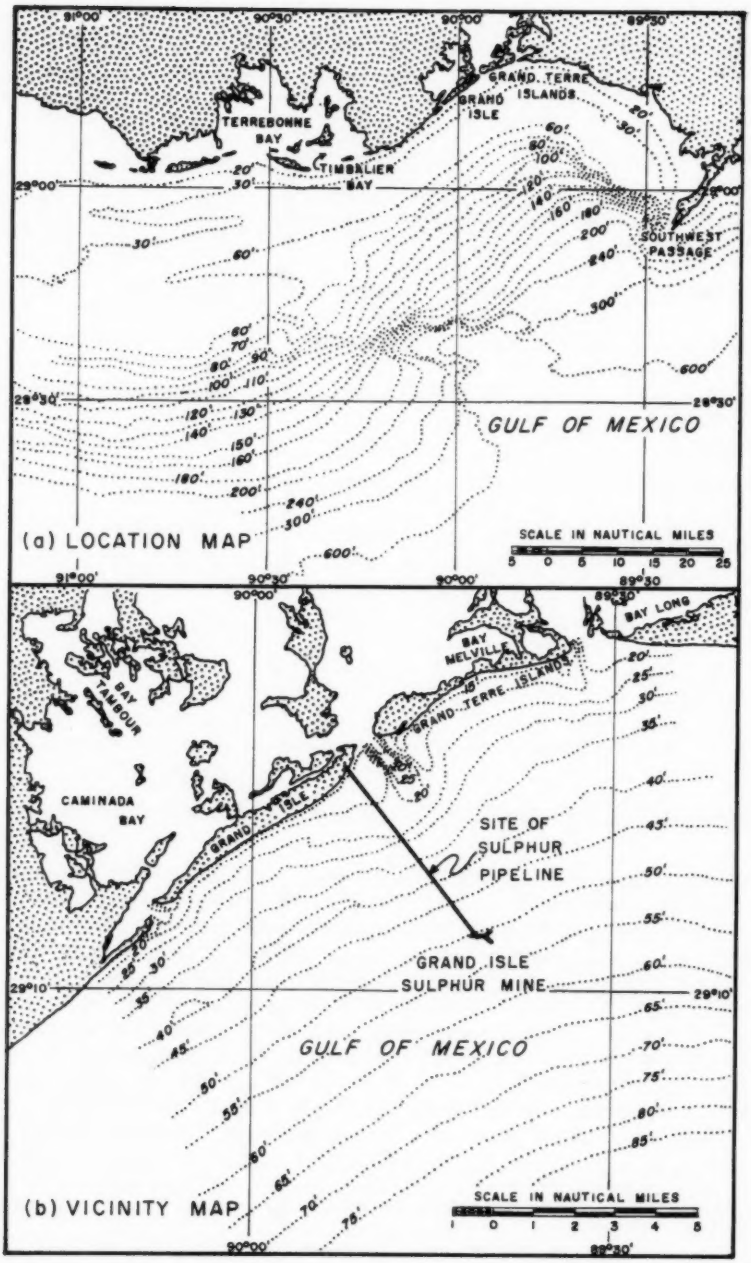

FIG. 2.—LOCATION OF SULPHUR PIPE LINE OFF GRAND ISLE, LOUISIANA, GULF OF MEXICO

TABLE 1.—DIMENSIONS AND PROPERTIES

Pipeline component	Dimensions			Section Moment of Inertia Neutral Axis, in in^4
	Outside diameter, in in.	Wall thickness, in in.	Cross-section area, in sq in.	
(1)	(2)	(3)	(4)	(5)
Outer Weight-Coat (Casing)	17.250	1.625	79.70	. . .
Casing Pipe	14.000	0.375	16.05	373.0
Air Insulation Annulus	13.250	0.818	31.97	. . .
Fiberglass Insuln. with Rollers	11.625	2.000	60.46	. . .
Hot water line	7.625	0.300	6.90	46.2
Annulus of Hot Water	7.025	0.512	10.47	. . .
Sulphur Line	6.000	0.288	5.17	21.1
Molten Sulphur	5.424	-	23.09	. . .
Return Water Line	4.500	0.237	3.17	7.2
Outer Weight-Coat (Return Water)	6.500	1.000	17.27	. . .
Return Water	4.026	-	12.72	. . .
Totals:			266.97	

The foundation was known to comprise extremely soft sediments, deposited on the continental shelf in geologic time by the Mississippi River deltaic system.[5,6] The questions at issue concerned the anticipated behavior of the pipeline in such a medium, having regard to the high temperatures the steel pipes would acquire from passage of the hot fluids and the possibility that the pipeline might be subject to exposure from the devastations of a Gulf hurricane. Reasonable assurance was needed that the pipeline would be both longitudinally and laterally stable when entrenched in the sediments and that coastal erosion in the area of Grand Isle would not lay bare the line within the probable life expectancy of the mine. The depth of burial of the pipeline and the floor heights of shore structures, needed to escape hurricane damage, were

5 "Near-surface Sediments of the Continental Shelf off Louisiana," by H. N. Fisk, Proceedings, 8th Texas Conf. on Soil Mechanics and Foundation Engrg., Univ. of Texas, Austin, Tex., 1957.

6 "Engineering Properties of Soils on the Continental Shelf of the Gulf of Mexico," by B. McClelland, Proceedings, 8th Texas Conf. on Soil Mechanics and Foundation Engrg., Univ. of Texas, Austin, Tex., 1957.

OF PIPELINE COMPONENTS

Dead Weight, in lb per ft	Material		Coefficient Thermal Conducty K, in BTU per ft °F per hr	Film Coefficient h BTU per ft °F per hr	Coefficient of Linear Expansion , in $(°F^{-1})$ $(x\ 10)^{-6}$
	Type	Yield Strength, in psi			
(6)	(7)	(8)	(9)	(10)	(11)
75-109 (range)	(Timcoat)	. . .	0.25	. . .	(6.90)
54.6	API 51 x 42 Bell and Spigot	42,000	26.00	. . .	6.90
-	Air	. . .	. . .	1.0 to 2.8	. . .
7.0	Fiberglass	. . .	0.025	. . .	(7.75)
23.5	T-1 Steel	90,000	. . .	. . .	7.75
4.2	Hot water at 300 °F (av.)	. . .	. . .	2630 to 420	. . .
17.6	T-1 Steel	90,000	. . .	. . .	7.75
18.0	Sulphur at 300 °F (av.)	. . .	. . .	. . .	. . .
10.8	API 5L Grade B5	35,000	. . .	. . .	. . .
15-21 (range)	(Timcoat)	. . .	. . .	. . .	. . .
5.0	Warm Water	. . .	. . .	. . .	. . .

204-244 Pipeline empty
231-271 Pipeline with fluids

additional specific unknowns. It is the purpose of this paper to describe the exploratory studies that yielded information on the vertical and thermal stability of the pipeline; limitations of length prevent discussion here of the hurricane and erosion problem.

Notation.—The letter symbols adopted for use in this paper are defined where they first appear and are arranged alphabetically, for convenience of reference, in the Appendix.

Principal Features of the Pipeline.—A schematic representation of a cross-section of the embedded pipeline, as it was conceived in 1958, is shown in Fig. 1. Fluid sulphur was to be conveyed in the innermost line of 6 in. (outside) diameter, arranged annularly within an insulated hot-water line of 7 5/8 in. diameter. Heat from the surrounding water would maintain the sulphur in the molten condition at about 300°F, and the insulation and annular airspace round this assemblage were expected to prevent serious heat loss to the outer casing pipe (of 14 in. diameter) that was to function as external support and protection for the system. Not shown in Fig. 1 is a return-flow water-line that, in 1958, was envisaged as a 4 1/2 in. outside diameter pipe strapped to

the casing pipe in a position immediately above or below it. Final construction of the pipelines included an additional 6 5/8 in. diameter fresh water pipeline,[2,3,4] that however, does not feature in the considerations of this paper.

The location of the offshore mine (Fig. 2) made the effective length of the pipeline approximately 35,000 ft. Over this distance the anticipated inlet water and sulphur temperatures at the mine were 320°F, and their outlet temperatures 280°F at the shore. In order to secure an equitable distribution of thermal stresses in the pipelines, it was prescribed that the outer casing pipe, when located on site at a probable temperature of 80°F, should be pretensioned by end-pulls of about 200,000 lb and anchored at both mine and shore-ends. The hotwater and sulphur lines, supported in the casing pipe at intervals by peripheral rollers, were then to be secured to the casing pipe at the mine-end and expanded at a temperature of about 190°F before fastening their ends to the shore anchorage. The whole pipeline was to be laid in an excavated trench 6 ft or 7 ft below the mudline and allowed a period for natural backfilling before becoming operational.

TABLE 2.—AVERAGE PROPERTIES OF PRINCIPAL SEDIMENT TYPES

Sediment Type	Classification and Grain Size	Density (lb per cu ft)		Water Content, in %	Angle of Repose (Dry)	Angle of Internal Friction	Atterberg Limits		
		Dry w_d	Wet w_w				LL	PL	PI
(1)	(2)	(3)	(4)	(5)	(6)	(7)	(8)	(9)	(10)
Sand	Grey or tan, loose, fine, w/small shells and silt inclusions 70%<0.1 m.m. 90%<0.2 m.m.	91 to 95	107 to 115	11 to 28	34°	20°	...	...	...
Clay	Soft, grey, mainly Montmorillonite, Illite and Kaolinite	39 to 77	86 to 110	40 to 130	...	0	44 to 108	20 to 30	10 to 83

Pertinent information concerning the pipelines, either given, or assumed for purposes of calculation, is contained in Table 1.

Properties of the Foundation.—Information provided by soil analyses of test borings along the pipeline site showed that to a distance from the coast of approximately 11,000 ft the foundation consists of loose grey or tan fine sand with frequent shell fragments and silt lenses. Beyond this distance, the medium comprises very soft grey clay with occasional sand lenses. The average properties of these sediments are recorded in Table 2; additional test results are presented later.

Relative distributions of the sediment types are shown in cross-sectional profiles along the pipeline site in Figs. 3, 4, and 5. These portray more specifically the variations within the clay medium of wet density, ultimate unconfined compressive strength and ultimate shear strength. The full-line contours defining value of these properties reveal a zone of very weak sedi-

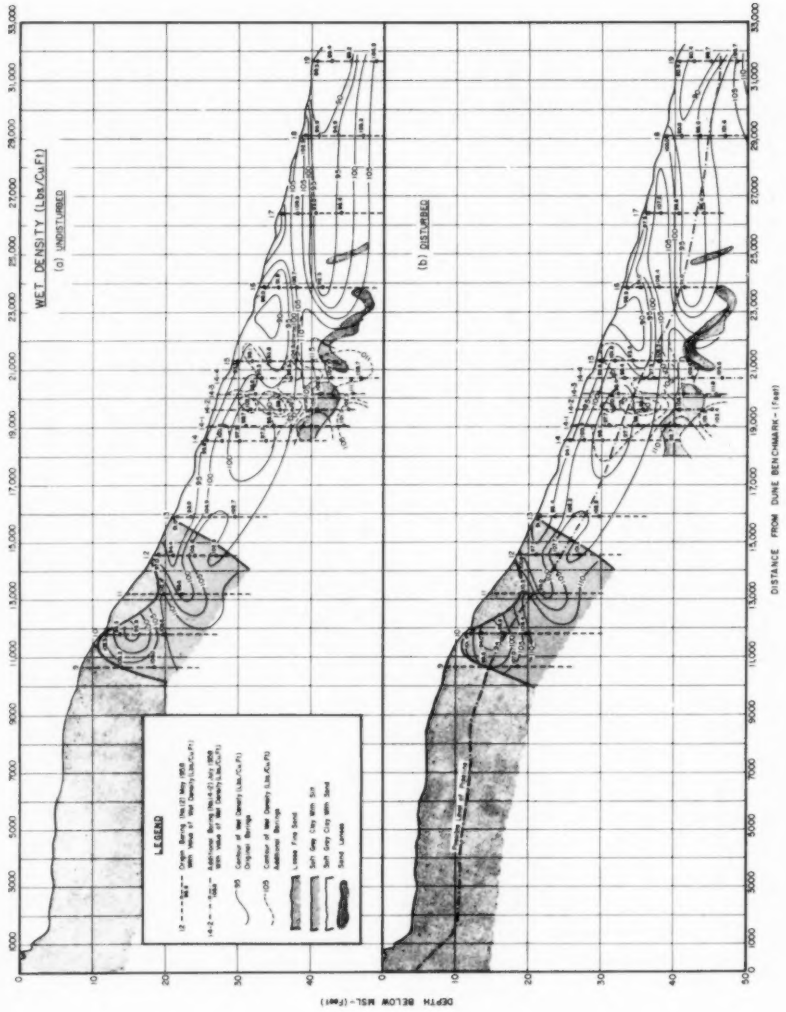

FIG. 3.—CONTOURED PROFILES OF WET DENSITY OF THE SEDIMENTS ALONG THE PIPELINE SITE

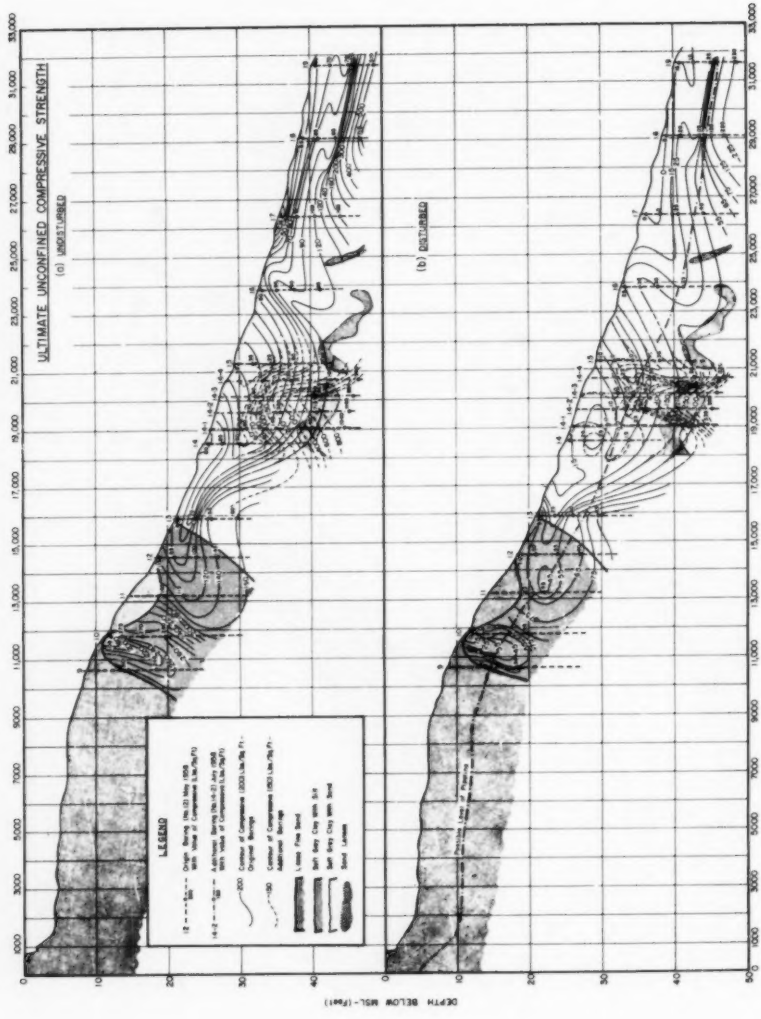

FIG. 4.—CONTOURED PROFILES OF ULTIMATE UNCONFINED COMPRESSIVE STRENGTH OF THE SEDIMENTS ALONG THE PIPELINE SITE

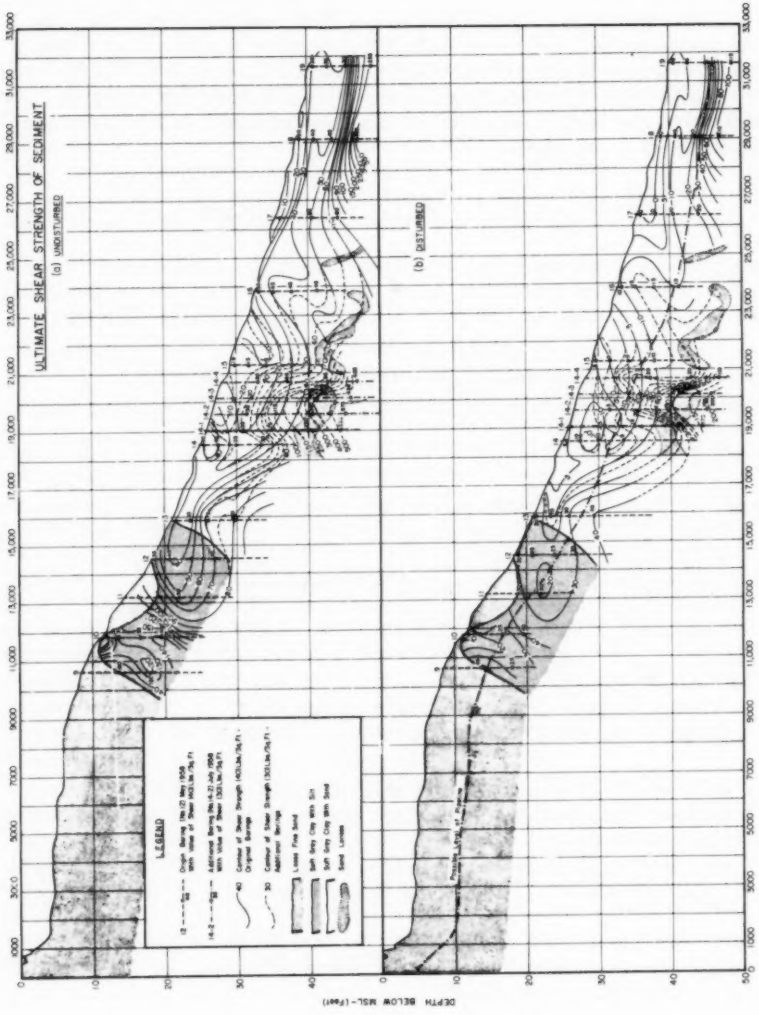

FIG. 5.—CONTOURED PROFILES OF ULTIMATE SHEAR STRENGTH OF THE SEDIMENTS ALONG THE PIPELINE SITE

ments at a distance from shore of some 18,000 ft to 22,000 ft. Additional deeper borings, made in the area, rather westward of the original line of borings, indicate that locally stiffer material may be encountered there in the form perhaps of a bar ridge[5] (dash line contours). This sub-surface consolidation is narrow, however, and the weak pocket surrounds it on each side. The considerable loss in strength of the clay when disturbed is evident in Figs. 3 and 4 in which the profiles (b) present test results on remolded samples. It must be supposed that the backfill material that ultimately confines the pipeline in its trench will suffer loss of strength comparable to that shown.

In the analysis of the foundation problem that follows, attention will be directed first to the vertical stability of the pipeline and then to the stability of the line under thermal effects.

VERTICAL STABILITY OF THE PIPELINE

Buoyancy of the Pipeline.—For the dimensions of the pipeline specified in Table 1, the displacement volume of the casing and return water line (with protective weight coating) is 1.86 cu ft per ft length of pipeline. The pipeline

TABLE 3.—BUOYANCIES OF THE SUBMERGED PIPELINE

Pipeline Condition	Dead Weight in Air, in lb per ft	Buoyancy			Negative Buoyancy		
		In sea water B_w, in lb per ft	In sediment B_s, in lb per ft		In sea water W_c, in lb per ft	In sediment, in lb per ft	
			Sand	Clay		Sand	Clay
(1)	(2)	(3)	(4)	(5)	(6)	(7)	(8)
Air-filled	204	119	42	93	85	162	111
	244	119	42	93	125	202	151
Operational (fluid-loaded)	231	119	42	93	112	189	138
	271	119	42	93	152	229	178

will thus have a buoyancy in sea water, B_w, of 119 lb per ft (64 lb per cu ft). For the total dead weights shown in Table 1, the net weight, or negative buoyancy, of the pipeline in sea water will range from 85 lb per ft to 125 lb per ft (46 lb per cu ft to 67 lb per cu ft) in the air-filled condition and from 112 lb per ft to 152 lb per ft (60 lb per cu ft to 82 lb per cu ft) in the operational condition.

When entrenched and backfilled in disturbed and semi-fluid silt or clay the force of uplift on the pipeline may be considered to be equal to the weight of interstitial (void or pore) water displaced by the pipes. If w_d be the dry density of the sand or clay (lb per cu ft), then $(r\ w_d)$ is the weight of water in unit volume, in which r is the moisture content (percentage). One cu ft of pipeline would thus have a buoyancy, B_s, in the sediment of $(r\ w_d)$. In terms of the wet density, w_w, this would be (in lb per cu ft)

$$B_s = \left(\frac{r}{1+r}\right) w_w \quad \ldots\ldots\ldots\ldots\ldots\ldots (1)$$

Taking representative mean values, w_w = 100 lb per cu ft and r = 100% (Table 2) for the clay, the uplift force in this sediment is thus $B_s \simeq 50$ lb per cu ft. It follows that the loaded pipeline would have an effective dead weight within the clay of 138 lb to 178 lb per running ft (74 lb per cu ft to 96 lb per cu ft), when operational. In the sand medium, with w_w = 110 lb per cu ft and r = 25% (Table 2), the buoyancy force is $B_s \simeq 22$ lb per ft (102 lb per cu ft to 123 lb per cu ft). These figures are summarized in Table 3.

It is to be determined whether, in the circumstances that a hurricane could so agitate the backfill over and around the pipe as to make the sediment semi-fluid, the pipeline would tend to become unstable and rise to the surface. The criterion for this happening could be considered to be a state in which the negative buoyancy of the pipeline in the sand or clay would be less than the negative buoyancy of the solids in the disturbed sediment.

If G_s be the specific gravity of the solids in the sediment it can be shown that the negative buoyancy, w_s, of the solids per cu ft of sediment would be

$$w_s = \frac{62.5}{r + \frac{1}{G_s}} \left(1 - \frac{64}{62.5\, G_s}\right) \quad \ldots\ldots\ldots\ldots \quad (2)$$

in lb per cu ft. For a typical value of G_s of 2.65, Eq. 2 reduces to

$$w_s = \frac{38.4}{r + 0.38} \quad \ldots\ldots\ldots\ldots\ldots\ldots \quad (3)$$

lb per cu ft. The value of r for a semi-fluid sand or mud could be expected to exceed the maximum shown in Table 2. Thus, if r ranged from 100% to 150%, the negative buoyancy of the solids would be from 27.8 lb per cu ft to 20.4 lb per cu ft and the conclusion must be that, so far from there being any tendency for the pipeline to rise, it would merely settle deeper in the agitated medium.

Vertical Equilibrium in the Sediments.—The approximate pressure of the loaded pipeline on the sand foundation in the excavated trench near the shore-end would be from 78 lb per sq ft to 106 lb per sq ft that would be well within the bearing capacity of the sand (estimated to be about 500 lb per sq ft). The sand foundation is not considered to present any instability problem except insofar as it may show a tendency to develop piping under the influence of the heat loss from the pipeline to the sediment under operating conditions. Further reference to this will be made later.

The load bearing capacity per unit length, W_m, of the silty clay sediments can be expressed in the form

$$W_m = \beta\, D\, \tau_m \quad \ldots\ldots\ldots\ldots\ldots\ldots \quad (4)$$

in which τ_m is the maximum shear strength of the sediment, and β a dimensionless coefficient. If β exceeds 5.14, the pipeline[7] would definitely sink. Adopting $\beta \simeq 2$ for safety,[8] the permissible maximum shear strength of the clay that should be mobilized (for D = 1.44 ft) is

$$\tau_m = 0.336\, W_m \quad \ldots\ldots\ldots\ldots\ldots\ldots \quad (5)$$

in lb per sq ft. Thus, for W_m ranging from 138 lb per ft to 178 lb per ft (96

[7] Theoretical Soil Mechanics, by Karl Terzaghi, John Wiley and Sons, Inc., New York, 1943.

[8] "Some Oceanographic and Engineering Considerations in Marine Pipe Line Construction," by R. O. Reid, Proceedings, 2nd Conf. on Coastal Engrg., Council on Wave Research, Engrg. Foundation, Berkeley, Calif., 1952, p. 749.

lb per sq ft to 124 lb per sq ft pressure), the minimum values of τ_m required to assure safe support of the pipeline range from 46 lb per sq ft to 60 lb per sq ft.

These values apply to undisturbed sediment that is presumed to exist at the bottom of the entrenchment. Fig. 5(a) shows that the contours of τ_m for 40 lb per sq ft, 50 lb per sq ft and 60 lb per sq ft are within 7 ft of the sediment surface for about half the distance over which the sediment is cohesive. Between about 17,000 ft and 27,000 ft from shore, however, these contours dip sharply and extrapolation suggests that the greatest depths attained by the 46 lb per sq ft and 60 lb per sq ft values are about 14 ft and 18 ft, respectively. The implication then is that somewhere in this zone the pipeline will tend to sink below the level of a prepared 7 ft deep trench. If positive sinking be taken as occurring when $\beta \simeq 5$ in Eq. 4, then the critical range of ultimate shear strength would be 19 lb per sq ft to 25 lb per sq ft, which is encountered in the center of the weak pocket over a depth range of 7 ft to 9 ft. The pipeline could be expected to sink here and stabilize itself in a curve approximately paralleling the contours of Fig. 5(a) at depths somewhere between 7 ft and 14 ft for the lightest weight-coat and between 9 ft and 18 ft for the heaviest weight-coat.

On the basis that the lightest weight-coat (Table 1) would probably be used it is possible to investigate the stresses that might ensue from the pipeline sagging without adequate support across the pocket of weak sediment, until held like a catenary by the tensions generated at the abutments of stiffer support. It is found[8,9] that such a situation could not obtain without the pipeline resting on supporting foundation at about 13 ft or 14 ft beneath the mudline near the center of the pocket. In the event that the pipeline has two unsupported spans of 225 ft at each end of the pocket, it is estimated that the induced flexural and tensile stress (combined) in these sections will not exceed 4300 lb per sq in.

THERMAL STABILITY OF THE PIPELINE

Thermal Properties of the Sediments.—Annual temperature variations at the mudline and within the sediment below 15 ft of water have been recorded in the Atchafalaya Bay area off the coast of Louisiana. These data[10] (Fig. 6) show that the overall mean temperature within the sediments in that area tends to be about 72°F. At 10 ft depth below the mudline the amplitude of the annual temperature fluctuation is about 3°F; near the mudline a design range of temperature over the year from 50°F to 90°F would seem to be indicated and should be applicable to the Grand Isle area.

The fluctuations in temperature within the sediment, measurable in Fig. 6 at the different levels, both short period (a few days) and long period (annual), provide a means[9] for estimating the thermal diffusivity (specific conductivity), k, of the clay sediment. The value of k, so found is 0.014 ft^2 per hr, that agrees

---

9 "Coastal Engineering Problems in the Laying of a Sub-marine Liquid Sulphur Pipeline in the Gulf of Mexico," by Basil W. Wilson, Tech. Report No. 187-1 (ref 58-24F) Texas Agric. and Mech. Research Foundation, College Station, Tex., December, 1958.

10 "Transfer Processes Operating at the Ocean Boundaries; Temperature Data; Data Report (Section 1), Texas Agric. and Mech. Research Foundation, College Station, Tex., December, 1952.

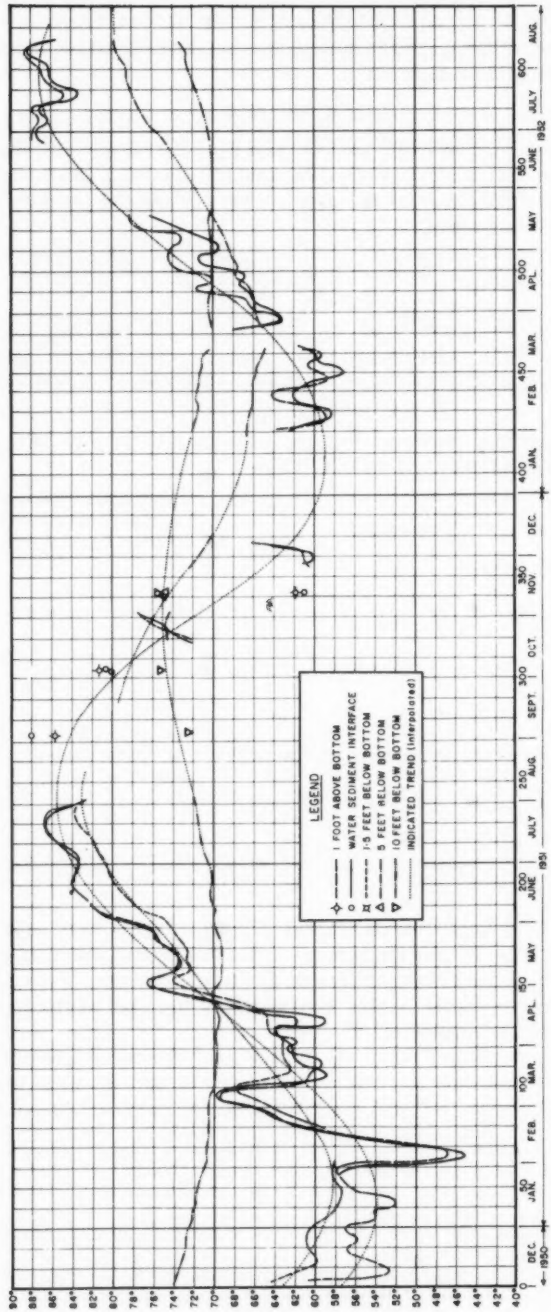

FIG. 6.—ANNUAL TEMPERATURE VARIATIONS AT THE MUDLINE AND WITHIN THE SEDIMENTS BELOW 15FT OF WATER AT OIL PLATFORM (LAT. 29°6' N; LONG. 91°34' W), ATCHAFALAYA BAY REGION, LOUISIANA, GULF OF MEXICO

quite well with a value of 0.011 ft^2 per hr found by Reid[11] for a different area of the Gulf.

If C_w be the specific heat of the wet sediment, then the thermal conductivity K of the wet sediment is given by

$$K = w_w C_w k \quad \ldots\ldots\ldots\ldots\ldots\ldots (6)$$

For w_w in lb per cu ft, k in ft^2 per hr, and C_w in BTU per °F, the units of K will be BTU per °F per ft per hr. The specific heat C_w can be expressed in terms of the specific heat of the dry solids C_d and the specific heat of sea water C_s by the relationship

$$C_w = \frac{C_d + r C_s}{1 + r} \quad \ldots\ldots\ldots\ldots\ldots\ldots (7)$$

Laboratory determinations[12] of C_d for samples of the sediments show an average value of 0.22 calories per gram per °C. Accordingly, with $C_s \simeq 1.0$, dependence of C_w on r for a range of values of moisture content from 48% to

TABLE 4.—COEFFICIENTS OF THERMAL CONDUCTIVITY OF SEDIMENTS; EXPERIMENTAL DERIVATION

Depth and Degree of Saturation	Temperature θ, in °F	Thermal Conductivity K (BTU per °F per ft per hr)	
		Sand	Clay
(1)	(2)	(3)	(4)
Just below mudline S = 0.963	40	1.25	0.72
	50	1.27	0.73
	60	1.30	0.79
	70	1.32	0.83
	80	1.33	0.86
	90	1.36	0.91
Pipeline level S = 0.956	100	1.36	0.95
	110	1.37	0.98
	120	1.38	1.01
	130	1.39	1.04

80% at the pipeline depth yields values for C_w from 0.45 to 0.56. These together with k = 0.014 ft^2 per hr, permit evaluation of the thermal conductivity K in terms of Eq. 6. An average value of K = 0.71 BTU per °F per ft per hr is thus obtained from typical boring test data for the clay at the pipeline depth of 6 ft to 7 ft below the mudline.

The thermal conductivities K of samples of the wet sediment were later determined[13] by refined experimental methods and found to vary slightly with temperature from 1.2 to 1.4 for the fine sand and 0.7 to 1.0 for the soft clay (Table 4).

11 "Oceanographic Analysis of Marine Pipe Line Problems: Engineering," by R. O. Reid, Final Report, Texas Agric. and Mech. Research Foundation, College Station, Tex., June, 1951.

12 "Thermal Conductivity of Soils," by C. M. Shilstone, Report, Shilstone Testing Lab., New Orleans, La., June, 1958.

13 "Experimental Determination of Soil Properties," by B. J. Fluker, Tech. Report, Texas Engrg., Experiment Sta., College Station, Tex., August, 1958.

Heat Flow from Pipeline to Water-Sediment Interface.—On the assumption that the thermal properties of the pipeline components accord with Table 1, the equivalent coefficient of thermal conductivity, K_e, over the annular layers

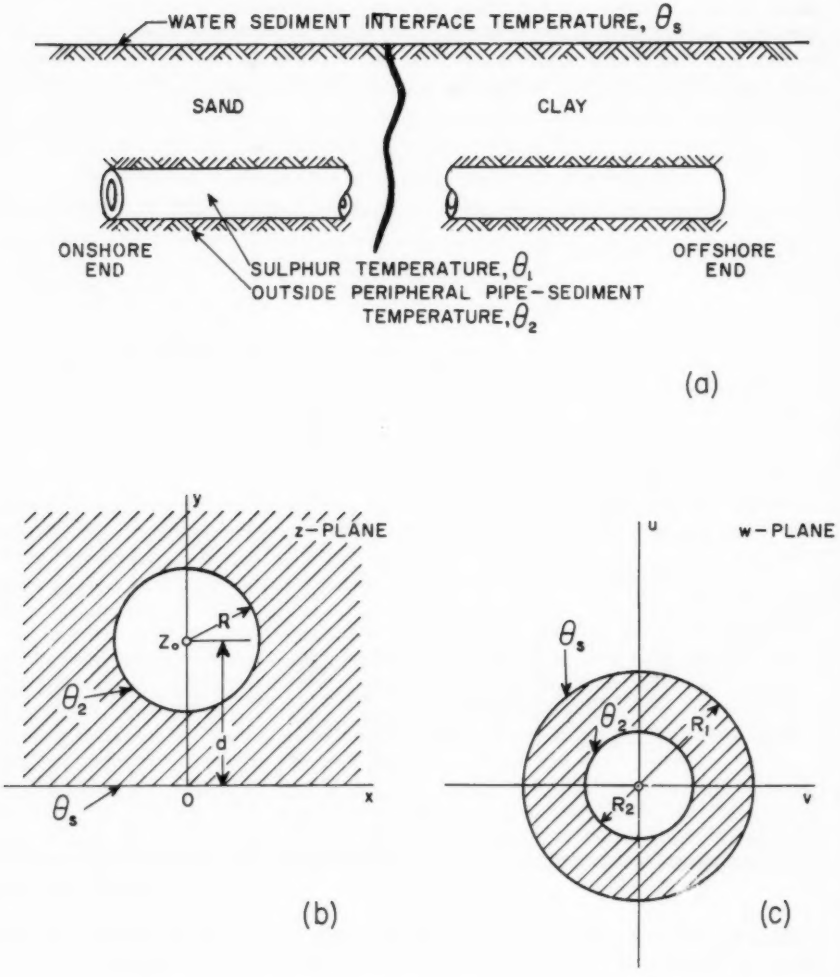

FIG. 7.—HEAT FLOW FROM PIPELINE TO MUDLINE; (a) SCHEMATIC REPRESENTATION; (b) ADAPTATION TO THE COMPLEX Z-PLANE; (c) CONFORMAL REPRESENTATION IN THE W-PLANE

from inside to outside of the pipeline, is estimated[9] to be about 0.045 to 0.048 BTU per °F per ft per hr.

It is now assumed that the heat flow from the entrenched pipeline through the sediment reaches a steady state condition in which the temperature, θ_s,

at the mudline remains constant. Determination of the temperature, θ_2, prevailing at the external periphery of the casing pipe weight-coat, may conveniently be analyzed with the aid of the theory of complex variables and the use of conformal mapping. Thus, the pipeline of Fig. 7(a) may be schematicized in the z-plane of Fig. 7(b) by a circle of radius R with uniform temperature θ_2 at height d above the x-axis, along which the temperature is uniformly θ_s. This maps conformally into the w-plane as two circles concentric with the origin of the u, v-axis.[14] The boundary at constant θ_2 is a circle of

TABLE 5.—PERIPHERAL TEMPERATURES AT THE PIPE-SEDIMENT INTERFACE UNDER PIPELINE OPERATING CONDITIONS

Sediment Type	Season	Temperature at Mudline θ_s, in °F	Temperature of Sulphur θ_1, in °F	Thermal Conductivity of Mud K, in BTU per ft per °F per hr	Temperature at Pipe Surface θ_2, in °F
(1)	(2)	(3)	(4)	(5)	(6)
Sand	Winter	50	320	1.30	77
		50	280	1.30	74
	Laying Condition	80	300	1.35	102
	Summer	90	320	1.37	113
		90	280	1.37	109
Clay	Winter	50	320	0.85	91
		50	280	0.85	85
	Laying Condition	80	300	0.90	111
	Summer	90	320	0.97	121
		90	280	0.97	116

radius R_2, that at constant θ_s a circle of radius R_1. The flow of heat, per unit time, Q, through the annular layer (the sediment) in the w-plane is

$$Q = \frac{2\pi K(\theta_2 - \theta_s)}{\log\left(\frac{R_1}{R_2}\right)} \quad \ldots\ldots\ldots\ldots (8)$$

14 Dictionary of Conformal Representations, by H. Kober, Dover Publications, Inc., New York, 1957.

whereas the same heat, flowing from the hot water to the outer periphery of the pipeline, is

$$Q = \frac{2\pi K_e(\theta_1 - \theta_2)}{\log\left(\frac{D}{D_1}\right)} \quad \ldots\ldots\ldots\ldots (9)$$

in which D and D_1 are, respectively, the diameters of the casing pipe weight-coat (outside) and of the hot water line (inside). Consequently, on equating Eqs. 8 and 9, the unknown temperature θ_2 is found to be

$$\theta_2 = \frac{K_e\,\theta_1 \log\left(\frac{R_1}{R_2}\right) + K\,\theta_s \log\left(\frac{D}{D_1}\right)}{K_e \log\left(\frac{R_1}{R_2}\right) + K \log\left(\frac{D}{D_1}\right)} \quad \ldots\ldots\ldots (10)$$

Further, the ratio R_1/R_2 in the w-plane is given by

$$\frac{R_1}{R_2} = \frac{d}{R}\left[1 + \sqrt{1 - \left(\frac{R}{d}\right)^2}\right] \quad \ldots\ldots\ldots\ldots (11)$$

For K_e = 0.048 BTU per °F per ft per hr, d = 6.7 ft, D = 2 R = 1.44 ft, D_1 = 0.59 ft and K values adapted from Table 4, the external peripheral temperatures of the pipeline, θ_2, are assessed in Table 5 for extreme winter and summer conditions. For a mudline temperature of 80°F, the distribution of temperature and lines of heat flow throughout the sediments follow the patterns of Fig. 8.

Laying and Prestressing the Outer Casing Pipe.—Having regard to the fact that the pipeline in the as-laid condition (filled with air) will exert on the foundation an average pressure of 59 to 87 lb per sq ft, the question arises whether the prestressing of the casing pipe can be accomplished as desired. The conditions at the shore-end where the foundation is mainly fine sand are examined first.

In Fig. 9(a) the pull P_c on the casing pipe is shown resisted by a distributed frictional force q per unit length, which is assumed independent of the elongation of the pipeline under the pull. Taking the origin at the shore of an x-axis along the pipeline, the tensile stress, σ_x, developing in the casing at any distance x, will be

$$\sigma_x = \frac{P_c - q\,x}{A_c} \quad \ldots\ldots\ldots\ldots\ldots (12)$$

in which A_c is the cross-sectional area of the casing pipe. The value of q may be considered to be

$$q = \mu_c\, W_c \quad \ldots\ldots\ldots\ldots\ldots (13a)$$

and

$$\mu_c = \tan\phi \quad \ldots\ldots\ldots\ldots\ldots (13b)$$

in which μ_c is the coefficient of friction of the casing on the sand, W_c the negative buoyancy per unit length of the pipeline in sea water, and ϕ the angle of internal friction for submerged sand. For W_c = 85 lb per ft to 125 lb per

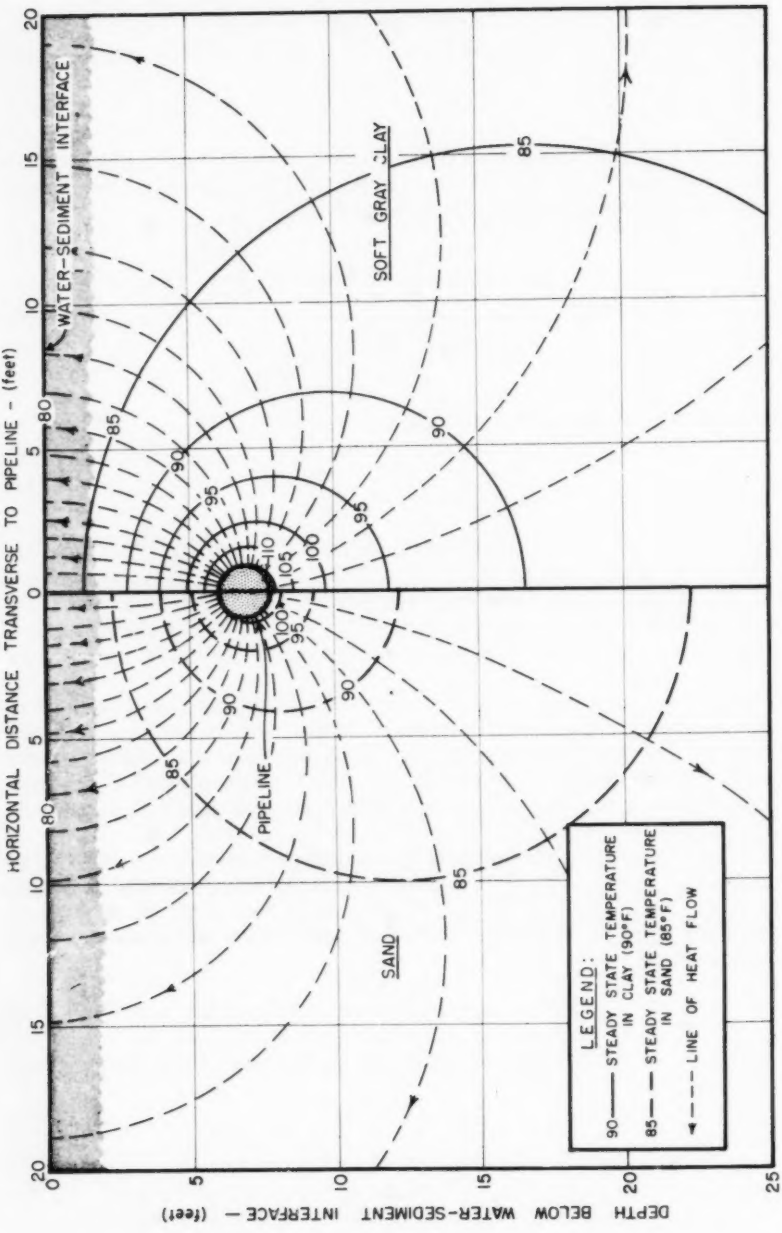

FIG. 3.—STEADY STATE HEAT FLOW THROUGH THE SEDIMENTS UNDER PIPELINE OPERATING CONDITIONS

ft, $\phi = 20°$, q is found to be from 31 lb per ft to 45 lb per ft and the distance a (Fig. 9(a)) in which the prestress from the pull $P_c = 200{,}000$ lb vanishes is therefore from 6500 ft to 4500 ft.

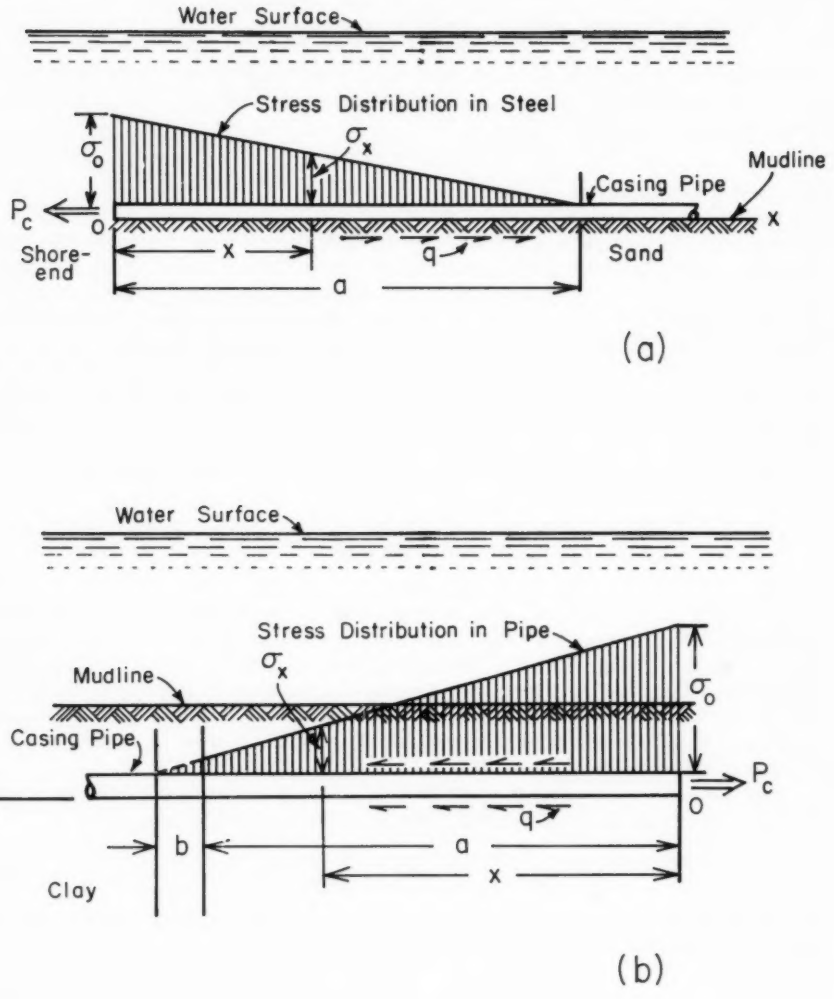

FIG. 9.—PRESTRESSING OF THE CASING PIPE BY APPLICATION OF END PULLS (a) SHORE-END (b) OFF-SHORE-END OF THE PIPELINE

Consideration of the offshore-end of the line is more intricate. Here the resistance q will depend on the cohesion of the clay and will not in general be independent of the elongation of the pipeline under the pull. The situation is

represented in Fig. 9(b) in which the origin is again taken at the end of the pipe. Over a distance a from the origin, at which the elongation will be large, the resistance q per unit length is assumed to be directly proportional to the maximum shear strength τ_m of the clay near the mudline. Thus,

$$q = \pi D \tau_m \quad \ldots\ldots\ldots\ldots\ldots\ldots \quad (14)$$

assuming the pipeline to be surrounded by the soft clay at the mudline. Beyond x = a, the resistance q will be some function of the elongation, u, the simplest form of which would be

$$q = \gamma u \quad \ldots\ldots\ldots\ldots\ldots\ldots \quad (15)$$

in which γ is a constant.

To arrive at some idea of the frictional properties of a sample of the cohesive clay (moisture content 68%) from the pipeline site, a simple test was devised, which is self descriptive in Fig. 10(a). Extraction of the model pipe yielded the test results of Fig. 10(b) from which a reasonable value of γ would be about 4300 lb per sq ft. The ultimate shear stress developed was of the order of 0.14 psi to 0.15 psi which is in fair agreement with the cohesion c found from Mohr circle stress analyses of typical data from the borings (Fig. 11). The test was decisive in indicating that the influence of Eq. 15 would extend over but a very short distance b (Fig. 9(b)) which, relative to a, could be neglected.

The tensile stress from the end pull P_c may thus be expressed as

$$\sigma_x = \frac{P_c}{A_c} - \frac{\pi D}{A_c} \int_o^x \tau_m \, dx \quad \ldots\ldots\ldots\ldots \quad (16)$$

In this, τ_m is a function of x, as indicated in Fig. 12(a), which is derived from Fig. 5. The integral of τ_m with respect to x is represented then by the area under the full-line curve of Fig. 12(a) for undisturbed sediment or the dotted-line curve for disturbed clay. The distance a from the mine-end of the pipeline over which the prestress σ_x declines to zero is readily found from Eq. 16 by trial and error and graphical integration of the areas. For undisturbed sediment it is only about 1400 ft and, for clay that has been weakened by disturbance, no more than about 9300 ft.

The expected amounts of elongation u of the pipeline under the end-pulls P_c may be evaluated from the basic stress-strain relationship

$$\frac{du}{dx} = \frac{\sigma_x}{E} \quad \ldots\ldots\ldots\ldots\ldots\ldots \quad (17)$$

in which E is the modulus of elasticity in tension of the steel. In the case of the shore-end of the casing pipe, Eqs. 12 and 17 yield

$$u_x = \left[\frac{P_c}{E A_c} - \frac{q}{2 E A_c} (x + a) \right] (x - a) \quad \ldots\ldots\ldots \quad (18)$$

Eq. 18 gives, for x = 0, $u_o = \frac{-a P_c}{2 E A_c}$, which, for $E = 30 \times 10^6$ lb per sq in., indicates an end-elongation u_o of from 1.3 ft to 0.9 ft corresponding to the estimates of a of 6500 ft and 4500 ft, respectively, cited previously. In the case of the mine-end of the casing pipe, Eqs. 16 and 17 give

$$u_o = \frac{-a P_c}{E A_c} + \frac{\pi D}{E A_c} \int_o^a \int_o^x \tau_m \, dx \, dx \quad \ldots\ldots\ldots \quad (19)$$

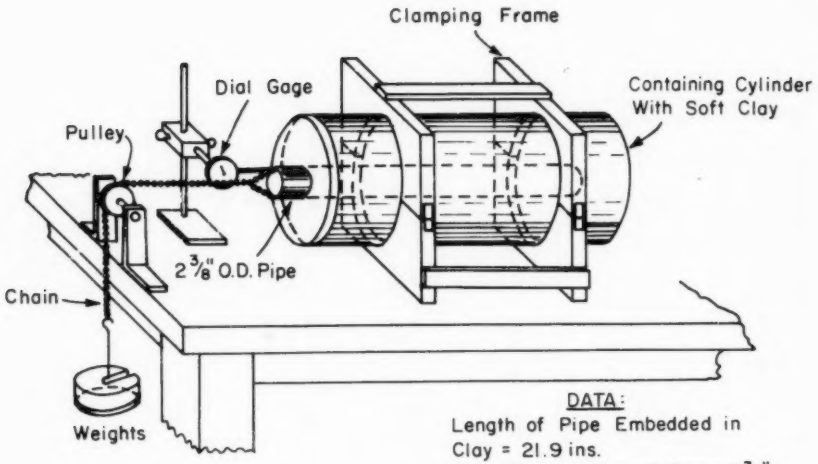

(a)

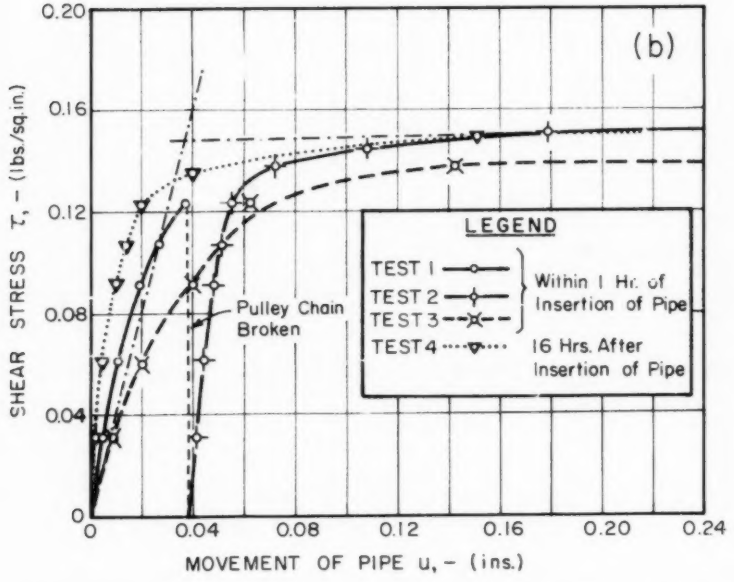

FIG. 10.—EXPERIMENTAL DETERMINATION OF CLAY SEDIMENT RESISTANCE TO LONGITUDINAL PIPELINE MOVEMENT; (a) EXTRACTION TEST APPARATUS (b) TESTS RESULTS

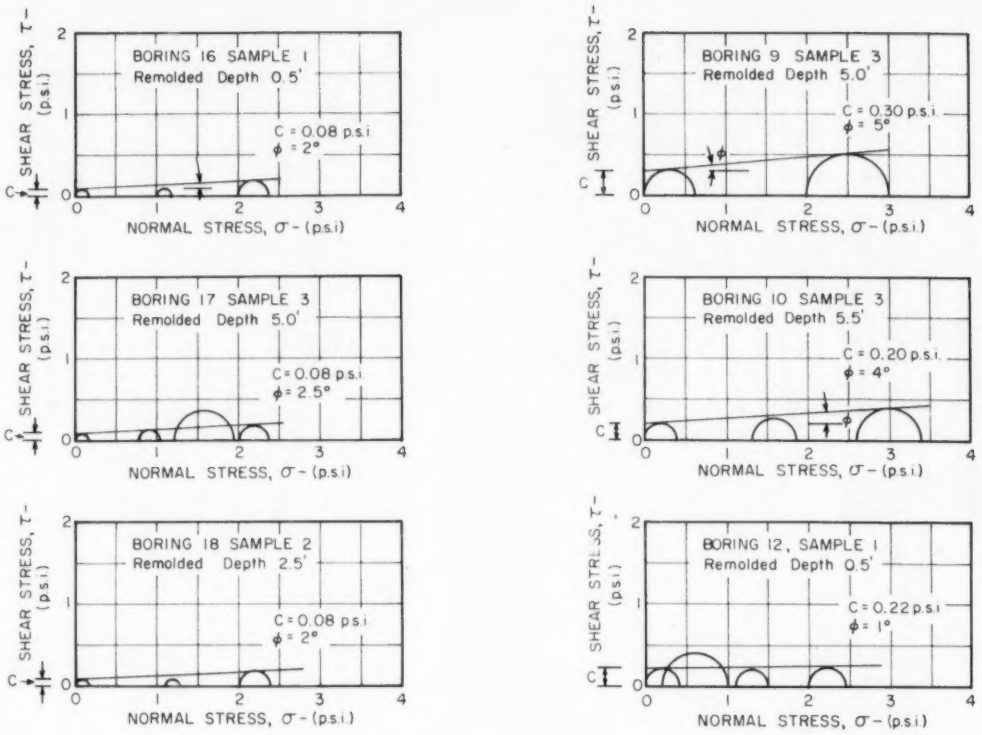

FIG. 11.—SAMPLE MOHR-CIRCLE STRESS ANALYSIS OF TEST DATA FOR COHESIVE CLAYS FROM BORINGS ALONG PIPELINE SITE (SPECIAL LARGE STRAIN QUICK-TRIAXIAL SHEAR TESTS, UNDER VARIOUS CONFINING PRESSURES, OR REMOLDED UNDRAINED SAMPLES)

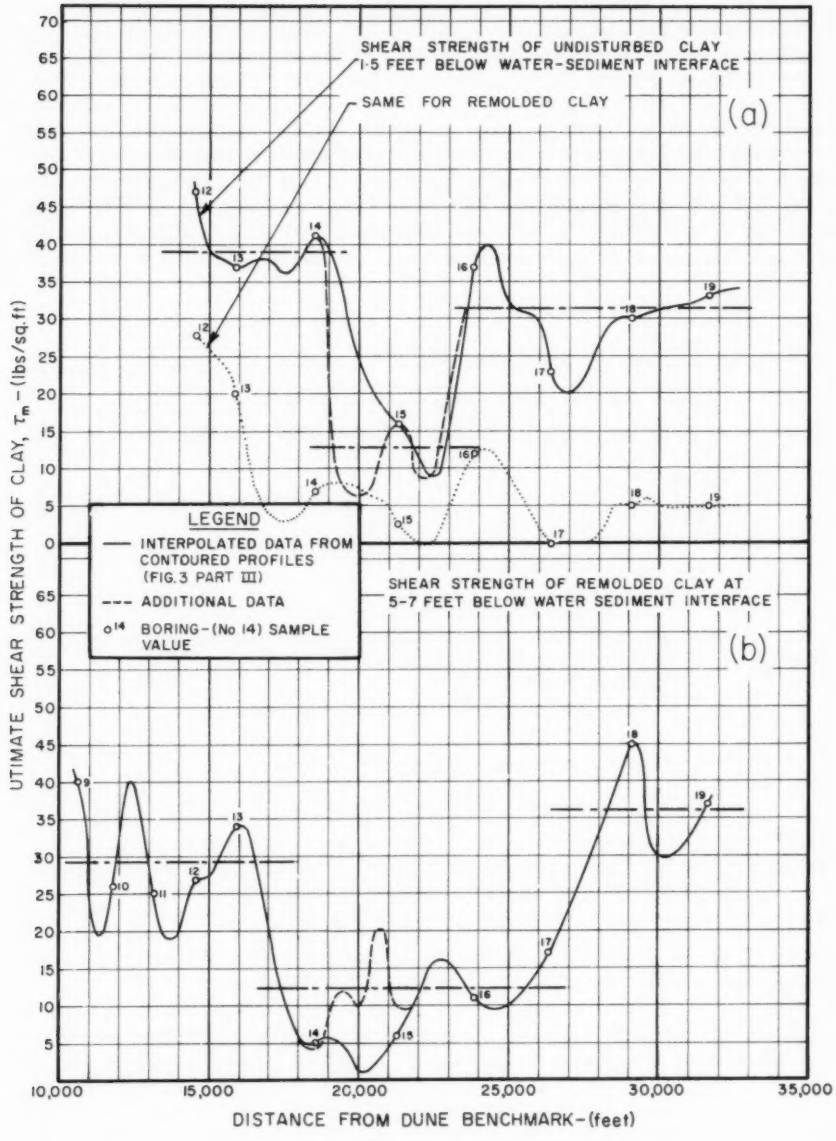

FIG. 12.—VARIATIONS OF SHEAR STRENGTH IN THE CLAY SEDIMENTS ALONG THE PIPELINE SITE; (a) AT 1.5 FT BELOW MUDLINE (UNDISTURBED AND REMOLDED); (b) AT 5 FT - 7 FT BELOW MUDLINE (REMOLDED)

which, if τ_m conforms to the strength of disturbed sediment (a = 9300 ft), results in an elongation of 1.7 ft, or, if the sediment is essentially undisturbed (a = 1400 ft), only 0.24 ft.

These computations suggest then that any effective prestressing of the casing pipe would be unattainable because of the high cumulative resistance of the sediments along the pipeline. (During laying of the pipeline in June, 1959, end pulls from 260,000 lb to 300,000 lb were applied to the casing and two external water lines (roughly the same stress condition for the casing and return water line treated in the text.). Measured expansion at the shore-end was only 7 in. (prediction 10 in. to 15 in.), at the mine-end only 2.5 ft (prediction 1.7 ft), instead of the hoped-for 12 ft.) End-pulling the casing pipe would leave the central portion entirely unstressed and, after anchoring of the ends, slow yield of the sediments would ultimately allow the non-uniform

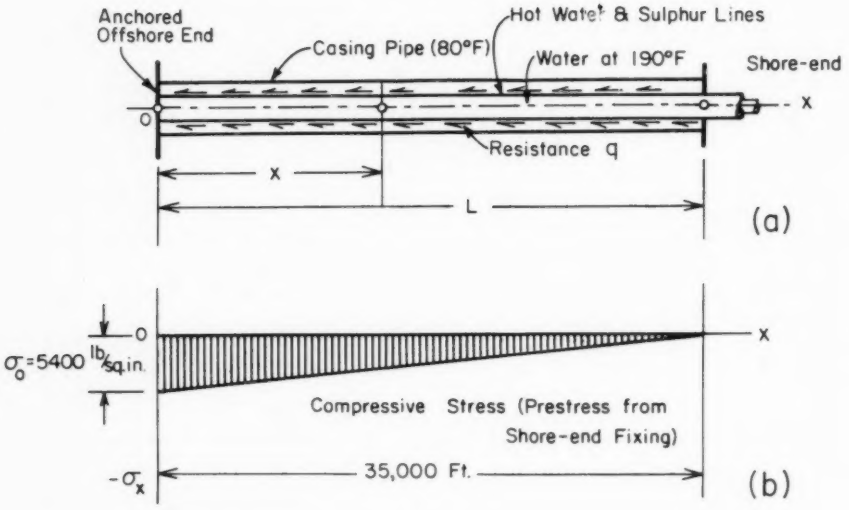

FIG. 13.—FIXING OF THE INTERNAL LINES IN THE CASING PIPE; (a) SCHEMATIC REPRESENTATION; (b) RESULTING STRESS IN INNER LINES

prestress to equilize at a very low value of stress along the entire pipeline, tending, essentially, to defeat the purpose of the prestress.

Fixing of the Sulphur and Hot Water Lines.—The fixing of the inner lines is portrayed schematically in Fig. 13(a) with reference to an origin taken at the offshore end of the pipeline. Expansion of the inner lines generates a small amount of friction in the rollers which carry them within the casing pipe; this is assumed constant and designated q per unit length. The cumulative resistance forces push on the offshore anchorage, in consequence of which a compressive stress develops in the inner lines that at any point x will be

$$\sigma_x = -\frac{q\,(L - x)}{A_s + A_h} \quad \ldots\ldots\ldots\ldots \quad (20)$$

in which L is the total length of the casing pipe and A_s and A_h are the cross-sectional areas of the sulphur and hot-water lines, respectively. (The negative sign is introduced to indicate compressive stress.) Taking $q = \mu_h(W_s + W_h)$ in which μ_h is the effective coefficient of friction of the roller bearings and

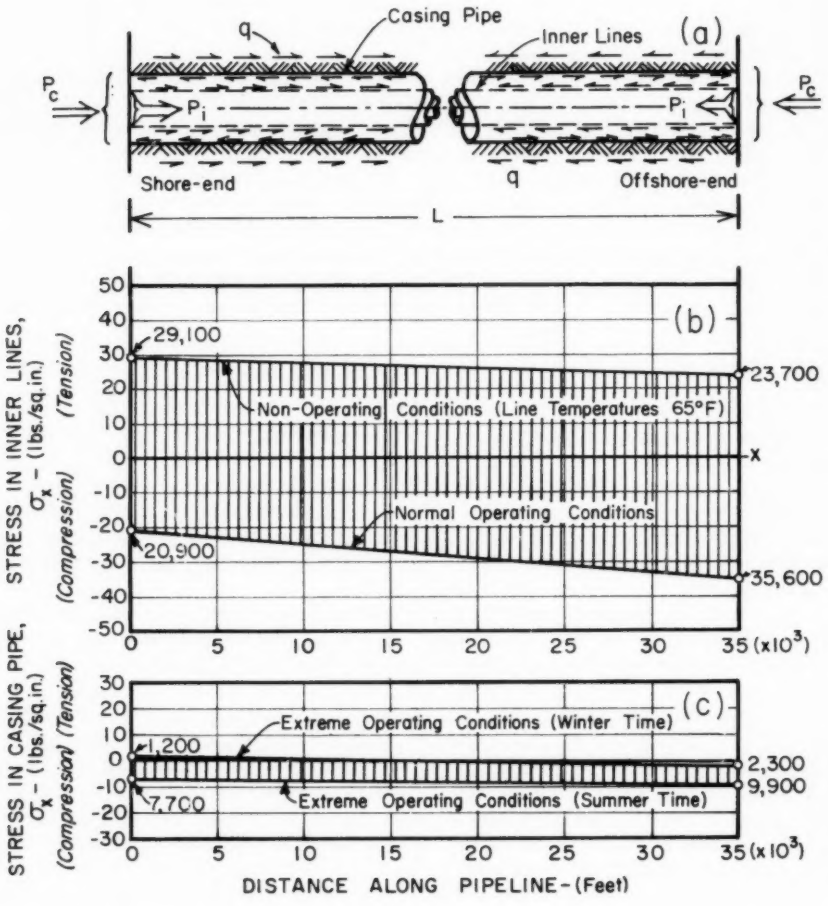

FIG. 14.—THERMAL STRESSES INDUCED IN PIPELINE UNDER OPERATING CONDITIONS; (a) SCHEMATIC REPRESENTATION; (b) STRESSES IN INNER LINES; (c) STRESSES IN CASING PIPE

W_s and W_h are the dead weights (in air) of hot-water-loaded sulphur and hot-water lines respectively, we find, for the particulars given in Table 1, with $\mu_h = 0.03$, a linear distribution of stress from 5400 lbs per sq in. at x = 0 to zero at x = L as shown in Fig. 13(b).

The elongation of the inner lines under the temperature rise, θ, from 80°F to 190°F may be shown to be

$$u_L = \alpha_i \theta L - \frac{q L^2}{2 E (A_s + A_h)} \quad \ldots\ldots\ldots\ldots (21)$$

in which α_i is the coefficient of linear expansion of the steel of the inner lines (see Table 1) and is computed to be 26.7 ft. (It is understood that actual expansion was of the order of 27 ft.)

Thermal Stresses in the Pipelines under Normal Operation.—Under operating conditions of the pipeline with the inner lines fastened to the casing, the ends anchored and the pipeline buried, it is assumed that the anchorages do not permit any sensible breathing or elongation of the pipeline. Accordingly, the tendencies towards expansion of the inner lines under the rise, θ_i from the fixing temperature of 190°F to the operating temperatures of 300°F ± 20°F are thwarted by the end-forces P of the anchorages (Fig. 14(a)) and result in thermal compressive stress throughout the line distributed as shown in Fig. 14(b) with a variation from 35,600 psi at the mine-end to 20,900 psi at the shore end (inclusive of the fixing prestress). The stress σ_i from these end constraints is computed from

$$\sigma_i = - E \alpha_i \theta_i \quad \ldots\ldots\ldots\ldots\ldots\ldots (22)$$

The casing pipe (and return water line), however, will also be subject to a temperature rise, θ_c, from the fixing temperature of 80°F to the values shown in Table 5, thereby acquiring stresses, σ_c, given by $\sigma_c = - E \alpha_c \theta_c$, in which α_c is the coefficient of linear expansion of the casing steel (Table 1). Under extreme summer conditions, (Table 5), thermal compressive stress in the casing would vary from about 9900 psi at the mine-end to 7700 psi at the shore-end, whereas under severe winter conditions thermal stress in the casing pipe would be quite small (Fig. 14(c)).

In the event of an unavoidable shut-down of operations in water, resulting in a drop of all line-temperatures to 65°F (Fig. 6), the induced thermal tensile stress in the inner lines would vary from about 23,700 psi at the mine-end to 29,100 psi at the shore end (Fig. 14(c)).

Longitudinal Stability of the Pipeline under Thermal Forces.—With end anchorages inhibiting expansion of the pipeline the latter would be prone to buckle unless prevented by the lateral restraints of soil forces. The condition is posed in Fig. 15(a) in the rather hypothetical case of half-wave buckling of the pipeline over its entire length L. The deflections y under the compression of the forces P_i and P_c pertaining to the inner lines and casing pipe respectively are, of course, not necessarily vertical. Buckling is resisted by normal soil forces p per unit length, considered proportional to the deflection. The soil modulus E_s appearing in this relationship

$$p = - E_s y \quad \ldots\ldots\ldots\ldots\ldots\ldots (24)$$

would be constant for a perfectly elastic foundation but may be expected to show some departure from constancy in a cohesive sediment as will be discussed later. The end conditions of the line are assumed to approximate hinges because any end moments will be of small importance due to the length of the line.

In buckling under thermal stress there will be actual elongation of the lines and no change in span length L. Thermal stress will tend to be relieved

by the buckling so that the forces P_c and P_i will diminish as the deflection y increases. If δ be the increase in length of the pipeline resulting from the buckling, then the relief of force will amount to $E A_c \delta/L$ for the casing and $E A_i \delta/L$ for the inner lines (in which A_c and A_i are respective cross-sectional areas), so that the work done by the thermally induced forces will be $\left(P_i - \frac{1}{2} E A_i \delta/L\right)\delta$ on the inner lines and $\left(P_c - \frac{1}{2} E A_c \delta/L\right)\delta$ on the casing pipe. Following Den Hartog,[15] it may be shown that the deflection δ is given by

$$\delta = \frac{1}{2} \int_0^L \left(\frac{dy}{dx}\right)^2 dx \quad \ldots\ldots\ldots\ldots\ldots\ldots \quad (25)$$

The work performed by the thermal forces then is

$$\frac{1}{2}\left(P_i + P_c\right)\int_0^L \left(\frac{dy}{dx}\right)^2 dx - \frac{E}{8L}\left(A_c + A_i\right)\left[\int_0^L \left(\frac{dy}{dx}\right)^2 dx\right]^2 \quad \ldots \quad (26)$$

By the principle of virtual work this equals the energy stored in the foundation and the energy of bending, that are, in that order,

$$\frac{1}{2}\int_0^L E_s y^2 dx + \frac{1}{2}\int_0^L E\left(I_c + I_i\right)\left(\frac{d^2y}{dx^2}\right)^2 dx \quad \ldots\ldots\ldots \quad (27)$$

in which I_c and I_i are the section moments of the casing pipe and the internal lines, respectively. Denoting

$$P = P_c + P_i \quad \ldots\ldots\ldots\ldots\ldots\ldots (28a)$$

$$A = A_c + A_i \quad \ldots\ldots\ldots\ldots\ldots\ldots (28b)$$

and

$$I = I_c + I_i \quad \ldots\ldots\ldots\ldots\ldots\ldots (28c)$$

the equality of Eqs. 26 and 27, with the Raleigh procedure of adopting a shape $y = y_o \sin \frac{\pi x}{L}$, leads to

$$\frac{P}{2}\left(\frac{\pi}{L}\right)^2 y_o^2\left(\frac{L}{2}\right) - \frac{E A}{8 L}\left(\frac{\pi}{L}\right)^4 y_o^4\left(\frac{L}{2}\right)^2 = \frac{E_s}{2} y_o^2\left(\frac{L}{2}\right) + \frac{E I}{2}\left(\frac{\pi}{L}\right)^4 y_o^2\left(\frac{L}{2}\right) \quad \ldots \quad (29)$$

The result given by Den Hartog[15] for the case of a hinged member under compression from constant end forces P is the same as Eq. 29, but without the second term on the left hand side. The critical buckling load P_{cr}, as given by Eq. 29, is

$$P_{cr} = E_s\left(\frac{L}{\pi}\right)^2 + E I\left(\frac{\pi}{L}\right)^2 + \frac{E A}{8}\left(\frac{\pi}{L}\right)^2 y_o^2 \quad \ldots\ldots\ldots \quad (30)$$

The third term on the right hand side of Eq. 30 arises only in the case of compression from thermally induced forces and represents additional compression that the pipeline could withstand because of the tendency towards immediate stress relief on buckling. If it can be shown that the forces P (Eq. 28) are less than P_{cr}, computed from just the first two terms of Eq. 30, then the pipeline will be quite definitely stable against any condition of buckling.

As shown by Den Hartog, the liklihood of a very long pipeline buckling into a single half-wave is quite remote. The tendency is for the line to buckle into a series of alternating half-waves, Fig. 15(b), of length l. The condition in fact

15 Advanced Strength of Materials, by J. P. Den Hartog, McGraw-Hill Book Co., Inc., New York, 1952, p. 262.

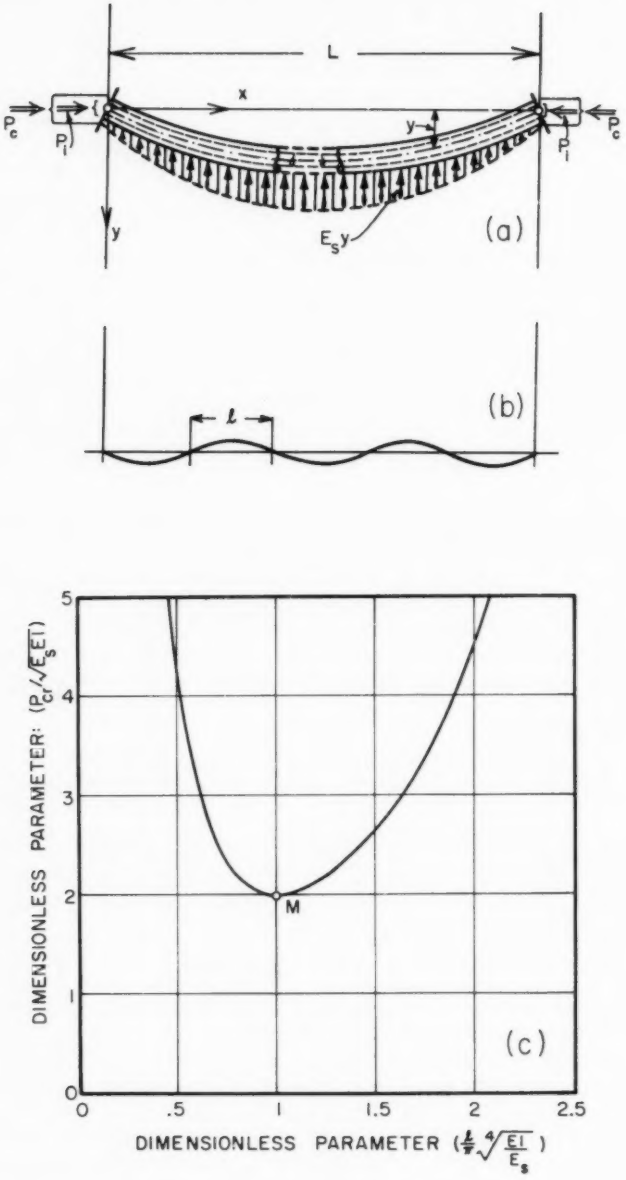

FIG. 15.—STABILITY OF THE PIPELINE AGAINST BUCKLING UNDER THERMAL STRESS; (a) SCHEMATIC REPRESENTATION; (b) MULTI-HALF-WAVE BUCKLING; (c) DIMENSIONLESS REPRESENTATION OF CRITICAL BUCKLING LOAD [ADAPTED FROM DEN HARTOG, 1952]

that a very long member buckles into a half-wave of specific length l is defined by the minimum value of P_{cr} which will just make that length unstable. This condition, represented by the point M in Fig. 15c, yields

$$P_{cr} = 2\sqrt{E_s E I} \quad \ldots\ldots\ldots\ldots\ldots\ldots (31a)$$

$$l = \pi \sqrt[4]{\frac{E I}{E_s}} \quad \ldots\ldots\ldots\ldots\ldots\ldots (31b)$$

which result is given also by Hetenyi[16] by use of another method.

Evaluation of the Soil Modulus, E_s.—The use of a soil modulus in the relationship of Eq. 24 is now firmly established in foundation engineering.[17,18,19] However, it is generally conceded that E_s usually increases with depth and that at a given depth it decreases as the deflection y increases.[17,18] The value of E_s to be adopted in Eq. 31 must therefore take cognizance of the depth of the pipeline and of the remolded nature of the material.

As remarked previously, the cohesive sediments covering a fairly wide area of the coastal region west of the Mississippi delta are very similar.[5] They comprise mainly montmorillonitic clay with inclusions of Illite and Kaolinite.[20] For such material F. D. Gaul,[19] A.M. ASCE, has found a value of E_s = 6900 lb per sq ft to be applicable in laboratory experiments of a laterally loaded pile; this is thought to be rather high. Fortunately, test data exist from field measurements of a laterally loaded pile in the neighborhood of Timbalier Island about 4 miles off the Louisiana coast, some 25 miles west of Grand Isle.[21] These data, comprising measurements of p and y (Eq. 24), have been correlated with standard laboratory tests of the sediments obtained from borings made on the site by B. McClelland, M. ASCE, and J. A. Focht,[18] M. ASCE. These authors show that the relationships of p to y for different depths follow trends that are similar to the relationships of deviator stress, σ, to strain, ϵ, in the quick triaxial shear-strength tests. According to their correlation, which they hold to be generally applicable to cohesive materials, the soil modulus can be evaluated from

$$E_s = 11\left(\frac{\sigma}{\epsilon}\right) \quad \ldots\ldots\ldots\ldots\ldots\ldots (32)$$

---

16 Beams on Elastic Foundations, by M. Hetenyi, Univ. of Michigan Press, Ann Arbor, Mich., 1946, p. 145.

17 "Non-Dimensional Solutions for Laterally Loaded Piles with Soil Modulus Assumed Proportional to Depth," by L. C. Reese and H. Matlock, Proceedings, 8th Texas Conf. on Soil Mechanics and Foundation Engrg., Special Publication No. 29, Bur. of Engrg. Research, Univ. of Texas, Austin, Tex., 1957.

18 "Soil Modulus for Laterally Loaded Piles," by B. McClelland and J. A. Focht, Jr., Proceedings, ASCE, Vol. 82, No. SM 4, October, 1956.

19 "Model Study of a Laterally Loaded Pile," by R. D. Gaul, Proceedings, ASCE, Vol. 84, No. SM 1, February, 1958.

20 "The Clay Minerals of Recent Marine Sediments to the West of the Mississippi Delta," by R. F. McAllister, thesis presented to the Agric. and Mech. College of Texas, in College Station, Tex., in 1958, in partial fulfillment of the requirements for the degree of Doctor of Philosophy.

21 "An Investigation of Lateral Loads on a Test Pile," by A. L. Parrack, Tech. Report Proj. 31, Texas Agric. and Mech. Research Foundation, College Station, Tex., 1952, (unpublished).

Here, obviously, because σ/ϵ is not a linear function and varies with depth, E_s must generally be a function of both depth and strain. From the nature of the $\sigma - \epsilon$ relationships obtained from the boring tests along the pipeline site, it would appear that they can be satisfactorily curve-fitted by an equation of the form

$$\epsilon = C\,\sigma^n \quad \ldots\ldots\ldots\ldots\ldots\ldots \quad (33)$$

in which C is a constant and n a numerical exponent. Evidence of this is presented in Fig. 16 for typical stress-strain curves taken at random. The values of C and n necessary to obtain the best possible curve-fits are plotted in Fig. 17 against distance along the pipeline. The conditions of immediate interest concern the values of C and n for the remolded clay at the pipeline depth, approximated by the test data at 5.5 ft below the mudline in Fig. 17(c). The constant C is found to vary from 15 to 37; that of n from about 1.9 to 2.3. It seems reasonable to adopt mean values of C = 25, n = 2.0.

On eliminating σ between Eqs. 32 and 33

$$E_s = 11\,C^{-1/n}\,\epsilon^{(1-n)/n} \quad \ldots\ldots\ldots\ldots\ldots \quad (34)$$

when for the values of C and n quoted

$$E_s = 2.2\sqrt{\frac{1}{\epsilon}} \quad \ldots\ldots\ldots\ldots\ldots\ldots \quad (35)$$

The graph of Eq. 35 is shown in Fig. 18 and reflects the dependence of E_s on the deflection. Because the ultimate strength of the cohesive material is reached in many cases when the strain exceeds about 6%, a mean value of E_s up to this limit of strain would seem to be a satisfactory criterion for adoption. We take therefore, in accordance with Fig. 18, E_s = 17 psi or 2450 lb per sq ft.

This value may be compared with the result of the extraction test (Fig. 10) for which γ was found to be 4300 lb per sq ft in the relationship of Eq. 15. Restating Eqs. 15 and 24 in terms of shear stress, τ, and normal stress, σ

$$q = \pi D \tau = -\gamma u \quad \ldots\ldots\ldots\ldots\ldots\ldots (36a)$$

and

$$p = D\sigma = -E_s y \quad \ldots\ldots\ldots\ldots\ldots\ldots (36b)$$

For u = y and a shear strength taken as one-half of the compressive strength ($\sigma = 2\tau$), the ratio p/q yields

$$E_s = \frac{2}{\pi}\gamma \quad \ldots\ldots\ldots\ldots\ldots\ldots \quad (37)$$

From this one might thus expect E_s to be $(2/\pi \times 4300)$ or about 2740 lb per sq ft, which is in fair agreement with the value of 2450 lb per sq ft given previously.

The Critical Buckling Load.—The pipeline has the choice of buckling in any direction. If the return water line is strapped below the casing pipe, the second moment of area of a cross-section of the system about a vertical axis will be less than that about a horizontal axis and will therefore favor lateral buckling of the pipeline. Lateral buckling would seem to be favored also by two other circumstances, namely, that vertical buckling would require penetration into stiffer material at greater depth in the case of a downward half-wave at the same time that an adjacent upward half-wave would necessitate the lifting of the pipeline against its own submerged weight as well as the overburden soil pressure.

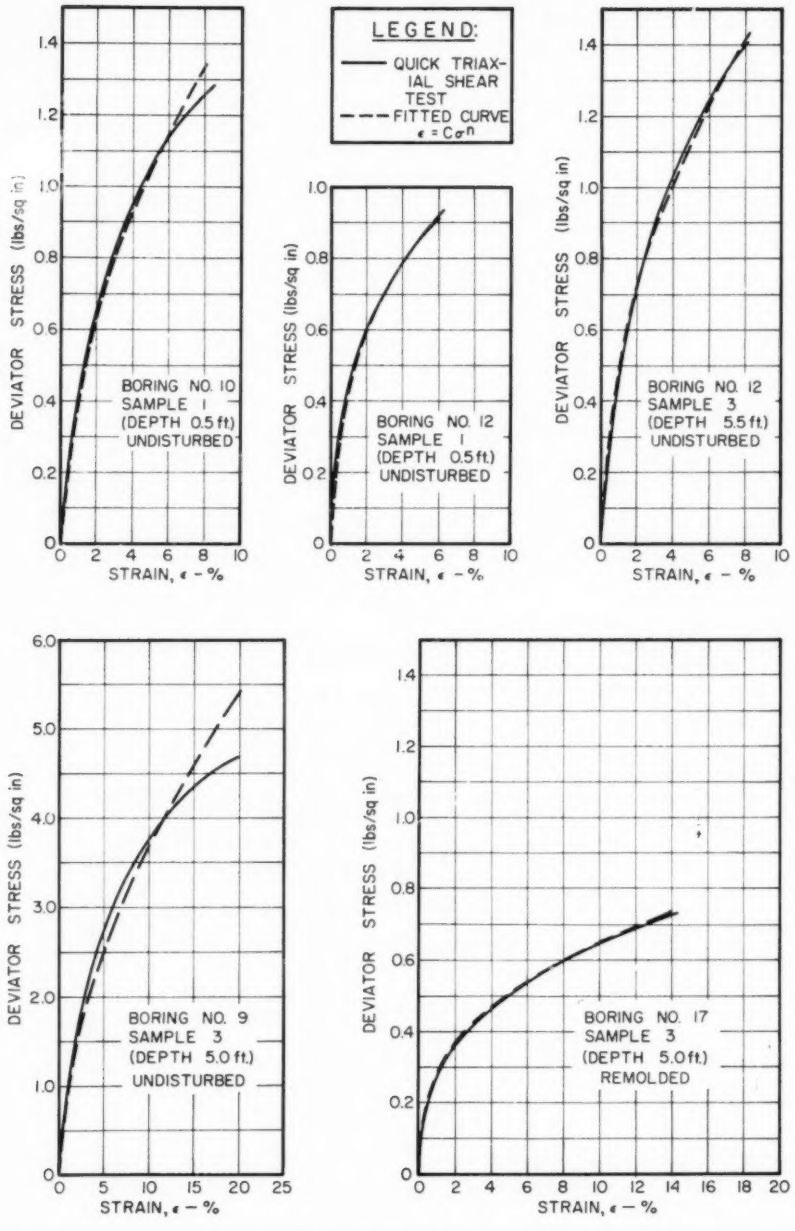

FIG. 16.—TYPICAL SAMPLES OF QUICK TRIAXIAL SHEAR TEST STRESS-STRAIN RELATIONSHIPS, CURVE-FITTED BY THE EQUATION $\epsilon = C_{\sigma} n$

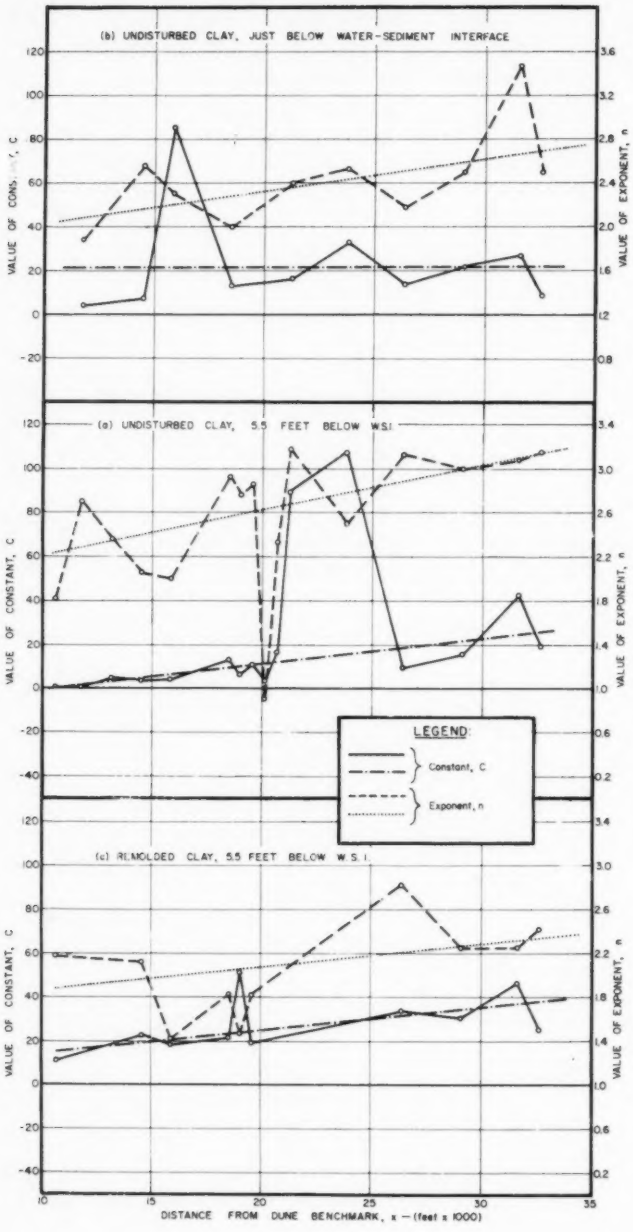

FIG. 17.—VARIATIONS ALONG PIPELINE OF VALUES OF CONSTANT C AND EXPONENTS, n, OF EQUATION $\epsilon = C_{\sigma}{}^{n}$ FITTED TO STRESS-STRAIN TEST DATA

Assuming lateral buckling then, the second moment of area (I) of the pipeline system about a vertical axis is I = 448 in.^{4}, when for E_s = 2450 lb per sq ft and E = 30 x 10^6 psi, the critical load P_{cr} is found to be 956,000 lb, and the critical half-wave length l = 44 feet. (For such a hinged length, without lateral support, the Euler critical load would be π^2 E I/l^2 or 476,000 lb.) Because actual load P from the induced thermal stresses at the mine-end of the

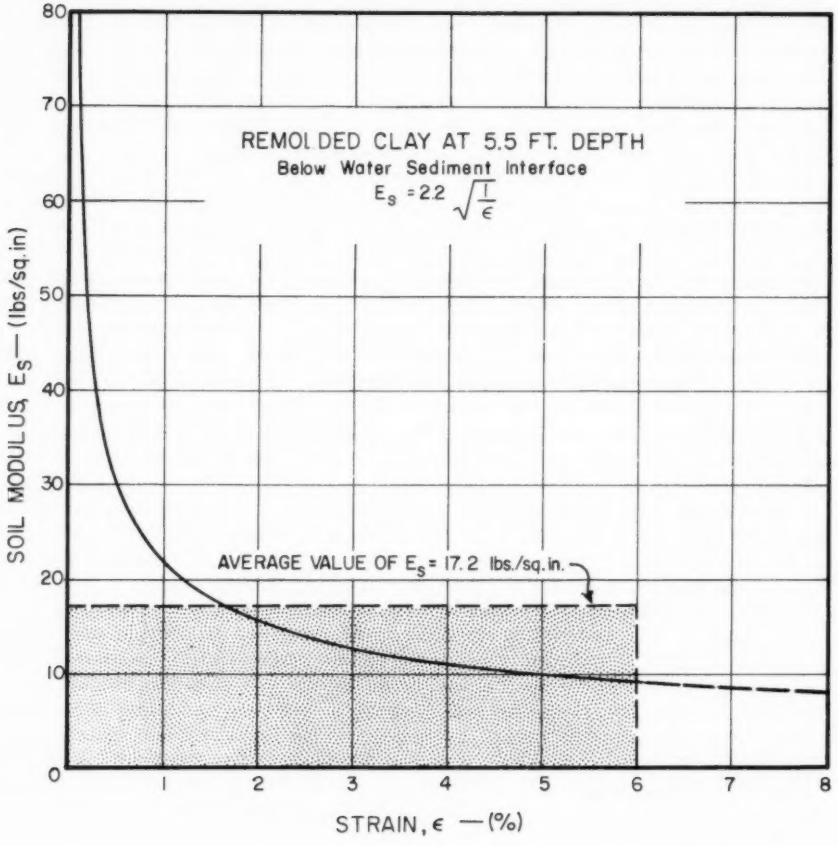

FIG. 18.—DEPENDENCE OF SOIL MODULUS, E_S, ON STRAIN, ϵ FOR REMOLDED CLAY AT DEPTH OF PIPELINE

pipeline is $(\sigma_i A_i + \sigma_c A_c)$, we find (for σ_i = 35,600 psi, A_i = 12.07 sq in., σ_c = 9900 psi and A_c = 19.73 sq in.) P = 625,000 lb. It seems, therefore, that the pipeline has a considerable margin of safety against decompression through buckling.

Effect of the Heat on the Sediments in Contact with the Pipeline.—All previous considerations of this paper up to this point have been based on the sup-

position that the foundation behaves in accordance with the properties determined from the test borings. The remaining important consideration concerns the influence of the heat flow from the pipeline on the properties and behavior of the foundation.

The possibility can be envisaged that in the fine sand sediments at the shore-end of the pipeline convection currents may be set up in the pore water which, through reduction of intergranular pressures, could lead to semi- or quicksand conditions and promote limited settlement of the line. The settlement could presumably continue until the convection currents became diffused to ineffective magnitudes at the greater depths. The amount of such settlement would seem to be unpredictable in the present state of our knowledge.

In the soft grey clay sediments prevailing along two-thirds of the length of the line, the chief concern might be that thermal osmosis will result in a migration of interstitial water from the heated zone, leading to a reduced water content in the clay in contact with the pipeline. This, it is thought, could produce some degree of desiccation and shrinkage of the medium that might induce tensile stresses in the casing pipe and lead to subsidence of the pipeline.

Regarding the imposition of tensile stresses in the casing pipe from shrinkage of the clay medium it would seem that the process of expulsion of void water from the clay in the neighborhood of the pipeline along the heat flow lines would be a fairly gradual process. The developing shrinkage stresses should therefore have time to disperse through the same process referred to in Section 8 in respect of the prestress, namely, that of a continuing slippage or creep taking place at the ultimate shear strength of the heated clay, assumed reduced from the liquid to the plastic limit. It might also be thought that any actual tensile stress imposed on the casing pipe as result of clay shrinkage might even be beneficial in that it would help to provide a condition of tension to offset the compressive stress in the line and thereby achieve naturally the prestress condition that is sought from preliminary endpulling of the casing pipe. It seems that the problem of the effect of clay shrinkage on the pipeline cannot be resolved in any very definite quantitative terms and that experience or experiment must decide this issue.

Regarding the anticipated subsidence of the line, this would seem to be unavoidable in the absence of a porous bedding and backfill, because the expulsion of void water by the thermal osmosis would lead to a consolidation of the clay in reverse along the heat flow lines. Because upwelling of material from below the pipeline cannot be expected, the line must necessarily sink. The degree of settlement likely to ensue, however, must obviously be limited by the increasing strength of the medium encountered beneath the pipe and the tendency at some stage for the clay there to reach stability from consolidation brought about by progressive bonding. Again, it does not seem possible to predict the amount of settlement that might be involved.

CONCLUSIONS

Laying of the 7-mile sulphur pipeline at a depth of 6 ft to 7 ft below the mudline off the eastern end of Grand Isle, Louisiana, involves its burial in very fine sand and silt over a distance of 11,000 ft from the shore and in extremely soft grey clay over the remaining distance out to the mine structures. In these media, the lightest density of weight-coat for pipeline protection, (135 lb per cu ft in the range of densities treated in this paper), would seem to be best from the point of view of relieving the foundation of stress in areas

of weakness without danger of flotation of the line in the event of agitation of the backfill by hurricane waves and flood.

The sand sediments are expected to provide adequate support for the line although some settlement is possible as result of convection currents induced in the pore water by heat flow from the pipeline through the soil. In the cohesive clay further offshore, the pipeline should be generally stable at trench-bottom level except over a distance between 17,500 ft and 23,000 ft from the coast, where it will almost certainly sink to a depth somewhere between 7 ft and 14 ft below the mudline in a pocket of extremely weak sediment. The gradients involved in this sag would be very slight and combined tension and flexural stress resulting from the depression should not exceed about 4300 psi. Heat losses from the pipeline may induce other limited subsidence in the clay as a whole, as a consequence of thermal osmosis and partial desiccation of the medium in contact with the pipe. Progressive bonding and consolidation round the pipe, however, should ultimately arrest this movement.

Analysis of the heat flow from the pipeline through the soil suggests that casing pipe temperatures can range from 74°F to 121°F (Table 5). These temperatures affect the stress condition in the casing pipe, but not in the inner lines, if ends are anchored. The highest thermal stress anywhere is 35,600 psi compression at the mine-end of the inner lines under operational conditions; in the casing, maximum thermal stress should not exceed 10,000 psi compression. It is shown that even the weakened soil forces to be expected of disturbed backfill should be adequate to contain the tendency of the pipeline to buckle under this compression.

It is a final conclusion of this study that uniform prestressing of the casing pipe would inevitably be frustrated by the cumulative soil resistance mobilized along the line. Indeed, it is evident that these soil resistances really render any anchorages unnecessary, because the friction is sufficiently great cumulatively to be able to restrict end-expansions to small proportions. (In final construction of the pipeline costly anchorages were dispensed with.) A favorable feature of free end-breathing of the pipeline would be the relief from thermal stress at the ends that it would afford. The specific nature of this, however, is outside the province of the present paper.

ACKNOWLEDGMENTS

In certain areas of this study the valuable advice and assistance of R. O. Reid, R. E. Schiller, M. ASCE, and S. J. Buchanan, F. ASCE, were of great help to the writer and are here gratefully acknowledged. The latter would also express his appreciation to the Freeport Sulphur Company, for whom this study was undertaken, for permission to publish this material.

APPENDIX.—NOTATIONS

A_c = cross-sectional area of the steel of the casing pipe and return water line;

A_h = cross-sectional area of the steel of the hot water line;

A_i = cross-sectional area of the steel of the inner pipelines $(= A_h + A_s)$;

A_s = cross-sectional area of the steel of the sulphur line;

a = dimension of length (Figs. 9 and 19);

B_s = buoyancy of pipeline entrenched in the sediments;

B_w = buoyancy of pipeline in sea water;

b = dimension of length (Fig. 9);

C = constant of proportionality, Eq. 33;

C_d = specific heat of dry solids in sediments;

C_s = specific heat of sea water;

C_w = specific heat of wet sediments;

D = outside diameter of casing pipe, inclusive of weight-coat;

D_1 = inside diameter of hot water line;

d = depth below mudline, Fig. 7;

E = modulus of elasticity of steel;

E_s = modulus of soil foundation, Eq. 24;

G_s = specific gravity of sediment solids;

h = film coefficient of heat conduction, (Table 2);

I = second moment of area of steel cross-sections for all components of pipeline, about vertical axis;

I_c = value of I for casing pipe and return water line;

I_i = value of I for concentric inner lines;

K = coefficient of thermal conductivity of wet sediment;

K_e = value of K equivalent of annular combination of pipeline components;

k = thermal diffusivity (specific conductivity of heat) of wet sediment;

L = total length of pipeline;

l = critical half-wave length of buckling;

n = numerical exponent, Eq. 33;

P = total restraining force acting on end of pipeline;

P_c = value of P applicable to casing pipe and return water line;

P_{cr} = critical buckling load for the pipeline entrenched in sediment;

P_i = value of P applicable to inner lines;

p = lateral soil force on pipeline per unit length;

Q = quantity of heat flow per unit distance per unit time;

q = tangential friction force per unit length;

R = radius of casing pipe to exterior of weight-coat;

R_1 R_2 = radii, Fig. 7;

r = moisture content of sediment;

S = degree of saturation of sediment, (Table 4);

u = longitudinal elongation of pipeline;

u_o = value of u at origin x = o;

u_x = value of u at any point x from origin;

W_c = negative buoyancy of pipeline in sea water per unit length;

W_m = load bearing capacity of sediment per unit length;

w_d = dry density of sediment (lb per cu ft);

w_w = wet density of sediments (lb per cu ft);

w_s = density of solids per unit volume of sediment (lb per cu ft);

x = variable horizontal distance;

y = variable lateral deflection;

α_c = coefficient of linear expansion of steel of casing pipe and return water line;

α_i = coefficient of linear expansion of steel of inner lines;

β = dimensionless coefficient, Eq. 4;

γ = constant of proportionality, Eq. 15;

ϵ = dimensionless strain, Eq. 33;

θ = temperature difference, rise or fall in temperature;

θ_c = rise or fall of temperature of casing pipe relative to its fixing temperature;

θ_i = rise or fall of temperature of inner lines relative to their fixing temperature;

θ_s = temperature of water-sediment interface;

θ_1 = temperature of hot water;

θ_2 = temperature at exterior surface of casing pipe weight-coat;

μ_c = coefficient of friction of casing pipe on sand sediment;

μ_h = effective coefficient of friction of roller bearings carrying inner lines within casing pipe;

π = universal constant, 3.1416;

σ = normal stress in sediment, Eq. 32;

σ_c = longitudinal thermal stress in casing pipe and return water line;

σ_i = longitudinal thermal stress in inner lines;

σ_x = longitudinal stress in pipeline at any point distant x from origin;

τ = shear stress in cohesive sediments;

τ_m = ultimate shear strength of clay sediment; and

ϕ = angle of internal friction of sediments in submerged state.

Journal of the
SOIL MECHANICS AND FOUNDATIONS DIVISION
Proceedings of the American Society of Civil Engineers

COHESION AFTER NON-HYDROSTATIC CONSOLIDATION

By John H. Schmertmann,[1] A. M. ASCE, and John R. Hall, Jr.,[2] A. M. ASCE

SYNOPSIS

A study was made to determine the effect of non-hydrostatic consolidation on the cohesion and friction in two saturated clays using the CFS-test procedure. The results showed that cohesion is unaffected by non-hydrostatic consolidation. The value of friction at zero CFS-test strain is increased by non-hydrostatic consolidation but the variation of friction with strain is the same as in a hydrostatically consolidated sample. In addition a time transfer of cohesion to friction was observed.

INTRODUCTION

Notation.—The letter symbols adopted for use in this paper are defined where they first appear, in the illustration or in the text, and are arranged alphabetically, for convenience or reference, in the Appendix.

Review of CFS-test.—A previous paper[3] reported the first published results of the basic research on the components of soil strength being performed in Soil Mechanics Research Laboratory of the University of Florida. This reference reports the development of a triaxial compression test, termed the CFS (an abbreviation of cohesion-friction-strain)-test, designed to permit the com-

Note.—Discussion open until January 1, 1962. To extend the closing date one month, a written request must be filed with the Executive Secretary, ASCE. This paper is part of the copyrighted Journal of the Soil Mechanics and Foundations Division, Proceedings of the American Society of Civil Engineers, Vol. 87, No. SM 4, August, 1961.

1 Asst. Prof. of Civ. Engrg., Univ. of Florida, Gainesville, Fla.

2 Graduate Asst., Civ. Engrg. Dept., Univ. of Florida, Gainesville, Fla.

3 "An Experimental Study of the Development of Cohesion and Friction with Axial Strain in Saturated Cohesive Soils," by J. H. Schmertmann and J. O. Osterberg, June 1960 Research Conf. on Shear Strength of Cohesive Soils, ASCE, July, 1961.

putation of cohesion and friction at strain intervals during compression and thereby establish curves of the variation of cohesion and friction with strain. Since an understanding of the definitions used for cohesion and friction and the techniques of the CFS-test are necessary in order to follow the work reported herein, they are briefly reviewed in this introduction:

The angle of internal friction ϕ_ϵ at any strain is the angle for which the tangent is the ratio of the change in shear stress to the change in normal effective stress occurring on the plane of Mohr envelope tangency at that strain, during a stress change occurring without significant change in soil structure.

The cohesion c_ϵ of a soil, at any strain ϵ, is the shear stress developed on the plane of Mohr envelope tangency at that strain, if the effective stress on that plane could be reduced to zero with proportionally the same change in soil structure as occurs in the determination of ϕ_ϵ.

For saturated soils, the effective stress at a point is defined as the total stress less the pore water pressure measured by a piezometer at that point. The plane of Mohr envelope tangency is the plane of maximum stress obliquity for the frictional component of strength. The expression "without significant change in soil structure" is, as of 1961, interpreted to be a void ratio change of less than 1% in the same soil, caused solely by a change in pore pressure.

From the foregoing, one may see that the cohesion and friction definitions used herein have a physical significance which one can "feel" and work with in the laboratory. The expressions "cohesion" and "friction" are retained herein for continuity with the previous work.[3] However, other expressions for these components, such as "pore pressure insensitive" and "pore pressure sensitive," may eventually be preferred. There is no claim that these are basic mechanical properties of a soil. The definitions were chosen with the hope that they will eventually prove useful in engineering application and thereby justify their existence. The writers are optimistic that this is the case. This work presents only part of the results from a research program active at the University of Florida, under the direction of the senior writer, and therefore represents only a part of the experimental evidence that will eventually be presented for the evaluation of the engineering significance of the CFS-test definitions and procedures.

Fig. 1 helps to explain the CFS-test technique. An axial deviator stress, σ_a, is imposed on a soil specimen in the triaxial chamber by subjecting the specimen to a constant rate of compressive strain. During this strain the pore water pressure is externally controlled to maintain a constant value of major principal effective stress, $\bar{\sigma}_1$, on any horizontal plane such as 1-1 in Fig. 1 (a). The control is by periodic manual adjustments of pore water pressure, u, to maintain a value of

$$u = \sigma_a + (\sigma_h - \bar{\sigma}_1) \quad \ldots\ldots\ldots\ldots\ldots\ldots (1)$$

in which σ_h is the constant cell pressure and $\bar{\sigma}_1$ is held constant at a pre-selected value. Thus,

$$u = \sigma_a + (\text{a constant}) \quad \ldots\ldots\ldots\ldots\ldots\ldots (2)$$

One of the pre-selected $\bar{\sigma}_1$ values is the $(\bar{\sigma}_1)_{high}$ indicated in Fig. 1(b). Two successive deviator stress-strain data points are obtained at this $(\bar{\sigma}_1)_{high}$, as represented by points a and b. The pore pressure is then increased to reduced $\bar{\sigma}_1$ to the pre-selected value of $(\bar{\sigma}_1)_{low}$. In the work reported herein the $(\bar{\sigma}_1)_{high}$ value was 95% $(\bar{\sigma}_1)_c$ imposed during consolidation, and the $(\bar{\sigma}_1)_{low}$ was 75% $(\bar{\sigma}_1)_c$. The increased pore pressure reduces the frictional component of

strength and thus reduces the deviator stress the speciman can support at that strain. Because the test is strain controlled, the result is a measured reduction in deviator stress instead of an increase in strain. After sufficient time for $\bar{\sigma}_1$ equilibrium at the lower value, two additional stress-strain data points

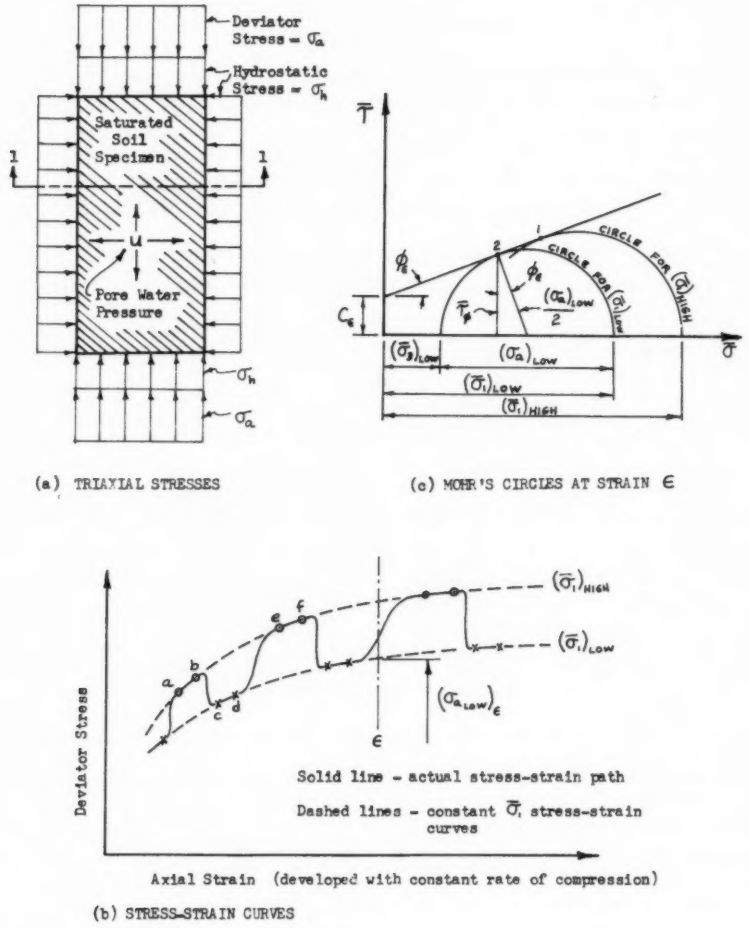

FIG. 1.—TECHNIQUE OF CFS-TEST

are obtained, as represented by points c and d. The pore pressure is then reduced to raise $\bar{\sigma}_1$ to the (σ_1) high value which results in increased friction and measured deviator stress: Points e and f are obtained to define two stress-strain curves, one for each $\bar{\sigma}_1$ as shown by the dashed lines in Fig. 1 (b).

At any value of strain, such as ϵ in Fig. 1 (b), a Mohr circle can be drawn representing the stress conditions for the specimen at each $\bar{\sigma}_1$ value. The two circles obtained are shown in Fig. 1 (c). The angle made by the tangent line 1-2 with the $\bar{\sigma}$ axis is ϕ_ϵ, which is then used in Eq. 3 to obtain c_ϵ. Eq. 3 is derived from the relationships shown in Fig. 1 (c):

$$c_\epsilon = \frac{\frac{\sigma_a}{2} - \sin\phi_\epsilon\left(\frac{\sigma_a}{2} + \bar{\sigma}_3\right)}{\cos\phi_\epsilon} \quad \ldots\ldots\ldots\ldots\ldots (3)$$

The values of ϕ_ϵ and c_ϵ thus obtained are plotted against strain, yielding a curve of cohesion-friction-strain behavior for the soil specimen tested.

Purpose.—In any field situation the soil is actually consolidated under non-hydrostatic stress conditions rather than the convenient hydrostatic consolidation usually employed in the laboratory triaxial test. It is therefore important to know if non-hydrostatic consolidation results in materially different subsequent strength behavior when compared to hydrostatic consolidation. All previous CFS-test work followed hydrostatic consolidation.

TABLE 1.—SUMMARY OF RESEARCH PROGRAM

Test Series (1)	Soil Type (2)	Number of Tests (3)	$(\bar{\sigma}_1)_c$ (4)[a]	$\left(\frac{\bar{\sigma}_1}{\bar{\sigma}_1}\right)_c$ Ratio Used (5)[a]	Consolidation Method (6)
I	Kaolinite	4	1.80 kg/cm^2	1.0, 1.2, 1.4, 1.6	Standard (see procedures)
II	Kaolinite	4	3.65 "	1.0, 1.2, 1.4, 1.6	Standard
III	Boston Blue Clay	4	3.65 "	1.0, 1.2, 1.4, 1.6	Standard
IV	Kaolinite	1 2	5.73 " 3.65 "	1.6 1.6	Standard, but increased time in secondary.
V	Kaolinite	2	3.65 "	1.6	1. σ_1/σ_3 kept constant during loading 2. $(\sigma_1-\sigma_3)$ added after consolidation to $(\bar{\sigma}_3)_c$

[a] Approximate.

The writers were especially interested in further study of the cohesion component of strength. One result of the previous work[3] was that the value of maximum principal effective stress, $\bar{\sigma}_1$, seemed much more important than soil structure in determining cohesion behavior. However, the possible importance of anisotropic structure was not studied. Such a study was one of the purposes of the work reported herein.

If cohesion is anisotropic due to anisotropy of soil structure, then the work by A. Casagrande, F. ASCE, and N. Carrill indicates[4] that for a constant value of maximum cohesion, and a constant position of the plane of maximum cohesion, the cohesion developed on the potential failure planes should vary measurably with significant variations in the degree of structural anisotropy. In this study,

4 "Shear Failure of Anisotropic Materials," by A. Casagrande and N. Carrillo, Contributions to Soil Mechanics 1941-1953, Boston Soc. of Civ. Engrs., p. 122.

TABLE 2.—SUMMARY OF TEST CONDITIONS

Series	Test Number	Sample Type Number	Test Date, 1959-60	$(\bar{\sigma}_1)_c$	$\left(\frac{\bar{\sigma}_1}{\bar{\sigma}_3}\right)_c$	Axial Consolidation Compression, $h_i - h_{o_a}$, in centimeters	Computed Values			
							Before consolidation		After CFS-test	
							e	S%	e	S%
(1)	(2)	(3)	(4)	(5)	(6)	(7)	(8)	(9)	(10)	(11)
I	H-17	DWEPK 795	1-21	1.80	1.00	0.258	1.059	100.5	0.958	101.2
	H-18	" 793	1-24	1.83	1.22	0.378	1.057	100.9	0.948	100.2
	H-19	" 792	1-26	1.84	1.42	0.469	1.057	100.9	0.945	100.8
	H-21	" 790	2-14	1.83	1.59	0.57	1.057	100.6	0.945	100.3
II	H-13	DWEPK 799	12-12	3.65	1.00	0.399	1.064	99.8	0.899	99.6
	H-14	" 798	1-10	3.81	1.21	0.546	1.064	99.6	0.883	100.0
	H-15	" 797	1-13	3.69	1.39	0.686	1.053	100.6	0.887	99.7
	H-16	" 796	1-19	3.56	1.58	0.818	1.055	100.6	0.901	100.8
III	H-22	BBC 539	2-20	3.65	1.00	0.233	0.744	99.8	0.645	100.0
	H-23	" 538	2-23	3.66	1.20	0.35	0.758	97.6	0.651	98.2
	H-24	" 537	2-25	3.67	1.41	0.47	0.732	99.0	0.652	97.9
	H-25	" 536	3-10	3.66	1.60	0.59	0.750	98.4	0.652	98.3
IV	H-20	DWEPK 791	2-9	5.73	1.57	1.15	1.068	99.3	0.846	100.0
	H-26	" 789	3-17	3.65	1.60	1.03	1.056	100.3	0.882	100.2
	H-29	" 785	3-31	3.67	1.61	0.835	1.064	99.9	0.887	99.9
V	H-27	DWEPK 788	3-20	3.71	1.63	0.70	1.051	100.2	0.906	99.6
	H-28	" 787	3-24	3.64	1.60	0.96	1.060	100.1	0.895	98.9

the maximum cohesion was assumed to be kept constant for the specimens of a test series by keeping initial soil structure, $\bar{\sigma}_1$, the plane of $\bar{\sigma}_1$ (horizontal), and void ratio constant within the series. The degree of anisotropy of the soil structure was varied by changing the $\bar{\sigma}_1/\bar{\sigma}_3$ ratio to which the specimens were consolidated prior to CFS-testing. This ratio was varied from 1.0 to 1.6 and it is assumed that significant variation in structural anisotropy was produced. Comparison of the results of such tests were then used to judge the possible anisotropic behavior of the cohesion component of soil strength.

Scope.—Table 1 summarizes the scope of this investigation. In this investigation two machine-remolded, near-saturated clays were used. Kolinite was chosen as the main clay because previous research[3] showed it had strength properties similar to a variety of clays of natural composition and had advantages of (a) additional structural sensitivity, in spite of machine remolding, (b) known minerology, and (c) relatively high permeability which aids the convenience of CFS-testing. Four of the five series used duplicate specimens of koalinite so that these series may be compared directly. To evaluate possible effects of mineralogy and grain size distribution, Series III was performed in an identical manner to Series II except that Boston blue clay was used. This is an illite-type clay with considerable silt. It is important to note that both kaolinite and illite are platey clay minerals and the results presented herein may be limited to clays with similar type clay minerals.

Series I and II are duplicates, except that the stresses in II are approximately double those of I. The stress was doubled to determine whether the magnitude of stress was a significant variable. The values of 1.80 kg per sq cm and 3.65 kg per sq cm were chosen for convenience. The ratio $\left(\bar{\sigma}_1/\bar{\sigma}_3\right)_c$ was limited to 1.6 because of excessive compressive strain encountered at higher values. Series IV was included to evaluate possible influences of the technique used to obtain the non-hydrostatic consolidation.

Table 2 presents additional detail about test and specimen conditions.

TESTING PROCEDURES

Equipment Used.—The triaxial and anisotropic loading equipment used was developed by the Norwegian Geotechnical Institute. A complete description of the equipment shown in Fig. 2 is available.[5] The NGI cell piston design was modified to accommodate a 1/4-in. piston running in ball-bearing sleeves.[6]

An SR-4 load cell was developed to replace the use of a proving ring. This cell has a compression of 0.006 mm per kg versus 0.090 mm per kg for a proving ring of the same load capacity (30 kg). This increase in rigidity enabled the tests to be run at a more constant rate of strain. The design of the load cell is reported elsewhere.[7]

---

5 "Triaxial Equipment Developed at the Norwegian Geotechnical Institute," by A. Andresen, J. Bjerrum, E. DiBiago, and B. Kjaernsli, Norwegian Geotech. Inst. Publications No. 21, Oslo, 1957.

6 "Prestress induced in Consolidated-Quick Triaxial Tests," by A. Casagrande and S. D. Wilson, Proceedings, 3d Internatl. Conf. on Soil Mechanics and Foundation Engrg., Switzerland, 1953, Vol. 1, p. 106.

7 "An Experimental Study of the Effect of Anisotropical Consolidation on the Cohesion and Friction in Saturated Clay," by J. R. Hall, Jr., thesis presented to the Univ. of Florida, at Gainesville, Fla., in June, 1960, in partial fulfillment of the requirements for the degree of Master of Science.

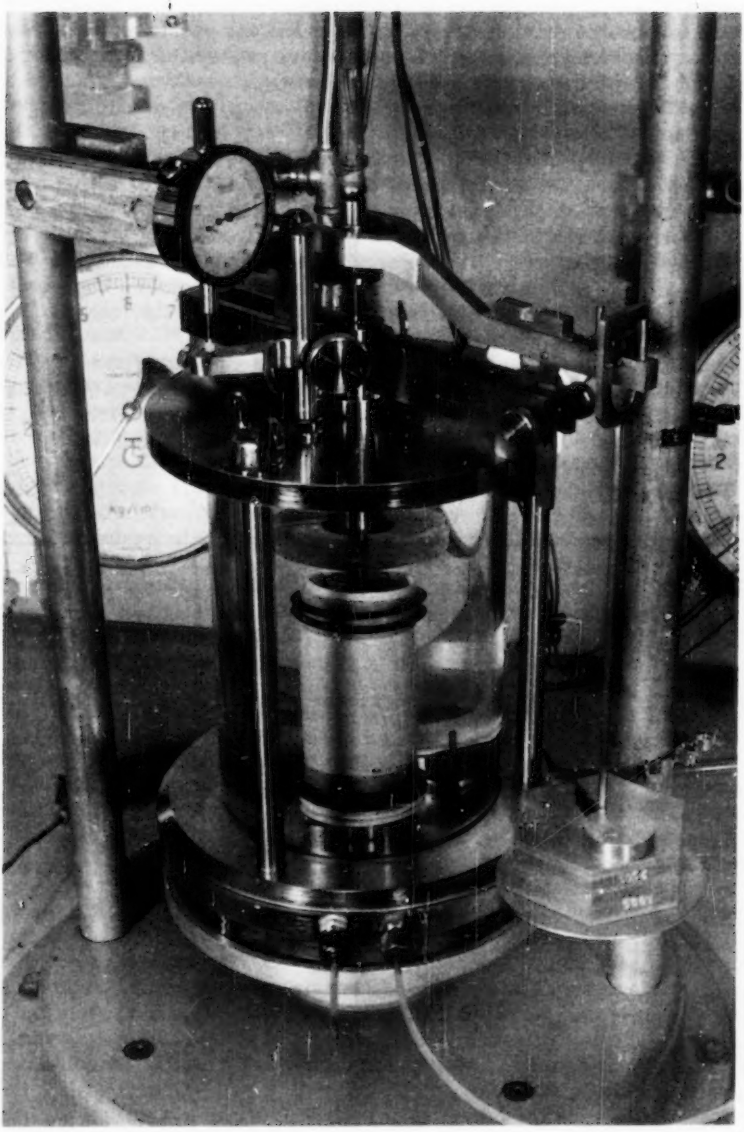

FIG. 2.—SPECIMEN DURING CFS-TEST AFTER ANISOTROPIC CONSOLIDATION

For preparation of duplicate remolded specimens with a high degree of saturation and structural duplication, a "Vac-Aire" extruder was used.[8] A helical particle-alinement structure results from the use of this extruder, and this, unfortunately, complicates the mental picture of the structural effect of subsequent non-hydrostatic consolidation. However, non-hydrostatic consolidation should develop some degree of anisotropic structure when compared to the starting condition.

Specimen Preparation.—The initial dimensions of all specimens were 8.00 cm high and 3.59 cm in diameter. Two clays were used. Table 3 lists the Atterberg limits, specific gravity, and grain size analyses of both.

Kolinite.—The kaolinite specimens were prepared from "as received" kaolinite powder. This was a particularly pure commercial kaolinite. The powder was mixed with distilled water to give a water content between 40% and 41%. A detailed description of this clay and a study of its geologic origin is available.[9] These specimens were designated DWEPK.

Boston Blue Clay.—The Boston blue clay was obtained from a pit in Cambridge, Mass. In remolding, the clay had to be allowed to partially dry in order to gain sufficient strength for extrusion into round bars. It was finally extruded at a water content of 26%. These specimens were designated BBC.

TABLE 3.—CLAY PROPERTIES

Clay	Liquid Limit, in %	Plasticity Index, in %	G used in calculations	Percentage Finer Than		
				200 sieve	50 μ	2 μ
DWEPK	52	21	2.609	100	100	60
BBC	38	19	2.810	98	87	53

Internal wool drains, together with filter paper strips along the sides and filter paper caps on the top and bottom, were used in triaxial tests. The specimens were sealed from the cell pressure media (water) with two latex membranes (each 0.056 mm thick) separated by a layer of grease. Further details concerning the preparation procedure are available.[3]

Testing Procedures.—

Non-hydrostatic Consolidation.—In order to reduce the void ratio variation within a test series, the tests were run so that the only variable was the minor principal stress applied during consolidation. The major principal stress applied during consolidation was held nearly constant within each series, giving essentially the same void ratio after consolidation in spite of the greatly different $(\bar{\sigma}_1/\bar{\sigma}_3)_c$ values of 1.0, 1.2, 1.4, and 1.6 (Table 2). With e and $\bar{\sigma}_1$ constant after consolidation, the effect of the non-hydrostatic consolidation could be better evaluated.

The method used for consolidating the specimens in Series I, II, III and IV, which is referred to as standard in Table 1, was as follows: Using the aniso-

8 "De-Aired, Extruded Soil Specimens for Research and for Evaluation of Test Proceedures," by H. Matlock, Jr., C. W. Fenske, and R. F. Dawson, A.S.T.M. Bulletin No. 177, October, 1951.

9 "Kaolinitic Sediments in Peninsular Florida and Origin of the Kaolin," by E. C. Pirkle, Economic Geology, Vol. 55, No. 7, November, 1960, p. 1382.

tropic loading device, the weights are suspended on a hanger which transmits the load to the piston of the triaxial cell through a system of knife edge supports with a lever-arm ratio of 5 (Fig. 2). The load to the piston is five times the load applied to the hanger. After noting the characteristic shape of the semi-log plot of the time-consolidation curves for kaolinite under a hydrostatic pressure of 3.65 kg per sq cm, it was observed that at approximately 6 ml decrease of volume, as measured by the amount of water drained from the specimen into a burette, the consolidation curve starts the turn into secondary consolidation. The total volume change was slightly more than 7 ml. It was decided to add the weights at equal intervals of volume change and to have all of the weights added by the end of 6 ml or 6/7 of the total consolidation. The weight increments used were determined by the convenience of the size of weights available. This load increment was usually 1 kg on the specimen, and from four to eleven increments were applied during the approximately 25 min required to consolidate 6 ml. The cell pressure was applied in one step at the beginning of consolidation and remained constant throughout the piston loading cycle. A similar procedure was used for the BBC in Series III and the kaolinite at $\bar{\sigma}_1$ = 1.80 kg per sq cm in Series I.

All of the anisotropic load was not added at the beginning of consolidation because the specimen was not able to support the total load without excessive strain or possible failure. By adding the load after equal increments of volume change, the specimen was given time to consolidate and thereby increase strength to support the following load increment without obviously excessive strain.

Two other methods of consolidation were used in Series V. For test H-27 the specimen was first consolidated hydrostatically under a pressure of 2.28 kg per sq cm. After the condolidation had proceeded 1,370 min in the secondary stage, following an approximate 50 min primary, the axial load was then applied in increments until the maximum stress, $\bar{\sigma}_1$, was equal to 3.71 kg per sq cm. In test H-28 the axial load and cell pressure were both increased in six increments such that the stress ratio σ_1/σ_3 was equal to 1.6 at all times. The specimen was allowed to consolidate for 8 hr between each increment. The final stresses on the specimen after consolidation were $\bar{\sigma}_1$ = 3.64 kg per sq cm and $\bar{\sigma}_3$ = 2.28 kg per sq cm.

In all tests for Series I, II, and III the time allowed for secondary consolidation after the final consolidation load increment varied between 17.4 hr and 19.7 hr.

Strength Testing.—As mentioned in the Introduction, the CFS-test was used for determining cohesion and friction as a function of strain. The compression rate of 0.0053 mm per min (0.0002 in. per min) was chosen the same for all tests. This rate permitted obtaining the required data for computing cohesion and friction over the range of approximately $\frac{1}{2}$% to 5% axial strain within a compression period of approximately 12 hr.

COHESION AND FRICTION

After non-hydrostatic consolidation the specimen is supporting a deviator stress,

$$\sigma_a = \sigma_1 - \sigma_3 \quad \ldots\ldots\ldots\ldots\ldots\ldots \quad (4)$$

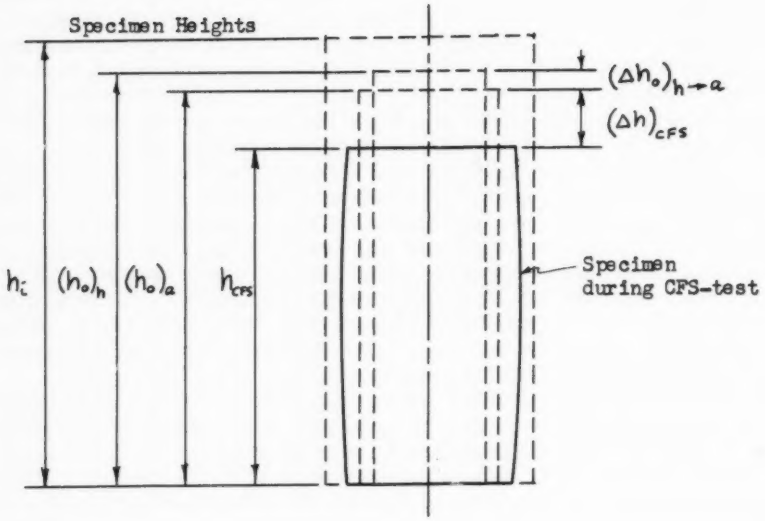

LEGEND

h_i = initial extruded height

$(h_o)_h$ = height after hydrostatic consolidation to $(\bar{\sigma}_1)_c$

$(h_o)_a$ = height after non-hydrostatic consolidation to same $\bar{\sigma}_1$; start of CFS-test

h_{CFS} = height during CFS-test

STRAINS

$\frac{(\Delta h_o)_{h\to a}}{(h_o)_a}$ = axial strain during non-hydrostatic consolidation = ϵ_a

$\frac{(\Delta h)_{CFS}}{(h_o)_a}$ = axial strain due to CFS-test = ϵ_{CFS}

Total strain = $\epsilon = \frac{(\Delta h_o)_{h\to a} + \Delta h_{CFS}}{(h_o)_h} \approx \epsilon_a + \epsilon_{CFS}$

FIG. 3.—DEFINITION OF SPECIMEN STRAINS

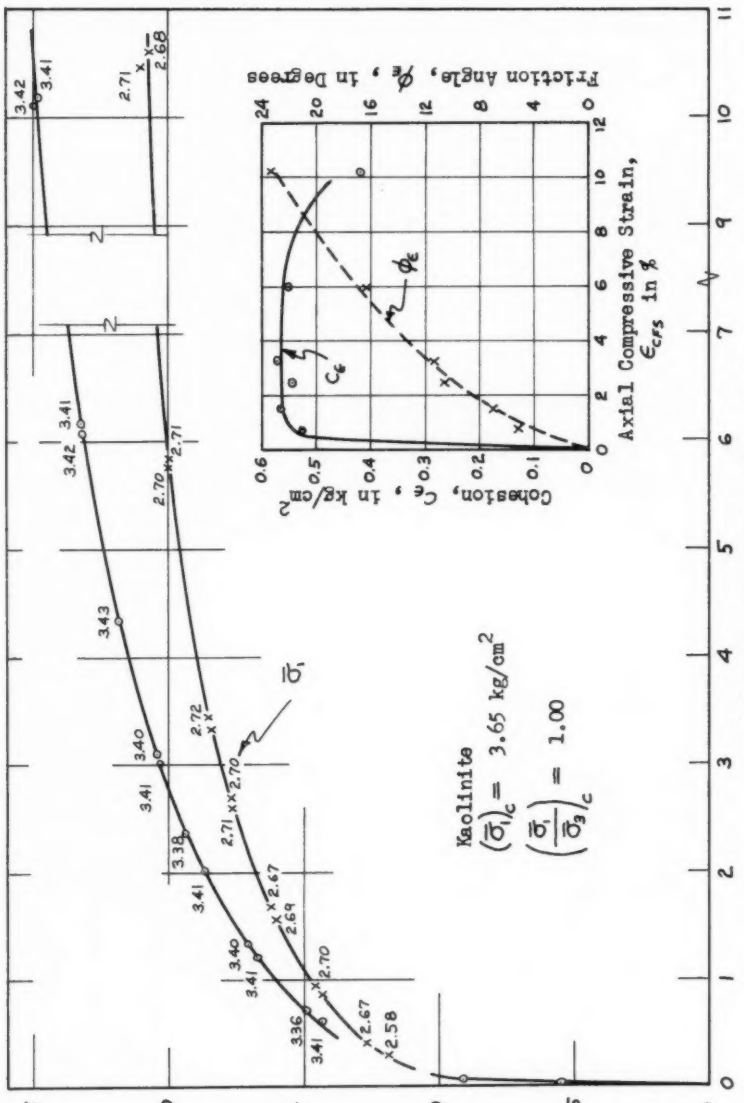

FIG. 4.—STRESS-STRAIN CURVES AND COMPUTED RESULTS FOR TEST H-13, SERIES II

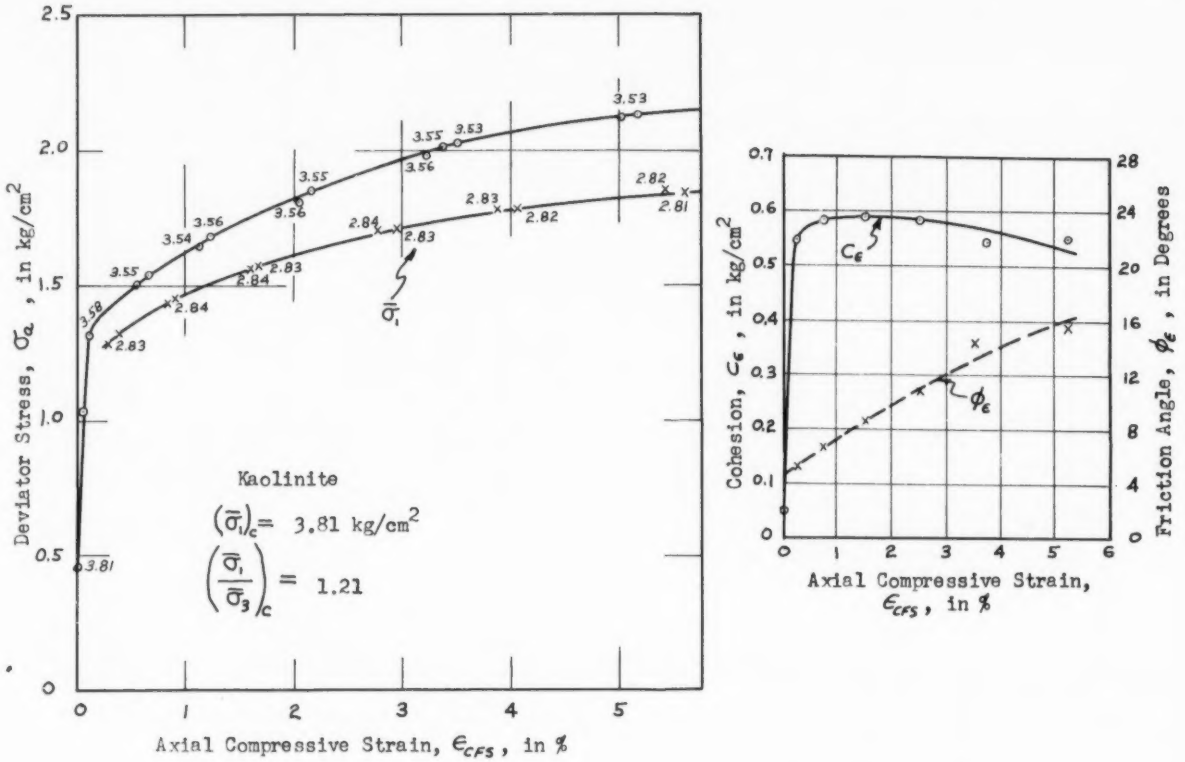

FIG. 5.—STRESS-STRAIN CURVES AND COMPUTED RESULTS FOR TEST H-14, SERIES II

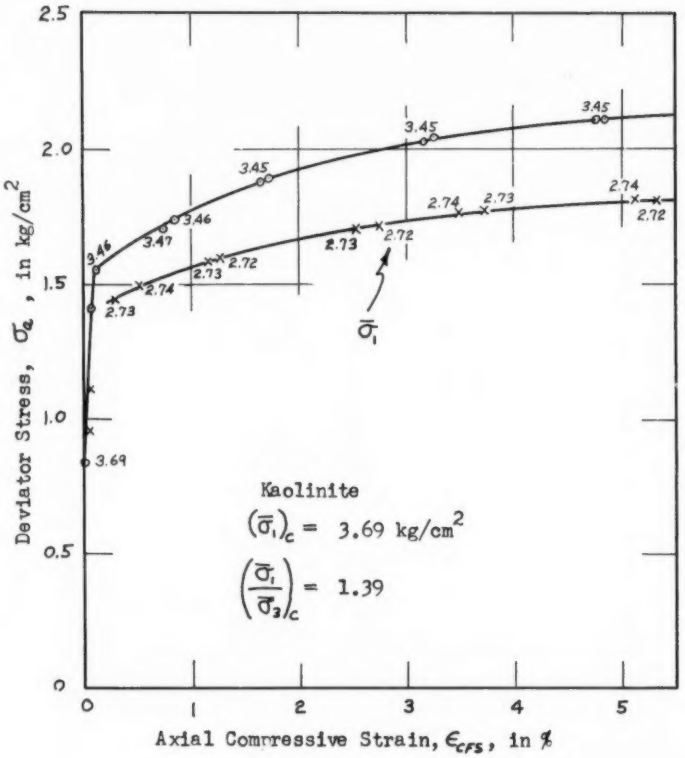

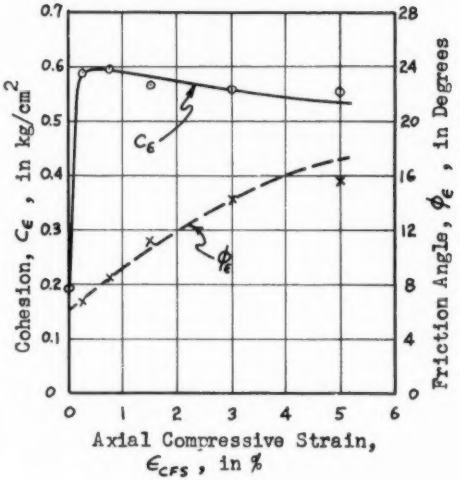

FIG. 6.—STRESS-STRAIN CURVES AND COMPUTED RESULTS FOR TEST H-15, SERIES II

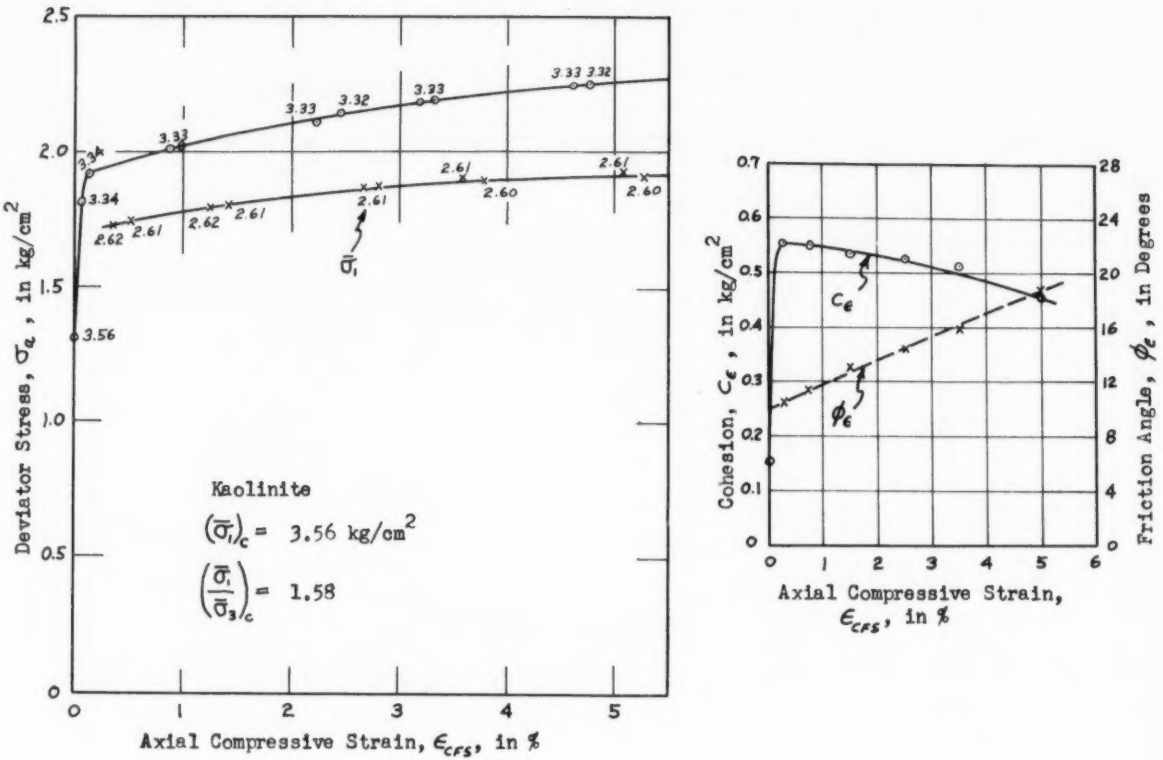

FIG. 7.—STRESS-STRAIN CURVES AND COMPUTED RESULTS FOR TEST H-16, SERIES II

and has undergone axial strain as shown in Fig. 3. In order to support this deviator stress, the values of cohesion and friction cannot both be zero. If the

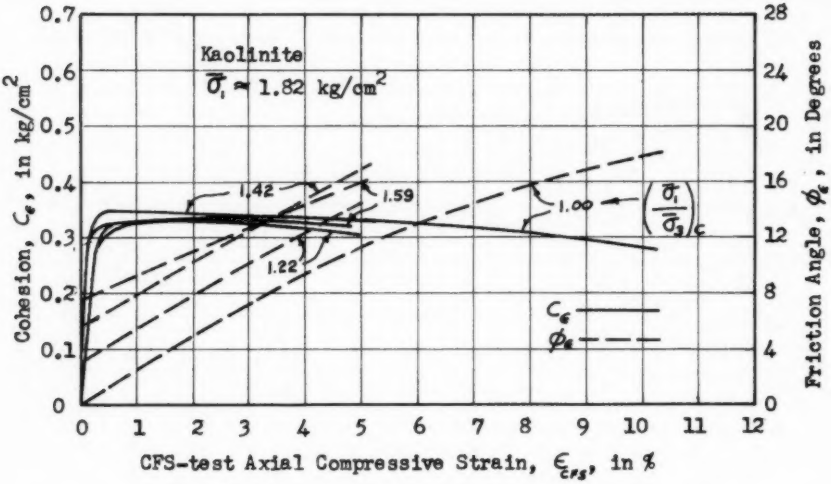

FIG. 8.—VARIATION OF COHESION AND FRICTION WITH CFS-TEST STRAIN FOR SERIES I

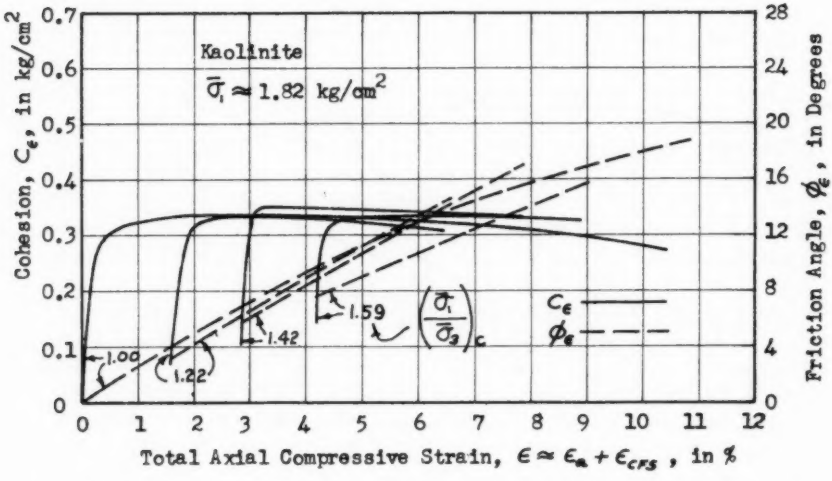

FIG. 9.—VARIATION OF COHESION AND FRICTION WITH TOTAL STRAIN FOR SERIES I

specimen is subjected to a hydrostatic state of stress, as in the case of hydrostatic consolidation, then at zero CFS-test strain both the cohesion and friction were assumed to be zero.

For the non-hydrostatic case, the following method was used to compute the values of cohesion and friction at zero CFS-test strain: The values of cohesion and friction are computed only at strains where the two required $\bar{\sigma}_1$ curves are

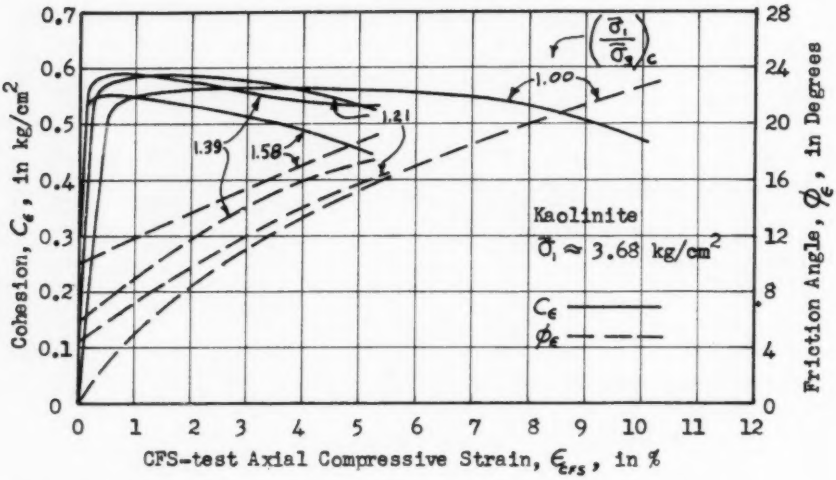

FIG. 10.—VARIATION OF COHESION AND FRICTION WITH CFS-TEST STRAIN FOR SERIES II

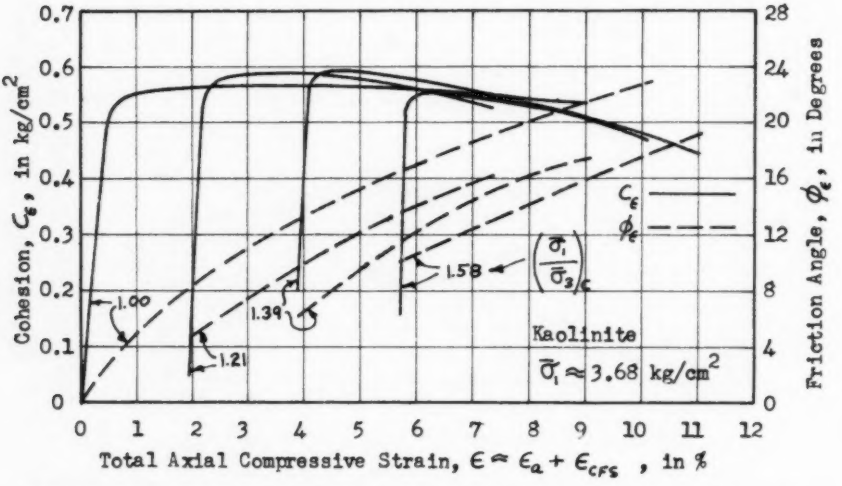

FIG. 11.—VARIATION OF COHESION AND FRICTION WITH TOTAL STRAIN FOR SERIES II

fully defined and c_ϵ and ϕ_ϵ are plotted against that strain. This may be seen in Figs. 4, 5, 6, and 7, that present the detailed results for Series II. Because it is impossible, from the data obtained, to draw the two curves for different ef-

fective stresses at small values of CFS-test strain (less than 0.25%), an extrapolation procedure was used. The extensive testing experience with DWE PK and BBC specimens hydrostatically consolidated for approximately 23 hr prior

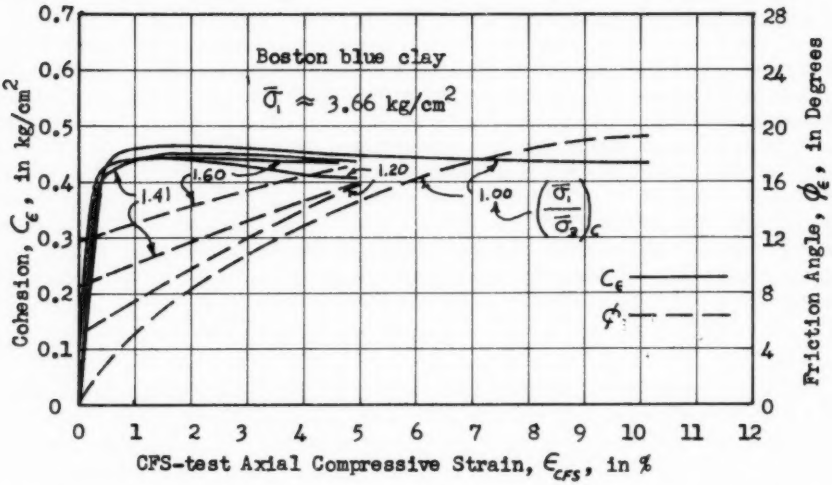

FIG. 12.—VARIATION OF COHESION AND FRICTION WITH CFS-TEST STRAIN FOR SERIES III

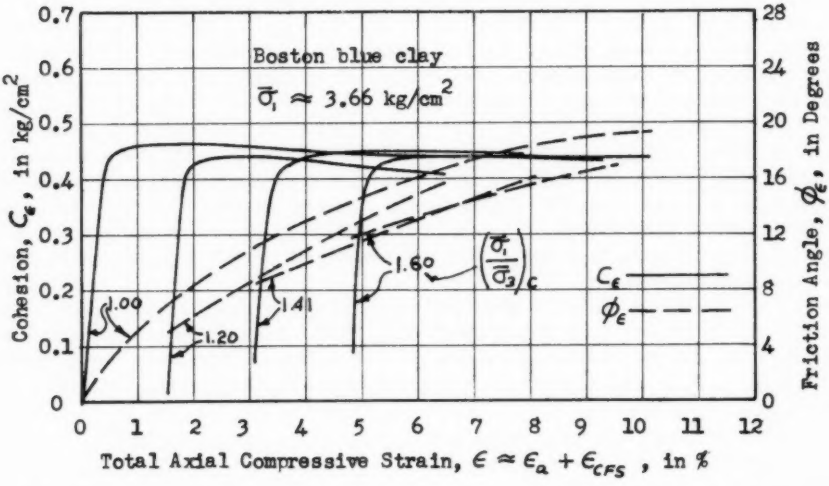

FIG. 13.—VARIATION OF COHESION AND FRICTION WITH TOTAL STRAIN FOR SERIES III

to shear testing indicated that at CFS-test strains of less than 1% the frictional component of strength varies much less rapidly with strain than the cohesion.[3] Thus, the friction was extrapolated to zero strain instead of the cohesion. This

value of friction was assumed to be the value at zero CFS-test strain and was used to compute the value of cohesion at zero strain by using Eq. 3. The initial values of cohesion and friction as computed by this method are shown on the curves plotted for the individual test (Figs. 4 to 7) as well as the curves showing each complete series (Figs. 8 to 13).

Series I, II, and III.—Series I, II, and III were performed in the same manner and are therefore presented together. This analysis began with a review of the strain history of each specimen, as shown in Fig. 3. After the initial extrusion the specimen was consolidated with $(\bar{\sigma}_1/\bar{\sigma}_3)_c$ ratios up to 1.6. The application of a deviator stress during consolidation resulted in axial compression greater than the height reduction measured during hydrostatic consolidation to the same value of $\bar{\sigma}_1$. This additional strain is designated ϵ_a. Then a strain ϵ_{CFS} was imposed during the CFS-test. Although the foregoing two strains were computed with a different reference height than the total strain ϵ, the percentage difference in the heights $(h_o)_a$ and $(h_o)_h$ is small and it is considered adequate to estimate the total strain due to deviator stress as

$$\epsilon = \epsilon_a + \epsilon_{CFS} \quad \ldots\ldots\ldots\ldots\ldots\ldots (5)$$

The cohesion-friction-strain curves for these series are presented in Figs. 8 to 13. Two strain coordinates are used. Figs. 8, 10, and 12 are based on the CFS-test strain, ϵ_{CFS}; Figs. 9, 11, and 13 on the estimated total deviator strain ϵ. From both these sets of figures it may be seen that the cohesion behavior is a function of $(\bar{\sigma}_1)_c$ and is unaffected by $(\bar{\sigma}_3)_c$. Thus, these results support the concept that cohesion is an isotropic property.

Considering only Figs. 8, 10, and 12, it appears that the friction-strain behavior was progressively displaced toward higher friction values with increasing values of $(\sigma_1/\sigma_3)_c$. However, these figures do not account for the deviator strain that occurred during the non-hydrostatic consolidation. When plotted on the basis of the estimated total strain, as in Figs. 9, 11, and 13, there is some displacement toward lower friction values with increasing $(\bar{\sigma}_1/\bar{\sigma}_3)_c$, but that the general friction-strain behavior is similar to that of the hydrostatically consolidated specimen. The values used for ϵ_a are critical in the foregoing comparison and it should be realized that the step-loading procedure used to apply the deviator stress during consolidation complicates the estimate of ϵ_a. The estimate used herein, as shown in Fig. 3, is probably not sufficiently refined to permit a conclusion regarding any displacement effect of non-hydrostatic consolidation on friction-strain behavior.

A conclusion is also not possible with regard to another important aspect of friction behavior, pore pressure development. Pore pressure is controlled in the CFS-test and thus its development in response to other factors possibly associated with non-hydrostatic consolidation was not considered in this research program.

Series IV.—Three tests were run to determine the effect of the length of time permitted for non-hydrostatic consolidation on the kaolinite. The three tests showed no important differences in their results. When the value of friction was extrapolated to zero CFS-test strain to compute cohesion at this strain, the computed value of cohesion ranged from -0.08 kg per sq cm to 0.00 kg per sq cm. The value of friction was then mathematically adjusted to suit a cohesion of zero.

The three Series IV tests were allowed to stand for 66 hr, 131 hr, and 299 hr, respectively, after the completion of primary consolidation. From the re-

sults of the Series IV and previous tests it was concluded that as the non-hydrostatically loaded specimen continues to consolidate in the secondary stage the deviator stress is initially carried by both cohesion and friction but is eventually carried totally by friction as the cohesion drops to zero. However, a zero cohesion is only possible for soils able to develop the required friction to carry the total load.

The conclusion of the cohesion to friction transfer is strongly supported by the unpublished experimental work of R. G. Bea,[10] A. M. ASCE, and his im-

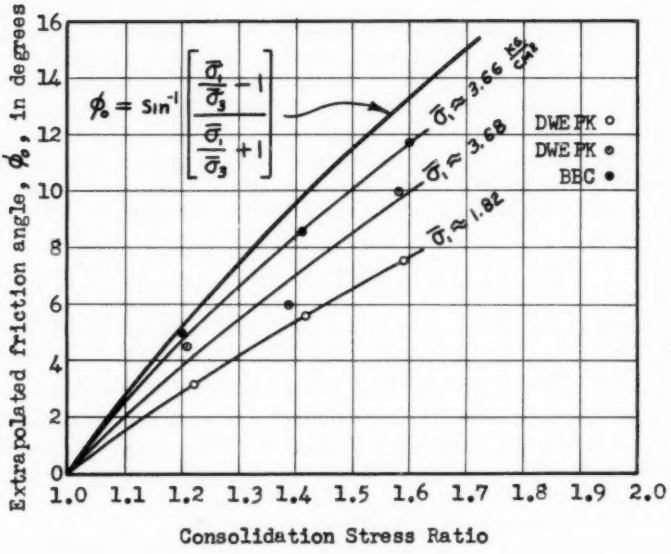

FIG. 14.—FRICTION ANGLE AT ZERO CFS-TEST STRAIN VERSUS CONSOLIDATION STRESS RATIO

portant contribution to its recognition is acknowledged. The present work on this subject is preliminary. Extensive additional research is in progress.

The tests in Series I, II, and III were conducted after secondary consolidation times between 17.4 hr and 19.7 hr. This was insufficient time for the cohesion to drop to zero, as seen in Figs. 9, 11, and 13. The value of friction angle at zero CFS-test strain, ϕ_0, versus consolidation stress is plotted in Fig. 14 for test Series I, II, and III, together with the curve representing the value

10 "An Experimental Study of Cohesion and Friction During Creep in Saturated Clay," by R. G. Bea, thesis presented to Univ. of Florida, Gainesville, Fla., in June, 1960, in partial fulfillment of the requirements for the degree of Master of Science.

of friction that would be obtained had the specimen consolidated over an adequate length of time for the cohesion to drop to zero. If cohesion is equal to zero, then it follows from Eq. 3 that

$$\phi_0 = \sin^{-1}\left[\frac{\frac{\bar{\sigma}_1}{\bar{\sigma}_3} - 1}{\frac{\bar{\sigma}_1}{\bar{\sigma}_3} + 1}\right] \quad \ldots\ldots\ldots\ldots\ldots\ldots (6)$$

The required time for the cohesion to drop to zero seemed to depend on $\bar{\sigma}_1$ as well as the type of clay. The BBC transferred cohesion to friction more rapidly than DWE PK, and the DWE PK at $\bar{\sigma}_1$ = 3.65 kg per sq cm more rapidly than the same clay at $\bar{\sigma}_1$ = 1.80 kg per sq cm.

Series V.—Tests H-27 and H-28 were consolidated as described under the heading "Testing Procedures" to determine the effect of the loading method used to arrive at the final principal stresses applied during consolidation. There was no significant difference between the results computed from these tests and the comparable tests of Series II which used the standard method. Considering the differences in the loading method used to consolidate the specimens it was concluded that the method of consolidation had no affect on the cohesion and friction of the kaolinite tested. However, it must be noted that the time allowed for secondary consolidation after the application of the last consolidation load increment was about the same for all tests compared.

CONCLUSIONS

The following is a summary of the conclusions in regard to non-hydrostatic consolidation and its affect on the cohesion and friction for the clays and experimental conditions of this study.

1. The anisotropic soil structure assumed to result from non-hydrostatic consolidation did not affect subsequent cohesion-strain behavior. This behavior also seems independent of the consolidation procedure when equal secondary consolidation times are used. The results suggest that cohesion is an isotropic property in the two platey clay mineral soils tested.
2. The value of friction at zero CFS-test strain, after approximately equal consolidation conditions, is increased by an increase of consolidation stress ratio, $(\bar{\sigma}_1/\bar{\sigma}_3)_c$. However, the variation of friction with strain is similar to that of a hydrostatically consolidated specimen.
3. During non-hydrostatic consolidation the deviator stress is carried at first by cohesion and friction but cohesion reduces and eventually drops to zero if the soil has adequate friction capability.

ACKNOWLEDGMENTS

The writers are pleased to thank the Engineering Sciences Division of the National Science Foundation, the Engineering and Industrial Experiment Station and the Graduate School of the University of Florida for their financial support of this research. F. E. Richart, Jr., F. ASCE, and W. H. Zimpfer, M. ASCE,

of the Civil Engineering Department of the University of Florida contributed thoughtful reviews of the original manuscript.

APPENDIX.—NOTATION

The following symbols have been adopted for use in the paper.

c_ϵ = cohesion at strain ϵ;

e = void ratio;

G = specific gravity of soil solids;

h_i = initial extruded height of specimen (Fig. 3);

h_{CFS} = specimen height during CFS-test (Fig. 3);

$(h_0)_a$ = specimen height after non-hydrostatic consolidation; start of CFS-test (Fig. 3);

$(h_0)_h$ = specimen height after hydrostatic consolidation (Fig. 3);

S = degree of saturation;

u = excess hydrostatic pore water pressure;

ϵ = axial compressive strain (Fig. 3);

ϵ_a = axial compressive strain during non-hydrostatic consolidation (Fig. 3);

ϵ_{CFS} = axial compressive strain due to CFS-test (Fig. 3);

μ = micron, 0.001 mm;

$\overline{\sigma}$ = effective normal stress;

σ_1 = major principal stress (horizontal plane);

$\overline{\sigma}_1$ = effective major principal stress;

$(\overline{\sigma}_1)_c$ = effective major principal stress developed during consolidation;

$(\overline{\sigma}_1)_{high}$ = higher valued $\overline{\sigma}_1$ curve during CFS-test (Fig. 1);

$(\overline{\sigma}_1)_{low}$ = lower valued $\overline{\sigma}_1$ curve during CFS-test (Fig. 1);

σ_3 = minor principal stress (vertical plane);

$\overline{\sigma}_3$ = effective minor principal stress;

$(\overline{\sigma}_3)_c$ = effective minor principal stress developed during consolidation;

$\left(\frac{\overline{\sigma}_1}{\overline{\sigma}_3}\right)_c$ = consolidation stress ratio, effective after primary consolidation;

σ_a = deviator stress = $(\sigma_1 - \sigma_3)$, applied through vertical piston;

σ_h = hydrostatic stress in triaxial cell;

$\bar{T}$ = shear stress;

$\bar{T}_\phi$ = shear stress on plane of maximum stress obliquity for frictional component of strength;

ϕ_0 = angle of internal friction developed at start of CFS-test $\left(\epsilon_{CFS} = 0\right)$; and

ϕ_ϵ = angle of internal friction at strain ϵ.

Journal of the
SOIL MECHANICS AND FOUNDATIONS DIVISION
Proceedings of the American Society of Civil Engineers

SECONDARY COMPRESSION OF CLAYS

By K. Y. Lo[1]

SYNOPSIS

Results of long term consolidation tests on five remolded and two undisturbed clays are reported. Most of the experiments were run until final settlements were attained. Basing on the present and past experimental evidences, the settlement-time curves of secondary compression can be classified into three types according to their characteristic behaviors. Briefly, for Type I curve, the rate of secondary compression gradually decreases with time; in Type II curve, the rate is proportional to the logarithm of time for a considerable range of time, then rapidly decreases, and for Type III curve, the rate increases with time, then gradually vanishes. All experimental curves fall into one of these categories.

The test results were analyzed in the light of a theory previously published. It was found that this theory is adequate for clays behaving according to curves Type I and II. For Type III curve, however, significant deviations of the predicted curve by this theory from the observed curve was noted. An extension of the theory was made and c mparison of the theoretical and experimental curves shows that the modified theory is satisfactory for this special case. As a result, all the observed phenomena can be accounted.

Observations on the entirely different and distinct behaviors between samples in the undisturbed and remolded state are described. Data for the relevant soil parameters, in particular the ratio of secondary to primary compressibility and the rate factor, together with their variations with water content and applied pressure are given.

Note.—Discussion open until January 1, 1962. To extend the closing date one month, a written request must be filed with the Executive Secretary, ASCE. This paper is part of the copyrighted Journal of the Soil Mechanics and Foundations Division, Proceedings of the American Society of Civil Engineers, Vol. 87, No. SM 4, August, 1961.

[1] Civil Engr., Norwegian Geotechnical Inst., Blindern - Oslo, Norway.

Environmental factors which have predominant influence on the accuracy of experimental results are studied.

INTRODUCTION

One of the subjects which arouse much controversy in the field of Soil Mechanics is secondary consolidation. (The term secondary consolidation is open to objections. As the compression proceeds under non-measureable excess pore pressure, the process can hardly be designated as consolidation. Other terms like secondary time effects and secular effects have been used. It appears, however, that the term secondary consolidation is not frequently used in the literature and will therefore be adopted indiscriminately in this paper as synonymous to secondary compression.) While for some clays oedometer tests have shown that secondary compression follows approximately a linear relationship when plotted against the logarithm of time,[2] deviations from Buisman's Law have been noted. In Mexico City Clay, for example, some experimental settlement-time curves exhibit a tendency for the compression to increase with the logarithm of time within the duration of the experiments.[3] For two remoulded clays, a Residual and a Glacial Silty Clay, the settlement curves reported by G. A. Leonards, M. ASCE, and B. K. Ramiah, M. ASCE, show[4] a distinct nonlinearity and approach horizontal asymptotes. The apparent confusion arises mainly from the lack of a simple and rational theory on which delineation of observations may be based, the extreme susceptibility of secondary consolidation to environmental changes, (particularly temperature). Also apparent is the fact that the tests on secondary consolidation have generally not been conducted to the stage of final equilibrium when no more compression occurs.

The literature on secondary consolidation is extensive. A brief review has been included in an earlier publication.[5] Of the theoretical treatments, the works of T. K. Tan[6] and M. A. Biot[7] appear to be most significant. These theories are, however, mathematically so complicated that the soil parameters involved cannot be conveniently determined, thereby both their experimental verification and practical application are hindered. A theory based on the assumption that the soil structure behaves as a rheological model has been developed.[5] The model used was originally presented by Tan and the theory may be shown to be a special case of the general theory of Biot. The advantages and disadvantages of the present theory will be evident as the analysis proceeds.

2 "Results of Long Duration Settlement Tests," by A. S. K. Buisman, Proceedings, First Internatl. Conf. on Soil Mechanics and Foundation Engrg., Vol. 1, 1936.

3 "Consolidation of Mexico City Volcanic Clay," by L. Zeevaert, Conf. on Soils for Engrg. Purposes, ASTM, STP, No. 232, 1958.

4 "Time Effects in the Consolidation of Clays," by G. A. Leonards and B. K. Ramiah, Symposium on Time Rate of Loading in Testing Soils, ASTM, Special Tech. Pub. No. 254, 1960.

5 "A Theory of Consolidation of Soils Exhibiting Secondary Compression," by R. E. Gibson and K. Y. Lo, Acta Polytechnica Scandinavica, 296/1961, Ci 10.

6 "Secondary Time Effects on Consolidation of Clays," by T. K. Tan, Publ. Acad. Sinica, 1957.

7 "Theory of Deformation of a Porous Viscoelastic Anisotropic Solid," by M. A. Biot, Journal of Applied Physics, Vol. 27, No. 5, 1956, p. 459.

The results of long term tests on five remolded clays and two undisturbed clays are reported herein. These data are analyzed in the light of the proposed theory which was found applicable to most of the clays tested. An extension of the theory is also made to include the rather unusual behavior of some clays revealed in the tests. Consequently it was found possible to describe the time-settlement relation of all the clays tested by a generalization of the model mentioned, with additional parameters also determinable from simple oedometer tests.

Notations.—The letter symbols used in this paper are defined where they first appear, in the illustration or in the text, and are arranged alphabetically, for convenience of reference, in the Appendix.

RECAPITULATION OF THEORY

For the sake of completeness and understanding of the method of analysis of test results, the basic ideas of the theory previously presented[5] will be briefly presented. For full details, readers are referred to the original paper.

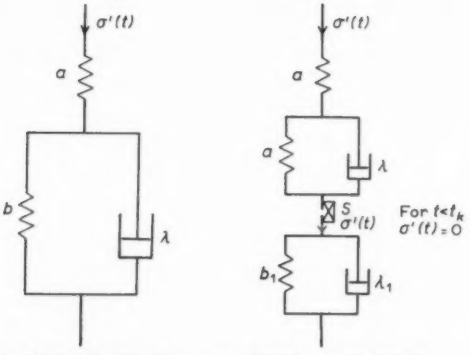

FIG. 1.—SCHEMATIC REPRESENTATION OF SECONDARY COMPRESSION

This theory is strictly one-dimensional, that is, motion of fluid and soil skeleton occur in one direction only. The assumptions involved in Terzaghi's theory of consolidation are retained with the exception that the soil skeleton is assumed to behave as a rheological model shown in Fig. 1(a).

When a time dependent effective stress $\sigma'(t)$ acts on the model, the Hookean spring a compresses instantaneously, but the settlement of the Kelvin element b-λ is retarded owing to the Newtonian dashpot λ. Due to the low permeability of clays, the effective stress $\sigma'(t)$ increases gradually with time from zero to the full value of the applied stress. Hence the compression of spring a is also gradual and is fully accomplished only when the applied stress has become fully effective.

Under the gradually increasing effective stress, the Kelvin body commences to compress. Initially the full load is taken by the Newtonian dashpot λ and is progressively transferred to the Hookean spring b as compression proceeds. This phenomenon of transference corresponds to the process of secondary consolidation occurring under sustained effective stress. After a long time has elapsed, the full effective stress will be taken by a and b, the dashpot λ sustaining no load. It is also clear, therefore, that secondary compression is present during the range of primary consolidation.

Through the model, an intrinsic time dependence of the effective stress-strain relation has been introduced. The consolidation phenomenon thus consists of two time-dependent porcesses such as the dissipation of pore water pressure and the creep of the soil skeleton under sustained effective stress. The effective stress-strain relationship can be expressed in the form

$$e = a\,\sigma'(t) + \int_0^t \sigma'(\tau)\, e^{-\frac{\lambda}{b}(t-\tau)}\, d\tau \quad \ldots\ldots\ldots (1)$$

in which e is the compressive strain, a denotes the primary compressibility, b refers to the secondary compressibility, $1/\lambda$ is the viscosity of the soil structure, t becomes the time after application of load, and τ represents a dummy variable.

If the continuity of flow of water through an element of soil is considered, then it can be shown that for small strains

$$\frac{k}{\gamma_w}\frac{\partial^2 \sigma'}{\partial z^2} = \frac{\partial e}{\partial t} \quad \ldots\ldots\ldots\ldots\ldots\ldots (2)$$

in which z is the space variable.

Eqs. 1 and 2, together with the appropriate initial and boundary conditions, define mathematically and one-dimensional problem completely.

The classical problem considered by K. Terzaghi, Hon. M. ASCE, is[8] a finite layer of clay subjected to a surface loading of infinite extent. The pressure is instantaneously applied and maintained constant thereafter. A complete solution through the use of integral transform method has been obtained for this problem considering secondary consolidation. The initial and boundary conditions for this problem are identical with those in the oedometer. This paper is only concerned with the verification of the basic assumption made in the theory and the evaluation of the soil parameters involved from laboratory results so that only the following asymptotic solution for large values of time is required.

$$e(t) = \Delta\sigma \left[a + b\left(1 - e^{-\frac{\lambda}{b}t}\right)\right], \quad t \geq t_a \quad \ldots\ldots\ldots (3)$$

in which $\Delta\sigma$ is the pressure increment and other symbols have been previously defined. Eq. 3 is only valid after an elapsed time t_a, at which the applied stress has become fully effective. Its usefulness lies in its sake for the purposes

8 "Die Berechnung der Durchlässigkeitsziffer des Tones aus dem Verlauf der hydrodynamischen Spannungserscheinungen," by K. Terzaghi, Akad, Wiss. Wien Abt. IIa, Vol. 132, 1923.

previously stated. To analyze the entire consolidation process, the complete solution given in another paper[5] has to be used.

METHOD OF ANALYSIS

On the basis of Eq. 3, two methods of determining the parameters a, b, and $1/\lambda$ have been developed and are used hereafter in the analysis of the test results. In the first method, a plot of $\log_{10} \frac{e(\infty) - e(t)}{\Delta\sigma}$, in which $e(\infty)$ is the final strain, against t furnishes all information about the parameters, but requires the value of final settlement to be obtained or estimated. The second method uses a plot of $\log_{10} (\delta_2 - \delta_1)$ against t_1, in which δ_2 and δ_1 are the settlements at times t_2 and t_1, respectively, the interval $\Delta t = t_2 - t_1$ being kept constant at any convenient value. This method can be used without resorting to final settlement, but involves the assumption that λ/b being constant during the working range.

TABLE 1.—PROPERTIES OF CLAYS TESTED

Clays tested (1)	L.L. (2)	P.L. (3)	P.L. (4)	% clay[a] $<2\mu$ (5)	No. of tests (6)	Range of water contents (7)	Range of applied stresses (8)
London Clay (brown)	75	30	45	52	10	30 - 70	0.5 - 4.0 t per sq ft
Grangemouth Clay	62	26	36	30	12	40 - 50	0.1 - 2.0 t per sq ft
Sodium Bentonite	530	120	410	>87	2	540	0.1 - 0.15 t per sq ft
Fornebu Clay, remolded	44	21	23	50	19	28 - 56	0.15 - 8.0 kg per sq cm
Fornebu Clay, undisturbed	44	21	23	50	17	26 - 47	0.15 - 8.0 kg per sq cm
Lilla Edet Clay, remolded	80	30	50	45	5	35 - 70	0.25 - 4.0 kg per sq cm
Lilla Edet Clay, undisturbed	80	30	50	45	10	50 - 100	0.25 - 4.0 kg per sq cm

[a] Dispersed with sodium hexametaphosphate.

Eq. 3 is purely a theoretical result, a consequence of our basic assumption of the validity of the model. For a clay to behave according to the theory, therefore, it requires that Eq. 3 should be satisfied within its range of validity as indicated theoretically. This, in turn requires that each of the two plots in question should give a straight line during the range of secondary consolidation, in which the excess pore water pressure has practically dissipated. The theory

is therefore conducive to direct experimental verification, and its validity and applicability easily assessed within its framework of assumptions.

EXPERIMENTAL PROCEDURE AND CLAYS TESTED

Long term oedometer tests were conducted on two British clays; remolded London Clay and Grangemouth Clay, Commercial Sodium Bentonite and on two Scandinavian Clays, Fornebu Clay and Lilla Edet Clay, both undisturbed and remolded. The index properties of the clays tested are shown in Table 1.

The geotechnical properties of London Clay have been investigated extensively.[9] The geotechnical properties of Lilla Edet Clay have been considered by L. Bjerrum and T. H. Wu,[10] M. ASCE, and the samples tested are nearly normally consolidated according to oedometer tests. The Fornebu Clay is normally consolidated and some relevant properties have been reported by Bjerrum, N. Simons and I. Torblaa.[11]

The experiments on the first three clays shown in the table were conducted while the writer was at Imperial College, using samples of 3 in. diameter and 3/4 in. thick in a brass ring. The last two clays were tested at the Norwegian Geotechnical Institute in a constant temperature room. The dimensions of the sample were 20 cm^2 in area and 2 cm high. The rings were lubricated with silicon grease to reduce side friction, and filter papers were placed on top and bottom of the sample to prevent the clay from being forced into the porous stone. In all cases drainage was permitted at both ends of the samples.

The majority of the tests was performed until ultimate settlements were reached and the temperatures recorded during the tests.

FACTORS AFFECTING THE VALIDITY OF EXPERIMENTAL RESULTS

Before proceeding to a description of the test results, it is necessary to briefly examine the factors which exert considerable influence on the accuracy of the experimental data.

Side Friction.—The effects of side friction on the consolidation behaviors of clays were investigated by D. W. Taylor who reported[12] that the total friction at the end of primary consolidation measured was less than 15% of the total applied load for undisturbed Boston Blue Clay and did not exceed 20% for the same clay in remolded state for a range of pressure up to 8 kg per sq cm. Basing on these data, T. W. van Zelst, M. ASCE, estimated[13] that the side friction is approximately 10% for a ring of 1.5-in. height and 100 sq cm^2 area. The results of their investigation led to the recommendation of the use of a ring of

9 "Tests on London Clay from Deep Borings at Paddington, Victoria and the South Bank," by A. W. Skempton and D. J. Henkel, Proceedings, Internatl. Conf. on Soil Mechanics and Foundation Engrg., London, Vol. 1, pp. 100–106.

10 "Fundamental Shear-Strength Properties of Lilla Edet Clay," by L. Bjerrum and T. H. Wu, Geotechnique, Vol. 10, No. 3, pp. 101–109.

11 "The Effect of Time on the Shear Strength of a Soft Marine Clay," by L. Bjerrum, N. Simons, and I. Torblaa, Proceedings, Brussels Conf. on Earth Pressure Problems, Vol. 1, pp. 148–158.

12 "Research on Consolidation of Clays," by D. W. Taylor, Publication Dept. of Civ. and San. Engrg., Serial, 82, 1942.

13 "An Investigation of the Factors Affecting Laboratory Consolidation of Clay," by T. W. van Zelst, Proceedings, Internatl. Conf. on Soil Mechanics and Foundation Engrg. Vol. 7, 1948, pp. 52–61.

suitable diameter to thickness ratio (perhaps 4) in order to reduce the side friction between the sample and the wall of the ring.

Measurements of side friction have been further conducted by S. Hansbo[14] and G. A. Leonards, M. ASCE, and P. Girault,[15] A. M. ASCE. For steel rings of 4-7/16 in. diameter and 1-1/2 in. untreated with lubricants, Leonards and Girault demonstrated that the friction per inch height is of the order of 17% of the applied load for undisturbed Mexico City Clay. In all tests reported herein, the brass rings were lubricated with silicon grease. It is likely that the side friction did not exceed 10% of the applied load in the majority of the tests. Because in general, the side friction increases from the start of the experiment with the effective stress to a value which remains approximately constant in the range of secondary consolidation, the actual pressure, which is the applied pressure reduced by friction, will also remain constant in this range. Provided that the side friction does not vary to any significant extent in the range of secondary compression, it will not interfere with the analyses which follow in the subsequent sections. However, it does alter the magnitude of the soil parameters computed from the test data as the side friction reduces the magnitude of the effective stress acting on the sample.

Vibration.—The effect of a sudden shock on the process of secondary compression is clearly indicated in the lowest curve on Fig. 3. (Different ordinate has been used for different settlement curves. The appropriate scale may be obtained by referring to the same symbol indicated in the curve and the scale.) The curve is displaced downwards abruptly, but retains the right shape. It was found that intermittent vibrations would disrupt the continuity of the curve and render the results useless. Any activating force is therefore undesirable during the run of the tests.

Temperature.—The most important factor which affects the experimental results on secondary consolidation is temperature variation during the tests. This influence is clearly depicted in Fig. 2. The change of temperature with time is shown in the upper part of the diagram and the close response of secondary compression to temperature fluctuations may be noted. An increase in temperature of approximately 3°C completely alters the shape and trend of the curves.

It is evident therefore, that the importance of temperature control in all tests on secondary consolidation cannot be overemphasized.

The susceptibility of secondary compression to temperature variation has an important bearing on the physical mechanism of secondary consolidation, however it is not expounded herein.

GENERAL CHARACTERISTICS OF SETTLEMENT-TIME CURVES

The number of tests performed on each clay, and the ranges of water content and applied pressure covered by the experiments are shown in Table 1. The presentation of all the results in graphical form would occupy too much space, and therefore only typical curves for each clay have been included. The settlement-time curves on a semi-logarithmic plot for the remolded clays

14 "Consolidation of Clays, with Special Reference to Influence of Vertical Sand Drains," by S. Hansbo, Proceedings, Swedish Geotechnical Inst., No. 18, 1960.

15 "A Study of the One-Dimensional Consolidation Test," by G. A. Leonards and P. Girault, 5th Internatl. Conf. on Soil Mechanics and Foundation Engrg., 1961.

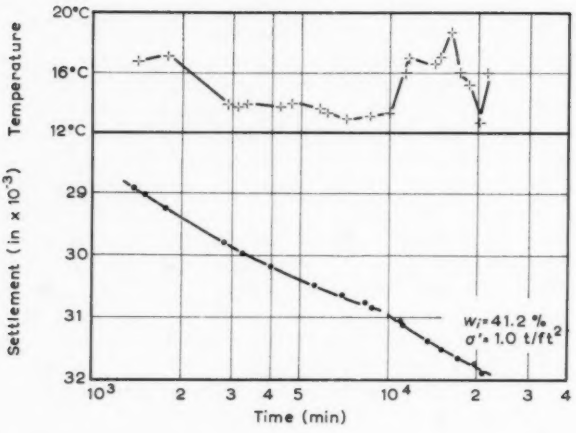

FIG. 2.—EFFECT OF TEMPERATURE ON SECONDARY CONSOLIDATION OF GRANGEMOUTH CLAY

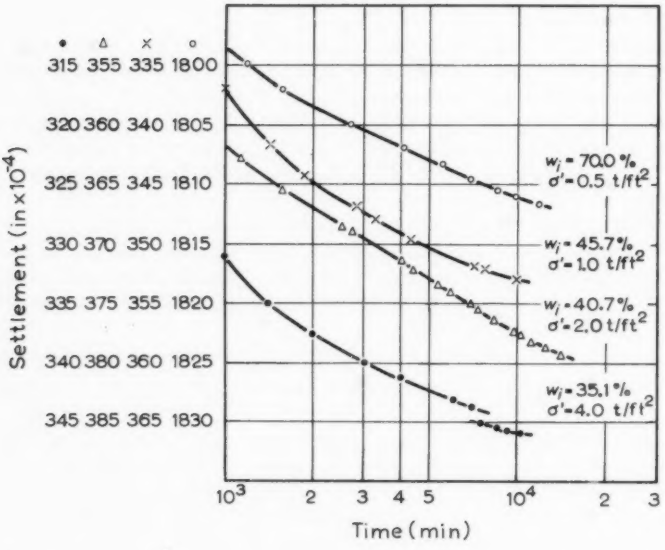

FIG. 3.—SETTLEMENT-TIME CURVES FOR REMOLDED LONDON CLAY (TEMPERATURE 20°C)

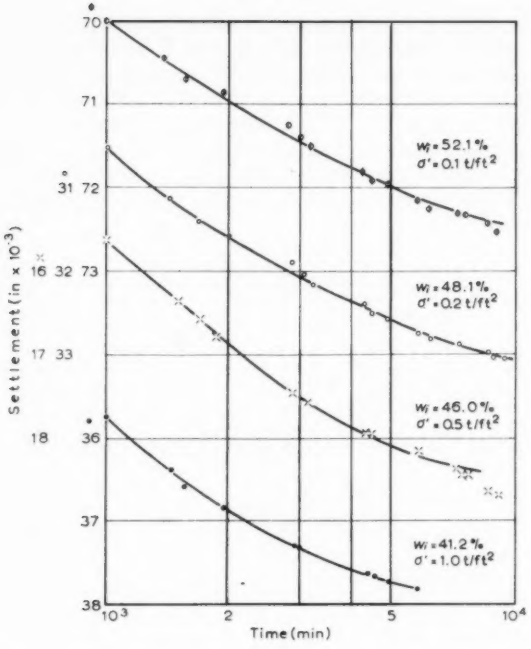

FIG. 4.—SETTLEMENT-TIME CURVES FOR REMOLDED GRANGEMOUTH CLAY (TEMPERATURE 19 °C)

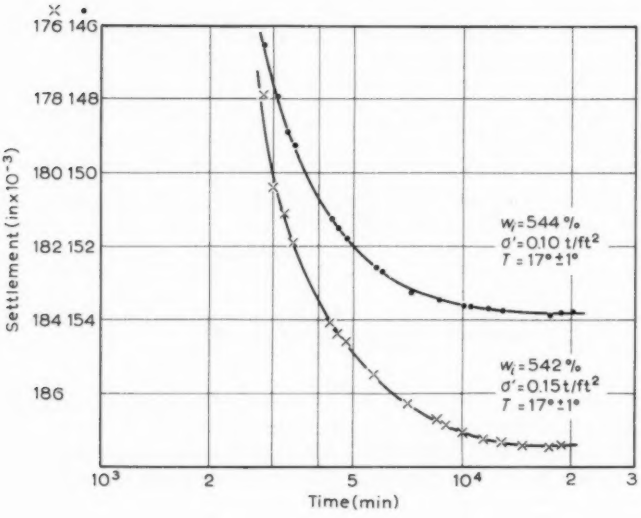

FIG. 5.—SETTLEMENT-TIME CURVES FOR SODIUM BENTONITE

are shown in Figs. 3 to 7, and those for the undisturbed clays in Figs. 8 and 9. For the settlement scale in Figs. 4, 5, 6, and 8, different ordinate has been used for different settlement curves. The appropriate scale may be obtained by referring to the same symbol indicated in the curve and the scale. In Fig. 8 the preconsolidation load p_c is approximately 0.6 kg per sq cm from e-log p curve. In Fig. 9 the secondary compression is too small to give any plot for the first two increments. For convenience, only the latter parts of the consolidation curves are presented, generally beginning with the reading taken at the

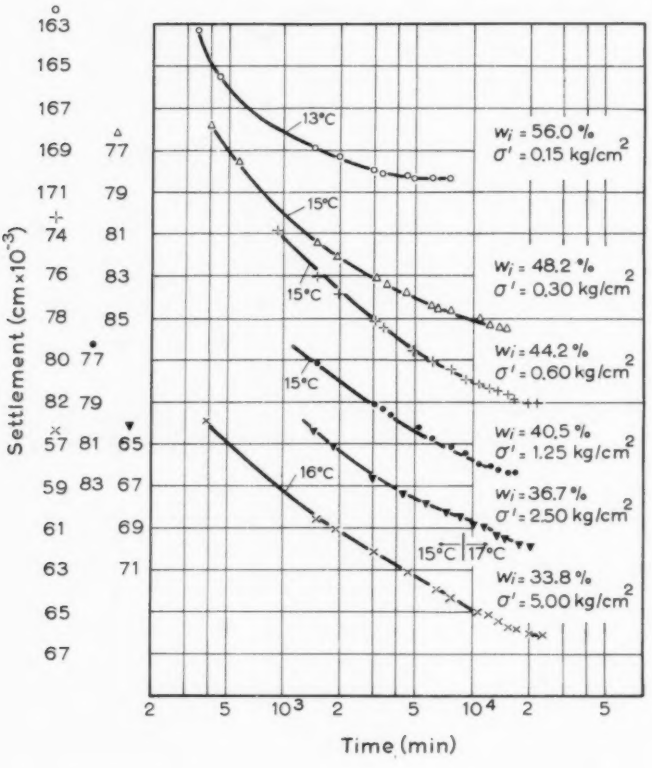

FIG. 6.—SETTLEMENT-TIME CURVES FOR REMOLDED FORNEBU CLAY (TEST SERIES II, SAMPLE NO. 3)

end of the first day. The scale for settlement has been exaggerated for the sake of clarity of presentation, and the shapes of the curves are therefore much distorted in the vertical direction. The numbers at the ordinate refer to the compression occurring under individual increments starting from zero for each loading.

In the course of investigation, the following general trends of the behavior of the secondary compression curves have been noted. For all the tests on re-

moulded clays, irrespective of the type of clay, the settlement-time curves during the secondary range have a similar shape throughout all the loading increments. With few exceptions, the ultimate settlement may be reached with-

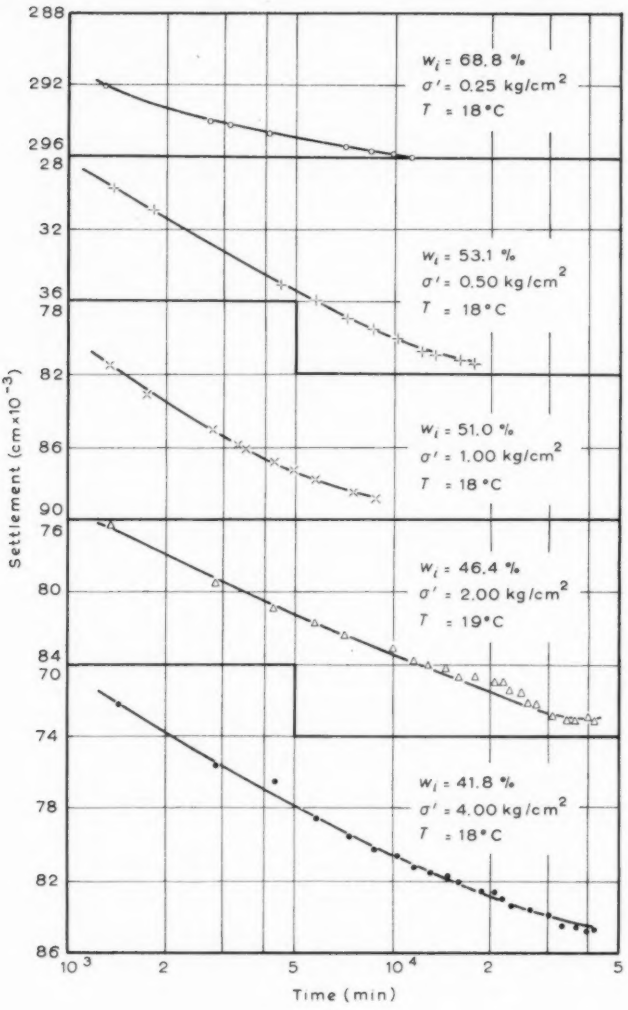

FIG. 7.—SETTLEMENT-TIME CURVE FOR REMOLDED LILLA EDET CLAY

in 3 weeks, the time required increasing slightly with the loading increments. The undisturbed samples, however, exhibit pronounced changes in the shape of the secondary compression curves for different load ranges. For pressure in-

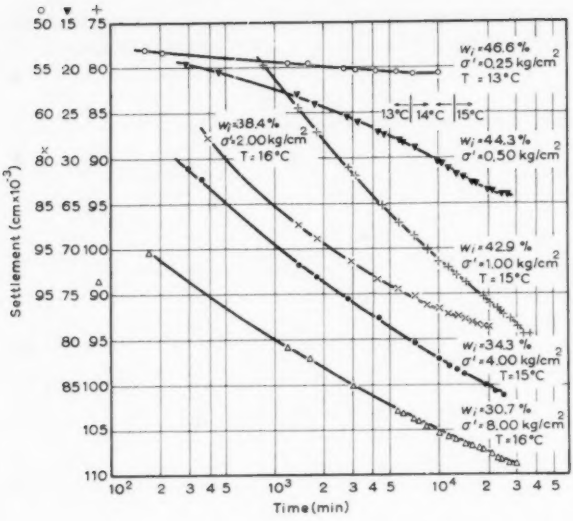

FIG. 8.—SETTLEMENT-TIME CURVE FOR UNDISTURBED FORNEBU CLAY

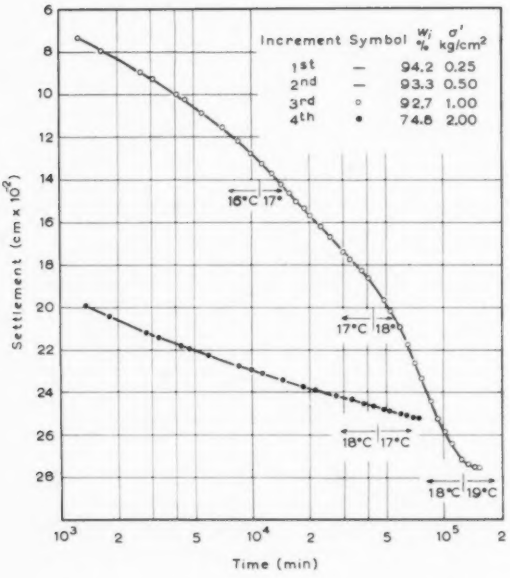

FIG. 9.—SETTLEMENT-TIME CURVES FOR UNDISTURBED LILLA EDET CLAY

crements below the preconsolidation load, the secondary time effect is small and the final settlement is reached within a period of less than a week. At pressures near the preconsolidation load, there is an abrupt change in the shape of the compression curve for the second and third increments in Figs. 8 and 9, and secondary compression becomes important. The shapes of the subsequent curves are similar to each other; some of them resemble those for the remolded clays.

TYPES OF SECONDARY CONSOLIDATION

An examination of the secondary compression curves in a settlement versus the logarithm of time plot in all the tests conducted, together with a study of

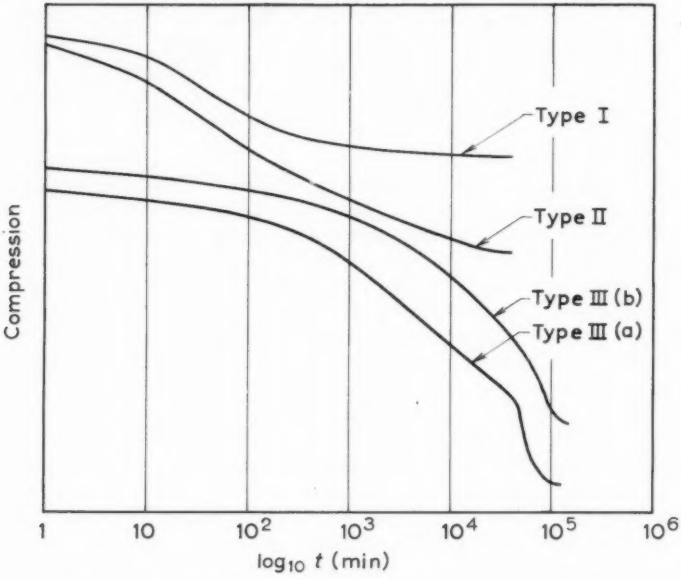

FIG. 10.—TYPES OF SECONDARY COMPRESSION CURVES

the available literature on the subject (Buisman,[2] Koppejan,[16] Zeevaert,[3] and Leonards and Ramiah[4]), indicates that there are three types of secondary compression curves which can be classified according to their characteristics as shown in Fig. 10, in which curves for the whole consolidation process are illustrated. Curve Type I has a gentle curvature concaving upwards, the rate of secondary consolidation decreasing with time and the curve becomes horizontal when the ultimate settlement is reached. The time required for this type of curve to reach final settlement is comparatively short, being of the order of 20 days or so. Most of the remolded samples of different clays and undisturbed

16 "A Formula Combining the Terzaghi Load-Compression Relationship and the Buisman Secular Time Effect," by A. W. Koppejan, Proceedings, 2nd Internatl. Conf. on Soil Mechanics and Foundation Engrg., Vol. 3, pp. 32–37.

Fornebu Clay tested fall within this group. Curves of Type II are characterized by the straight portion of the curve following approximately the logarithmic law for an appreciable range of time. The rate of compression decreases rapidly near the ultimate stage and becomes zero as the final settlement is attained. (It has been reported by R. Haefeli, M. ASCE, and W. Schaad,[17] that the compression curve continued to be straight after a testing period of 5 yr. The clay used was Kaolinite. It appears, however, that the settlement must terminate finally because the sample cannot be compressed to nothingness in the oedometer. In fact, the validity of the logarithmic law must be bounded, otherwise it would lead to the absurdity that the sample could vanish in a laterally-confined condition. Letting the settlement S equal the initial height of the sample h in Buisman's expression[2]

$$S = h_o\, p(\alpha_p + \alpha_s \log_{10})t \ ,$$

the corresponding time t' at which the sample vanishes is obtained:

$$t' = \exp.\, \alpha_s^{-1} \left(p^{-1} - \alpha_p\right)$$

which is clearly finite.)

Type III curve is concave downwards, the rate of secondary compression increases with the logarithm of time, then slows down gradually and finally vanishes. The acceleration of compression can be either gradual as in Type III(b) or abrupt as in Type III(a). Both types have been observed in undisturbed Lilla Edet Clay and examples may be found in Figs. 9 and 18(b). The ultimate settlement for this type of compression takes a long period to attain and tests have been running up to a 100 days or more to reach equilibrium.

Type I and Type II curves are those generally encountered, while Type III curve needs some special consideration.

The environmental factors which may affect secondary compression have been presented. During the tests on Lilla Edet Clay, no vibration from any accidental cause was noted. The temperatures varied but little throughout the duration of each increment, and this variance of the order of $\pm 1/2°$ C is thought to be insufficient to cause a sudden break. A comparison of these curves with Figs. 2 and 3 in which the effects of temperature and vibration are depicted gives a convincing evidence that this phenomenon must be a true behavior of the clay. Test results on remolded samples of the same clay did not show this peculiar behavior and therefore further confirms this point.

It is possible that the peculiar behavior of secondary compression as characterized by Type III curves is present only in natural deposits of a loose structure. The same phenomenon has not been observed in undisturbed Fornebu Clay, which although not quick, has a sensitivity varying from 4 to 8. On the other hand, the sensitivity of Lilla Edet Clay varies between 20 and 250. Since all remolded samples of Lilla Edet Clay and the other clays tested did not show this phenomenon, it must be a structural effect, which was developed during a time of geological scale after the deposition of the clay. This structural effect may then be destroyed in the course of remolding resulting in the absence of this phenomenon in remolded samples. It is quite likely that in the loosely de-

17 "Time Effect in Connection with Consolidation Tests," by R. Haefeli and W. Schaad, Proceedings, 2nd Internatl. Conf. on Soil Mechanics and Foundation Engrg., Vol. 3, 1948.

posited strata, the clay particles are kept in position by some form of cementation which develops into a bond by chemical processes, aided by the effect of time and overburden pressure. This loose structure is susceptible to a breakdown when a critical stress (or more likely strain) is exceeded leading to an accelerated compression. (The question which inevitably arises is: Which observed quantity governs the phenomenon of structural breakdown, the stress or strain? Experimental evidence obtained so far does not allow a definite conclusion to be drawn, but it is hoped that additional tests will clarify this point. Hereafter, therefore, we shall speak of a critical pressure loosely to mean that stress which has to be attained before this breaking of bonds can occur.) The recognition of this phenomenon has been noted by Bjerrum and Wu,[10] who reported the abrupt change in true cohesion (Hvorslev parameter) with water content at pressures near the preconsolidation load. The existence of the phenomenon of structural breakdown in other clays has been indicated by Bjerrum[18] as an implication from the low friction angle found in in-situ shear tests. It is suggested that a gradual structural breakdown would lead to a continuous curve concave downwards as shown in curve Type III(b) while a sudden breakdown would lead to curve Type III(a).

COMPARISON OF TEST RESULTS WITH THEORY

Figs. 11 to 17 show the analysis of test results of London Clay, Grangemouth Clay, Bentonite, Fornebu Clay and Lilla Edet Clay. (In Fig. 14 a different vertical scale other than that shown has been used for increment No. 3. In order not to confuse the figure, this is not shown.) These plots give the relevant soil parameters; the primary compressibility a, the secondary compressibility b, and the viscosity of the soil structure $1/\lambda$. As predicted by the theory, the curves closely approximate to straight lines at large times, while the deviations from linearity represents the hydrodynamic period of the consolidation process. It is obvious that remolded London Clay, Grangemouth Clay, Sodium Bentonite, Fornebu Clay (both remolded and undisturbed) and Lilla Edet Clay, all behave in satisfactory agreement with this theory. For each clay at some typical applied load, a theoretical curve has been worked out and compared with the observed curve (Fig. 18). (In Fig. 18(a) lines how observed curves and prints indicate corresponding theoretical computations.) The agreement for all cases are again not unreasonable, especially in view of the exaggerated settlement scale.

Undisturbed Lilla Edet Clay requires special consideration. Type III curves were observed in some loading increments for this clay, and the simple model of Fig. 1(a) is inadequate to describe the phenomenon. In the following section an extension of this model will be made which will permit analysis of the Type III behavior.

EXTENSION OF THEORY FOR TYPE III CURVE

The proposed model for describing the behavior of clays showing Type III curve characteristics is shown in Fig. 1(b). This model is a generalization of

18 "The Effective Shear Strength Parameters of Sensitive Clays," by L. Bjerrum, 5th Internatl. Conf. on Soil Mechanics and Foundation Engrg., 1961.

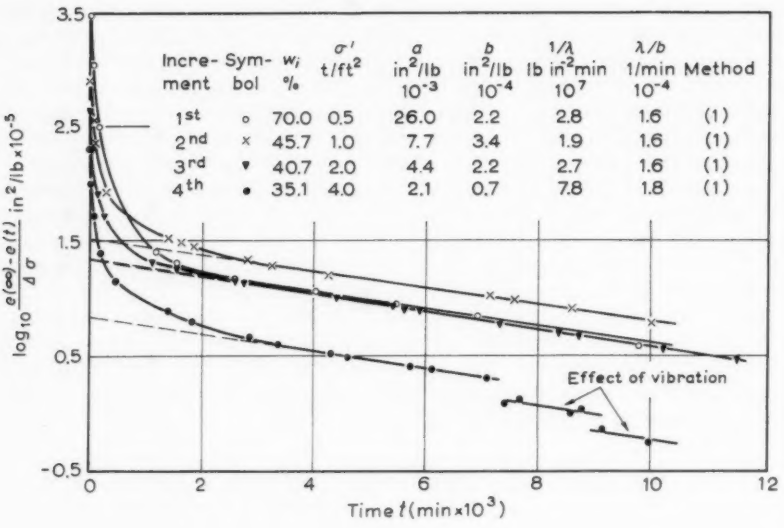

FIG. 11.—DETERMINATION OF SOIL PARAMETERS OF REMOLDED LONDON CLAY

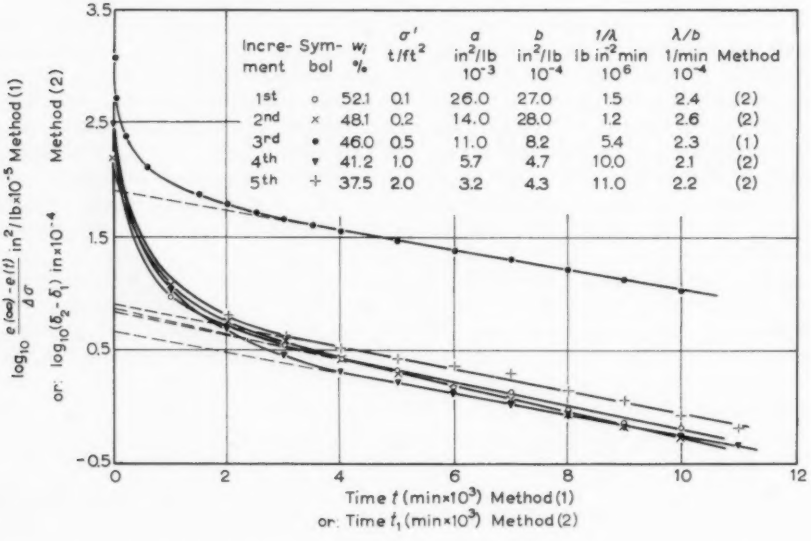

FIG. 12.—DETERMINATION OF SOIL PARAMETERS OF REMOLDED GRANGEMOUTH CLAY

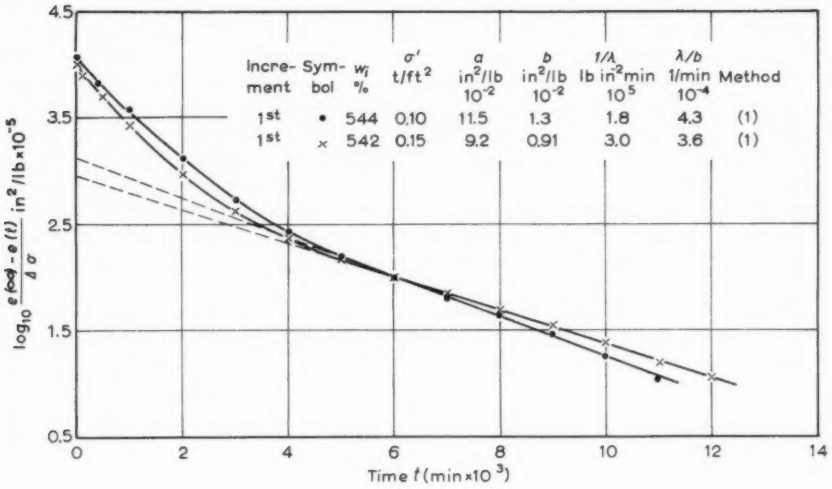

FIG. 13.—DETERMINATION OF SOIL PARAMETERS OF SODIUM BENTONITE

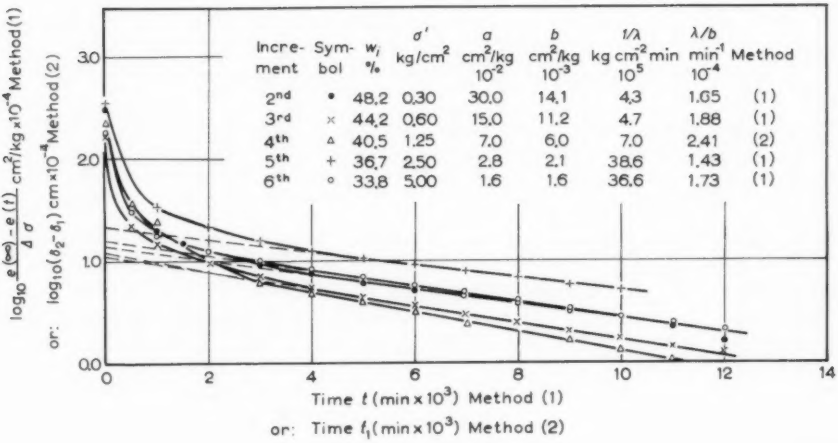

FIG. 14.—DETERMINATION OF SOIL PARAMETERS OF REMOLDED FORNEBU CLAY (TEST SERIES II, SAMPLE NO. 4)

the model of the theory previously presented.[5] To be satisfactory the model must be descriptive of the following experimental findings in undistrubed clays:

(a) No appreciable secondary consolidation occurs at pressures below the apparent preconsolidation load.

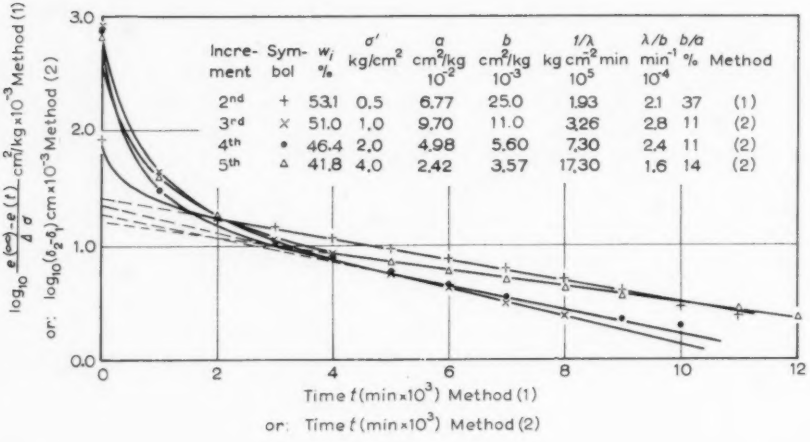

FIG. 15.—DETERMINATION OF SOIL PARAMETERS OF REMOLDED LILLA EDET CLAY

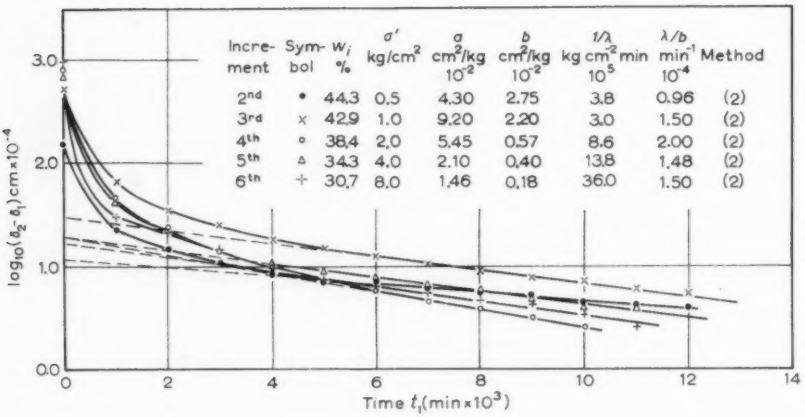

FIG. 16.—DETERMINATION OF SOIL PARAMETERS OF UNDISTRUBED FORNEBU CLAY

(b) When the applied pressure reaches a critical value, large amount of secondary compression occurs. The first stage of the secondary consolidation behaves in close agreement with Gibson and Lo's theory. Subsequently signifi-

cant deviations from the previous mentioned theory occur, the settlement being underestimated by this theory.

(c) The sample behaves in subsequent loadings according to Gibson and Lo's theory again.

The model in Fig. 1(a) has been previously described. The spring elements a and b behave according to Hooke's Law, while dashpot λ follows Newton's Law of ideal fluids, that is, the rate of strain is proportional to the acting stress. The spring a accounts for primary compression and the transference of stress from the dashpot to spring b constitutes the secondary effect. This model is coupled in series to another similar Kelvin body through an element S as shown in Fig. 1(b). The element S has the following mechanical properties: Below a certain critical value of an observed quantity such as stress (or strain), the element S is rigid and therefore sustains the stress $\sigma'(t)$ from the b-λ element, without transmitting it to the b_1 - λ_1 element. However, when this criti-

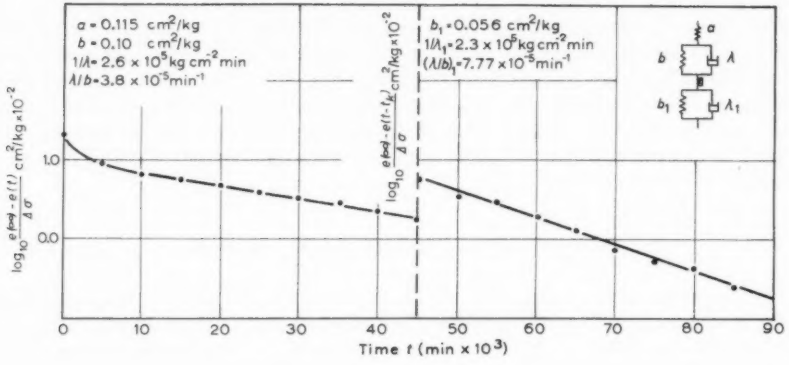

FIG. 17.—DETERMINATION OF SOIL PARAMETERS OF UNDISTURBED LILLA EDET CLAY (TEST SERIES II, SAMPLE NO. 2, 3RD INCREMENT; METHOD 1 WAS USED THROUGHOUT)

cal value is exceeded, the body S then loses its load-carrying capacity and $\sigma'(t)$ operates as well in the b_1 - λ_1 element. The strain required to transform the property of S to bring into action the additional part b_1 - λ_1 is assumed to be an infinitesmal of higher order so that the element S does not contribute to the compression of the whole model. When S is rigid, the b_1 - λ_1 element is in effect uncoupled and the consolidation proceeds according to the earlier theory. For stresses below the preconsolidation load, the fact that secondary consolidation is unimportant can be accounted for by letting the viscosity $1/\lambda$ approach infinity, and in these circumstances only the primary compressibility a contributes to the settlement. On the other hand, when structural breakdown occurs, the whole model is fully active as a result of the transformation of the bond element S. For subsequent loadings, the model of Gibson and Lo's theory applies again.

With the effective stress-strain relationship described by this model, the theory previously presented can be extended with little difficulty and the entire

process of consolidation can be accounted for. For the determination of the additional parameters b_1 and λ_1 use will be made of the asymptotic solution which may be shown to be

$$e(t) = \Delta\sigma \left[a + b\left(1 - e^{-\frac{\lambda}{b}t}\right) + b_1\left(1 - e^{-\frac{\lambda}{b_1}(t - t_k)}\right)\right] \quad t \geq t_k \quad \ldots (4)$$

in which t_k is the time at which an abrupt change in the observed settlement curve occurs. For $t_a \leq t \leq t_k$, Eq. 3 holds.

Using this procedure, the soil parameters for undisturbed Lilla Edet Clay have been computed. As an example, Fig. 17 shows a typical plot. The plot on the left hand side gives the soil parameters before structural breakdown occurs and the one on the right hand side yields the additional soil parameters required to account for the accelerated settlement after breakdown at the time roughly 4.5 by 10^4 min after application of loading. As predicted by Eq. 4, each of these plots was expected to be a straight line within the appropriate limits. The soil parameters are of the same order of magnitude in both stages. Fig. 18(b) shows a comparison between the experimental curve with (a) Terzaghi's theory, (b) Gibson and Lo's theory and (c) the modified theory for undisturbed Lilla Edet Clay (test series I, third increment, $\sigma' = 1.2$ kg per sq cm. Points computed from Gibson and Lo's theory and the modified theory are identical before the break. The divergence of the former theory from the experimental result is evident and it is apparent that the points from the modified theory fall close to the observed curve.

VARIATION OF SOIL PARAMETERS

The characteristic behavior of soils during consolidation can according to Gibson and Lo's theory be described by two factors, the compressibility ratio b/a and the rate factor λ/b. The ratio of b/a expresses the relative importance of secondary to primary compression, and the variation of this factor with water content for remolded London Clay, Grangemouth Clay and Fornebu Clay are shown in Figs. 19(b), 20(b), and 21(b), respectively. All three remolded clays show a slight decrease in the ratio of secondary to primary compressibility with increasing water content. Both for Grangemouth and Fornebu Clay the compressibility factor is of the order of 0,1 and for London Clay 0,05. For Lilla Edet Clay the variation of this parameter is more erratic, but the ratio is of the order of 0,15. Throughout the ranges of water content and applied pressures used in the experiments, it may be concluded that the fluctuations in magnitude of this factor are not significant for remolded clays.

The behavior of undisturbed samples are, however, distinctly different. For Fornebu Clay Fig. 22(b) shows a rapid rise in the b/a ratio for water contents approaching that corresponding to the preconsolidation load which is a result of sampling for this normally consolidated clay. At pressures above the preconsolidation load, the compressibility factor can be ragarded as a constant while for pressures below the preconsolidation load, secondary consolidation is so small that the secondary compressibility cannot be evaluated. A comparison of the compressibility factor in the undisturbed and remolded state indicates clearly that secondary consolidation is much more pronounced in the undisturbed state; the compressibility factor being twice or more and may rise

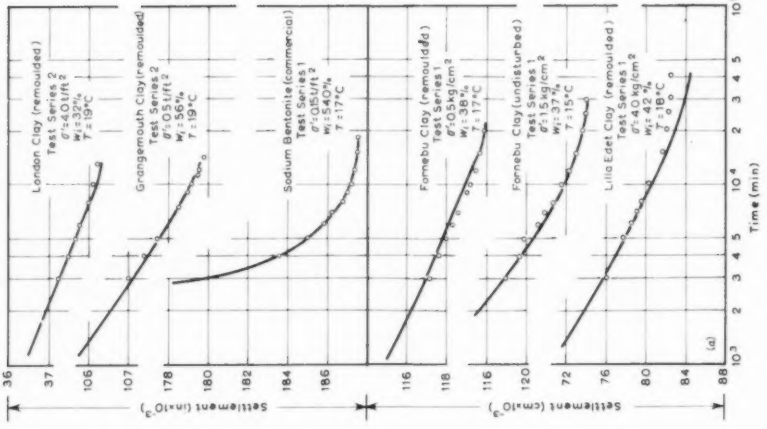

FIG. 18.—COMPARISON OF THEORETICAL AND EXPERIMENTAL CURVES

up to as much as 0,3 for Fornebu Clay. The same general trend of behavior is exhibited by Lilla Edet Clay, but with a much higher b/a ratio, ranging from

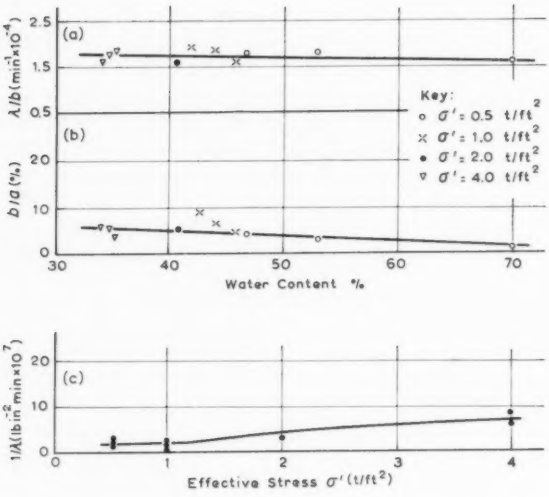

FIG. 19.—VARIATION OF SOIL PARAMETERS OF REMOLDED LONDON CLAY

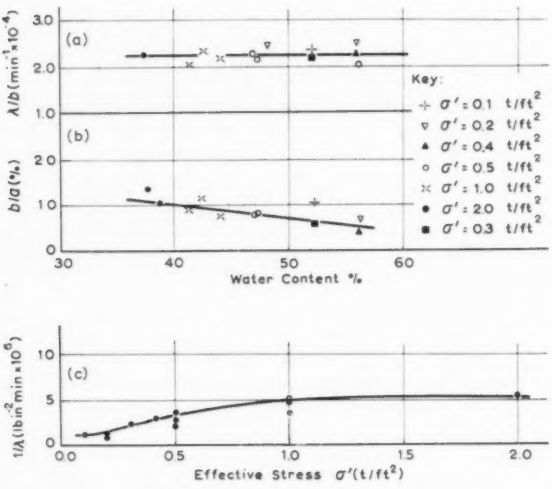

FIG. 20.—VARIATION OF SOIL PARAMETERS OF REMOLDED GRANGMOUTH CLAY

1,4 to 1,6, at pressures within a small range exceeding the preconsolidation loads. Thus in this clay the secondary settlement constitutes more than 60%

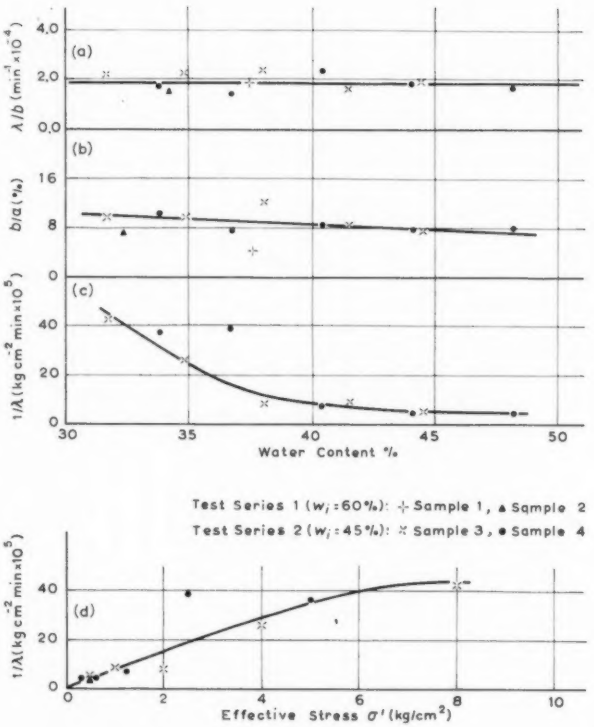

FIG. 21.—VARIATION OF SOIL PARAMETERS OF REMOLDED FORNEBU CLAY

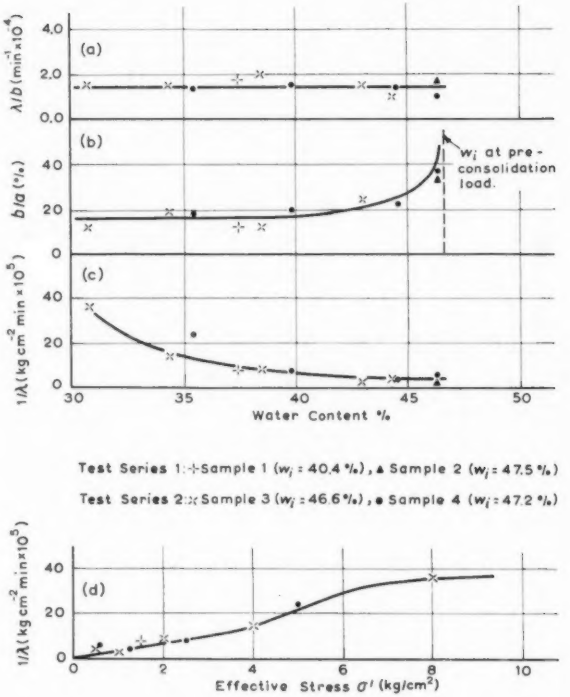

FIG. 22.—VARIATION OF SOIL PARAMETERS OF UNDISTURBED FORNEBU CLAY

of the ultimate compression. For pressures beyond this, the compressibility factor reduces to approximately 0,2 to 0,3.

The combination of parameters which governs the rate of secondary consolidation is the factor λ/b, as indicated in Eq. 3. The variation of λ/b with water content for London Clay, Grangemouth Clay and remolded and undisturbed Fornebu Clay are shown in Fig. 19(a), 20(a), 21(a), and 22(a). It is both interesting and surprising (and indeed fortunate) that there is little change in the λ/b ratio for each remolded and undisturbed clay. The value of this ratio for undisturbed Fornebu Clay is 1,4 by 10^{-4} 1 per min, while that for the remolded samples is 1,9 by 10^{-4} 1 per min indicating that the remolded samples will take less time to reach the equilibrium state.

The peculiar behavior of Lilla Edet Clay requires two rate factors to describe the process of secondary compression at pressures slightly larger than the preconsolidation load. No general conclusion can be drawn from the data at present available, nevertheless some idea of the magnitude of the rate factor may be obtained in Fig. 17. In the remolded state, the rate factor of Lilla Edet Clay varies in the range 1,6 - 2,8 by 10^{-4} 1 per min.

A knowledge of the compressibility factor and rate factor will not only enable us to have a general appreciation of the behavior of the clay during consolidation, but is also essential in the prediction of the time rate of settlement in field cases. A brief analysis on the application of the theory has been given previously.

The variation of the viscosity of the soil structure of the clays are shown in Figs. 19(c), 20(c), 21(c) and (d), and 22(c) and (d). The tendency for the viscosity to increase with increasing load and decreasing water content may be noted.

CONCLUSIONS

A study of the published data together with the experimental evidence obtained from five remolded and two undisturbed clays presented herein indicates that secondary compression curves can be classified into three types according to their characteristic shapes in a logarithm of time plot:

(a) Type I curve shows a gradual decrease of the rate of secondary consolidation until it finally reaches ultimate settlement.

(b) Type II curve is characterized by the proportionality of secondary compression with the logarithm of time for an appreciable range of time before the final settlement is reached.

(c) Type III curve shows an acceleration of the rate of secondary consolidation. This can be either gradual or abrupt. This phenomenon is believed to be due to the breakage of bond between the particles and occurs in loosely deposited soils. The rate, however, decreases at large times and becomes zero at the ultimate stage.

With the environmental factors well controlled, it has been shown by the experiments described that final settlement can be reached within practically attainable time for all three types of secondary compression. Analysis of curves Type I and II led to the conclusion that the clays behave satisfactorily according to a theory of one-dimensional consolidation considering secondary consolidation.[5] An extension of this theory is made, and the behavior of soils

according to Type III curve can be adequately described by the modified theory. Therefore, it is possible to analyze all three different types of curves of secondary compression. Additional parameters required to describe the soil behavior can be directly and easily determined by the methods developed. It has been found that most of the tests on remolded clays showed a secondary compression curve of Type I. The undisturbed samples may fall into any one of the three categories and exhibit marked variation in secondary compression both with respect to magnitude and rate depending on the applied pressure and the stress history. These phenomena can best be described by the two ratios b/a and λ/b.

The factor b/a is the ratio of secondary to primary compressibility and is a measure of the relative importance of compression due to pore water dissipation and that due to creep or breakdown of soil structure under sustained effective stress. A slight decrease of b/a with increasing water content has been found for remolded London, Grangemouth, and Fornebu Clay.

Tests on undisturbed samples of Fornebu and Lilla Edet Clay showed, however, that secondary compression is much more important in the in-situ condition. For pressures below the preconsolidation load, secondary compression is practically negligible. Within a small range of stresses exceeding the preconsolidation pressure, secondary compression becomes important. For Fornebu Clay, it amounts to more than 30% of the primary compression and for Lilla Edet, secondary compression constitutes approximately 60% of the total settlement. At higher pressures, the b/a ratio becomes almost constant and is somewhat smaller than that obtained at pressures near the preconsolidation load. An impression of the variation of b/a with water content may be obtained from Eq. 22 for Fornebu Clay.

With Lilla Edet Clay in particular, a rather abrupt increase in the rate of settlement during secondary consolidation has been observed. This phenomenon may be explained by the breaking of bonds between the soil particles (a structural breakdown), and this appears to confirm a hypothesis put forward by Bjerrum and Wu[10] who attributed the sudden change in true cohesion near the preconsolidation pressure to the destruction of bonding.

The ratio of λ/b governs the rate of secondary compression implicitly as a parameter in an exponential function of time. For remolded London, Grangemouth, and Fornebu Clay as well as undisturbed Fornebu Clay, this ratio is essentially a constant for each clay within the range of water contents and pressures used in the tests. Data from other clays are insufficient to draw any conclusion regarding this point. This is indeed a fortunate situation as it avoids the mathematical difficulty involved with nonlinearity. A comparison of undisturbed and remolded Fornebu Clay shows, however, that the λ/b ratio is smaller in the undisturbed state, indicating that the ultimate settlement requires longer time to complete in the undisturbed state.

The preceding conclusions are valid within the frame work of one dimensional consolidation. In applying the test results to practical cases, due consideration must be paid to field conditions. Special attention is drawn to the fact that, presented elsewhere,[5] the time rate of settlement involving secondary compression is not related by the ratio of squares of thickness and for treatment of the entire consolidation process, the complete solution has to be used.

Finally, it must be emphasized that variation in temperature has a predominant influence on both the rate and magnitude of secondary consolidation. For investigations on secondary compression, therefore, this environmental factor

must be controlled. Further study of the temperature effect would also probably lead to a better understanding of the mechanism of secondary consolidation. Reliable measurements of pore pressure during the entire process of compression are required to give a still more stringent test of the theory.

ACKNOWLEDGMENTS

The experiments on London Clay, Grangemouth Clay, and Bentonite were conducted while the writer was at the Soil Mechanics Laboratory, Imperial College, University of London. Those on Fornebu and Lilla Edet Clay were performed at the Norwegian Geotechnical Institute. The writer expresses his gratitude to the authorities concerned for permission to publish this work. Helpful analyses from R. F. Gibson of Imperial College are gratefully acknowledged. R. Kirkedam, the writer's colleague at the Norwegian Geotechnical Institute, has rendered valuable assistance in the preparation of this paper.

APPENDIX.—NOTATION

The following symbols, adopted for use in this paper, are collected herewith for reference:

a = primary compressibility, compressibility of spring a;

b = secondary compressibility, compressibility of spring b;

b_1 = compressibility of spring b_1;

$e(t)$ = strain at any time t;

$e(\infty)$ = ultimate strain;

k = permeability of soil;

t = time;

t_1 = time at which settlement δ_1 occurs;

t_2 = time at which settlement δ_2 occurs;

Δt = $t_2 - t_1$;

t_a = upper time bound of Eq. 3;

t_k = upper time bound of Eq. 4;

z = space variable;

γ_w = density of water;

δ_1 = settlement at time t_1;

δ_2 = settlement at time t_2;

σ' = vertical effective stress;

$\Delta\sigma$ = pressure increment for each loading step;

$1/\lambda$ = viscosity of dashpot λ;

$1/\lambda_1$ = viscosity of dashpot λ_1; and

τ = dummy variable of integration.

Journal of the
SOIL MECHANICS AND FOUNDATIONS DIVISION
Proceedings of the American Society of Civil Engineers

FIELD STUDY OF A CELLULAR BULKHEAD

By Ardis White,[1] M. ASCE, James A. Cheney,[2] M. ASCE,
and C. Martin Duke,[3] F. ASCE

SYNOPSIS

A detailed experimental analysis is presented of the sturctural behavior of a segment of a steel sheet pile cellular bulkhead in Long Beach Harbor, Calif. The bulkhead consists of 62-ft diam circular cells with connecting arcs and retains a 55-ft height of fine silty sand hydraulic fill. Measurements were made, beginning during construction and extending more than 4 yr, of sheet pile strains and deflections, pore water pressures, and soil and bulkhead movements.

The findings provide both empirical knowledge and a clearer understanding of cellular bulkhead performance. Of particular interest were the hoop tensions and associated lateral earth pressures, the consolidation phenomena, and the distortions of sheet piles and soil. Useful information was obtained about field instrumentation and the importance of certain construction procedures. The test results are provided in as full detail as feasible.

Note.—Discussion open until January 1, 1962. To extend the closing date one month, a written request must be filed with the Executive Secretary, ASCE. This paper is part of the copyrighted Journal of the Soil Mechanics Division, Proceedings of the American Society of Civil Engineers, Vol. 87, No. SM 4, August, 1961.

[1] Assoc. Prof. of Civ. Engrg., Univ. of Houston, Houston, Texas.
[2] Research Engr., Lockheed Aircraft Corp., San Jose, Calif.
[3] Prof. of Engrg., Univ. of California, Los Angeles, Calif.

INTRODUCTION

The steel sheet pile cellular bulkhead is still a young phenomenon, and while design methods have been developed[4,5] there have been to date (1961) only few attempts to obtain quantitative data on the performance of such structures in the field.[6] Such field studies have been undertaken in Japan.[7]

The behavior of soil itself as a structural material is not adequately understood, and the complex interactions between soil and steel in cellular bulkheads add greatly to the difficulty of attempting a rational design of such a structure. Laboratory and theoretical research can clarify some of the questions. Field observations, however, are necessary in order to gain empirical information for immediate use in design and to obtain an understanding of the complex interactions which occur. There are needed both sampling type field studies, involving simple measurements of the gross performance parameters on many bulkheads of differing design, and detailed field studies of particular cells in particular bulkheads. The latter study is presented herein.

Construction in 1952-1953 of the cellular bulkhead at Pier E in Long Beach Harbor, Calif., a part of the development program of that harbor,[8] afforded the opportunity for this study, and a cooperative field research program was established between the University of California and the Port of Long Beach. A pilot test was conducted at one cell. Another cell and adjacent arc of the bulkhead were fully instrumented for measurement of strains in the steel, pore pressures and settlements of the fill, and movements of the cell and arc. Observation was made of gross horizontal movement of all cells. The field measurements covered the period from July 1952 to September 1956. Previous reports appeared in the form of theses by White and Cheney.[9,10]

Pier E consists of 33 circular cells with connecting arcs on water side, as illustrated in Fig. 1. Original water depth varied from 30 ft to 50 ft at different locations along the bulkhead, as shown by the contour lines on the figure. The normal tide fluctuation has two highs and two lows per day, with a maximum annual range of approximately 8 ft. All elevations herein are referred to mean lower low water (MLLW).

Qualitative Description of Bulkhead Performance.—It will be useful herein to give a qualitative description of the structural behavior of a circular cell founded in sand. When the steel work has been completed, the cell may be thought of as a cylindrical assemblage of loosely attached sheet piles with their

---

4 "Stability and Stiffness of Cellular Cofferdams," by Karl Terzaghi, Transactions, ASCE, Vol. 110, 1945, p. 1083.

5 "Soil Mechanics," by D. P. Krynine, McGraw-Hill Book Co., New York, 1947.

6 "Shipways with Cellular Walls on a Marl Foundation," by Miller Fitzhugh and Karl Terzaghi, Transactions, ASCE, Vol. 112, November, 1947, p. 298.

7 Yasumaru Ishii, Transportation Technical Research Inst., Transp. Ministry, Kurihama, Japan (personal communication).

8 "Steel Sheetpile Cells Form Bulkhead for Long Beach Harbor Expansion," by R. R. Shoemaker, Civil Engineering, September, 1950.

9 "Field Study of a Cellular Sheet Pile Bulkhead," by Ardis White, thesis presented to the Univ. of California, at Los Angeles, in June, 1953, as partial fulfilment of the requirements for the degree of Doctor of Philosophy.

10 "Soil Behavior in a Cellular Bulkhead," by James A. Cheney, thesis presented to the University of California, at Los Angeles, in June, 1953, as partial fulfilment of the requirements for the degree of Master of Science.

lower ends embedded in sand. As pumping of hydraulic fill into the cell proceeds, the following occurs:

1. Lateral pressure of the fill deposited, and any hydrostatic excess due to water held in the cell above sea level, cause the cell to expand inelastically until the interlock slack is filled.

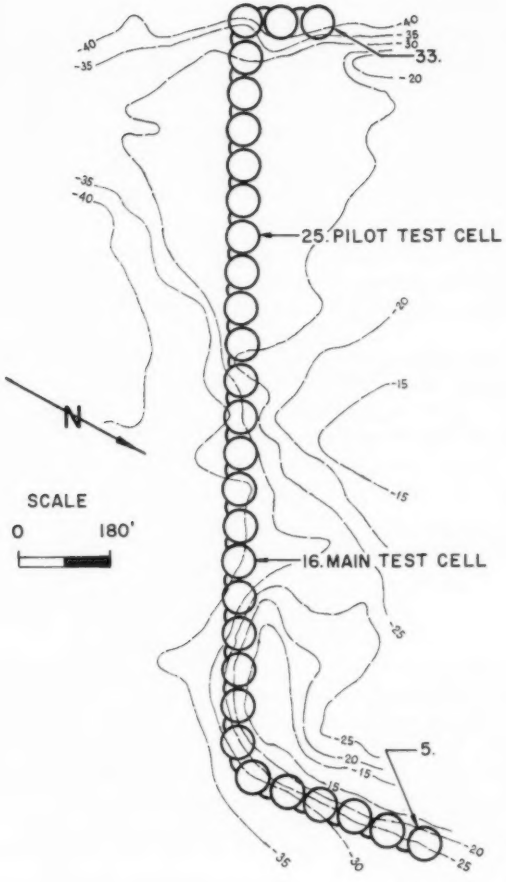

FIG. 1.—PLAN OF PIER E CELLULAR BULKHEAD

2. Weight of the fill causes an increase in outward pressure of the sand below the original bottom and the cell tends to expand at that level also until the interlock slack is filled over the full cell height.

3. As soon as the interlocks are tight, the cell ceases to be a loose assemblage of piles and becomes a more or less coherent steel cylinder. Theoreti-

cally there will then be an increment of hoop tension over most of the full height for each increment of fill placed or hydrostatic excess applied. While the hoop tension at any time will increase downward to a level in the vicinity of the natural ground, this effect probably will not be reflected in gross changes in shape of the cell because the corresponding deformations will then be largely elastic and therefore small.

4. In normal construction procedure, the cell becomes filled with water soon after pumping starts and remains full until the fill level reaches the top of the cell. Subsequently the water level falls slowly to sea level. Each increment of fill consolidates under its own weight and that of the fill placed above it, so that settlement of the lower fill is advanced by the time the last fill is placed. Essentially full settlement of a sand fill will have been accomplished before any backfill is placed behind the cell.

The cell may now be considered as a sand-steel structure possessing strength to resist horizontal loading. When fill is placed in back and on the sides, the cell will respond as follows:

1. Hoop tensions on the back and sides will be diminished slightly due to the inward pressures exerted by the backfill.
2. The cell as a whole will rotate and translate by small amounts on its base.
3. The cell will deform, with important shear stresses and strains set up on horizontal planes and on vertical planes parallel to the bulkhead centerline. Some sliding will occur at sheet pile interlocks in the side walls.
4. A surcharge placed behind the cell will aggravate the previous tendencies. Soil surcharge placed directly over the cell will aid it in resisting rotation, sliding, and distortion, and will also increase the hoop tensions.

On the basis of the filed study reported herein, an effort will be made to quantify some of the previous relationships for the particular bulkhead tested.

STRUCTURE AND MATERIALS

The construction procedure used at Pier E is illustrated approximately in Fig. 2, which is a photograph of Pier A in the same harbor. At the lower right of the figure is the king-pile support for the steel template, in the next position the template is in place, and succeeding positions show the subsequent phases of construction. The procedure at Pier E was different from that illustrated in Fig. 2 in that arcs were placed on the water side only and were placed before filling of adjacent cells.

Steel Structure.—The design features of the steel cells for the bulkhead are summarized in Fig. 3.

The sheet piles were typed SP-7a, 1/2-in. web, 76 ft long, and type SP-6a, 3/8-in. web, 69 ft long, manufactured by the Bethlehem Steel Company. The properties given by the manufacturer were:

Modulus of elasticity	29,500,000 psi
Poisson's ratio	0.28
Ultimate tensile strength	70,000 psi minimum
Yield point	38,500 psi minimum

Fig. 4 shows the method of fabrication of the T-pile between cell and arc.

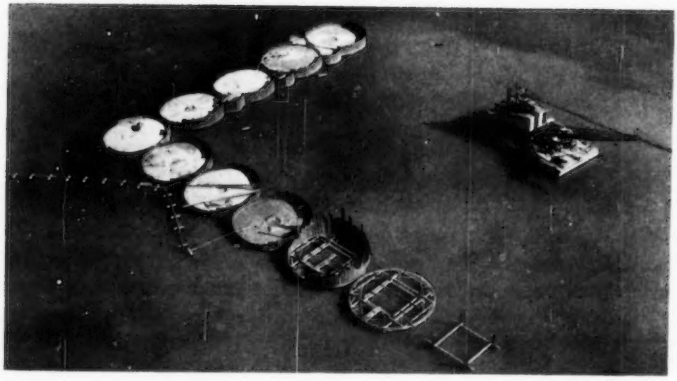

FIG. 2.—CONSTRUCTION VIEW OF TYPICAL CELLULAR BULKHEAD

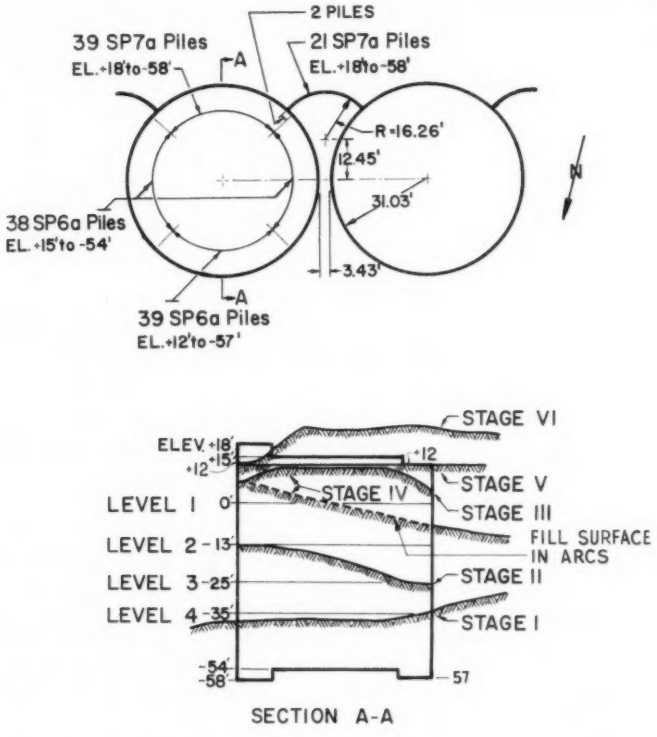

FIG. 3.—GENERAL STRUCTURAL FEATURES AND CELL 16 FILL STAGES

The test cells were built essentially in accordance with Fig. 3, but due to construction difficulties, the main test cell (Cell 16) was appreciably out of shape before any fill was placed. Details of this irregularity will be given with the test results.

Soil Characteristics.—The chronology of filling of the main test cell, together with a summary of the soil stratification and simplified soil property data (3-in. diam specimens) are given in Fig. 5. The dates on the fill profiles are for 1952. The soil below el -80, down to approximately el -110, was of essentially the same constitution as that at the higher levels. The fill in and be-

TABLE 1.—FILL STAGES, CELL 16

Stage	Date Completed	Description
I	9/8/52	Cell empty
II	9/18/52	Cell 4/10 full
III	9/27/52	Cell full
IV	10/30/52	Arcs full
V	8/22/53	Backfill up
VI	9/1/54	Surcharge on

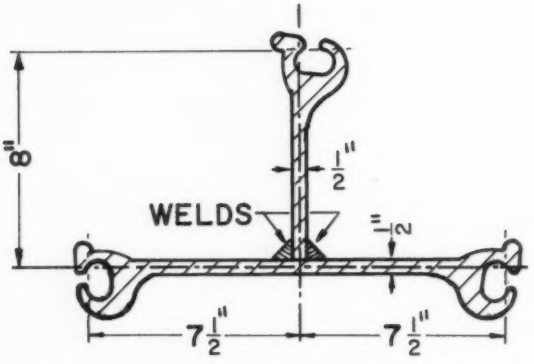

FIG. 4.—CROSS SECTION OF TYPICAL T-PILE

hind the cells was obtained by hydraulic dredging from the harbor south of the bulkhead. The fill stages shown in Fig. 3 and used as an independent variable in the presentation of test results are defined in Table 1.

Contrary to experience with the other cells, the water level in Cell 16 did not rise to the top and thus stabilize the cell during the early period of pumping, but remained essentially at sea level until September 19, 1952 (fill profile, Fig. 5). This is attributed to a rather free flow of soil and water under the northeast edge of the cell, due possibly to the low original ground level or to the jetting used in driving the test piles. On September 19, the ground level

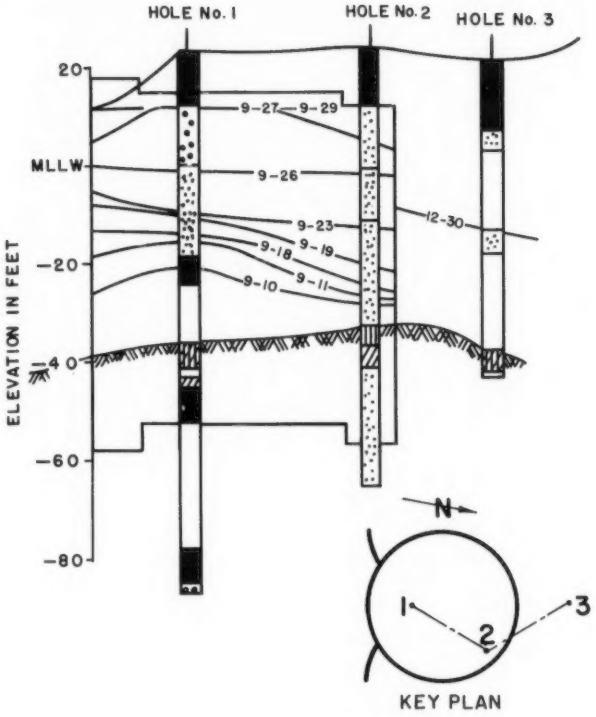

SYMBOL	DESCRIPTION [a]	UNIT DRY WEIGHT p.c.f.	COMP-RESSIVE INDEX [b]	COEF. OF PERMEABILITY cm/sec x 10^4	ANGLE OF INTERNAL FRICTION
	VERY FINE SAND	90	0.08	7.54	35°
	MEDIUM SAND	100	0.05	80.9	37°
	SILT	80	0.17	0.375	15° [c]
	CLAY	80	0.33	0.00045 *	15° [c]
	MEDIUM TO COARSE SAND	100	0.04	39.1	38°
	FINE TO MEDIUM	100	0.05	39.1	37°

[a] U.S. BUREAU OF CHEMISTRY AND SOILS GRAIN SIZE CLASSIFICATION.
[b] DECREASE IN VOID RATIO PER TENFOLD INCREASE IN PRESSURE IN COMPRESSIBILITY TEST.
[c] COHESION = 400 p.s.f.
* FROM CONSOLIDATION TEST - ALL OTHERS BY FALLING HEAD PERMEAMETER.

FIG. 5.—SUMMARY OF SOIL PROPERTIES

outside the northeast corner had risen several feet (corresponding with an effective penetration depth of approximately 30 ft) and the flow ceased, the water level came up in the cell, and the cell stabilized. It was normal procedure to pump into the cells in such a way that the fill piled up near the south face. At Cell 16, the unsymmetrical soil pressures accompanying this procedure further distorted the poorly alined cell before the interlocks became tight.

TEST PROCEDURES

The principal observational results were obtained at Cell 16, but supplementary information was gained at Cell 25 and with the bulkhead as a whole.

At Cell 25 a pilot test was conducted, with horizontal and vertical strainmeters, a driftmeter tube, and a pore-pressure settlement device. Work at Cell 25 covered the period June 1952 to March 1953, during which the cell was driven and filled and backfilled to el +4. The strainmeters were at Level 4 (Fig. 6) which, in the case of Cell 25, was 7 ft below natural ground.

Observations were made of the lateral movements of all cells.

Fig. 6 gives the locations of instruments in Cell 16. The strainmeters were mounted in pairs, one inside and one outside the cell at each location and orientation. The driftmeter tubes were used to obtain sheet pile deflections. The pore-pressure settlement devices were located at the four levels at points O through U. In addition to the measurements with the indicated instruments, observations of vertical and lateral movements were made with surveying instruments at the top of the cell.

Installation and observation at Cell 16 covered the period August 1952 to September 1956, during which the cell was driven, filled, and backfilled, a surcharge was applied, and, finally, work was done to realine the cell. Complete sets of observations were taken at approximately 10-ft intervals of fill in the cell and every 2 days or 3 days for approximately 3 weeks after completion of filling of the cell. On two occasions readings were taken at extremes of tide over a 24-hr period. Partial sets of readings were taken at decreasing frequencies up to September 1956.

Sheet pile strains and deflections were obtained on adjacent piles, one pile holding strainmeters and the other holding the square tubing for the driftmeter. Straight piles were selected for the test piles and the immediately adjacent piles to minimize irregularities in load transfer across the test piles.

Regional Subsidence.—During the test period, a general subsidence was progressing in the harbor area. The rate at Cell 16 was approximately 0.9 ft per yr and that at the reference bench mark on shore was approximately 1.1 ft per yr. The rotational effects of this subsidence were determined to have an unimportant influence on the test, and the differential settlements over the period of filling of the test cells were not significant. However, corrections for this effect were required for determining cell settlements over longer time periods.

Soundings and Tide Measurements.—Soundings and surveys were used to obtain fill surface configurations (Figs. 3 and 5) at the fill stages and at other times when instruments were read. Water levels inside and outside the cell were also recorded. Elevations were referred to a bench mark on a sheet pile at Cell 18, with periodic checks against the nearby shore station.

Soil Settlement and Pore Pressure.—The divide shown in Fig 7 was used to determine both the pore water pressure and the settlement of fill at the sev-

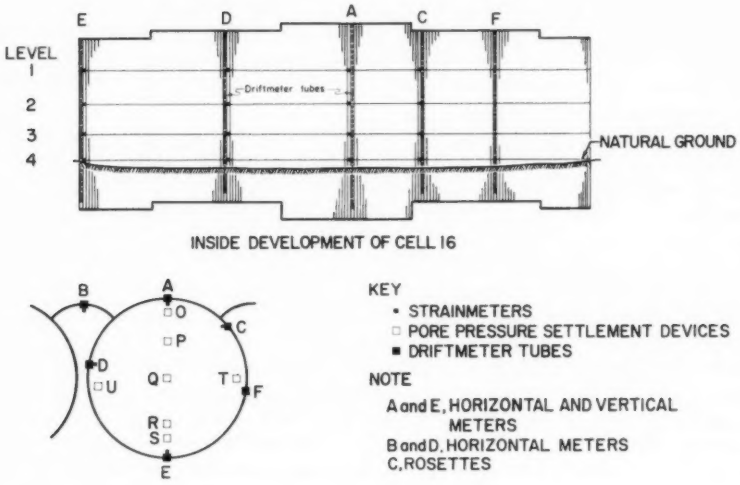

FIG. 6.—SCHEME OF INSTRUMENTATION

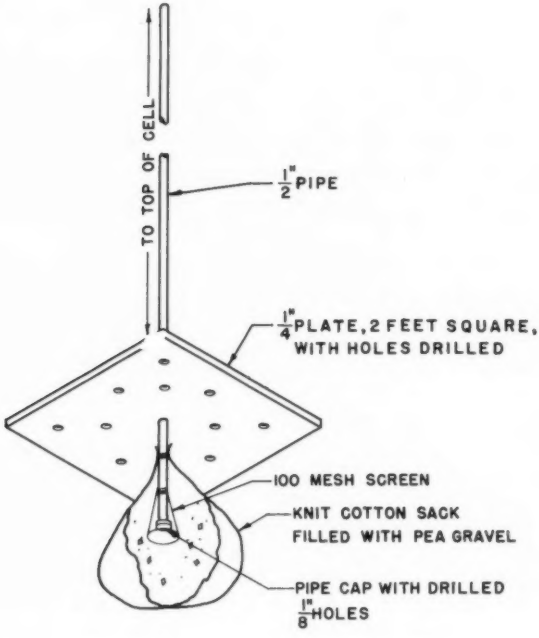

FIG. 7.—PORE PRESSURE-SETTLEMENT DEVICE

eral points at each level. The large plate was designed to cause the pipe to settle with the soil at the plane of the plate. Observations were made to 0.01 ft at the tops of the pipes with an engineer's level, utilizing the previous bench mark.

Pore water levels were obtained to 0.1 ft by means of an electric contact device lowered down the pipes.

The devices were installed as the fill reached the desired levels and were held in position temporarily by fastening them to timber piles laid across the top of the cell. When the fill had risen around the device sufficiently to support its weight, the fastening was changed to provide horizontal restraint only. Three of these devices at lower levels were lost due to large horizontal and vertical movements of the fill accompanying the early construction procedure.

Cell Deformation.—Relative horizontal deflections of points at 6-ft intervals along the length of seven piles were obtained by means of a driftmeter shown disassembled in Fig. 8.

This instrument is an oil well surveying device which gives a photographic record of the slope at any desired point within a pipe. In use, a photo-sensitive disc was placed in a special seat in the base of the driftmeter (bottom of Fig. 8), and the three small parts were assembled and screwed as a unit onto the base. A timing device was set and the three-part unit was placed in the hollow upper part of the instrument, to which the base was then screwed. The driftmeter was horizontally oriented, dropped down inside a square tube, and held at the proper depth with the steel tape. After an interval, the timing device activated a flashlight, which directed light down a hollow plumb bob onto the sensitive disc. The light burned for 1 min, causing a dark spot on the disc, the position of which indicated the two components of inclination of the driftmeter to 0.1°.

Mounting of the square tubes on the piles consisted of making up the proper lengths of 1 ¼-in. (outside dimension) sq galvanized iron tubing, using waterproof soldered joints, and fastening this tubing with welded clips to the pile. The tube was kept free of direct bond to the pile. The lower end of the tube was sealed and then protected by a short oblique section of 3-in. pipe welded to the pile. The piles with driftmeter tubes could be handled safely with a 3-point pickup, and were assembled in position in the cell and then carried to grade by jetting.

Marks were established at the tops of all instrumented piles and also at a pile in the northeast quadrant between D and E (Fig. 6). Horizontal movements of these marks were observed with surveying instruments to 0.03 ft, and vertical movements to 0.01 ft. Control of the horizontal movements was a point at the center of Cell 16, which was reestablished periodically by intersection of a line from shore and the theoretical centerline of the bulkhead. Control for the vertical movements was the previous bench mark.

The lateral movements of all cells were determined by surveys made after completion of backfilling behind the cell (March 18, 1953) and after applying surcharge (June 23, 1954).

Strains in Sheet Piles.—Carlson strainmeters were selected for the Pier E research work because of success with them in a previous research project in Long Beach Harbor.[11] They were mounted in pairs on opposite sides of a

[11] "Field Study of a Sheet Pile Bulkhead," by C. Martin Duke, Transactions, ASCE, Vol. 118, 1953, pp. 1131-1196.

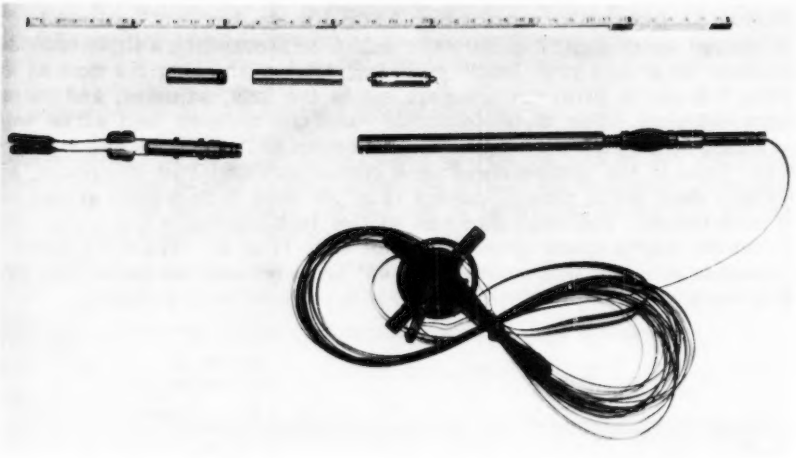

FIG. 8.—DRIFTMETER

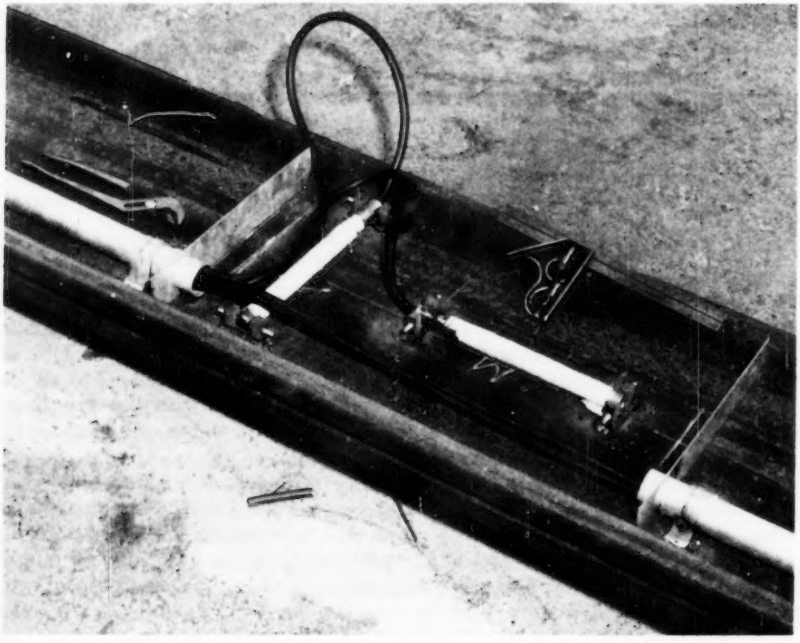

FIG. 9.—TYPICAL STRAINMETER INSTALLATION

pile to permit correction for bending strains. Fig. 9 illustrates a typical installation.

U-shaped meter lugs (Fig. 10) were welded in place using a jig to establish accurately the proper gage length of 10 in. After positioning the conduit and welding it in place, strainmeters were set in the lugs, adjusted, and the set screws tightened. The three-conductor neoprene-covered lead wires were then pulled up through the conduit for collection at the top of a pile and were labled. Ends of the strainmeters were coated with anti-rust compound, and individual sheet metal channel covers (Fig. 10) were tack-welded at one end over each meter. The final step was that of tack-welding a flat sheet metal box over the entire space between conduit ends (Fig. 9). The third meter in the rosettes at Pile C was mounted at a 45° angle between horizontal and vertical meters.

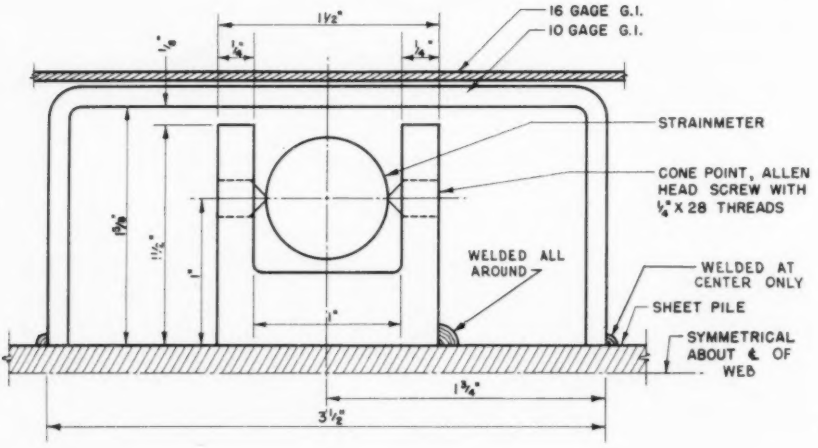

FIG. 10.—DETAIL OF STRAINMETER INSTALLATION

To prevent damage to the strainmeters while moving the piles, a timber pile was lashed to each strainmeter test pile and was kept in place until the test pile was in a vertical position ready to be placed in the cell. The timber pile was then removed, and the test pile was interlocked with the previously driven adjacent pile and was jetted to grade. The lead wires were grouped at the piles and were later extended to a central point.

Only one strainmeter or its lead wire, at Pile E, Level 3, became defective up to the time of completion of backfilling (August 22, 1953), but subsequently several lead wires were lost or destroyed due to construction operations accompanying surcharging and the later realinement of the cell. Of the meters whose lead wires were still intact in September 1956, approximately 75% were still yielding plausible readings.

Zero strain readings used in the computations were those obtained on September 8, 1952, when filling began. Since at that time the interlocks were

loose, readings at Levels 1, 2, and 3 could be made only to the nearest 40 by 10^{-6} of strain. Zero readings at Level 4, and subsequent readings at all levels were reproducible to the nearest 8 by 10^{-6}.

DATA PRESENTATION

Soil and Water Behavior.—Tables 2 and 3 present the data on soil settlement and pore pressure in Cell 16 for the various instrument locations. Also given in Table 3 are the elevations of the tide and of the free water level in the cell. These data are illustrated in Figs. 11, 12, 13, and 14.

TABLE 2.—SUMMARY OF SOIL SETTLEMENTS, CELL 16[a]

Level	Point	Stage II		Stage III			Stage IV			Stage VI
		9-9 1952	9-18 1952	9-22 1952	9-26 1952	9-29 1952	10-4 1952	10-15 1952	1-23 1953	9-2 1954
El 12	P						0.0	0.21	0.47	2.65
	Q					0.0	0.19	0.36	0.44	1.96
	R						0.0	0.21	0.27	1.14
	S						0.0	0.23	0.31	1.05
1	P				0.0	0.61	0.78	0.94	. . .	2.97
	Q				0.0	0.66	0.80	0.99	1.07	2.47
	R				0.0	0.51	0.65	0.82	. . .	2.71
	S				0.0	0.48	0.62	0.76	. . .	1.50
	T				0.0	0.29	0.38	0.52	. . .	. . .
	U				0.0	0.51	0.65	0.80	. . .	. . .
2	P			0.0	0.41	0.62	0.79	0.98	. . .	. . .
	Q			0.0	0.53	0.88	1.01	1.17	1.23	2.59
	R			0.0	0.55	0.82	0.93	1.07	1.07	1.95
	S			0.0	0.47	0.69	0.79	0.91	0.91	1.59
	T			0.0	0.35	0.47	0.55	0.67	. . .	. . .
	U			0.0	1.93	2.20	2.32	2.42	. . .	. . .
3	R	0	1.72	2.00	2.50	2.69	2.80	2.92	2.92	3.83
	S	0	-0.09	0.88	1.23	1.34	1.41	1.51	1.53	2.15
	T	0	1.27	1.48	1.65	1.72	1.77	1.88	. . .	. . .
	V	0	1.57	1.65	2.10	2.24	2.29	2.39	. . .	. . .

[a] Tabular values are in feet.

Figs. 11 and 12 show the soil settlements at the four levels during and shortly after the filling of the cell. Fig. 11 illustrates the geometrical distribution of final settlement on September 22 and October 15, 1952, and Fig. 12 shows the average time rates at Levels 1, 2, and 3 in relation to depth of fill. The dotted line in Fig. 12 is the fill-depth curve for the northeast edge where soil and water flowed under the cell in the early filling period.

Figs. 13 and 14 are typical of the pore pressure distribution at the time when filling in Cell 16 was just completed (Stage III). Fig. 13 gives the experimentally determined equipotentials at one instant, and Fig. 14 portrays the manner in which pore pressures at three levels responded to transient inside and outside water levels.

TABLE 3.—SUMMARY OF PORE WATER DATA, CELL 16[a]

Level		1					2						3				Tide
Point		P	Q	R	S	T	P	Q	R	S	T	U	R	S	T	U	Going
9-10-52	C												4.4	4.4	4.4	4.1	
Noon	P												5.0	4.8	5.6	4.2	up
	S												4.4	4.4	4.4	4.1	
Stage II	C												1.5	1.5		1.5	
9-18-52	P												1.3	2.3		1.9	down
3 PM	S												1.1	1.1		1.1	
9-22-52	C						11.2	11.2	11.2	11.2	11.2	11.2	11.2	11.2	11.2	11.2	
8 PM	P						11.2	10.4	10.9	11.0	7.1	11.5	8.9	9.4	9.5	9.4	up
	S						1.0	0.8	0.8	0.8	0.8	0.8	0.8	0.8	0.8	1.0	
Stage III	C						11.0	11.0	11.0	10.5	11.0	11.0	11.0	11.0	11.0	11.0	
9-25-52	P						10.1	7.4	9.6	9.4	7.4	10.4	8.8	8.8	8.6	8.8	up
11 AM	S						5.0	4.8	4.8	4.8	4.8	4.8	4.8	5.0	5.0	5.0	
9-27-52	C	11.3	11.3	11.3	11.3	11.3	11.3	11.3	11.3	11.3	11.3	11.3	11.3	11.3	11.3	11.3	
12 Noon	P	9.9	9.4	9.3	9.4	9.5	8.5	8.3	8.2	8.4	7.7	9.4	7.3	7.6	7.2	7.5	up
	S	4.0	4.0	4.0	4.0	4.0	4.1	4.0	4.0	4.0	4.0	4.0	4.0	3.6	3.6	4.1	
10-4-52	C	...	...	...	...	...	11.9	11.4	...	...	...	...	11.5	11.5	11.5	11.9	
11 AM	P	9.0	...	8.4	8.4	8.5	8.2	8.0	7.6	7.6	7.6	9.1	7.2	7.8	4.8	7.9	down
	S	4.6	...	4.6	4.6	4.6	4.2	4.5	4.5	4.5	4.5	4.5	4.5	4.5	4.6	4.2	
10-10-52	P	6.4	...	6.2	7.4	6.3	5.6	5.8	5.9	5.7	7.3	5.8	5.3	5.4	4.9	5.3	
	S	3.8	...	3.8	3.8	3.8	3.8	3.8	3.8	3.8	3.8	3.8	3.8	3.8	3.8	3.8	up
12-12-52	P	...	...	6.4	5.6	3.9	...	3.7	5.0	6.1	4.6	4.5	3.8	4.0	5.8	4.1	...
9 AM																	
1-9-53	P	...	...	3.6	9.1	9.5	...	...	...	...		4.0	3.1	3.2	3.1	3.3	...
12 Noon																	

[a] Tabular values are in feet, MLLW datum
C: Elevation of water surface in cell
P: Elevation of water in standpipe
S: Sea level

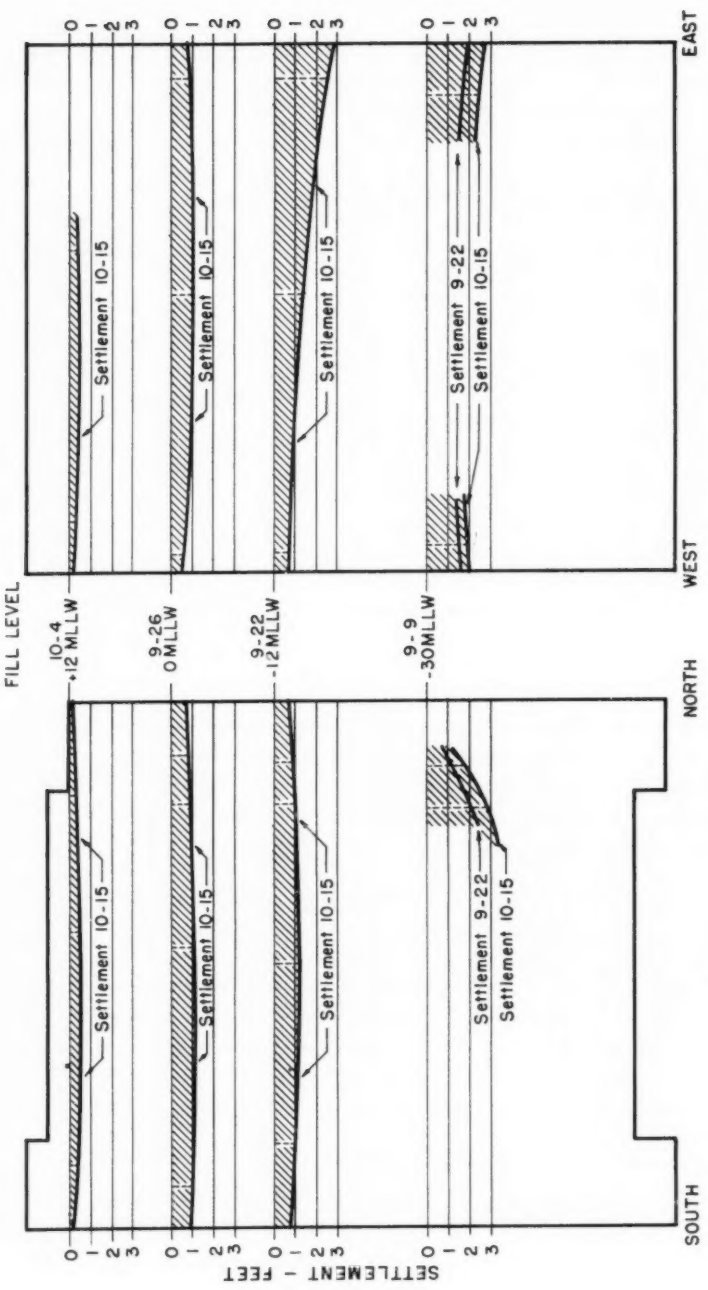

FIG. 11.—SOIL SETTLEMENT PROFILES

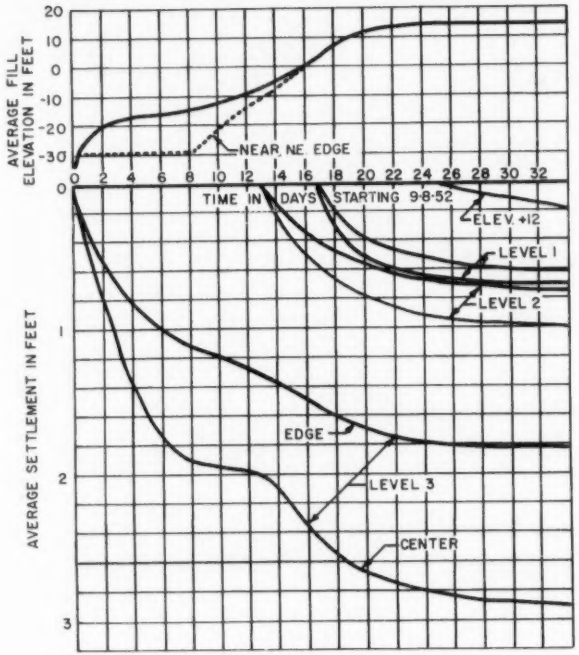

FIG. 12.—TIME-SETTLEMENT CURVES FOR FILL

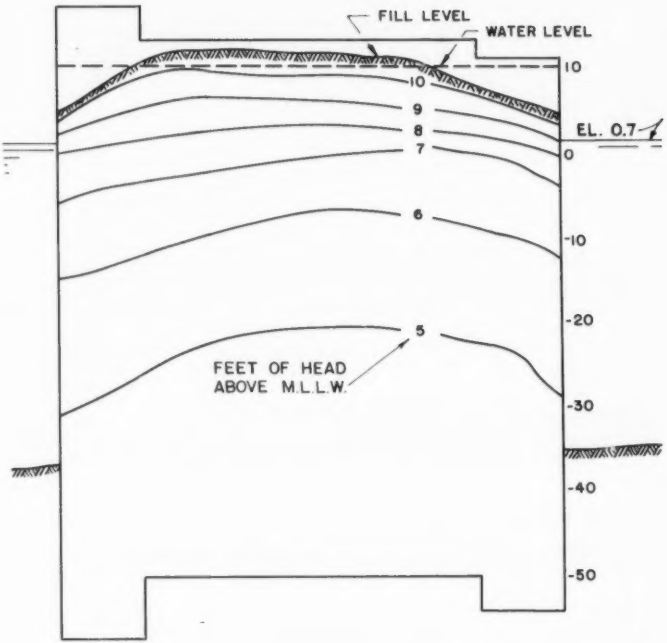

FIG. 13.—PORE PRESSURE DISTRIBUTION, SEPTEMBER 28, 1952, 1:15 P.M.

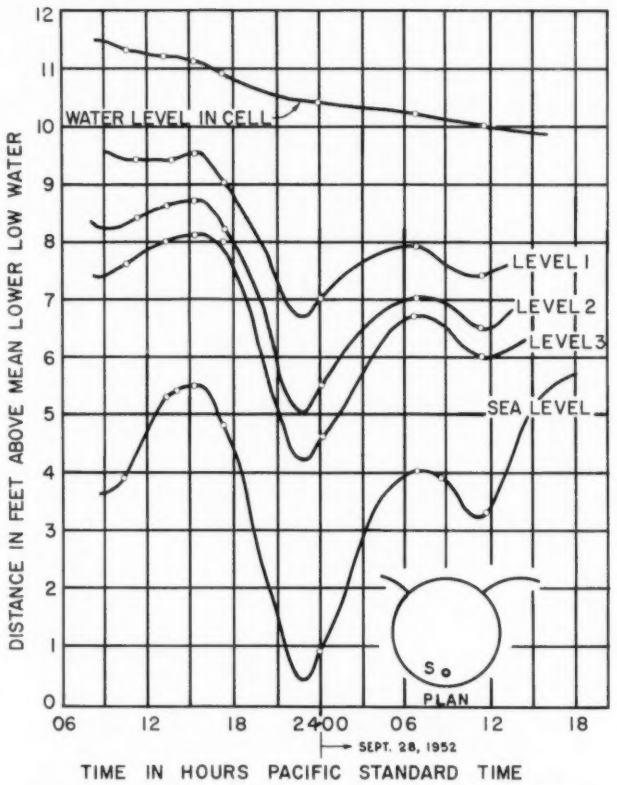

FIG. 14.—EFFECT OF TIDE ON PORE PRESSURE AT POINT S, SEPTEMBER 27, 28, 1952

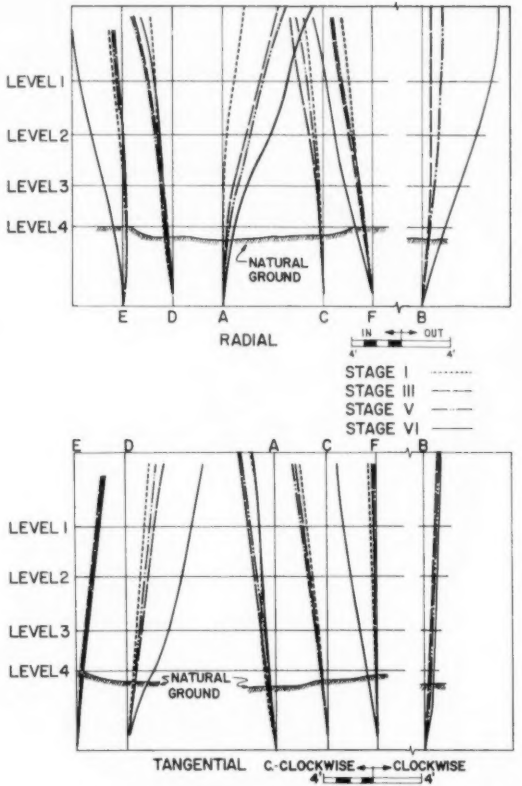

FIG. 15.—SHEET PILE PROFILES

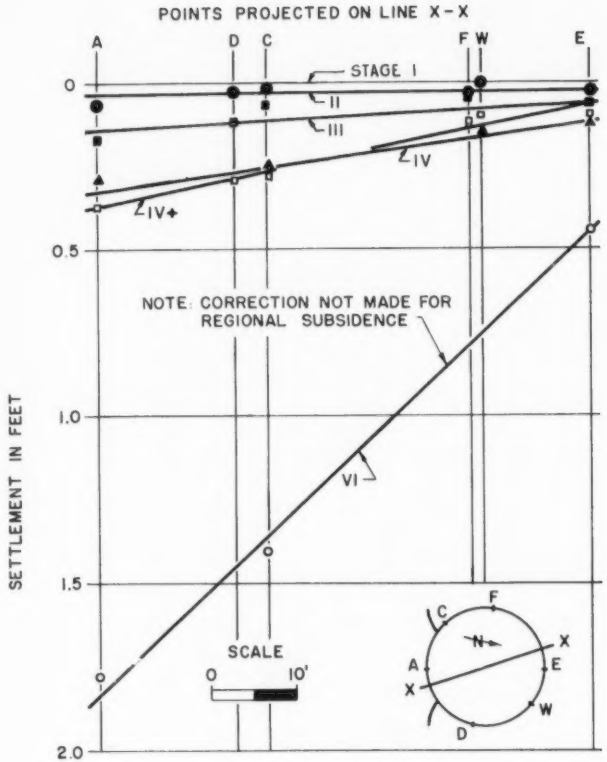

FIG. 16.—SHEET PILE SETTLEMENT

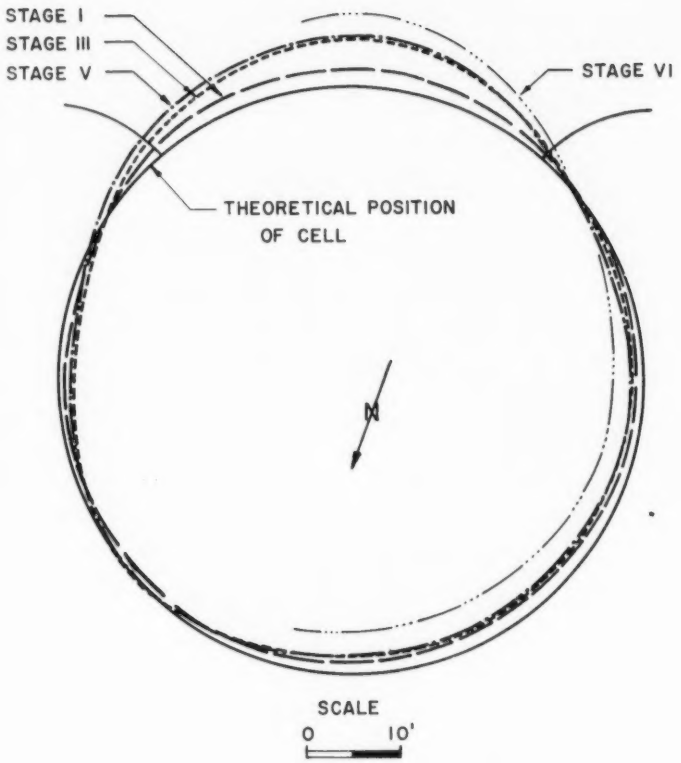

FIG. 17.—MOVEMENTS OF TOP OF CELL

Cell Deformation.—The data on deformation and movement of Cell 16 are given in Figs. 15, 16, 17, and 18.

Fig. 15 shows the two components of horizontal deflection of each instrumented pile at each fill stage. The bottom of the pile was taken as reference, and the curves were constructed by successive upward projections of the an-

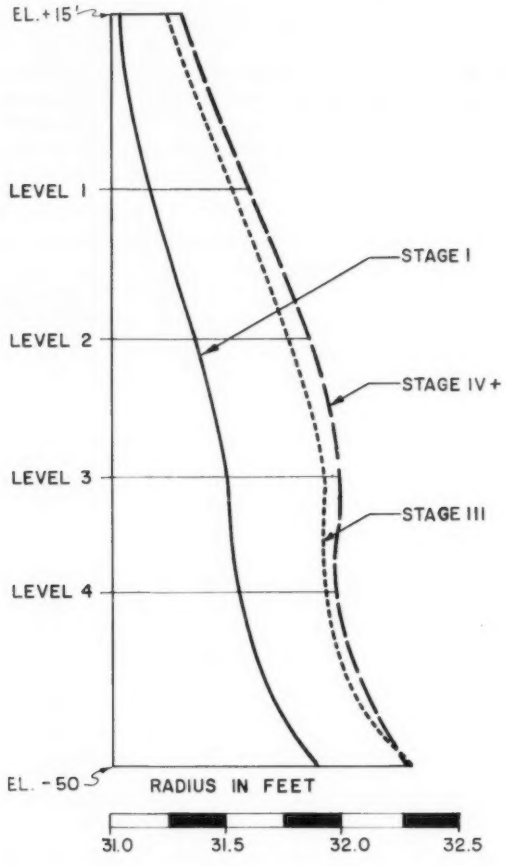

FIG. 18.—AVERAGE RADII

gles obtained in the driftmeter measurements. Pile deflections at the pilot cell were observed a few times during filling. The deformations were similar to those for Pile E, Cell 16, for the corresponding loading.

Fig. 16 shows the changes in elevation and slope of the top of the cell. It was obtained by projecting the changes in elevation at six points around the cell on the radial plane x - x, which is the plane of resultant horizontal movement of the cell.

Fig. 17 shows the changes in shape and position of the cell for the various stages, based on surveying data. Fig. 18 combines the radius measurements at the top with the driftmeter readings to obtain an average deformation of the cell in a radial plane.

In Table 4 are shown the horizontal deflections of the tops of Cells 11 through 31 (Fig. 1), based on surveying data corresponding with application of the surcharge.

Stresses in Sheet Piles.—In Table 5 are given the horizontal hoop tensions in the sheet piles, computed from the measured strains. The vertical stresses were also computed but are not included herein because they were quite small and were more or less randomly distributed about a zero mean.

The method of computation of the stresses will be explained. The strain at each location was first computed, for each date, as the average of the strains measured on the two sides of the pile, using the readings of September 8, 1952,

TABLE 4.—PIER E CELL DEFLECTIONS, STAGE IV TO STAGE VI

Cell Number	Southward Deflection, in Feet 3/18/53 to 6/23/54
11	0.7
12	-0.1
13	-0.1
14	0.6
15	1.7
16	2.3
17	0.7
18	1.9
19	0.2
20	0.3
21	0.1
22	0.0
23	0.4
24	1.0
25	0.3
26	0.8
27	0.6
28	0.8
29	0.5
30	0.5
31	0

just before filling was started, as the zero strain value. The strains were then converted to stress, using the steel properties previously given, and utilizing biaxial stress theory to obtain principal strains, principal stresses, and finally horizontal and vertical normal stresses. The horizontal stresses were then converted to hoop tensions in kips per lin in. of pile, as shown in Table 5.

In the application of biaxial stress theory, three procedures were necessary as follows:

1. At Pile C, since there were strain rosettes, it was possible to obtain the desired normal stresses uniquely from the strain measurements.
2. At Piles A, B, E, and the pilot test, there were horizontal and vertical strainmeters at each location. The normal stresses were obtained with the

TABLE 5.—SUMMARY OF HOOP TENSIONS, CELL 16[a]

Level	Pile		Stage II			Stage III							Stage IV				Stage V	Stage VI	
		9-12 1952	9-18 1952	9-21 1952	9-24 1952	9-27 1952		9-28 1952				10-4 1952	10-30 1952	10-31 1952	10-31 1952	3-7 1953	8-22 1953	7-3 1954	9-1 1954
		2 pm	2 pm	4 pm	7 pm	3 pm	8 pm	2 am	8 am	3 pm	7 pm	12Noon	3 pm	9 am	3 pm	3 pm	1 pm	11 am	
1	A	1.0	-0.3		0.6		3.0			2.7	2.5	1.7	3.1			1.9	4.4	4.4	4.3
	B								0.1				0.6	0.1	0.8	0.7	1.9		
	C	0.6	0.8			1.8	3.3	3.7	3.1			3.3	3.3	4.7			3.3		3.6
	D	-0.1	-0.1	0.5	0	1.6	3.6	2.2	1.3			1.4		2.0	2.1	1.3	1.3	1.3	1.4
	E	0	0.1	-0.6	-1.0	1.6	1.3	2.6	1.1			1.2	1.5	1.3	1.2	1.6	0.4		1.0
2	A	0.6	0.5	0.9	1.3	3.7	2.8				1.5	2.6		2.4	2.7	3.0	3.6	3.6	
	B												0.5	1.0	0.8	1.7	1.6	3.3	3.9
	C	0.5	0.6	-0.4				1.8	1.7			1.6			2.6		3.1		3.3
	D	0.4	0.7	-0.3	1.4	3.2	3.1	3.2	2.9			2.9		2.7	3.0	3.0	3.1	2.8	2.5
	E	-0.1	0.1	0.7	-0.2	2.6	2.3	2.6	1.6			1.2	1.9	0.8	1.9	1.5	1.9		2.1
3	A	1.1	1.1	1.3		4.4	4.0			4.1	2.6	3.3		4.5	4.5	4.2	5.0	7.2	6.8
	B								0.2				0.1	1.8		4.2	1.8	3.3	3.6
	C	1.1	1.7				3.8	3.7	3.7			3.4	3.2	3.5			3.5		4.5
	D	0.9	0.7	1.2	1.5	2.8	2.9	2.9	2.8			3.1	3.5	2.9		3.1	2.9		2.7
	E																		
4	A	1.9	2.3	3.0		5.5	5.5			5.9	7.0	5.7		6.0	5.8	5.6	4.6	6.4	
	B								0.6				0.3	0.3		1.7	1.2	1.8	2.8
	C		2.1			3.4	4.5	4.4	4.5			4.0		4.2	4.2		4.5		
	D	2.2	2.8	-0.1	3.8	5.8	5.9	6.1	5.9			6.0	6.0	5.6	6.4	5.6	5.3		
	E	0.7	1.9	1.6	2.2	1.0	3.6	4.5	3.5			4.9	4.1	4.9	4.7	2.9	2.6		3.6

[a] Tabular values are in kips per lin in. of sheet pile.

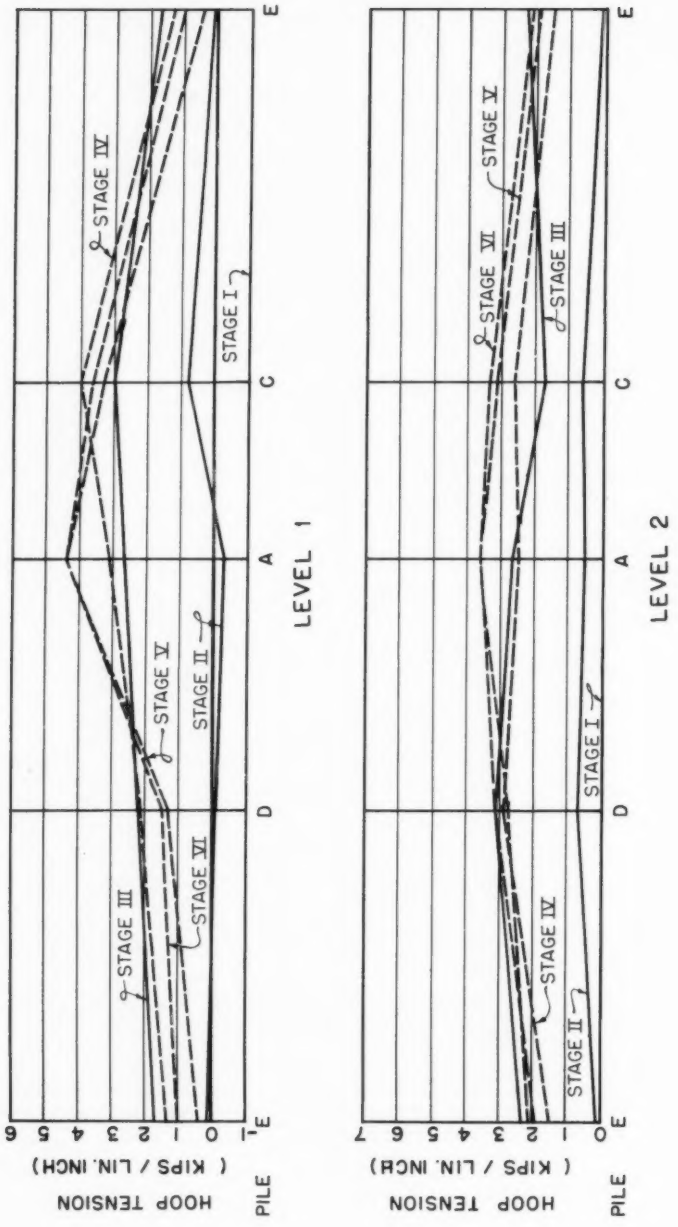
HOOP TENSION
(KIPS / LIN. INCH)
PILE
E
A
C
D
E
STAGE I
STAGE II
STAGE III
STAGE IV
STAGE V
STAGE VI
LEVEL 1
LEVEL 2

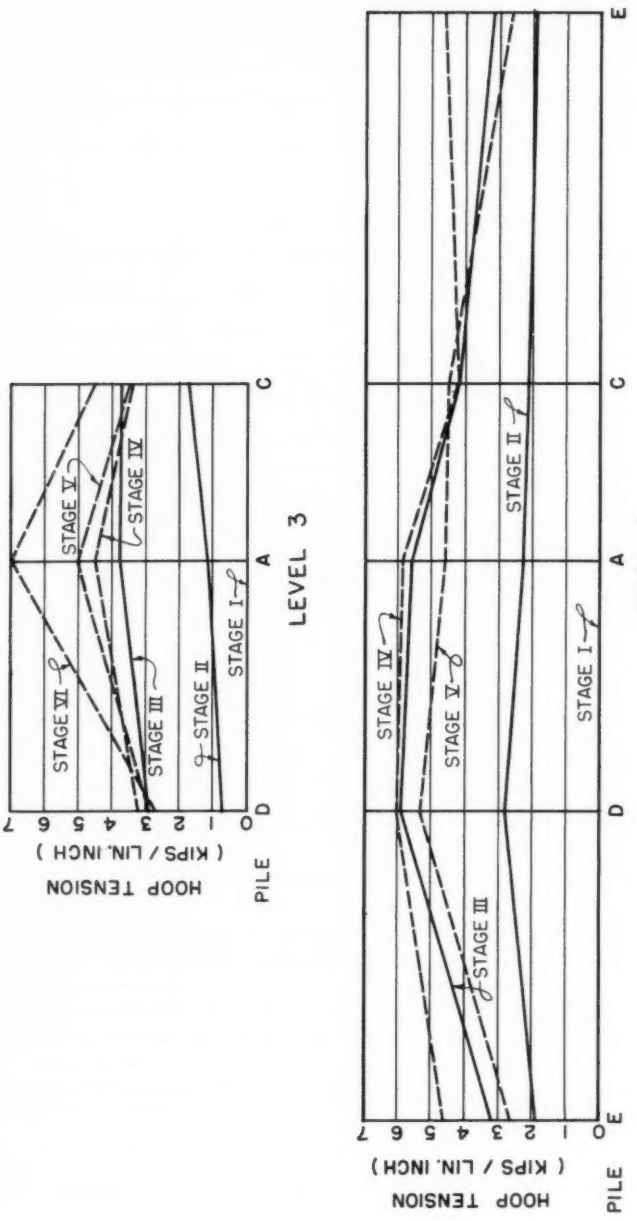

FIG. 19.—SUMMARY OF HOOP TENSIONS

assumption that the measured strains were the principal strains. This procedure is rational for these four piles, because, due to symmetry, the interlock friction theoretically is zero for each of them at all times.

3. At Pile D, only horizontal meters were used, and the horizontal stresses were obtained by assuming that the vertical stresses were zero and increasing the computed horizontal stresses by 10%. This procedure was based on a detailed study of strains and stresses from the two- and three-element rosette gage installations.

TABLE 6.—AVERAGE HOOP TENSIONS, CELL 16

Level	Pile	Stage II	Stage III	Stage IV	Stage V	Stage VI
		Cell 4/10 Full	Cell Full	Arcs Full	Backfill Up	Surcharge On
1	A	-0.3	2.7	3.1	4.4	4.4
	C	0.8	3.0	4.0	3.3	3.6
	D	-0.1	2.2	2.1	1.3	1.4
	E	0.1	1.7	1.3		1.0
	Avg.	0.1	2.4	2.6	3.0	2.6
2	A	0.5	2.7	2.5	3.6	3.6
	C	0.6	1.7	2.6	3.1	3.3
	D	0.7	3.1	2.9	3.1	2.7
	E	0.1	2.3	1.5	1.9	2.1
	Avg.	0.5	2.5	2.4	2.9	2.9
3	A	1.1	3.8	4.5	5.0	7.0
	C	1.7	3.7	3.4	3.5	4.5
	D	0.7	2.9	3.2	2.9	2.7
	E					
	Avg.	1.2	3.5	3.7	3.8	4.7
4	A	2.3	5.6	5.9	4.6	6.4
	C	2.1	4.2	4.2	4.5	
	D	2.8	5.9	6.0	5.3	
	E	1.9	3.2	4.6	2.6	3.6
	Avg.	2.3	4.7	5.2	4.3	5.0

[a] Tabular values are in kips per lin in. of sheet pile.

In Figs. 19, 20, and 21, the average hoop tensions in Cell 16 are shown graphically in their relation to some of the other variables. These figures were plotted from the data in Table 6, which was prepared by averaging stage data from Table 5. Fig. 19 shows how the tensions varied around the cell at each fill stage for each meter level. Fig. 20 gives the chronological picture of development of tensions at the four levels, averaging the data on all piles at each level. The same information in Fig. 20 is plotted in Fig. 21 against level for each fill state.

The few tension determinations from the pilot test are given as follows:

Date	Hoop Tension (kips per lin in.)	Fill Condition
7/20/52	0	Cell empty
7/26/52	1.0	Fill at el 0
7/30/52	1.7	Cell full

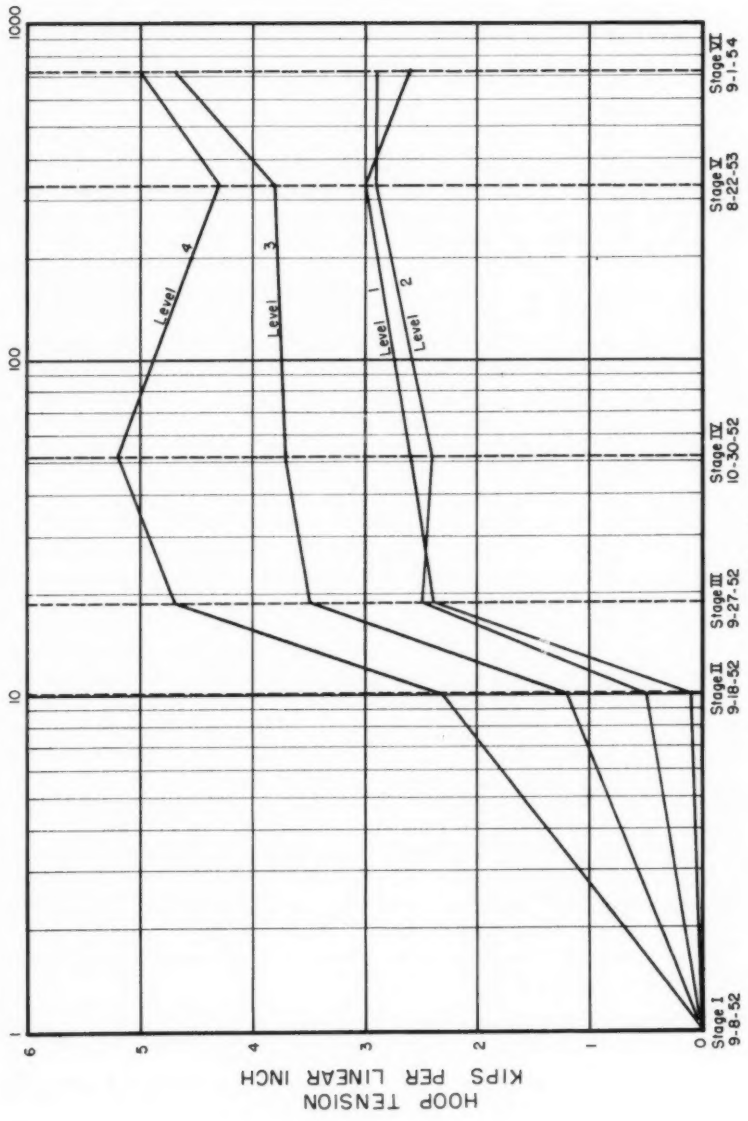

FIG. 20.—AVERAGE HOOP TENSION VERSUS TIME

Date	Hoop Tension (kips per lin in.)	Fill Condition
9/ 5/52	1.3	
9/28/52	2.4	Arcs full
1/ 9/53	2.0	Backfill at el 4
3/ 7/53	1.6	Backfill at el 4

PERFORMANCE DURING FILLING OF CELL

Soil Settlement.—Soil settlement entered the study of cell behavior in three ways. First, the soil within the cell consolidated under its own weight. Second, the weight of the filled cell caused consolidation of the original ground. Third, the lateral pressure of the fill depostied unsymmetrically in the cell (Fig. 3), and later of the backfill, produced a differential settlement resulting in a southward tipping. Superimposed on these effects was the regional subsidence in the Long Beach-Wilmington area.

The maximum settlements of the pore pressure-settlement devices were found at depth rather than at the surface. Points some distance down in the cell settled as much as 1.2 ft (Fig. 11), excluding the estimated effects of the previously described soil flow beneath the cell. This is because the fill farther down in the cell was in place longer, was more heavily loaded, and experienced some settlement before the top material was placed.

The maximum soil settlement shown in the north-south porfile (Fig. 11) occurred in the center of the cell, with smaller settlements at the edges. This could be caused by the effects of wall friction. The apparent inconsistency at the lower levels of the east-west profile is because the early soil flow beneath the east face of the cell near point U.

Some sliding and shifting of the fill within the cell occurred while the pore pressure-settlement devices were still in shallow fill. This caused erratic movements of some of the lower settlement points and made difficult the accurate determination of consolidation settlements.

Pore Pressures.—The changes in water level in the pore pressure pipes were due to three pressure effects such as hydrostatic excess due to consolidation, rising and falling tides, and seepage of water out of the cell. The consolidation pressure can be determined analytically from the measurements at a given time if the sea level and the flow net through the cell are known.

Unfortunately, data from the borings as well as the features of the profile plots of pore pressure data (Figs. 12 and 13) indicated that a theoretical prediction of the flow net is not feasible. The flow net can be obtained, however, from the measurements if the assumption is made that the consolidation hydrostatic excess does not change between successive extremes of tide. The level of water in the standpipe is given by

$$P = C\left(1 - \frac{m}{n}\right) + S\left(\frac{m}{n}\right) + h \quad \ldots\ldots\ldots\ldots \quad (1)$$

in which, C is the water level in the cell; S denotes the sea level; h represents the excess hydrostatic pressure due to consolidation; and

$$\frac{m}{n} = \frac{\text{number of potential drops from fill surface to a given point.}}{\text{total number of potential drops}}$$

If subscripts 1 and 2 represent high and low tide, respectively

$$\frac{m}{n} = 1 \frac{(P - S)_1 - (P - S)_2}{(C - S)_1 - (C - S)_2} \quad \ldots\ldots\ldots\ldots (2)$$

which defines the flow net empirically. Once the flow net is determined, h may be computed.

This computation was carried out for point "S" (Fig. 6) for September 27, 1952 (Fig. 14), and it was determined that h = 1.2 ft. However, because the result is obtained from the difference between relatively large numbers, a small probable error in pore pressure reading leads to a larger probable error in the computed hydrostatic excess. Therefore, the previous value, while significant, must be considered qualitative.

Early in the filling, when the sea level and the water level in the cell were the same, the existence of hydrostatic excess due to consolidation was obvious. Between September 10 and September 12, h ranged from 0 ft to 1.2 ft.

Movement of Top of Cell 16.—Fig. 17 shows that the top of Cell 16 was far out of its theoretical position before any fill was placed. Except on the east side, it was initially too far east and south, and the cell continued to move in these directions during filling. This movement probably was mainly due to uneven deposition of fill and to the early flow of soil beneath the cell.

The initial irregularity of Cell 16, shown in Fig. 17, is believed to have been caused by one or more of the following: (1) a damaged template was used in forming this cell, (2) jetting was done to place the test piles, (3) relatively shallow penetration king piles were used to support the template, and (4) relatively shallow penetration of sheet piles resulted from the low natural ground level. Great difficulty was encountered in closing this cell, the most irregular one in the bulkhead.

Fig. 16 shows that the maximum sheet pile settlement, at point A, on completion of filling of the cell was approximately 0.2 ft. The greater settlements on the south side of the cell are consistent with the data on southward tilting provided in Figs. 15 and 17.

During filling, the driftmeter data showed rotations at the lower ends of the square tubes (3 ft above the end of pile) of approximately 0.1° for all test piles except at D, in which the value was 2.0°.

Radius Versus Depth Curves.—Correlation of radius measurements at the top of the cell (Fig. 17) with the driftmeter data (Fig. 15) permitted the construction of Fig. 18, representing average radial sheet pile deformation. The general shape of the curves clearly indicates outward movement of the bottom of the cell, increasing with height of fill. The initially large bottom radius (Stage I) suggests the possibility that an interlock may have been injured during pile driving or perhaps that an insufficient number of points was used to define accurately the shape of the cell. The lateral distance between the curves for Stage I and Stage IV represent both an elastic and an inelastic (interlock takeup) deformation of the cell wall. The elastic portion of this deformation is so small, theoretically, that the deflection measurements could not detect it with useful accuracy.

Hoop Tensions.—Perhaps the most interesting data are those arising from the measurement of strains in the sheet piles. Fig. 19 facilitates comparison of the hoop tensions for the different fill levels and at different points around the cell. The lower tensions for Pile E may be because the natural ground lev-

el there (Fig. 3) was higher than it was on the south side of the cell. For the cell full (Stage III) condition, the tensions were otherwise comparatively uniform around the cell, except for Level 4.

The highest hoop tension for Stage II (cell 4/10 full) was 2.8 kips per lin in. at Level 4, Pile D, as shown in Table 5. Because only one set of readings was obtained for this condition, the same tension appears in Table 6. When the cell had been filled, several sets of readings were taken, and the highest individual tension obtained was 6.1 kips per lin in. (at Pile D), with a corresponding average value of 5.9 kips per in. This high stress at D may have been due to the large local radius of curvature (the cell wall was almost straight), or to the high rate of filling at that point which occurred when the soil flow under the cell was nearby stopped abruptly.

Fig. 20 reveals a systematic pattern of development of horizontal tensions during filling.

The rosette installation at Pile C were made with the thought of studying the complex structural situation near the T-pile connection between cell and arc. The data were examined carefully in this regard, but the results were inconclusive.

Sets of strain readings were taken at short intervals in 2 days to study the affects of tidal changes on hoop tensions. The average horizontal stresses increased with a drop in tide and decreased with a rise in tide, as shown in Table 5.

Only a few values of hoop tension were botained for the pilot cell, Cell 25. These were of low magnitude, because the strainmeters were approximately 7 ft below the natural ground, where the cell wall was not as free to expand as it was at points intrumented on the main test cell.

Hoop Tension as a Function of Fill Height.—Fig. 21 indicates for Levels 2, 3, and 4 an almost linear distribution of the average hoop tension in Cell 16 with regard to elevation for the Stage II condition (cell 4/10 full), and a similar trend is shown for Stage III (cell full). The stresses obtained for Level 1, however, are much higher than would be obtained by linear extrapolation from Levels 2, 3, and 4. The high average stresses at Level 1, Stage III, are influenced by the high individual stresses at C and A. The fill was slightly higher at A than elsewhere in the cell, during most of the filling procedure. It is possible that action of the T-pile near C caused an increase in hoop tensions in the cell at the latter point.

Fig. 3 shows that the top of the fill for Stage II was between Levels 2 and 3, nowever, Fig. 21 clearly indicates a positive average hoop tension at Level 1, which was 13 ft above Level 2. The curve for Stage III in Fig. 21 seems to imply an appreciable hoop tension at the top of the cell for the cell-full condition.

To study this point further, Fig. 22 was drawn by correlating fill-height above meter level with strain measurements at Levels 3 and 4. In Fig. 22, data are included for fill levels intermediate to those of Table 5. The fill-heights above meter level were insufficiently large at Levels 1 and 2 to justify graphing the data at these levels. It is confirmed by these curves that tensions exist at a given level before the fill surface has risen to that level. The dashed line in Fig. 22 represents the trend of the relationship for the greater fill heights. The line passes through the origin, susgesting that the relationship becomes linear after the fill surface has risen appreciably above the meter level.

This phenomenon may be examined analytically if it is assumed that the lateral earth pressure increases in proportion to fill depth and that the cell behaves elastically. The pressure distribution is as indicated in Fig. 23 (a). If a horizontal cut in the cell wall were made at the fill surface, the lower portion of the cell would expand as in Fig. 23 (b) and develop the angle

$$\theta = \frac{K\gamma R^2}{n E t} = \frac{K\gamma}{K} \quad \ldots\ldots\ldots\ldots\ldots \quad (3)$$

in which θ is the rotation of each cell element in the vertical plane; K denotes the ratio of horizontal to vertical earth pressure; γ represents the soil unit

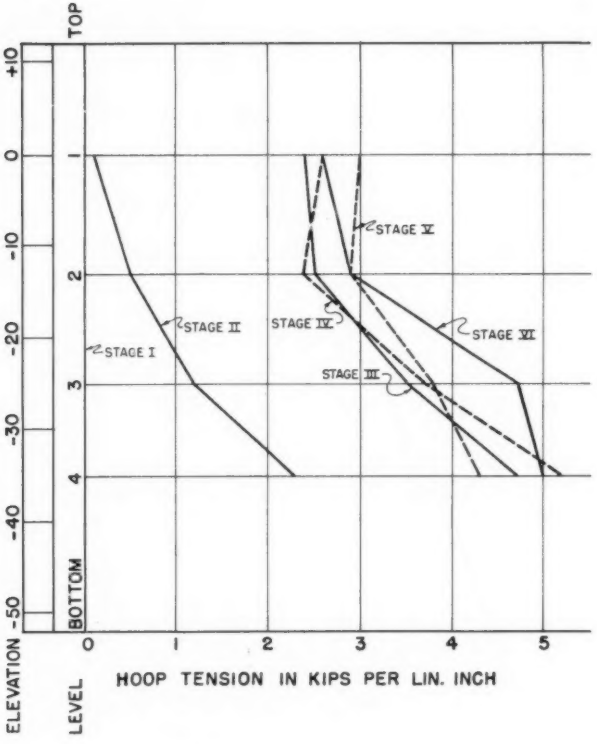

FIG. 21.—AVERAGE HOOP TENSION VERSUS FILL LEVEL

weight; R refers to the cell radius; n is a coefficient depending on extensibility of sheet pile interlocks; E represents the modulus of elasticity of the steel; t denotes the effective cell wall thickness; and k is a derived parameter equivalent to a modulus of subgrade reaction. The solution is corrected for the effect of the cut by providing edge moments (Fig. 23 (c)) and edge shears (if re-

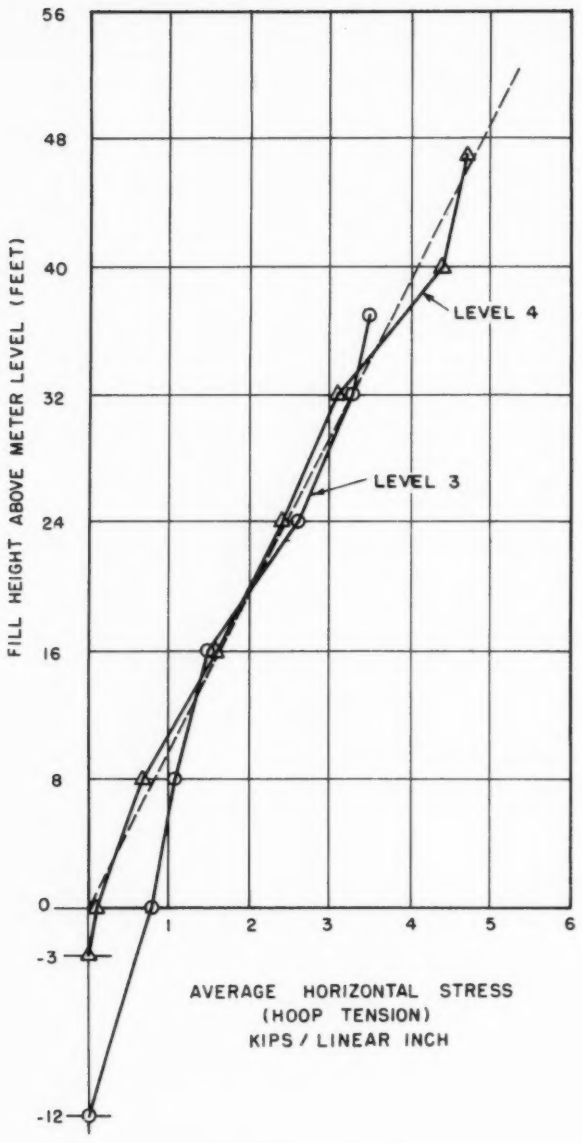

FIG. 22.—AVERAGE HOOP TENSION VERSUS FILL HEIGHT ABOVE METER LEVEL

quired) to eliminate the physical discontinuity. To solve for M_o, the redundant edge moment, one needs the influence coefficient [12] for edge rotation due to a unit applied edge moment. The edge moment required to eliminate the discontinuity in slope is obtained by dividing $\frac{\theta}{2}$ by the influence coefficient. Fig. 24 shows the theoretical hoop tension curves thus obtained for two values of the parameter k. The curve for k = 84 corresponds to a continuous steel cylinder, while that for k = 7 includes a reasonable allowance for interlock extensibility.[13]

This analysis verifies qualitatively the implication of Figs. 21 and 22, but the observed effect considerably exceeds that shown in Fig. 24. The difference might be reconciled by considering the analysis the transverse slipping of the sheet pile interlocks.

Coefficient of Lateral Earth Pressure.—From Table 5, the hoop tensions at high tide at Levels 1, 2, 3, and 4 for the cell-full condition (Stage III) are found

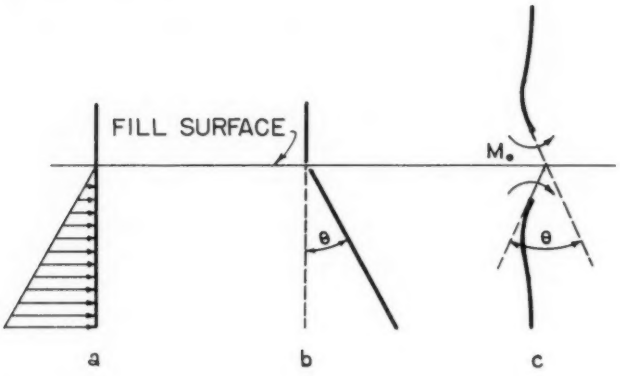

FIG. 23.—ANALYSIS OF EFFECT OF DISCONTINUITY OF LATERAL PRESSURE

to be 1.4, 2.5, 3.6, and 3.9 kips per lin in., respectively. These hoop tensions may be transformed into lateral fill pressures by the use of thin shell theory, assuming in accordance with the analysis leading to Fig. 24 that the horizontal loading discontinuity effect is zero when the cell is full. The lateral pressures shown in Fig. 25 (a) are thus obtained. The value at top of cell is shown as zero on the basis of theory.

In accordance with the data of Fig. 14 and Table 3, the high cell water level and the lateral water pressures and seepage forces from the flow net must be considered. The computation is made for the case where the water outside the cell is at high tide, 5.5 ft, because the water levels are fairly stationary at this time. The net lateral water pressure, which is subtracted from the total horizontal pressure, is shown in Fig. 25 (b).

---

[12] "Formulas for Stress and Strain," by R. J. Roark, McGraw-Hill Book Co., Third Ed., 1954.

[13] "Cellular Sheet Piling Structures—A Detailed Study of the Stressing in Circular Walls," by L. Descans, L'Ossature Metallique, Brussels, January, February, 1954.

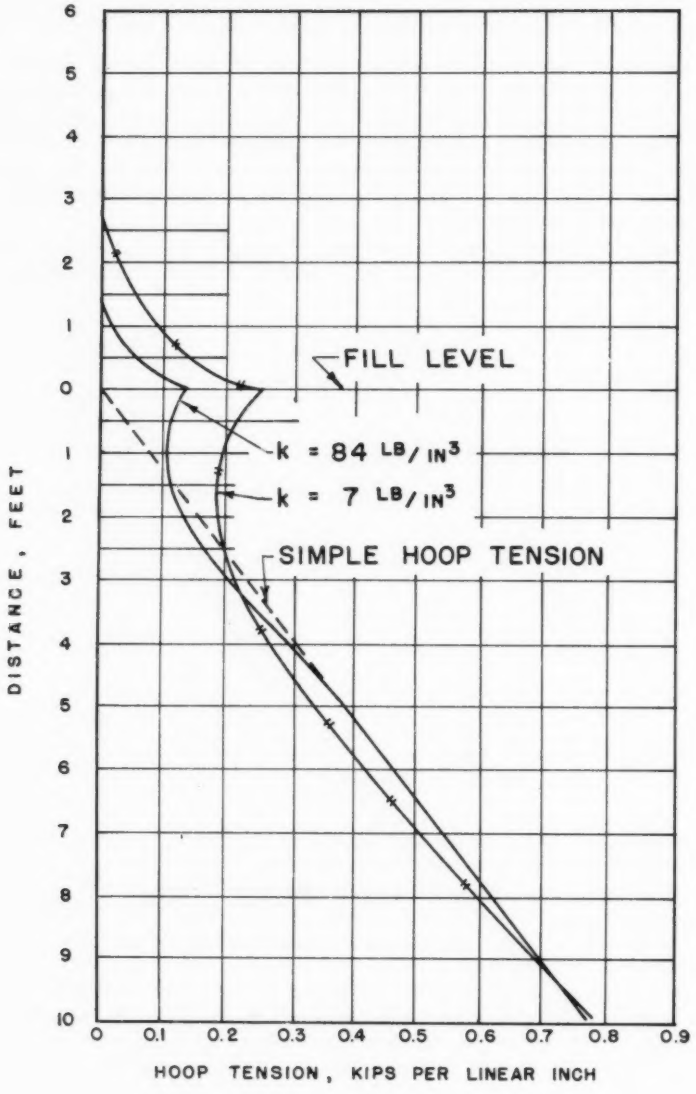

FIG. 24.—EFFECT OF LATERAL PRESSURE DISCONTINUITY ON HOOP TENSION

Effective soil unit weights[14] of 120 and 60 lb per cu ft above and below water level, respectively are used in the computation of vertical soil pressure (Fig. 25 (c)). The seepage force of the downward flowing cell water (Fig. 25 (d)) is added. Friction between the cell wall and the settling soil is neglected.

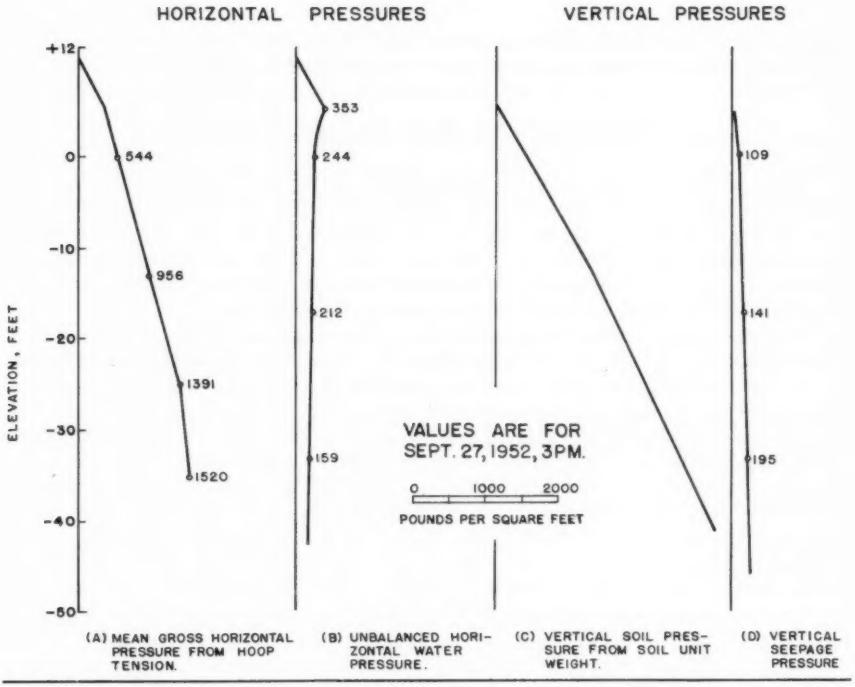

FIG. 25.—HORIZONTAL AND VERTICAL PRESSURES, STAGE III, HIGH TIDE

The coefficient of lateral earth pressure is obtained as the average of the quotients of the net horizontal and vertical soil pressures at the four datum levels. By this method, it is found, for Stage III, that

$$K = 0.54$$

Approximately the same value was obtained from a similar computation using the Stage III average hoop tensions with outside water level taken at mean sea level. For design, the engineer must consider the total lateral pressure, not just the portion due to soil as determined herein.

During the early stages of filling the cell, the water levels inside and outside the cell were the same. Thus it is probably acceptable herein to neglect

14 "A Soils Study for Pier E Test Cell No. 16," by L. T. Evans, Long Beach Harbor Dept., January 3, 1955.

the seepage and consolidation hydrostatic forces in determining the coefficient of lateral earth pressure. Fig. 22 may be utilized for this purpose, taking K as inversely proportional to the slope of the curve. The proportionality constant will be the reciprocal of saturated soil unit weight times the cell radius. This computation yields for the early filling stages

$$K = 0.66$$

using the average (dashed) line in Fig. 22. The value in Eq. 5 would be corrected downward if pore pressure due to consolidation were large.

PERFORMANCE AFTER FILLING OF CELL

Settlements and Deflections.—Movements of the cell and the soil under the effects of time and of increases in loading following the completion of filling are shown in Figs. 15, 16, and 17, and in Tables 2 and 4. The indicated vertical movements over the period from late 1952 to 1954 are subject to correction for the effects of regional subsidence, but the horizontal movements and rotations were not significantly influenced by these effects.

The movement of the cell as a whole, as illustrated in Figs. 15, 16, and 17, showed nothing significant through Stage V, where the backfill was raised to el 12. The surcharge load, however, carried to el 25 or el 26 corresponding with Stage VI, caused a large deflection away from the backfill. The resultant effect was a southerly tipping of the sheet piles of more than 3°, which was contributed to by a 1° southerly rotation of the cell as a whole. The net cell racking, more than 2°, created relatively large shearing distortions of the soil within the cell. The reason why the movement stopped at this point is the consequent reduction, toward the active value, of the horizontal pressure of the backfill against the cell. Note from Fig. 1 and Table 4 that other deep-water cells also experienced exceptionally large moments away from the backfill.

The soil in the cell also settled with respect to the steel, between Stages IV and VI, by 0.4 ft at the cell top and 0.3 ft at Level 2 (from Table 2 and Fig. 16).

Hoop Tensions.—Figs. 19 through 21 and Tables 5 and 6 show the effects on hoop tensions of the events subsequent to filling of the cell. Computation of coefficient of lateral earth pressure after filling behind the cell and in the arcs, and after adding the surcharge, is difficult to do with confidence and precision. The asymmetry of fill-loading and the forces applied to the cell at the T-piles create a complex stress system.

Soil unit weights[14] of 116 and 60 lb per cu ft above and below water level, respectively, were used, and it was assumed that both cell water level and sea level water at el 4.3 (approximate mean sea level adjusted for regional subsidence).

With the backfill up and the surcharge on, the horizontal earth pressures should be approximately balanced on the north face of the cell. At the south face, however, the surcharge should be more directly reflected in hoop tension. Because of the uncertainty as to shear flow between steel and soil around the cell circumference, the lateral earth pressure is computed by using the south face hoop tensions at Piles A and C only. This leads to an approximate value of

$$K = 0.53$$

which is essentially the same as in Eq. 4. Apparently then, subject still to the theoretical limitations previously mentioned, the large cell distortions did not greatly affect the hoop tensions, and the hoop tension increases between Stages III and VI may be assignable primarily to the increase of fill depth associated with the surcharge.

The largest hoop tension observed in the test, approximately 7 kips per lin in., occurred at Level 3, Pile A, in Stage VI (Fig. 19 and Table 6). Tensions at Piles A, C, and D generally exceeded those at Pile E, especially during the latter phases of construction. This pattern can be explained in terms of the existence of soil pressure on both faces at Pile E and of the comparatively large water depth at Pile A.

The comparatively small hoop tensions at Pile B (Table 5) apparently follow from the facts that the connecting arc radius (Fig. 3) is much smaller than the cell radius, and the soil in the arc space is confined in a bin-like manner.

SELECTED FINDINGS

The test data have been presented in as complete detail as was feasible, in order that others may use them appropriately. The following summary emphasizes some of the significant findings as developed herein.

1. The coefficient of lateral earth pressure was obtained as 0.66 during the filling of the cell, 0.54 shortly after the cell was filled, and 0.53 2 yr later after application of a 14-ft surcharge. The apparent independence of the latter values with respect to large cell deformation is an important point. Unbalanced pore pressures must also be included in computation of hoop tension.
2. The large movement accompanying application of the surcharge consisted of a 1° rotation of the cell as a whole and an added 2° shearing distortion of the sheet piles and the contained soil.
3. The maximum hoop tensions occurred at Level 4, approximately at the original ground level. The largest individual hoop tension determined was 7 kips per lin in., at Level 3, Pile A, Stage VI.
4. The soil in the cell required 10 days after completion of filling to reach approximately 90% consolidation. During and before this time, pore pressures due to consolidation reached values of the order of 1.2 ft of sea water.
5. The filling procedure used in construction is a major factor in cell alinement. Specifications should require adequate outside soil depth before filling; the symmetrical depositing of fill in the cell, and the arising of cell water level to the top before the fill rises more than $\frac{1}{4}$ to $\frac{1}{2}$ of the cell height. The latter measure tightens the interlocks and stiffens the cell during filling.
6. Hoop tensions where necessary were satisfactorily determined from measurements with horizontal strainmeters alone, with an appropriate correction being made in the computations. This implies possibilities for simplification in future studies.

ACKNOWLEDGMENTS

The Pier E test program was conceived in 1949 by R. R. Shoemaker with C. M. Duke, and then considered by a special committee of the Soil Mechanics

Group of the Los Angeles Section, ASCE, headed by B. N. Hoffmaster, M. ASCE. The program was developed through studies among University of California and Long Beach Harbor Department personnel and the Executive Committee of the Soil Mechanics Group (S. S. Green, F. ASCE, Chairman). It was also influenced through correspondence with Karl Terzaghi, Hon. M. ASCE, G. P. Tschebotarioff, F. ASCE, and D. P. Krynine, F. ASCE. Roy W. Carlson, M. ASCE, advised as to the methods of mounting the Carlson strainmeters. L. T. Evans, M. ASCE, consultant to the Harbor Department, conducted the exploration and testing of soils.

The instrumentation was financed by the Long Beach Harbor Department. Personnel of the University of California, Los Angeles, planned and supervised the instrumentation, made most of the observations, and reduced the data.

Active representatives of the Long Beach Harbor Department were Shoemaker, Hoffmaster, Raymond Berbower, M. ASCE, and L. L. Whiteneck. Engineering students L. S. Deutsch, A. M. ASCE, G. Muir, R. Rundle, W. Hook, O. F. Hackett, G. G. Nelson, and R. J. Loy contributed to the experimental work. R. J. Houghton, M. ASCE, prepared the figures.

To the engineers previously named, and to the many others who aided in conducting the project, the writers extend their sincere appreciation.

Journal of the
SOIL MECHANICS AND FOUNDATIONS DIVISION
Proceedings of the American Society of Civil Engineers

PILE HEAVE AND REDRIVING

By Earle J. Klohn,[1] M. ASCE

SYNOPSIS

Upward pile movement or "pile heave" commonly occurs whenever large numbers of closely spaced piles are driven. Pile heave is generally attributed to displacement of the foundation soils during subsequent driving of adjacent piles. The majority of engineers appear to be of the opinion that all heaved piles must be redriven. Very few documented case histories dealing with this problem are available in the engineering literature.

This paper presents detailed field data with analyses pertaining to pile-heave problems that developed during construction of end-bearing pile foundations for a large industrial plant. Two individual areas within the plantsite are selected for detailed study. Pile heave occurred at both areas. However, whereas in one area the heaving constituted a serious foundation problem necessitating the redriving of all heaved piles, in the other area it presented no problem and redriving was not necessary. The successful performance of the completed pile foundations at both areas is confirmed by settlement observation data maintained on the buildings since construction.

The paper shows that each pile-heave problem must be evaluated on its own merits. In order to carry out such an evaluation, adequate data concerning such items as subsoil profile, magnitude of pile heave, magnitude of ground heave, pile penetration diagrams, and pile loading tests must be gathered and studied. From such a study, the mechanics of the specific pile heaving process

Note.—Discussion open until January 1, 1962. To extend the closing date one month, a written request must be filed with the Executive Secretary, ASCE. This paper is part of the copyrighted Journal of the Soil Mechanics Division, Proceedings of the American Society of Civil Engineers, Vol. 87, No. SM 4, August, 1961.

[1] Partner, Ripley, Klohn and Leonoff Ltd., Consulting Engineers, Vancouver, B. C.

may be determined and consequently its probable effects on the performance of the completed structures evaluated.

THE PROJECT AND THE PILE PROBLEMS INVOLVED

The paper is based on data obtained during construction of a large expansion to an existing pulp mill located at tidewater on Canada's West Coast. A plan of the development showing both the original and expanded mill layouts is presented on Fig. 1. The original pulp mill, built in 1946, was supported on timber end-bearing piles driven into underlying glacial outwash deposits. Ap-

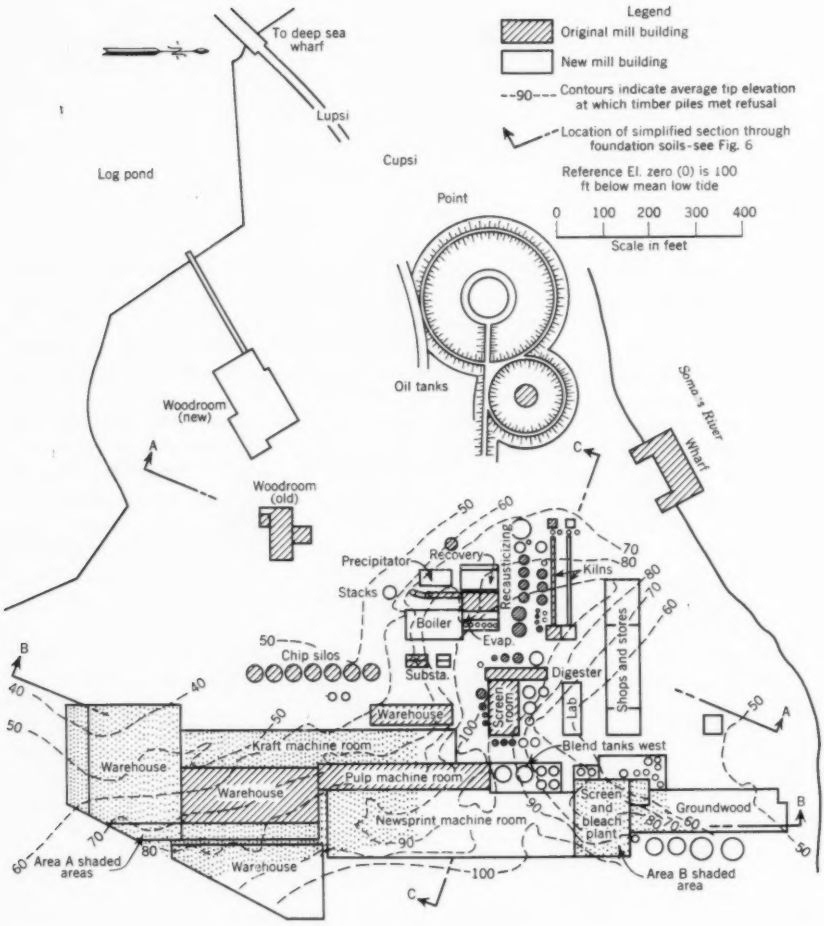

FIG. 1.—PLAN OF MILL AREA

proximately 6,000 piles, most of which were 35 ft or less in length, were driven for support of the original mill. Settlement observations maintained on the original mill buildings since their construction indicated that the foundations had performed satisfactorily and that no foundation settlement problems had developed. (Settlement records indicated average building settlements ranging between 0.02 ft and 0.03 ft for the period 1946 to 1955.)

The 1955 mill expansion program involved the construction of several large and heavily loaded buildings. Support of these structures required the driving

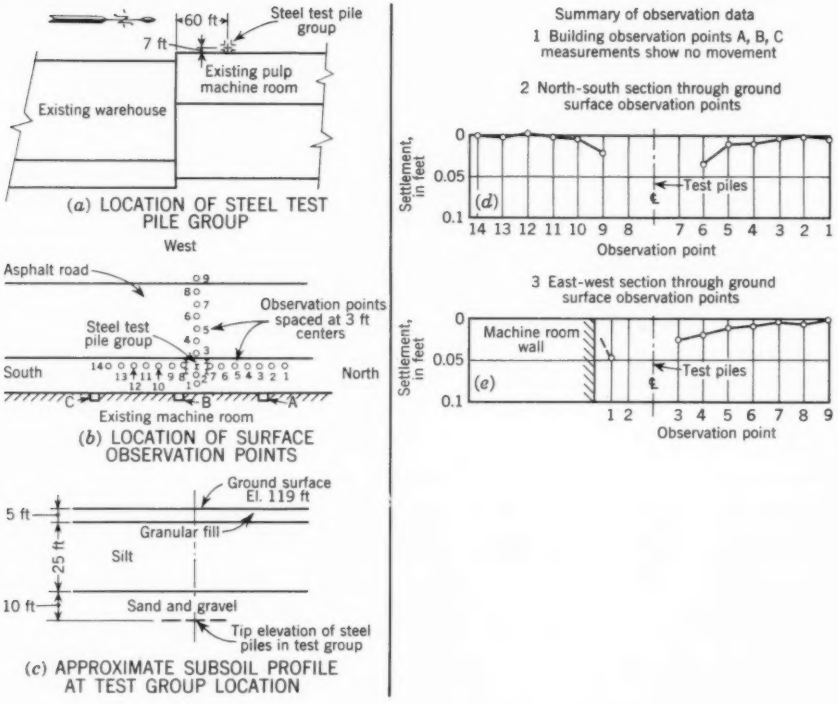

FIG. 2.—GROUND SURFACE MOVEMENTS DURING DRIVING OF STEEL TEST PILE GROUP

of large groups of piles of greater length and at closer spacing than had previously been necessary for the original mill. Approximately 26,000 timber end-bearing piles ranging in length from 10 ft to 125 ft and having an average length of about 50 ft were required. In many instances the new structures joined directly onto existing mill buildings containing equipment sensitive to movement. As this equipment had to be kept in continuous operation throughout the construction period, disturbance of these buildings also had to be prevented.

Construction of pile foundations for the new buildings therefore had to satisfy two distinct requirements:

(1) Damage to existing buildings during pile driving for the new mill structures must be prevented.
(2) A satisfactory pile foundation, free from harmful settlements, must be achieved for the new mill structures.

The first requirement, prevention of damage to existing buildings owing to soil displacement from pile driving, was satisfied by using steel H piles within a distance of approximately 10 ft from existing buildings. These piles offered two advantages:

(1) They permitted use of a higher allowable load per pile (50 tons), thereby reducing the number of piles in a group from 16 timber to 6 steel.
(2) Being low displacement piles a group of them displaced a relatively small volume of soil.

The decision to use steel H piles was partially based on data obtained from a test group of 5 steel piles driven adjacent to an existing mill building. Briefly, these data (presented in Fig. 2) showed that the existing building was not affected by driving the test-pile group and that subsidence of the ground surface did not exceed 0.01 ft beyond a distance of 10 ft from the centre of the test-pile group.

During construction of the mill expansion, benchmarks were set on the exterior walls of existing buildings and on sensitive equipment foundations within the buildings. Level observations were maintained on the bench marks throughout the driving of the steel piles. These observations indicated that driving the steel piles had no measurable effect on the existing buildings except at one local area where maximum settlements of 0.01 ft were reported. The steel piles were therefore considered a success, having performed their design function of limiting the soil desplacement to a value that would not affect the existing adjacent pile foundations. A photograph showing steel piles driven next to the pulp machine room is presented in Fig. 3. All steel piles were driven before driving of timber piles was started. This figure also illustrates the difference in size between steel and timber pile groups. Fig. 4 shows ground heave for a large timber pile group and indicates the kind of soil displacement problem that steel piles may have prevented alongside the buildings.

During the initial stages of the driving, several steel H piles developed very high penetration resistances at relatively shallow depths and, before the problem could be assessed, the field forces attempted to achieve further penetration by continuing to hammer the piles. The attempt appeared successful as the piles were driven several feet deeper. It was noted, however, that the upper ends of the piles had both rotated and moved laterally. To check on this behavior several piles were pulled so that their tips might be examined for damage. Fig. 5 presents photographs of two such piles.

The extensive damage caused by overdriving is quite apparent, as is the corkscrew shape of one of the pile tips, a shape that explains the pile rotation that developed during driving. As a result of these findings, all overdriven piles in this local area were pulled and replaced.

To satisfy the second foundation requirement, provision of pile foundations free from harmful settlements, an evaluation of the effects of pile heave on future foundation behavior was required. Carrying out such an evaluation con-

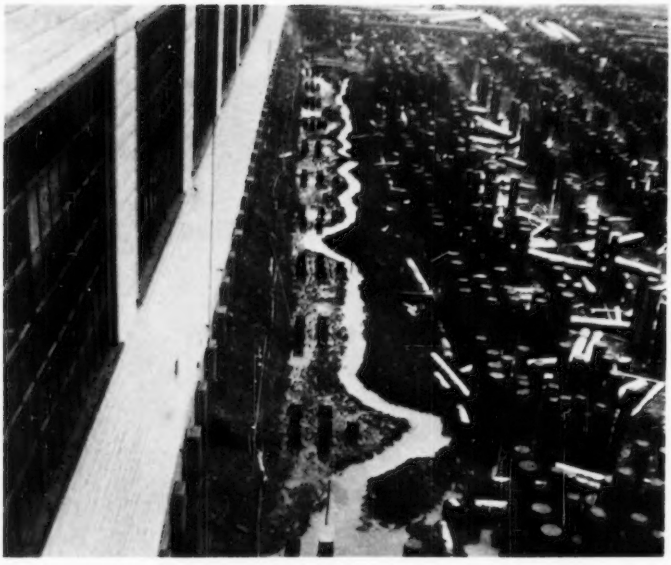

FIG. 3.—STEEL PILE GROUPS LOCATED ADJACENT TO EXISTING PULP MACHINE BUILDING

FIG. 4.—GROUND HEAVE AT AREA B

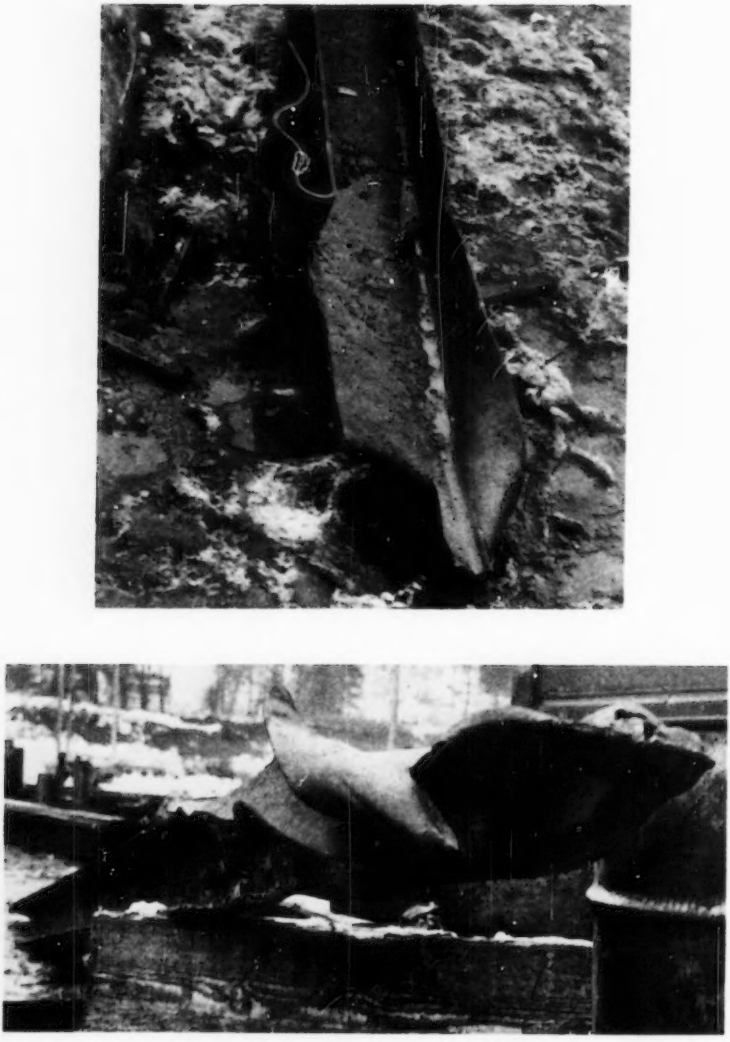

FIG. 5.—STEEL PILE TIPS DAMAGED BY OVERDRIVING

stituted the major foundation consideration at this site and the following sections of the paper deal exclusively with this item.

GENERAL LAYOUT AND SOIL CONDITIONS

A general layout of the pulp and paper mill showing both the original and the new mill buildings is presented in Fig. 1. Also shown in this figure are contour lines depicting the average tip elevations at which the timber end-

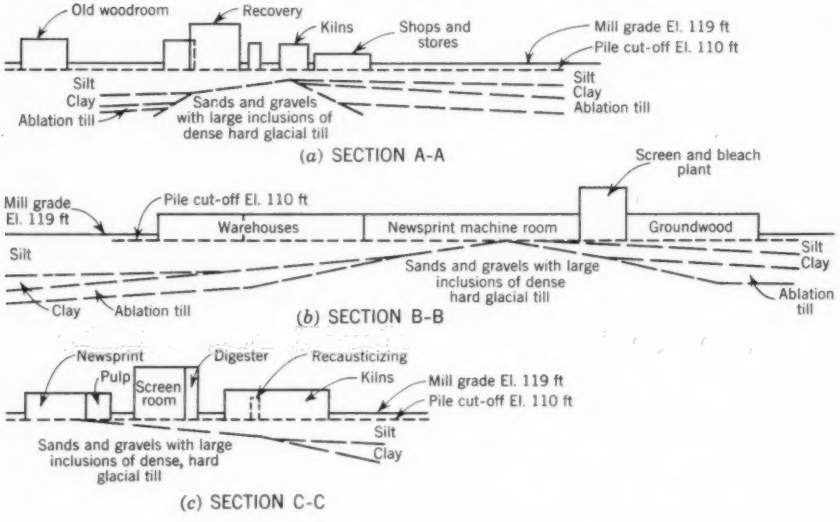

FIG. 6.—TYPICAL SIMPLIFIED SECTIONS THROUGH FOUNDATION SOILS

bearing piles met refusal. These contours indicate that the mill straddles a buried spur of hard material that slopes downwards in a westerly direction. Geological opinion is that the spur was carved by erosion from a thick sheet of glacial outwash material. This deposit, into which all end-bearing piles were driven, is extremely variable, as proved by both the foundation exploration and construction programs. It consists mainly of medium-to-dense sands and gravels. However, it does contain large inclusions of dense hard glacial till and an erratic scattering of boulders. In one area extensive pockets of

clean loose sand were noted. In some areas the outwash material is directly overlain by recent deposits of silt and clay which extend to the present ground surface. In other areas a soil deposit, referred to in this paper as "ablation till," occurs between the top surface of the outwash material and the overlying silts and clays. The ablation-till deposit consists of a well-graded mixture of particle sizes ranging from clay to fine gravel. The material has the appearance of glacial till, but is not dense.

During the last retreat of the Pleistocene ice sheet, sea levels rose and flooded the glacial deposits, burying them beneath fine grained marine sediments. With increasing depth below the present ocean floor their grain size decreases from silt to clay size. The silts are non-plastic and have natural water contents ranging between 35% and 45%. The clays have natural water contents ranging between 30% and 50%, liquid limits of 40% to 50%, and plastic limits of 18% to 22%. The natural water content of the clay is usually slightly below its liquid limit.

Typical sections through the foundation soils at this site are shown in Fig. 6. More detailed subsoil data relating to particular pile problems are presented in those sections of the paper in which the problems are discussed.

PILE HEAVE

The term "pile heave" as used in this paper refers to the upward movement of a previously driven end-bearing pile caused by the subsequent driving of additional piles in the immediate vicinity. A pile is heaved by the upward component of movement of the soil displaced by these subsequent piles. The magnitude of pile heave to be expected at this site was not known beforehand. A search was made of the engineering literature in an attempt to find data that would provide some guidance in evaluating this problem. Several references (1) (2) (3)[2] were located; although these did not treat pile heave in extensive detail they did indicate that heaved piles must be redriven or settlements approximately equal to the original heave might occur under the completed building loads. This opinion was also reflected by the requirement of most building codes (4) (5) (6) that heaved piles must be redriven. As the mill structures are extremely sensitive to settlement the designers considered that settlements in excess of 0.03 ft would be intolerable. Using this criterion, a maximum allowable pile heave of 0.03 ft was tentatively selected. For piles that heave in excess of this figure redriving would be considered.

Pile heaves far in excess of the maximum tolerable settlement value (0.03 ft) occurred as soon as pile driving got under way. Obviously, unless assurance could be given that the heaved piles would not settle excessively under future applied building loads, redriving of most piles would be necessary. The added costs and the additional time involved if redriving was required would be most critical for this project. Therefore procedures had to be evolved as quickly as possible to evaluate the pile-heave problem as the driving operation progressed across the site.

Effects of Pile Heave on End-Bearing Piles.—For end-bearing piles that derive a large percentage of their allowable bearing capacity from point resistance (for example, those driven through soft highly compressible soil to rock), pile heave during construction can be the cause of excessive settlement of the pile foundations at some later date when they are loaded. This problem

[2] Numerals in parenthesis refer to corresponding items in the Appendix—Bibliography.

will develop if heave during construction causes the pile tips to lift off the bearing stratum. When such piles are loaded, they will settle until their tips are once again in intimate contact with the bearing stratum. Thus, settlements approximately equal in magnitude to the original pile heave may occur.

On the other hand, for end-bearing piles that appreciably penetrate the bearing stratum and derive a large percentage of their allowable bearing capacity from skin friction developed within this stratum, pile heave may not pose a future settlement problem. For example, if the frictional resistance developed within the bearing stratum by the embedded lower portion of the pile exceeds the upward drag exerted on the pile by the soft overlying sediments displaced during the driving of adjacent piles, then these upper soils will heave without moving the pile. But soil displacement will also occur within the bearing stratum itself, due to the pile penetrations. Such displacement may result in appreciable pile heave; however, as this heave is caused by a general upward movement of the bearing stratum soils it is unlikely to result in a decrease in the resistance that the pile can develop within the bearing stratum. Therefore future foundation settlement due to pile heave is unlikely to be a problem provided the heave is caused by displacement within the bearing stratum as opposed to displacement within compressible soils overlying the bearing stratum.

Both types of pile heave were encountered at this site, and an example of each has been selected for analysis. At Area A, pile heave is attributed to soil displacement within the bearing stratum. At Area B, it is attributed to displacement of the overlying compressible soils that lifted the pile tips off the bearing stratum.

Area A.—The boundaries of Area A are outlined on Fig. 1, a general plan of the millsite. Pile driving, pile-load testing, and subsoil data pertaining to this area are presented in Figs. 7 to 10 inclusive. A photograph showing pile-driving operations in this area is presented in Fig. 7. Typical pile penetrations diagrams are presented in Fig. 8. These diagrams illustrate the general pattern of pile resistance during driving, and show how this resistance builds up as the pile penetrates the bearing stratum. All piles were of Douglas Fir and were driven using a No. 1 vulcan hammer. In Fig. 9 are presented the results of 4 pile-loading tests made on representative end-bearing foundation piles. Pertinent information relating to subsoil profile, pile dimensions, method of test, etc., are noted in the figure for each individual pile test. In Fig. 9 all test piles were of Douglas Fir. The piles were driven using a No. 1 vulcan single acting steam hammer. The rate of loading for pile tests equals one load increment every 15 min. Permanent pile movement was measured by unloading the test pile to zero load and recording the permanent settlement the previous load had produced. In Fig. 10 are presented the results of a series of pile-loading tests carried out on a timber friction pile driven into the soft marine deposits. The rate of loading for the test was one increment of load every hour. Also shown in Fig. 10 are field and laboratory test data obtained from a drill hole made approximately 3 ft from the test pile. The test pile and drill hole data are considered representative for the marine deposits encountered at Area A.

A review of the data obtained on each individual pile during driving indicated that the majority of foundation piles had heaved as adjacent piles were driven. Although the recorded pile heave values varied erratically, apparently most piles had heaved between 0.10 ft and 0.20 ft. Settlements of this magnitude

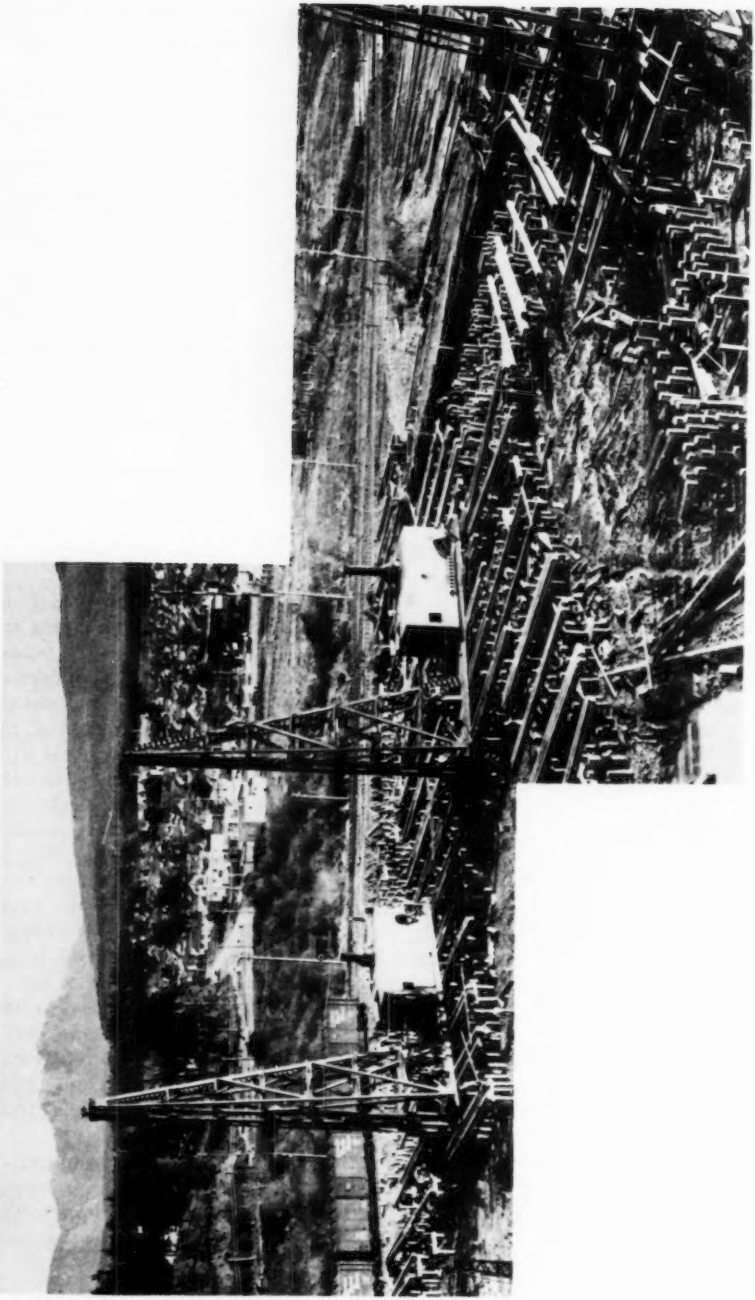

FIG. 7.—PILE DRIVING AT AREA A (LOOKING EAST)

in the completed building were intolerable and unless assurance could be given that the heaved piles would not settle, redriving would be necessary. Such an operation would be both costly and time consuming and was to be avoided if possible.

The pile-driving records indicated that foundation piles in Area A penetrated an average distance of 15 ft to 20 ft into the relatively incompressible ablation till and the underlying sand and gravel materials before meeting refusal. The marine deposits that overlie the ablation till are very soft and offered little resistance to penetration of the piles. The frictional resistance that the piles would develop within the bearing stratum was judged to be greater

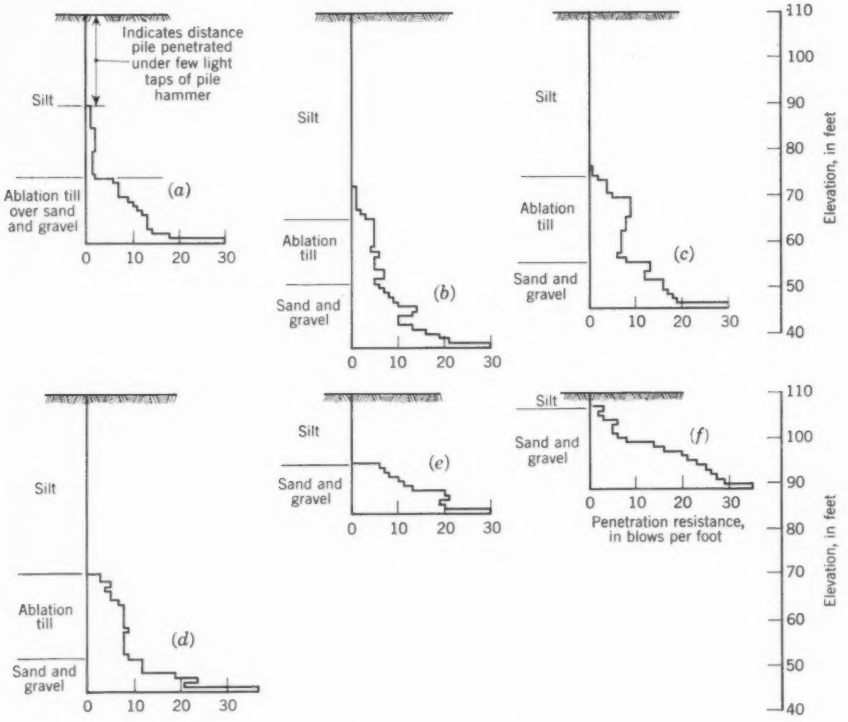

FIG. 8.—TYPICAL PILE PENETRATION DIAGRAMS WITH SIMPLIFIED SUBSOIL PROFILES—AREA A

than the upward drag that would be exerted on them by subsequent displacement of the soft marine soils. The observed pile heaves were therefore apparently caused by displacements within the ablation till and underlying sand and gravel soils. If this were the case, then intolerable settlement of the heaved piles at some future date would not occur.

To check this appraisal of the heave problem several pile-loading tests were run. All test piles produced load-settlement curves similar to those shown in Fig. 9. Approximate computations were carried out to determine what portion of the total load applied to the test pile was carried by skin friction developed in the soft marine deposits and what portion by the lower

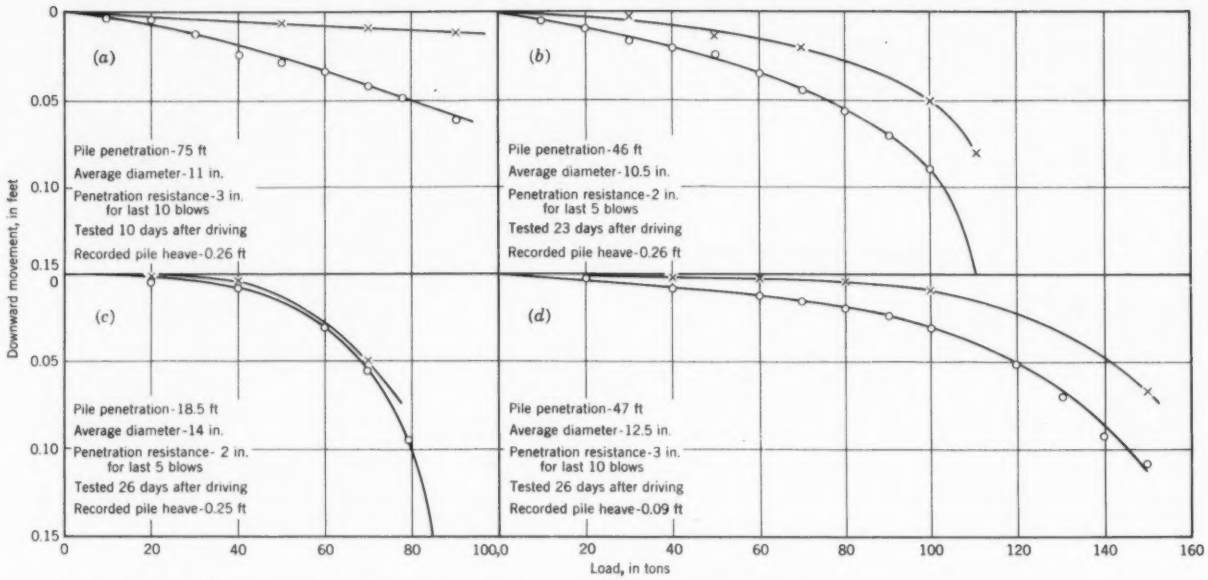

Test pile	*a*	*b*	*c*	*d*
Simplified subsoil profile	0 ft-45 ft silt 45 ft-75 ft ablation till overlying sand and gravel	0 ft-35 ft silt 35 ft-46 ft ablation till overlying sand and gravel	0 ft-2 ft silt 2 ft-18.5 ft sand and gravel	0 ft-30 ft silt 30 ft-47 ft sand and gravel

Total downward pile movement

Permanent downward pile movement

FIG. 9.—TYPICAL PILE LOADING TEST DATA—AREA A

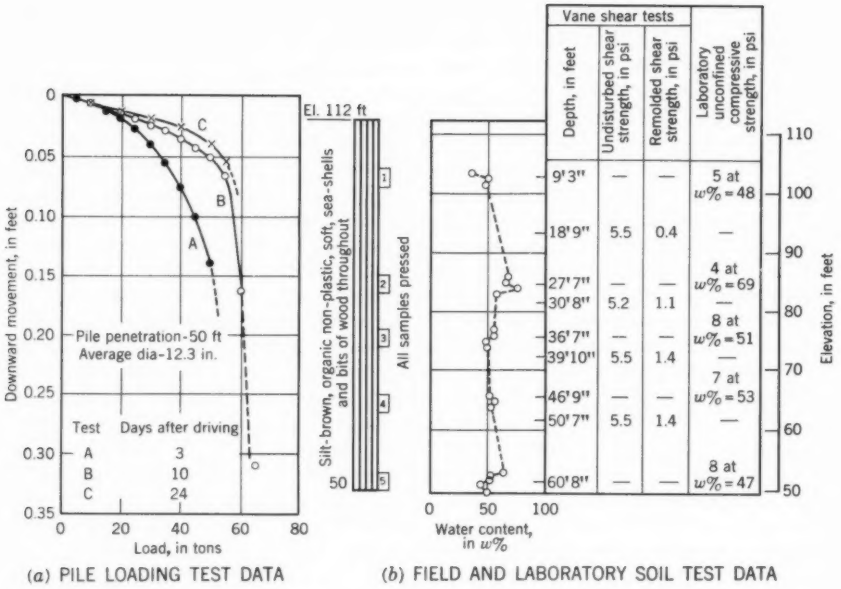

(a) PILE LOADING TEST DATA (b) FIELD AND LABORATORY SOIL TEST DATA

FIG. 10.—PILE LOADING TEST DATE AND FIELD AND LABORATORY SOIL TEST DATE—FOR FRICTION PILE IN MARINE DEPOSITS

FIG. 11.—PILE DRIVING AT AREA B (LOOKING NORTH)

end of the pile embedded in the bearing stratum. Ultimate skin friction values for the marine deposits were obtained from the friction pile-loading test (Fig. 10). In every case the computations indicated that the load carried by the section of pile embedded in the bearing stratum was from 2 to 6 times the design pile load of 20 tons. Admittedly such computations are approximate only, as subsoil conditions at the test pile location may vary somewhat from those assumed for computation purposes. However, when viewed in conjunction with all the available data these computations were considered to confirm the preliminary appraisal that pile heave would not present a future settlement problem. Foundation piles were therefore cut off and capped without redriving.

Settlement observations maintained since construction of the mill expansion (1956) confirm that pile heave did not present a potential settlement problem in Area A. The average recorded settlement to date (July 1960) for the warehouse building is 0.01 ft. The initial settlement readings were made when the building was partially constructed and while an estimated 30% of the final live-plus-dead loads was acting on the pile foundations. For the completed structure the average live-plus-dead load acting over the entire plan area of the building is approximately 2000 psf. As would be expected, the warehouse structure has readily absorbed these very small settlements and is in excellent condition.

Area B.—The boundaries of Area B are outlined in Fig. 1, a general plan of the millsite. Pile driving, pile testing, and subsoil data pertaining to this area are presented in Figs. 11 to 14 inclusive. A photograph showing pile driving operations in this area is presented in Fig. 11. Typical pile penetration diagrams illustrating the general pattern of pile resistance during driving, are presented on Fig. 12. All piles were of Douglas Fir and were driven using a No. 1 vulcan hammer. In Fig. 13 are presented the results of 3 pile-loading tests made on representative end-bearing foundation piles. Pertinent information relating to subsoil profile, pile dimensions, method of test, etc., are noted on the figure for each individual pile test. All test piles were of Douglas Fir. The piles were driven using a vulcan No. 1 single acting steam hammer. The rate of loading for pile tests equals one load increment every 15 min permanent pile movement was measured by unloading the test pile to zero load and recording the permanent settlement the previous load had produced. In Fig. 14 are presented a summary of field and laboratory data for 3 test holes located near Area B.

Pile heave observation data obtained on each individual pile in Area B clearly indicated that large heaves occurred during the driving operation. Most piles apparently heaved between 0.3 ft and 0.4 ft. However, large variations in heave were recorded for individual piles within any one pile group and maximum pile heaves of 1 ft or greater were noted in several instances. The large pile heaves were also accompanied by appreciable heaving of the ground surface in the vicinity of each pile group (Fig. 4).

The pile driving data for Area B, particularly the pile-penetration diagrams, definitely showed that the behavior during driving of a large percentage of the end-bearing piles in this area differed appreciably from that of the piles previously driven in Area A. Two major differences were noted in the pile behavior:

(1) The overlying marine deposits offered appreciable resistance to driving.
(2) The piles did not slowly build up resistance to further penetration; instead they refused suddenly.

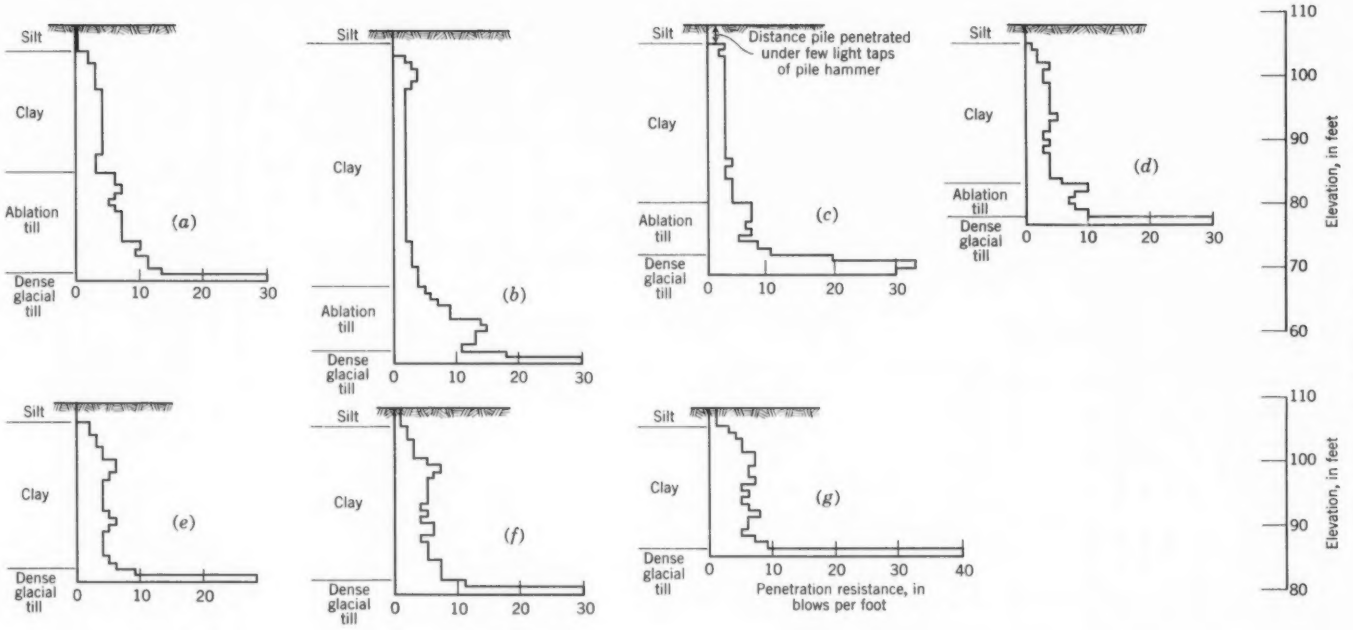

FIG. 12.—TYPICAL PILE PENETRATION DIAGRAMS WITH SIMPLIFIED SUBSOIL PROFILES—AREA B

These observations clearly indicated that the subsoil profile at Area B was appreciably different from that at Area A. The available test-hole data implied that the overlying marine deposits in this area were medium-to-stiff clays rather than silts. The bearing stratum appeared to be a dense glacial till. To check these items, 3 additional test holes were immediately drilled. These test holes confirmed that the marine deposits at Area B were medium-to-stiff clays. They also confirmed that the bearing stratum was a dense hard glacial till into which the timber piles could not penetrate more than one or two feet. In the area that exhibited large pile heaves, the overlying clay appeared to rest directly on the dense, hard glacial-till bearing stratum.

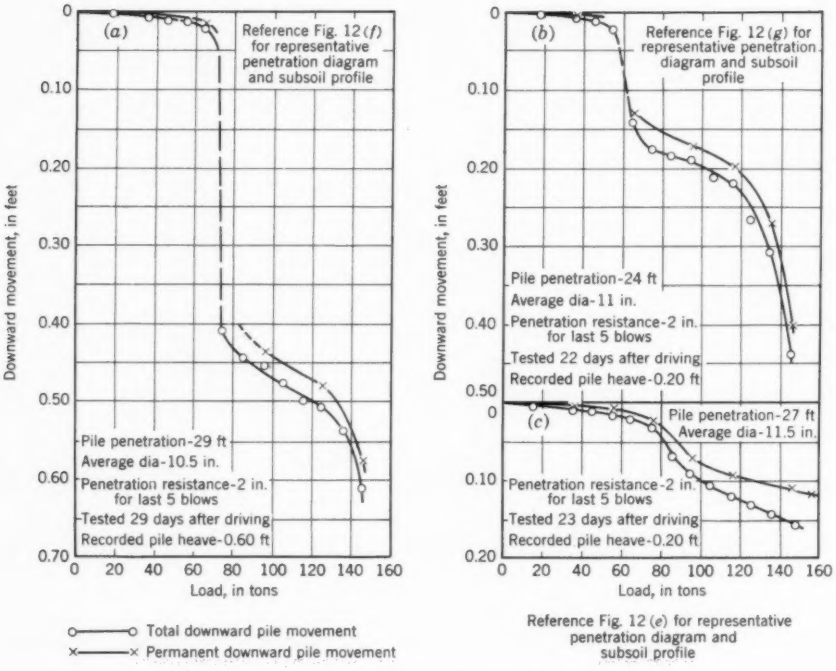

FIG. 13.—TYPICAL PILE LOADING TEST DATE—AREA B

These data were interpreted to indicate that pile heave at Area B posed a serious foundation problem. It was reasoned that those piles that had met sudden refusal, without appreciable penetration into the bearing stratum, had offered little resistance to the upward drag exerted on them by the displaced clay and that consequently they had heaved, lifting their tips out of contact with the bearing stratum. Unless redriven until their tips were again in sound contact with the bearing layer these heaved piles were potentail sources of large foundation settlements under future applied building loads.

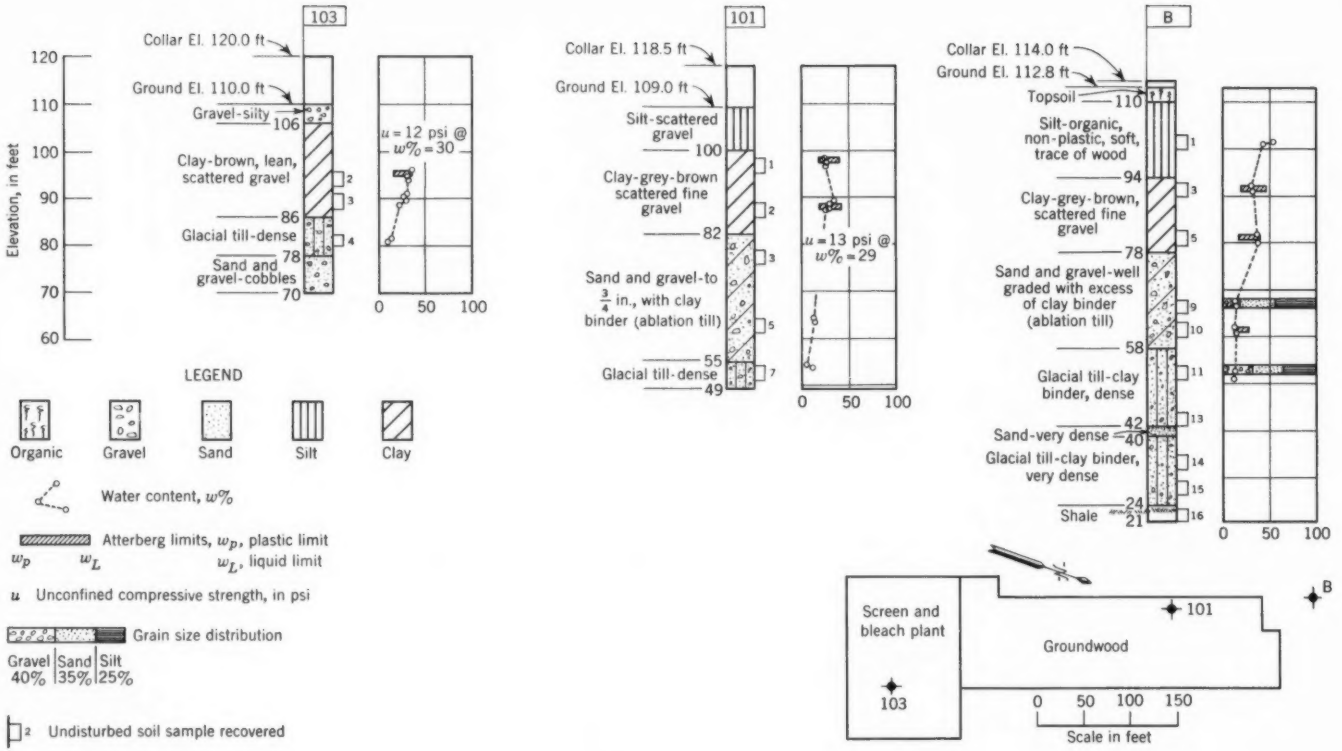

FIG. 14.—TEST HOLE DATE—AREA B

To check this appraisal of the pile heave problem and confirm the necessity for redriving the heaved piles, several representative piles were selected for pile-loading tests. Each pile was loaded until it reached what appeared to be its ultimate bearing capacity. At this constant load the pile moved downwards. However, after having settled a distance that ranged from 0.1 ft to 0.4 ft for different test piles, the pile stopped moving under the constant load. Loading of the test pile was then continued until it again moved downwards under constant load. In every case this final or ultimate load that caused continuous movement of the pile appreciably exceeded the one that caused the initial pile movement. A suggested explanation for this observed behavior of the test piles is as follows:

(1) Initially, a pile was driven through the overlying marine clay and met practical refusal on contacting the dense glacial till. As a result, the pile tip did not penetrate more than one or two feet into the till layer.

(2) When subsequent piles were driven in the same pile group, they displaced large volumes of the overlying clay soil so that the ground heaved around the pile groups.

(3) The displaced clay exerted large upward forces on the previously driven pile. These forces exceeded the resistance to upward movement that the pile could develop with its small penetration into the bearing stratum. Consequently the pile moved upwards.

(4) In moving upwards the pile tip lost contact with the bearing stratum, and the pile in effect became a friction pile supported by the overlying clay soil.

(5) When load tested, the pile behaved initially as a friction pile supported in the overlying clay, and when the ultimate skin friction value of this material was reached, the pile failed, moving suddenly downwards until the tip again came into contact with the bearing stratum. With the pile tip in contact with the bearing stratum, the pile stopped moving. Additional loads were then applied until ultimate failure was reached.

(6) The ultimate failure load represented the ultimate total bearing capacity of the pile, equal to skin friction in the overlying clay plus point resistance in the glacial till bearing stratum.

The pile-loading test data were interpreted to confirm the original appraisal that pile heave at Area B posed a major foundation problem at this site. Displacement of the overlying marine clay during pile driving had apparently caused the pile tips to lift off the bearing stratum. In their heaved condition, the foundation piles were, in effect, friction piles supported by the overlying clay. As such they would undergo with time large settlements under the applied building loads. Settlements of this kind would be intolerable for the proposed structures. Redriving of all piles in this area was therefore required to ensure that the pile tips achieved sound contact with the bearing stratum.

PILE REDRIVING

Redriving heaved piles in Area B was a difficult operation requiring careful planning and close supervision. On the one hand, heaved piles had to be redriven sufficiently hard that they moved downwards a distance at least equal

to the observed heaves. On the other hand, excessively hard redriving that might cause brooming or breaking of the piles could not be tolerated.

The shorter the waiting period between driving and redriving, the smaller would be the skin friction forces that must be overcome during the redriving operation. The available loading-test data indicated that 12 hr after driving the piles had developed approximately 75% of the skin friction they would develop three weeks after driving. Beyond 3 weeks, the rate of increase of ultimate bearing capacity with time was estimated to be slow. Obviously, unless the heaved piles could be redriven within a few hours after the initial driving they would have to overcome large frictional resistances during the redriving operation. Unfortunately on this project, obtaining the required pile heave observations, and redriving the piles, required a minimum time interval of approximately 48 hr. This delay was caused by several factors, including the large number of piles in each pile group, the type of pile driving equipment in use of the site, and the construction procedures that had been developed for driving piles over the site area. This time lag between driving and redriving made the redriving operation somewhat more difficult than might normally be the case.

In order to develop suitable criteria for redriving heaved piles, several representative piles in the area were selected for testing. The piles selected for this purpose had originally been driven several days previously. Briefly, the driving tests consisted of applying 10 blows to the pile with a No. 1 vulcan hammer (5000 lb ram, 15,000 ft lb per blow) and then measuring the penetration achieved. All test piles were redriven to a minimum penetration resistance of 1 in. for 10 blows and some of the piles were redriven until at least three consecutive sets of 10 blows had each produced less than 1 in. of penetration. Several of the test piles were then pulled and examined for damage. In every case those piles that had moved 1 in. or more under the first 10 blows of the hammer and had subsequently been redriven to a final penetration resistance of 1 in. per 10 blows had undamaged tips. Even those piles that had been subjected to exceptionally hard redriving forces showed only moderate tip damage. Brooming and splitting of the pile tops appeared to be the more critical problem. This behavior was considered normal since a large percentage of the energy applied to the pile heads during driving never reached the pile tip, but instead was dissipated by the frictional resistance the pile had developed in the overlying clay soils.

After reviewing the results of the pile redriving and pulling tests these conclusions were drawn:

(1) Unless the pile moved 1 in. or more under the first 10 blows of the pile hammer, the second or third set of 10 blows still did not produce movements in excess of 1 in. per set of 10 blows. In addition, the exceptionally hard driving was likely to damage or break the pile.

(2) Piles which moved a distance of 1 in. or more under the first 10 blows of the hammer normally could be driven several inches before tightening up again. This tightening up was interpreted to indicate that the pile tip was once again in contact with the bearing stratum.

(3) Piles which moved 1 in. or more under the first 10 blows of the hammer and were subsequently driven to a final penetration resistance of 1 in. per 10 blows would not have their tips damaged by the stresses developed in the pile during the redriving operation.

On the basis of these conclusions, the following procedures were developed for redriving the heaved piles:

(1) The pile was given 10 blows with the No. 1 vulcan hammer. If the pile moved 1 in. or more, it was given an additional 10 blows.
(2) This procedure was repeated until a penetration of less than 1 in. for 10 blows was reached.

The boundaries of the critical areas where pile redriving was considered necessary were delineated on the basis of a study of both the pile-heave observation data and pile-penetration diagrams. Generally, pile re-driving was extended over those areas where the pile-penetration diagrams indicated that the piles had met sudden refusal without appreciable penetration into the bearing stratum. All piles in the areas selected for redriving were redriven, regardless of whether or not the observation data indicated excessive heave. The redriving areas were purposefully made to overlap adjacent areas where pile heaving did not appear to be a problem, so as to ensure that no piles which required redriving were missed. As a general rule, 1 in. or more of penetration was achieved for the first 10 blows in areas where pile heaving was considered critical, whereas less than 1 in. of penetration for the first 10 blows was obtained in those areas bordering the critical area that were purposefully overlapped during redriving.

At most locations a direct correlation between observed pile heave and observed pile penetration during redriving (pile redrive) was not evident for each individual pile. However, a review of the heave data in terms of average values per pile group, indicated that in areas considered critical for pile heave the average redrive value was approximately equal to the average heave value for the same pile group. These data were interpreted to indicate that the redriving operation was successful and had accomplished its objective of driving back down into the bearing stratum those piles that had been unseated by the original pile heaving.

Settlement observation data maintained since construction of the mill expansion (1956) show that the redriven pile foundations have performed satisfactorily. The average settlement to date (July 1960) for the screen and bleach plant, which is located in Area B, is 0.02 ft. The initial settlement readings were made when the building was partially constructed and while an estimated 40% of the final live-plus-dead loads was acting on the pile foundations. For the completed structure the average live-plus-dead load acting over the entire plan area of the building is approximately 3,000 lb per sq ft. As would be expected, the screen and bleach plant has readily absorbed these very small settlements and is in excellent condition.

CONCLUSIONS

There are many aspects of foundation behavior that are not subject to exact pre-determination by theoretical analyses. Pile heaving, and the effects of pile driving on existing adjacent buildings, are two of these. Evaluation of such problems requires the gathering and studying of detailed field observation data as well as a knowledge of the theoretical principals involved.

The effects of pile heave on the ultimate performance of a pile foundation will depend on the mechanics of the heaving action. Each pile heave problem

must be individually evaluated. To carry out such an evaluation, adequate information concerning such items as subsoil profile, magnitude of pile heave, magnitude of ground heave, pile penetration diagrams, and pile loading tests must be gathered and studied. The data presented show that whereas in some instances pile heave may constitute a serious foundation problem necessitating the redriving of all heaved piles, in other instances it may present no problem and redriving is not required.

Where piles are driven adjacent to existing foundations, damaging movements may be caused by the soil displaced during driving. At this site the use of low-displacement steel H piles was successful in limiting the soil displacement to values that did not affect the existing foundations.

ACKNOWLEDGMENTS

Owner of the pulp and paper mill project is MacMillan and Bloedel Ltd. The project was designed and constructed under the supervision of H. A. Simons Ltd., Consulting Engineers, Vancouver, B.C. Senior soil mechanics consultant was K. Terzaghi. The writer's firm acted as general soil mechanics consultants to the designers and in this capacity worked in close cooperation with Mr. Terzaghi. The writer is indebted to Mr. Terzaghi for his valuable guidance and recommendations during the site investigation and construction stages of the work and for his encouragement in the preparation of this paper.

APPENDIX - BIBLIOGRAPHY ON PILE HEAVE

1. Soil Mechanics in Engineering Practice, by Karl Terzaghi and Ralph B. Peck, John Wiley and Sons Inc., New York, N.Y. 1st Ed., 1948, p. 477.
2. Pile Foundations, by Robert D. Chellis, McGraw-Hill Book Co. Inc., New York, N.Y., 1st Ed., 1951, p. 116, p. 414.
3. "The Pile Foundations For The New John Hancock Building In Boston" by Arthur Casagrande, Journal, Boston Soc. of Civ. Engrs., Vol. 34, 1947, p. 297 (Reprinted by Harvard Graduate School of Engrg. as Soil Mechanics Series No. 30).
4. "National Building Code of Canada," 1953 Sect. 4.2.2.4.13.
5. "Foundation Code of the City of New York," 1948, Sect. C-26-405.1, item j.
6. "Proposed Revision to Boston Building Code," Journal, Boston Soc. of Civ. Engrs., July, 1960, Sect. 2980, item h.
7. "A Pile Load Test" by D. F. Coates, The Engineering Journal, March, 1956, p. 228.

Journal of the
SOIL MECHANICS AND FOUNDATIONS DIVISION
Proceedings of the American Society of Civil Engineers

IMPACT WAVES IN SAND: IMPLICATIONS OF AN ELEMENTARY THEORY

By Blaine R. Parkin[1]

SYNOPSIS

Some implications of an elastic-plastic theory for the propagation of unidimensional compression waves in dry Ottawa sand are examined. The theory, which contains an explicit strain-rate effect, has previously been found to give good agreement with experiment. Results from it are compared with elastic and plastic theories of wave propagation in soils. Problems associated with the use and experimental determination of "dynamic" stress-strain curves are considered. Laws of similitude required by the present theory are examined. Tentative design data on the response of impact pressure gages are developed.

INTRODUCTION

Notation.—The letter symbols adopted for use in this paper are defined where they first appear, in the illustrations or in the text, and are arranged alphabetically, for convenience of reference, in the Appendix.

Note.—Discussion open until January 1, 1962. Separate discussions should be submitted for the individual papers in this symposium. To extend the closing date one month, a written request must be filed with the Executive Secretary, ASCE. This paper is part of the copyrighted Journal of the Soil Mechanics and Foundations Division, Proceedings of the American Society of Civil Engineers, Vol. 87, No. SM 4, August, 1961.

[1] Engineer, RAND Corp., Santa Monica, Calif.

A detailed comparison between a theory of elastic-plastic wave propagation in a strain-rate sensitive material and experimental results[2,3,4] for impact wave propagation in columns of dry Ottawa and Fort Peck sands have been previously presented.[5] The fact that the theory has the striking ability to reproduce a number of important experimental trends with considerable precision would seem to give it credibility as a mathematical model for these particular soils.

Of course, there is a difference between saying that a particular phenomenological theory is credible, and saying that a theory for the dynamic response of even a relatively simple soil such as dry sand has been established. Much experimental and theoretical work remains to be done before it is possible to say that any theory of dynamic soil behavior has been established. However, the very encouraging comparisons obtained with the drastically simplified theory suggests that it may have some implications of practical value. For this reason results from the present theory will be compared with some other theories of wave propagation in soils. Also, problems connected with the derivation of "dynamic" stress-strain curves from experimental stress histories at fixed points in a sand will be examined. The laws of similitude implied by the present theory will be examined and the present theory will be used to investigate the response of drum-type pressure gages to impact loading.

Because these topics are considered mainly within the framework of the experiments examined previously.[5] The theoretical basis of that analysis will be summarized for completeness. Thus the sand is treated as an elastic-plastic continuum which, for one-dimensional motions, can be described by

$$\frac{\partial p}{\partial x} + \rho \frac{\partial v}{\partial t} = 0 \quad \ldots\ldots\ldots\ldots\ldots\ldots (1)$$

$$\frac{\partial \epsilon}{\partial t} + \frac{\partial y}{\partial x} = 0 \quad \ldots\ldots\ldots\ldots\ldots\ldots (2)$$

and

$$E \frac{\partial \epsilon}{\partial t} - \frac{\partial p}{\partial t} = \begin{cases} k\left[p - f(\epsilon)\right], & p \geq f(\epsilon) \\ 0, & p < f(\epsilon) \end{cases} \quad \ldots\ldots\ldots\ldots (3)$$

The quantities t and x denote the time and the Lagrange coordinate along the sand column respectively. The quantity $\epsilon(x, t)$ denotes the compressive longitudinal strain, $p(x, t)$ denotes the compressive longitudinal stress, and the stress $f(\epsilon)$ is a function which defines the static stress-strain curve. The Young's modulus E is defined as the slope of the static stress-strain curve

---

[2] "The Behavior of Soils Under Transient Loadings," by R. V. Whitman, Proceedings, 4th Internatl. Conf. on Soil Mechanics and Foundation Engrg., Butterworths Scientific Publications, London, 1957.

[3] "The Behavior of Soils Under Dynamic Loadings, 3," by R.V. Whitman, et al., Final Report on Laboratory Studies, M.I.T., Dept. of Civ. and San. Engrg. Soil Mechanics Lab., August, 1954, AFSWP-118, Contract DA-49-129 Eng-227, Office of the Chf. Engr., ASTIA No. AD-64032.

[4] "The Behavior of Soils Under Dynamic Loadings, 2, Interim Report on Wave Propagation and Strain-Rate Effect," by D. W. Taylor and R. V. Whitman, M.I.T., Dept. of Civ. and San. Engrg. Soil Mechanics Lab., July, 1953, AFSWP-117, Contract DA-49-129 Eng-227, Office of Chf. Engr., ASTIA No. AD-28-650.

[5] "Impact Waves in Sand: Theory Compared with Experiments on Sand Columns," by Blaine R. Parkin, Proceedings, ASCE, Vol. 87, No. SM3, June, 1961.

$f'(\epsilon)$ at zero stress. The longitudinal particle velocity is denoted by $v(x, t)$. The initial density of the sand is assumed to be given by the constant ρ. The strain rate constant is k. In the idealized material obeying Eqs. 1, 2 and 3 disturbances propagate with the speed of sound $c = \sqrt{E/\rho}$. Eqs. 1, 2 and 3 have been given previously by Malvern.[6,7]

We shall apply the preceding equations to the mechanical system shown schematically in Fig. 1. In Fig. 1 m denotes the mass of the gage; S is the stiffness of the gage spring; V(t) refers to the gage velocity, at impact end; v(0, t) represents the sand particle velocity, at the impact end; and v(l, t) denotes the sand particle velocity, at the reaction end. In this illustration the sand occupies the interval between x = 0 and x = l. The stress gage at each end of the sand column consists of two lumped parameter elements; a mass m and a spring of stiffness S. The system is started from rest by giving impulsively

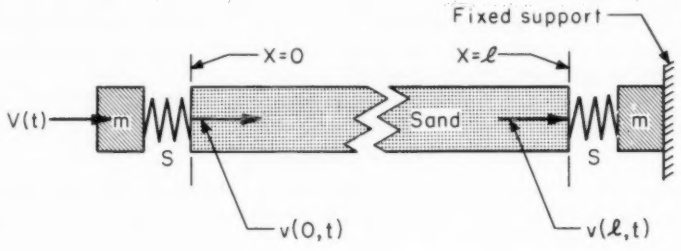

FIG. 1.—IDEALIZED EXPERIMENTAL ARRANGEMENT

the velocity V_0 to the mass of the right hand gage. Thus Eqs. 1, 2 and 3 are subject to the initial conditions

$$V(0) = V_0 \quad \ldots\ldots\ldots\ldots\ldots\ldots \quad (4a)$$

and

$$p(x, 0) = \epsilon(x, 0) = v(x, 0) = 0 \quad \ldots\ldots\ldots\ldots \quad (4b)$$

in which V_0 is the initial impact gage velocity. The boundary conditions which apply on the right hand or the impact end of the column are

$$m \frac{dV}{dt} + p(0, t) = 0 \quad \ldots\ldots\ldots\ldots\ldots\ldots \quad (5)$$

and

$$\frac{dp}{dt} = S\left[V(t) - v(0, t)\right] \quad \ldots\ldots\ldots\ldots\ldots\ldots \quad (6)$$

and as a result of the constitutive Eq. 3,

$$E \frac{d\epsilon}{dt} - \frac{dp}{dt} = \begin{cases} k\left[p(0, t) - f(\epsilon)\right], & p \geq f(\epsilon) \\ 0, & p < f(\epsilon) \end{cases} \quad \ldots\ldots\ldots \quad (7)$$

6 "Plastic Wave Propagation in a Bar of Material Exhibiting a Strain-Rate Effect," by L. E. Malvern, Quarterly of Applied Mathematics, Vol. 8, pp. 405, 1951.

7 "The Propagation of Longitudinal Waves of Plastic Deformation in a Bar of Material Exhibiting a Strain-Rate Effect," by L. E. Malvern, Transactions, ASME, Vol. 18, 1951, p. 203.

At the left hand or reaction end the boundary conditions are

$$\frac{dp}{dt} = S\,v(1, t) \quad \ldots\ldots\ldots\ldots\ldots\ldots \quad (8)$$

and

$$E\frac{d\epsilon}{dt} - \frac{dp}{dt} = \begin{cases} k\left[p(1, t) - f(\epsilon)\right], & p \geq f(\epsilon) \\ 0 & , p < f(\epsilon) \end{cases} \quad \ldots\ldots\ldots \quad (9)$$

Eqs. 1 through 9 determine the functions $p(x, t)$, $\epsilon(c, t)$, $v(x, t)$ and $V(t)$. In some cases near the start of the motion, the function $V(t)$ in Eqs. 5 and 6 will not vary greatly from its initial value V_o. These two equations can then be approximated with the single boundary condition

$$\frac{dp}{dt} = S\left[V_o - v(0, t)\right] \quad \ldots\ldots\ldots\ldots\ldots\ldots \quad (10)$$

It will be necessary herein to refer to experimental conditions discussed previously.[5] Values of the parameters k and S will be used which are derived from the Ottawa sand data with no corrections being applied to them. Thus from the writer's previous work[5]

$$k = 2.62 \times 10^4 \text{ per sec}$$

and

$$S = 4.6 \times 10^3 \text{ lb per cu in.}$$

This value of S corresponds to the impact gage stiffness. The corresponding value for the stiffness of the reaction gage used in the tests is uncertain but it appears that the value

$$S = 18 \times 10^3 \text{ lb per cu in.}$$

is a satisfactory choice. The gage mass m had the dimensions of mass per unit area. In gravitational units the value of m obtained from the data given by R. V. Whitman, M. ASCE[2] is

$$m = 0.00494 \text{ lb sec}^2 \text{ per cu in.}$$

The values of other physical constants appropriate to Ottawa sand having an initial void ratio e of about 0.53 are

$$E = 40{,}000 \text{ psi}$$

$$\rho = .00016 \text{ lb sec}^2 \text{ per in.}^4$$

and

$$c = 15{,}600 \text{ in. per sec}$$

in which c is the elastic wave speed.

COMPARISON OF THEORIES

In this section we shall not attempt to exhaust the topic. For example if the reader wishes to compare the present results with those obtained from a visco-elastic-plastic type of theory he must compare the present findings with those of R. H. Smith and Nathan M. Newmark,[8] F. ASCE. Moreover, di-

[8] Numerical Integrations for One-Dimensional Stress Waves, by R. H. Smith and N. M. Newmark, Civ. Engrg. Structural Research Series, No. 162, A Technical Report to the Office of Naval Research Dept. of the Navy under Contract Nonr 1834(03) Proj. NR064 183, Dept. of Civ. Engrg., Univ. of Illinois, Urbana, Ill., August, 1958.

rect calculations for an elastic-plastic material will not be found in this paper, although we shall give some attention to the determination of "dynamic" stress-strain curves by the use of such a theory.

Elastic Wave Propagation.—In many investigations concerning the dynamic response of soil it is customary to consider the soil as an elastic substance. The elastic parameters for the soil are derived from measurements of seismic wave speeds in the medium. Such a procedure might be useful for cohesionless masses of sand as long as the amplitudes of the stress waves do not differ greatly from zero. Otherwise it would seem that the plasticity of the medium must be considered.

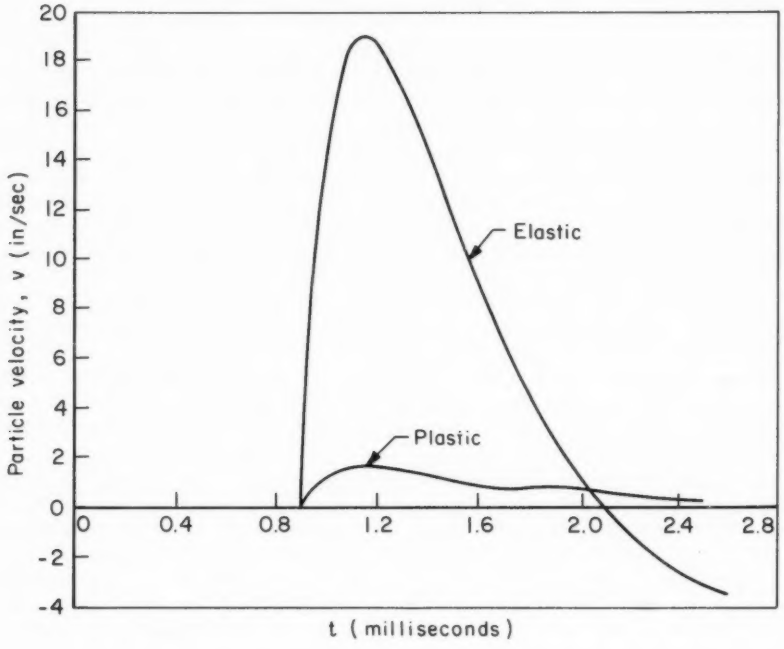

FIG. 2.—PARTICLE VELOCITIES VERSUS TIME (REACTION END, 14 IN. COLUMN)

In support of this view results are compared from the present theory with those of wave propagation in an elastic medium having the same wave speed and density as the idealized Ottawa sand. It is imagined that 14-in. columns of both substances are subjected to identical impacts at $V_0 = 60$ in. per sec. The impact-end and reaction-end stress gages of both columns have stiffnesses as specified previously. Similarly the strain-rate parameter k for the idealized sand is that specified in the "Introduction." An example from these calculations is shown in Fig. 2 in which the curve labeled "plastic" results from the present theory.

It has already been noted[5] that the peak stress at the impact end of the column is significantly overestimated by elastic-wave calculations. As was shown,[5] the degree of this overestimate depends upon the values assigned to the parameters k and S in the plastic theory. Of course this finding is obtained from preliminary estimates of the behavior of the elastic column which approximates only the first stress peak at the impact end of the rod. More elaborate calculations show several stress peaks at both reaction and impact ends of an elastic column which result from waves being reflected at these surfaces. The highest compressive stress occurs for the present configuration at the reaction end of an elastic column as the result of the first reflection. On the other hand, the present theory, which includes plasticity, shows that the reaction-end stress is essentially limited by the static strength of the sand, even though some strain rate and reflection effects may be present. These factors combine to produce dramatic differences in reaction end response of the two media in terms of stresses, particle accelerations, particle velocities and particle displacements. It was found that peak values of these quantities differ by an order of magnitude.

Finally it is observed that the striking differences in the response of the plastic and the elastic media are in large part due to the method by which the wave motions are excited in them, and that these waves are longitudinal waves in bars. Changes in either of these factors would result in quantitative variations in the response of both elastic and plastic materials, although in many situations the qualitative sense of the present results will be preserved.

Simple Waves and Dynamic Stress-Strain Curves.—In this paper a possible constitutive relationship for a homogeneous granular medium has been studied which relates the properties of the substance under dynamic conditions to those measured under static conditions. To find such a constitutive relationship which is valid for any solid substance poses many difficult problems. It is rather remarkable that the simple law used here represents dry sand as well as it does.

Of course, the present viewpoint is not the only one which might be considered for studies of wave propagation in homogeneous solids. Indeed, a view which certainly antedates that of the present study concerns substances in which the constitutive relationship, or stress-strain law, depends only on the instantaneous strain and not at all on the rate of straining. In such cases one imagines that the stress-strain law appropriate to the medium in a dynamic situation may or may not resemble the static stress-strain curve of the substance. As already noted, the essential idea is that whatever the detailed nature of the dynamic stress-strain curve, it must be dependent only upon the strain. There is only an incidental interest in any relationship between the static and the dynamic stress-strain curves. The problem then, is to determine the form of this dynamic stress-strain curve from observations of wave propagation in the medium. If the medium were truly strain-rate independent for the range of strain rates of interest, the dynamic stress-strain curve would then form the basis for predictions of the response of the medium to various dynamic loads. There has never been doubt that two theoretical models, one including strain-rate effects and the other excluding this factor, will generally lead to differing results. The purpose here is to examine whether or not the additional concept of the dynamic stress-strain curve, when used with a theory which excludes strain rate effects, can lead to satisfactory estimates concerning the process of wave propagation in a strain-rate sensitive soil.

The first investigator to address himself to this problem as it might apply to wave propagation in soils appears to have been G. I. Taylor.[9] Taylor sought to determine the plastic stress-strain relationship that the material must obey in order that the velocity-time relationship observed at a fixed station within a plastic bar may be dynamically possible. Later C. W. Lampson[10] used similar ideas to determine dynamic stress-strain relationships from pressure observations at points in soil close to the point of high explosive detonations. Lampson's results are derived from experiments in which spherical or at least axial symmetry prevailed, and he used a heuristic procedure to correct his pressure-time data for the effects of spherical spreading. This complication is not considered herein. Rather, like Taylor, a physical space of only one dimension defined by the longitudinal extent of the sand column is considered.

The possibility that one might be able to deduce dynamic strains and particle velocities from stress (or strain) measurements at fixed stations in a soil is grounded in the theory of simple waves.[11] This theory is valid for media which exhibit no strain-rate sensitivity. (Strictly speaking the equations of motion in the material must be "reducible."[11] For example, simple wave solutions cannot be found for spherically symmetric motions even if there is no strain-rate effect.) One manifestation that this theory might be applicable in a given situation is that travel-time curves of constant stress level in the medium should plot as straight lines. In spite of the fact that the present theory includes a strain-rate effect Malvern noted that, in a Lagrange diagram, contours of constant strain from his calculations resemble closely similar contours deduced from simple wave theory. However, Ottawa sand appears to be far more strain-rate sensitive than the metal considered by Malvern, so that travel time curves of constant stress from the present theory show a modest curvature. The particular example chosen for study corresponds to an impact at 115 in. per sec in a semi-infinite column of sand. Travel-time curves were plotted for a short interval following the impact. The resulting plot does not resemble a simple wave solution until disturbances have traveled at least 6 in. into the sample. At later times when stress relaxation effects occur the resemblance is lost. Therefore for the present case it is plausible to use simple wave theory for the calculation of dynamic stress-strain curves only during the first part of the loading when the stress is rising. Clearly, the results obtained depend upon the position in the medium as well as the intensity of the impact.

One useful question might concern the application of a simple-wave analysis to experimental data in the following way. Suppose for example, that experimental travel-time curves of constant stress in a strain-rate sensitive material have been obtained. Suppose further that this material is accurately described by the present theoretical model. Can simple-wave analysis be used to obtain at least approximate histories of the particle velocities and

9 "Propagation of Earth Waves from an Explosion," by G. I. Taylor, Paper written for Ministry of Home Security, 1940. See The Scientific Papers of G. I. Taylor, Vol. I, "Mechanics of Solids," Cambridge Univ. Press, 1958, pp. 456.

10 Final Report on Effects of Underground Explosions, by C. W. Lampson, NDRC Report No. A479, OSRD Report No. 6645, 1946. See Also Appendix B, pp. 410 in The Effects of Atomic Weapons, U. S. Govt. Printing Office and the Combat Forces Press, Washington, D. C., 1950.

11 Supersonic Flow and Shock Waves, by R. Courant and K. O. Friedrichs, Interscience Publishers, Inc., New York, 1945, Sec. 99, pp. 240.

strains in the medium? Figs. 3 and 4 dynamic stress-strain curves and particle velocity versus time curves for two fixed stations in the sand are presented in answer to this question. These positions are located at x = 2 in. and at x = 12 in. from the impact end of the sample. At both stations it will be noted that, at a given stress, the strain calculated from the simple wave

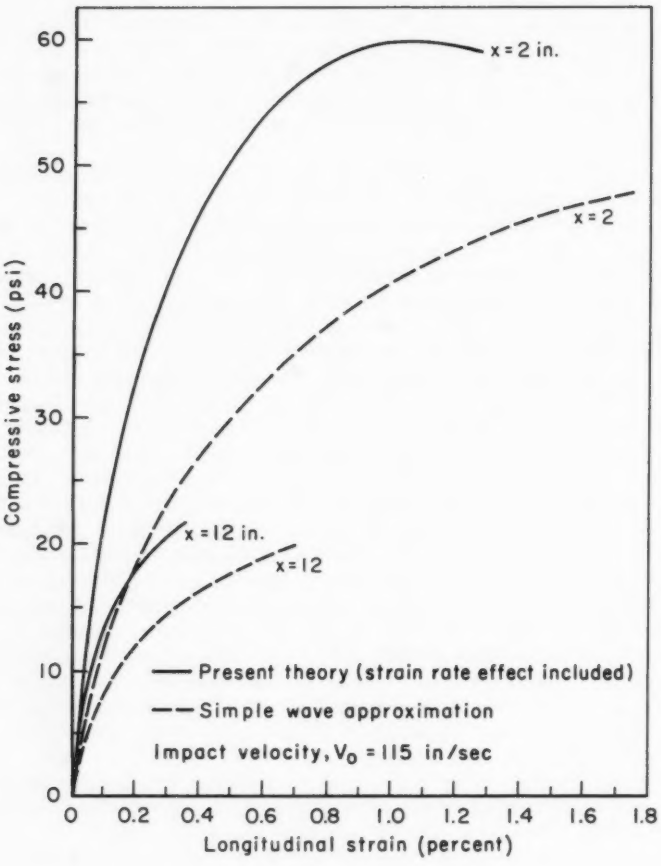

FIG. 3.—DYNAMIC STRESS-STRAIN CURVES OBTAINED FROM THE PRESENT THEORY COMPARED WITH DYNAMIC STRESS-STRAIN CURVES OBTAINED BY USE OF SIMPLE-WAVE THEORY

assumption exceeds the strain calculated from the present theory by a factor of approximately two. Similarly, at a given instant of time, and therefore at a given stress, the particle velocity obtained from simple wave computations exceeds that obtained from the present theory by nearly 50% at x = 12 in. When x = 2 in. this excess in particle velocity amounts to about 20%. Evidently

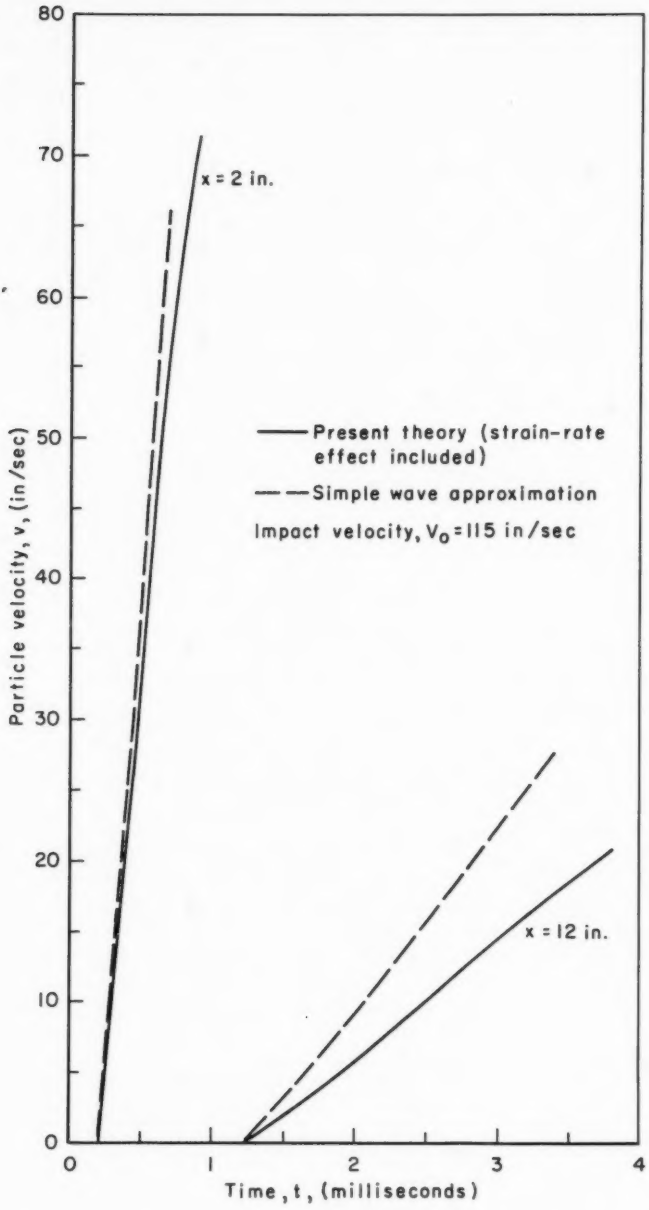

FIG. 4.—COMPARISON BETWEEN PARTICLE VELOCITY-TIME CURVES CALCULATED BY MEANS OF STRAIN-RATE SENSITIVE AND SIMPLE WAVE THEORIES

the simple wave approximation is chiefly of qualitative value in soil dynamics problems where appreciable strain-rate effects are involved. On the other hand comparison of these results with the elastic calculations examined previously indicates that the plastic behavior of the soil is an essential ingredient which, even more than strain-rate effects, must be accounted for in discussions of intense wave propagation in soils.

SIMILITUDE

Dynamic tests on sand bring into prominence certain properties of the material which are not of crucial importance in static tests, and the question then arises as to the proper method of extrapolating results from dynamic tests in the laboratory in order to predict the dynamic behavior of a sand formation in the field, or as to the proper method of correlating existing laboratory results. Of course, the information now available does not permit a complete answer to this question. However, the success obtained with the present theory leads to the hope that its use to indicate a partial answer will not be premature.

The aims and methods of the theory of similitude certainly do not need illucidation here. It is sufficient to note that characteristic physical quantities for the present idealized substance are defined by the parameters ρ, E, k and $f(\epsilon)$. If we call the characteristic length l, we find from the usual sort of analysis that we may relate the characteristic time to this length by means of the characteristic wave speed c given in the Introduction. In particular it is found that if quantities (kl/c) and $f(\epsilon)/E$ have the same values in the laboratory as they do in the field, then scaling laws of the sort proposed by Lampson,[10] or in a slightly more general form by Parkin,[12] are valid. (G. Birkhoff[13] has grouped such scaling laws under the heading of Mach similitude.) The first of these two quantities $\left(\frac{l\,k}{c}\right)$, is similar in form to the quantity which must be held constant in order that these scaling laws may be used for linear viscoelastic substances. This result could have been foreseen from the existence of a certain likeness of the differential Eqs. 1, 2 and 3 to the equations of motion for a Kelvin-Voigt solid.

The similarity requirements brought about by the plasticity of the medium depends upon the value $f(\epsilon)/E$. And as also found for the elastic-plastic material,[12] this requirement indicates that motions in the two materials will be similar only if every ordinate of their static stress-strain curves are properly proportioned. This proportionality must be constant, ordinate for ordinate, at every strain within the range of interest. The formal stringency of this condition is obvious. General knowledge of the precision with which it must be satisfied would be desirable. From the particular cases studied here it was found that for some purposes it may be possible to relax this requirement whereas for others it must be rigidly satisfied. In this connection it is noteworthy that R. L. Bjork[14] has found that a condition similar to the writer's

12 A Review of Similitude Theory in Ground Shock Problems, by B. R. Parkin, The RAND Corp., Santa Monica, Calif., Research Memorandum RM-2173, April, 1958 (ASTIA Doc. No. AD156012).

13 Hydrodynamics, by G. Birkhoff, Princeton Univ. Press, 1950.

14 Numerical Solutions of the Axially Symmetric Hypervelocity Impact Process, by R. L. Bjork, The RAND Corp., Santa Monica, Calif., RAND Paper No. P-1661, April, 1959.

plasticity requirement must be satisfied in order that experimental results from hypervelocity impact of metals may be properly scaled with impact velocity. In this case the pressures involved are so high that the metals become fluid and it becomes necessary to speak of an equation of state rather than a stress-strain curve. In the present case the existence of two parameters which must be specified, in order that the customary scaling laws may be validly applied, places rather severe restrictions upon the scaling of laboratory results. This difficult situation may be severely aggravated if the nature of the external agency which produces the motion in the medium must also be taken into account. For example, if one wished to scale the results obtained from the system illustrated in Fig. 1, he must be certain that the additional parameters $U_0 = \frac{V_0}{c}$, $\alpha = \frac{S\,c}{E\,k}$ and $\beta = \frac{S}{m\,k^2}$ are kept invariant in the transformation, although as shall be seen in the subsequent analysis of the linearized theory, there are some conditions of limited applicability in which the last of these added constraints may be ignored.

LINEARIZED THEORY

In order to linearize the equations of motion, Eqs. 1, 2 and 3, it is necessary only to replace the nonlinear static stress-strain relationship in Eq. 3 by a linear function. In terms of the dimensionless stress $\sigma = p/E$ such a linear function may be written as

$$f(\epsilon) = E\left[\sigma - \sigma_0 - \theta\,(\epsilon - \epsilon_0)\right] \quad \ldots\ldots\ldots\ldots \quad (11)$$

in which θ determines the slope of the line and $(E\,\sigma_0, \epsilon_0)$ give the coordinates of an arbitrarily chosen point upon it. For example if $\epsilon_0 = \sigma_0 = 0$ and $\theta = 1$ the medium will be taken to be elastic, whereas if $\theta = 0$ for some σ_0 and for some range in ϵ, the substance is perfectly plastic within this ϵ-interval.

In order to systematize the calculations it is helpful to introduce dimensionless variables similar to those used by Malvern.[6] Thus,

$$y = \frac{x\,k}{c} \quad \ldots\ldots\ldots\ldots\ldots\ldots\ldots \quad (12a)$$

$$\tau = k\,t \quad \ldots\ldots\ldots\ldots\ldots\ldots\ldots \quad (12b)$$

$$\sigma = \frac{p}{E} \quad \ldots\ldots\ldots\ldots\ldots\ldots\ldots \quad (12c)$$

and

$$u = \frac{v}{c} \quad \ldots\ldots\ldots\ldots\ldots\ldots\ldots \quad (12d)$$

Introducing these new variables and Eq. 11 into the equations of motion yields the linear system

$$\frac{\partial u}{\partial \tau} + \frac{\partial \sigma}{\partial y} = 0 \quad \ldots\ldots\ldots\ldots\ldots\ldots \quad (13a)$$

$$\frac{\partial u}{\partial y} + \frac{\partial \epsilon}{\partial \tau} = 0 \quad \ldots\ldots\ldots\ldots\ldots\ldots \quad (13b)$$

and

$$\frac{\partial \epsilon}{\partial \tau} - \frac{\partial \sigma}{\partial \tau} = \sigma - \sigma_0 - \theta\left(\epsilon - \epsilon_0\right) \quad \ldots\ldots\ldots\ldots \quad (13c)$$

It may be required to find solutions to Eqs. 13 corresponding to a variety of conditions. However, the present examination will be restricted to consideration of the first part of the motion of particles near the impact end of a sand column. In this case the simplified boundary condition of Eq. 10 may be used on the surface x = 0. Since no reflections at the surface x = 1 will be considered conditions at that point may be replaced by the condition that all stresses, strains and particle velocities must vanish at large distances from x = 0. Thus, the modified boundary conditions may be written in terms of dimensionless variables as

$$\frac{d\sigma}{d\tau} = \alpha \left[U_o - u(0, \tau) \right] \quad \ldots\ldots\ldots\ldots\ldots\ldots (14a)$$

and

$$\sigma(\infty, \tau) = 0 \quad \ldots\ldots\ldots\ldots\ldots\ldots (14b)$$

In Eq. 14a the quantity U_o denotes the dimensionless variable corresponding to the impact velocity V_o and the parameter α denotes the dimensionless ratio

$$\alpha = \frac{S\,c}{E\,k} \quad \ldots\ldots\ldots\ldots\ldots\ldots (15)$$

Because the motion is started from rest, the initial conditions are given by

$$\sigma(y, 0) = u(y, 0) = \epsilon(y, 0) = 0 \quad \ldots\ldots\ldots\ldots (16)$$

The linearized theory will be used herein to consider only those cases for which that part of the static stress-strain curve through the origin is approximated by a straight secant. Therefore ϵ_o and σ_o are made equal to zero in Eqs. 11 and 13. The Laplace transform of $\sigma(y, \tau)$, $u(y, \tau)$ or of $\epsilon(y, \tau)$ are denoted by superscribing a bar over the appropriate symbol as follows (the parameter s is not to be confused with the displacement s(x, t) previously defined[5]):

$$\bar{\sigma}(y, s) = \int_o^\infty \sigma(y, \tau) e^{-s\tau}\, d\tau \quad \ldots\ldots\ldots\ldots (17)$$

Eqs. 13 and 14 may then be transformed to find that $\bar{\sigma}(y, s)$ is given by

$$\bar{\sigma} = \frac{\alpha\, U_o\, e^{-ys\sqrt{\frac{s+1}{s+\theta}}}}{s\left[s + \alpha\sqrt{\frac{s+1}{s+\theta}} \right]} \quad \ldots\ldots\ldots\ldots\ldots (18)$$

For an elastic solid $\theta = 1$, the linearized theory becomes exact, and Eq. 18 reduces to

$$\bar{\sigma} = U_o \left[\frac{1}{s} - \frac{1}{s+\alpha} \right] e^{-ys} \quad \ldots\ldots\ldots\ldots\ldots (19)$$

The inverse of this transform is known to be[15]

$$\sigma(y, \tau) = \begin{cases} U_o \left[1 - e^{-\alpha(\tau - y)} \right], & (\tau - y) \geq 0 \\ 0, & (\tau - y) < 0 \end{cases} \quad \ldots\ldots\ldots (20)$$

---

15 Modern Operational Mathematics in Engineering, by R. V. Churchill, McGraw-Hill Book Co., Inc., New York, 1944.

If Eq. 20 is expressed in terms of real time and space instead of the dimensionless variables τ and y it will be seen that this result is independent of the strain-rate parameter, k. This well-known relationship has been rederived here because it will be needed later and, because it emphasizes the fact that when a spring suddenly pushes against the end of an elastic rod the elementary theory of one-dimensional wave propagation predicts a monotonic rise in the stress immediately after the impact to a maximum limiting value. When U_o is constant as assumed, an initial stress spike or peak does not occur. The rate of stress rise for a particular elastic material depends only upon the gage stiffness, S.

Impact Gage Response in a Strain-Rate Sensitive Medium.—Because the primary interest is in events which occur at the impact surface y = 0, we shall put y = 0 in Eq. 18. In this special case the transform becomes

$$\bar{\sigma}(0, s) = \alpha U_o \left\{ \frac{s+\theta}{s^3 + \theta s^2 - \alpha^2 s - \alpha^2} - \frac{\alpha (s+1)(s+\theta)}{s\left(s^3 + \theta s^2 - \alpha^2 s - \alpha^2\right)} \frac{1}{\sqrt{(s+1)(s+\theta)}} \right\} \quad . . \quad (21)$$

and its inverse may be found with the aid of a convolution. The precise nature of the inverse depends upon the order and the affix of the poles of $\bar{\sigma}(0, s)$ in the complex s-plane. Simple poles which are located on the real axis in the s-plane lead to real exponential functions in the inverse, and poles which are located off this axis imply an inverse transform involving trigonometric functions. In order to determine when we will have one or the other of these solutions, we must find the positions in the complex s-plane of the zeros of the cubic,

$$q(s) = s^3 + \theta s^2 - \alpha^2 s - \alpha^2 \quad \ldots\ldots\ldots\ldots \quad (22)$$

for various values of θ and α.

It may be verified that if the condition

$$\theta^3 + \frac{\alpha^2}{4}\theta^2 + \frac{9}{2}\alpha^2 \theta - \alpha^2\left(\frac{24}{7} - \alpha^2\right) \geq 0 \ldots\ldots\ldots \quad (23)$$

is satisfied all roots of $q(s) = 0$ will be real. As it happens, $q(s) = 0$ has one root which is real and positive for all θ in $0 \leq \theta \leq 1$, but if the condition of Eq. 23 is not satisfied the remaining roots will be complex. If only the equality in Eq. 23 is considered this equation defines a locus of points in a $\theta - \alpha$ plane which divides the plane into two regions. In one area the solution $\sigma(0, t)$ will involve circular functions. In the egion of the $\theta - \alpha$ plane exterior to this area $\sigma(0, t)$ will involve hyperbolic functions. Fig. 5 shows that portion of the $\theta - \alpha$ plane which is of physical interest. Points inside the curve correspond to solutions involving complex roots so that an initial spike in the impact stress records is to be expected. If a point (α, θ) lies on the curve or in the area outside of it, the fact that the linearized solution does not contain complex exponentials is not sufficient to exclude an initial spike from the impact stress record. Whether or not the linearized result predicts a monotonic stress rise without an initial peak depends upon the precise location of the particular point (α, θ) with respect to the locus. In passing it is noted that according to Eq. 20 all points on the line $\theta = 1$, that correspond to an elastic medium, are not in a domain of the $\alpha - \theta$ plane where initial stress spikes occur. When the point (α, θ) does not lie on this line the question of whether or not a stress spike will occur is not simply resolved.

In order to clarify this point and to test the accuracy of the linearized theory the inverse transform $\sigma(0, \tau)$ was determined and the resulting formulas were evaluated numerically for values of α and θ corresponding to the points A, B and C of Fig. 5. The numerical results from the linearized theory were then compared to corresponding results from the nonlinearized theory. The linearized theory was found to give results which were in satisfactory agreement with stress histories obtained by the method of characteristics.

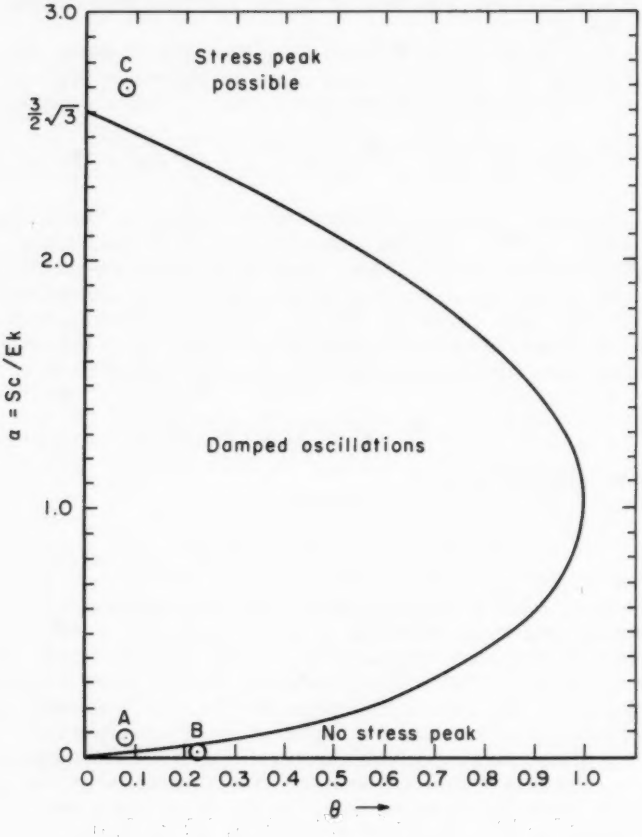

FIG. 5.—IMPACT GAGE RESPONSE DIAGRAM

In the numerical evaluation of the linearized theory the value of α at point A was computed from known values of E and c for Ottawa sand together with the gage stiffness S and the strain-rate parameter k from the introduction. The selection of a proper value of θ is somewhat bothersome because we must know in advance the range in the strain, $\epsilon(0, \tau)$, which will occur shortly after impact. For a given material the amount of strain will depend largely

upon the impact velocity V_0. This property is used in the present study by selecting the slope of the secant to the static stress-strain curve θE, so that this line intersects the static curve $f(\epsilon)$ at $\epsilon = 0$ and at that value of ϵ corresponding to the peak stress immediately after an impact. For Ottawa sand the necessary data may be taken from the calculations that lead to Fig. 8 of the writer's previous work.[5] The results for ϵ and $f(\epsilon)$ give values of θ for a range of impact velocities V_0 as shown in Fig. 6. Thus it is seen that the point A of Fig. 5 falls within the experimental range for Ottawa sand. Fig. 6, although constructed in a rather arbitrary manner, is useful because it indicates, at least qualitatively, how one might account for the value of V_0 in his choice of θ. It seems likely that for impact velocities that are significantly greater than those considered here, it would introduce little error if one were

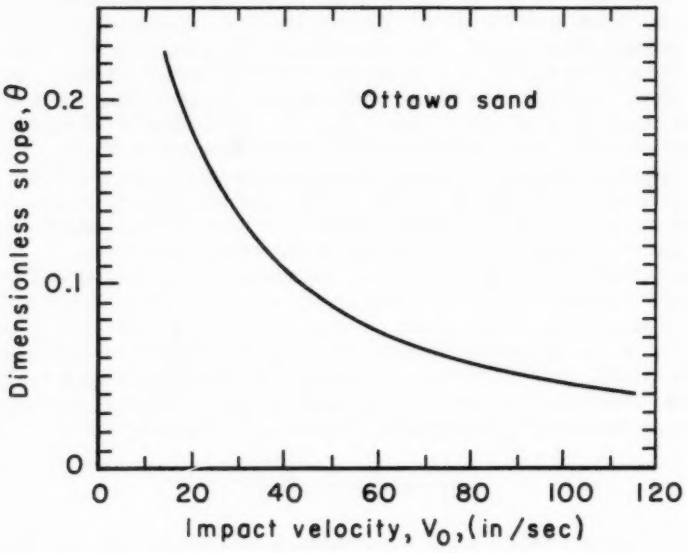

FIG. 6.—EFFECT OF IMPACT VELOCITY UPON CHOICE OF LINEAR STRESS-STRAIN CURVE SLOPE

to carry out the present development of the linearized theory with $\theta = 0$. (This additional simplification has been found useful for the calculations of the initial response of the impact gage to a second impact.)[16]

The three examples from the linearized theory at points A, B and C in Fig. 5 and the result given by Eq. 20 for the elastic medium permit a full interpretation of Fig. 5. It seems clear from both the linearized and the nonlinear theories that if α and θ are chosen so that the point in the $\alpha - \theta$ plane lies below the lower branch of the curve of Fig. 5 then the impact stress-time

[16] Impact Wave Propagation in Columns of Sand, by B. R. Parkin, The RAND Corp., Santa Monica, Calif., Research Memorandum RM-2486, November, 1959, ASTIA No. AD234961.

record should show no peak. If the point (α, θ) is inside this locus the first part of the stress-time record should show a peak. Moreover, for this case the linearized theory indicates that the solution is oscillatory in form and that these oscillations are damped. Finally, when the point (α, θ) is above the upper branch of the curve a stress peak may be expected in the impact records. This peak is not associated with oscillatory solutions; and as $\theta \rightarrow 1$, that is, as the medium approaches perfect elasticity, the stress spike should vanish.

CONCLUSIONS

The consequences of choosing alternative theoretical assumptions regarding the propagation of longitudinal stress waves in dry Ottawa Sand have been compared. For example, suppose calculations are matched to the experimental seismic wave speed but the study of large amplitude wave propagation in the medium are based upon the theory of elasticity. Then compared to the present theory, or any other theory that accounts for the plasticity in the medium, elastic calculations can lead to significant overestimates of stresses, particle displacement, particle velocities and particle accelerations in the soil.

On the other hand one might wish to include the assumption of plasticity in his calculations but use a "dynamic" stress-strain curve in order to avoid taking account of strain-rate effects. If strain-rate effects are important then, depending upon the magnitude of the strain-rate parameter, it appears that this procedure may lead to results which are no more accurate than would be obtained by a straightforward neglect of all strain-rate effects.

In the present simplified theory the occurrence of the impact stress peak of the experiments is ascribed entirely to an interaction of the strain-rate sensitivity and static stress-strain properties of the medium with the elastic compliance of the impacting stress gage. On this basis it has been possible to derive design criteria for impact stress gage response under a variety of conditions. The possible usefulness of these results in experimental assessments of the strain-rate sensitivities of soils may be noted.

ACKNOWLEDGMENTS

The preceding results have been made available through the efforts of Mrs. Susan Belcher who carried out the numerical work, of Mrs. Madelon Lopez who prepared the manuscript, and of G. I. Margadonna and his staff who have drawn the illustrations.

APPENDIX.—NOTATION

The terms used in this paper are listed here for convenience of reference and for the use of discussers:

c = elastic wave speed;

E = Young's modulus (slope of static stress-strain curve at zero stress);

f, $f(\epsilon)$ = static stress-strain curve;

k = strain-rate parameter;

m = mass of gage per unit area;

p = compressive stress;

S = gage spring stiffness (pressure/deflection);

t = time;

$u = \frac{v}{c}$ = dimensionless particle velocity;

$U = \frac{V}{c}$ = dimensionless impact gage velocity;

$U_o = \frac{V_o}{c}$ = dimensionless initial impact gage velocity;

v = particle velocity;

V = impact gage velocity;

V_o = initial impact gage velocity;

x = Lagrange coordinate along sand column;

y = dimensionless Lagrange coordinate along sand column;

$\alpha = \frac{S\,c}{E\,k}$;

$\beta = \frac{S}{m\,k^2}$;

ϵ = compressive longitudinal strain;

ρ = initial density of sand;

$\sigma = \frac{p}{E}$ = dimensionless compressive stress; and

$\tau = kt$ = dimensionless time.

Journal of the
SOIL MECHANICS AND FOUNDATIONS DIVISION
Proceedings of the American Society of Civil Engineers

DISCUSSION

Note.—This paper is a part of the copyrighted Journal of the Soil Mechanics and Foundations Division, Proceedings of the American Society of Civil Engineers, Vol. 87, No. SM 4, August, 1961.

DYNAMIC TESTING OF PAVEMENTS[a]

Addendum to Closure by W. Heukelom and C. R. Foster

W. HEUKELOM[35] and C. R. FOSTER,[36] F. ASCE.—The final paragraph of the closure published on page 153, in the April 1961 Journal of the Soil Mechanics and Foundations Division (Proc. Paper 2804) should be deleted and replaced by the following:

The numerical evaluation of the damping force, considered by A. A. Eremin, M. ASCE, is not based on Eq. 15 but on a combination of Eqs. 15 and 16 from which it can be determined that

$$S \sin \phi = \omega A \quad \ldots\ldots\ldots\ldots\ldots\ldots (29)$$

The value of A is determined by measuring S and ϕ at a known frequency ω.

The writers are grateful to O. M. Christof Ehrler for his remarks and questions. The relationship between the elastic stiffness R and the dynamic deflection of the medium is basically given in Eq. 8. A closer consideration reveals that

$$R = p\, a\, G_m \quad \ldots\ldots\ldots\ldots\ldots\ldots (30)$$

in which G_m is the shear modulus of the medium, p represents the factor which depends on the distribution of the load over the loaded area with radius of a:

$$p = \frac{\pi}{1-\mu} \quad \ldots\ldots\ldots\ldots\ldots\ldots (31a)$$

according to J. Boussinesq[37] for uniform stress,

$$p = \frac{3\pi}{2(1-\mu)} \quad \ldots\ldots\ldots\ldots\ldots\ldots (31b)$$

according to O. K. Frohlich[38] for parabolic stress distribution,

---

[a] February, 1960, by W. Heukelom and C. R. Foster (Proc. Paper 2368).

[35] Konin Klijkel Shell-Laboratorium, Ameterdam (N. V. De Bataafsche Petroleum Naatschappij).

[36] Coordinator of Research, Natl. Bituminous Concrete Assn., Texas Agric. and Mech. College, College Station, Tex. Formerly, Asst. Chf., Soils Div., Corps of Engrs., U. S. Army Engrs. Waterways Experiment Sta., Vicksburg, Miss.

[37] "Application des Potentiels," by J. Boussinesq, Paris, 1885.

[38] "Druckverteilung im Baugrunde," by O. K. Fröhlich, Vienna, 1934.

and

$$p = \frac{4}{1-\mu} \quad \ldots\ldots\ldots\ldots\ldots\ldots (31c)$$

according to I. N. Sneddon[39] for rigid plate conditions.

For the writer's tests, Eq. 31(b) gives the best fit. By comparing the observed values of R and G_m (from wave velocities), the following values of the dynamic Poisson ratio were derived according to Fröhlich:

Soft wet clay	$\mu = 0.42$
Soft loam	$\mu = 0.39$
Hard dry clay	$\mu = 0.37$
Sand	$\mu = 0.36$

from which the writers concluded that the dynamic Poisson constant of soils is 0.4 rather than the value 0.5 which is used in most cases.

Variations of the R-value during vibration have been observed, especially on clay soils and have, so far, been attributed to thixotropy. In the same way, the amplitude of the vibrations affects the stiffness, but this was found to affect primarily the observed value of M and to a much lesser extent the value of R. As far as the observations enable conclusions to be drawn, R can be considered constant.

The mass effect at low frequencies corresponds with

M = 1 to 5 tons for bare soils,

M = 3 to 10 tons for flexible pavements, and

M = up to 50 tons for heavy rigid pavements.

The mass of the vibration machine is 2 tons. The variation of the soil-mass was considered by H. Lorenz.[40]

The value of ϕ has been found to be small in the range of practical loading times t. For various reasons the actual loading time in sustained vibrations must be equal to

$$t = \frac{1}{\omega} = \frac{1}{2\pi f} \quad \ldots\ldots\ldots\ldots\ldots\ldots (32)$$

so that f = 50 cps corresponds to $t \approx 0.003$ sec. Under traffic conditions this is an extremely short time.

Real resonance has been observed at low frequencies of between 5 cps and 8 cps. It is doubtful whether resonance at higher frequencies is real. In the opinion of the writers it is more likely to be connected with variations in the observed mass, which can also give rise to a maximum in the amplitude-versus-frequency curve, thus resembling true resonance where, however, the phase angles would be much greater.

---

39 "Fourier Transforms," by I. N. Sneddon, London, 1951.

40 Grundbau-Dynamik, by H. Lorenz, Springer, 1960.

FOUNDATION VIBRATIONS[a]

Closure by F. E. Richart, Jr.

F. E. RICHART, JR.,[13] F. ASCE.—The writer wishes to thank all the discussers for their generous contributions of ideas and information on the general subject of vibrations of foundations. It is evident that much work remains to be done on the problem of developing satisfactory design procedures for foundations subjected to impulsive or repeated loads.

Coates feels that the repeated static load type of test has practical possibilities for evaluating the behavior of soils under dynamic loads. The writer agrees that a series of plate loading tests at several depths should give useful data, provided that the range of deformations corresponds to that encountered under dynamic loading conditions. In order to obtain reliable load-deformation curves within this loading range, special measuring techniques and apparatus must be used that are several orders of magnitude more sensitive than those customarily used for plate bearing tests. This increased difficulty of measurement also requires skilled test personnel. Consequently, the choice of methodused for local evaluations of a building site, by seismic methods, by steady state vibration methods, or by repeated static loadings depends on the budget available for site exploration. If the static method is to be used as the primary exploration procedure, the writer would still recommend that one of the dynamic methods be used as a check.

With regard to the problem of starting or stopping, the important problem to be resolved is the probable maximum amplitude of vibration to be encountered as the resonant frequency is passed. If the system is highly damped (low value of b) a low magnification of amplitude occurs over a rather wide range of frequency, but intolerable amplitudes of vibration should not occur. The amplitude of oscillation under the steady state condition represents the maximum value to be developed. If this theoretical maximum amplitude is larger than can be tolerated indefinitely, an estimate can be made of the largest amplitude to be developed during starting and stopping by the graphical phase-plane method (see, for example, Jacobsen and Ayre (64)).

The dynamic behavior of foundations subjected to impulsive loads, as by drop hammers can be estimated by use of Fig. 8 if the soil parameters are carefully evaluated for the entire range of stress involved.

In compliance with the suggestion by Coates and Eremin that Fig. 8 be presented with E as a parameter instead of G, Fig. 20 has been prepared as an alternate for Fig. 8(a). By using these coordinates the curves for the constant force oscillator nearly coincide, and those for the rotating mass oscillator appear to move closer together. However, the use of E instead of G as a para-

---

[a] August, 1960, by F. E. Richart, Jr. (Proc. Paper 2564).

[13] Prof. of Civ. Engrg., Univ. of Florida, Gainesville, Fla.

meter ordinarily will not eliminate the need for estimating an effective Poisson's ratio of the soil. The shear wave in a saturated soil is a much more reliable measure of the stiffness of the soil structure than is the compression wave, because the measured value of the latter is influenced by the presence of water. The writer prefers to use the shear modulus, G, as the soil stiffness parameter to be evaluated.

The use of E as a parameter in curves of amplitude factor versus frequency actually causes increased divergence of the curves that can be prepared from the information shown on Fig. 8(b). Consequently, this information is not shown on Fig. 20. It should be noted that Fig. 8(b) is plotted using a different pair of parameters as ordinate and abscissa than are used in Fig. 9(a) and Fig. 10(a). Because of this arrangement, a numerical value of amplitude of vibration for the rotating mass oscillator can be obtained without requiring any eval-

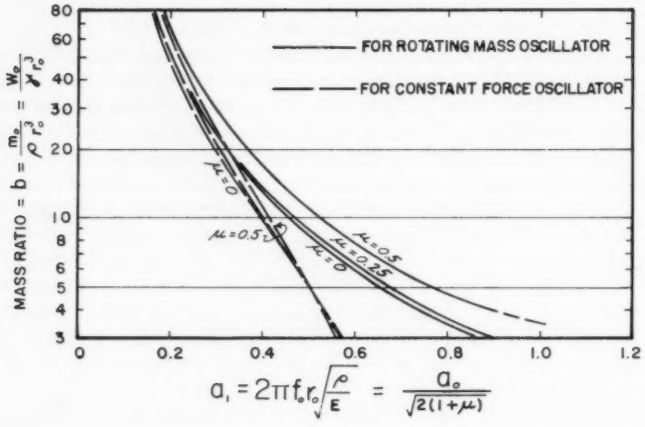

FIG. 20.—ALTERNATE PLOT OF MASS RATIO VERSUS FREQUENCY FACTOR RELATIONS FOR VERTICAL OSCILLATION

uation of G. The practical value of this diagram was pointed out to the writer by R. V. Whitman, M. ASCE, of MIT.

Coates and Perri are correct in pointing out that the radius of gyration of the rectangular prism for an axis through a center line in the base should be $1/3(h^2 + a^2)$. This changes the computed amplitude and frequency in Example B to 0.000176 radius and 218 rpm, respectively.

Alpan has raised objections to the possibility of resonance in a semi-infinite, homogeneous, isotropic elastic body and uses Polz (39) and Christopherson (40) as references to support his contention. Alpan has not carefully identified his referenced information with the problems to which they apply. In the first paragraph of the section under Vertical Impulses Acting at the Surface, the writer has noted that Lamb (17) did not find resonance resulting from a single concentrated load type of impulse which acted on the semi-infinite elastic medium. This is the basis for Christopherson's criticism of the method for determining

the soil constants by a single impulsive load as proposed by Crockett and Hammond. Polz also noted that resonance was not possible for the condition of a concentrated pulsating load, which is again consistent with Lamb's findings.

Resonant conditions may be obtained in semi-infinite, homogeneous, isotropic, elastic solids when the periodic loads are distributed over a finite contact area at the surface of the solid. The study by Polz (39) also showed this and by use of the curves given on Table 1 of his paper with the data for Example A, the computed amplitude of oscillation is very close to that computed from Fig. 8(b). (It should be noted that Polz considers only that case of a constant force type oscillator). It appears that Alpan has not considered the radius of the contact area, r_o, which appears in the expression for resonant frequency (Eq. 11) to represent the characteristic distance required to establish a natural frequency. The expression for frequency (Eq. 11) obtained for the circular contact area and the expression for frequency obtained by Polz (39) which contains a length parameter, h, are all dimensionally consistent with Eq. (21) as well as with the expression for frequency obtained by Lundgren (65) on the basis of dimensional analysis.

Alpan notes that the methods discussed in the paper did not include the problem of damping. The mass ratio, b, represents a measure of the dissapation of energy by elastic waves in the elastic body, but no internal damping of the soil is considered. In most cases, the amplitude of oscillation in the operating frequency range is the design criteria. Consequently, the internal damping in the soil will act to reduce the amplitude below that computed from the elastic theory, and, as reliable information becomes available on the damping capacity of various soils, this secondary correction can be made if desired.

The use of a "typical" value of a damping ratio, D, and the theory of a single degree of freedom system with viscous damping permits computation of the amplitude of vibration of a soil-oscillator system. The amplitude obtained by this method depends on the damping ratio chosen, and typical values have been accumulated for years for different test installations on different soils.

This value of damping ratio computed from test results lumps together the results of the internal damping of the soil and the dissipation of energy by waves through the soil. Consequently, there is little justification for using a particular damping ratio for conditions where the geometry and masses involved may be appreciably different from the test conditions. This is where the elastic half space theory has an advantage, because the results are presented in a manner that permits extrapolation of model test information to prototype conditions.

Relatively small mechanical oscillators have been used extensively to provide test information on the dynamic behavior of soils. Many of these tests have indicated a non-linear behavior of the soil under increasing load amplitudes. The writer pointed out that the amplitudes of motion developed by the oscillating mass often were large enough that the computed acceleration became greater than 1.0 g. This indicates that the oscillator jumped free of the ground during the upward motion. As a result, the contact pressure at the oscillator base varied between zero and a maximum during each oscillation, and the "hysteresis modulus of elasticity" had a lower slope than it would have had if the minimum pressure had been higher (Fig. 21(a)). This effect of range of stress on the effective modulus of deformation, or hysteresis modulus, was pointed out by Terzaghi (66) for repeated static loads on sands, and by Tschebotarioff (discussion of reference 33) for dynamic loads on foundations. Because

of this effect, in the conclusions to the paper the author recommended that oscillator tests utilize the same vibration parameters (which in this discussion refers to range of stress) as are to be used in the prototype.

The decrease in hysteresis modulus with increasing range of stress corresponds to the idea of a soft spring characteristic as discussed by Lorenz (45). Along with a decrease in the effective stiffness of a footing with increased load,

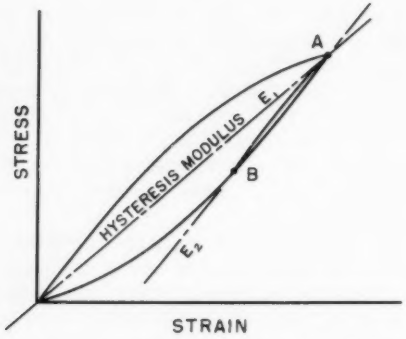

(a) EFFECT OF STRESS RANGE ON HYSTERESIS MODULUS

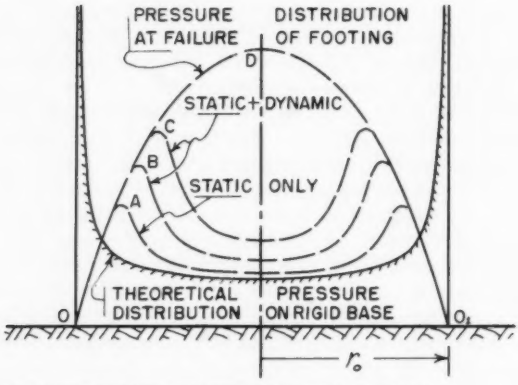

(b) PRESSURE DISTRIBUTIONS ON CIRCULAR BASE

FIG. 21.—FACTORS CONTRIBUTING TO NON-LINEAR BEHAVIOR FOUND AS DYNAMIC LOADS INCREASE

there must be a change in the pressure distribution at the footing base. Fig. 21(b) illustrates one concept of the change in maximum pressure distribution from curve A under static load alone, to curve B for static plus small dynamic loads, to curve C for larger dynamic loads. The maximum pressure cannot exceed some limiting value, which is represented by the curve ODO_1 corresponding to that for a cohesionless soil. Because the pressure distribution

changes from one where the majority of the load is carried near the perimeter of the footing to one where the pressure is concentrated nearer the center, the resonant frequency will be reduced (Sung, (3) and Richart (24)).

Finally, Alpan suggests that because the amplitude of oscillation computed from the elastic half-space theory was appreciably less than that he computed from the damped mass-point theory using an assumed typical value of the damping constant, that the former method was unsafe. The applicability of any theory for design purposes must be proved by field data obtained from operation of the actual installation. There is still a scarcity of reliable published information concerning the dynamic behavior of large footings under periodic loading. However, at the present time (1961) a comprehensive series of tests is being conducted at the United States Army Engineer Waterways Experiment Station, Vicksburg, Miss. for the Military Construction Division of the Office, Chief of Engineers, Washington, D. C. Vibratory tests are being carried out on four circular reinforced concrete bases of 62 in., 88 in., 108 in., and 124 in. in diameter using vertical, torsional, and rocking modes of oscillations. It is the writer's opinion that the results for vertical amplitude of oscillation from about the first forty tests agree well with the values computed using Fig. 8(b).

Perri has pointed out the expressions that may be used to evaluate amplitudes of oscillation and resonant frequencies of the coupled sliding and rocking motions for an undamped mass subjected to a periodic horizontal force. For such a system, the amplitudes of motion become infinite at the respective values of coupled resonant frequencies. Consequently, this particular type of analysis is of little use in evaluating the maximum anticipated amplitudes of oscillation at resonance.

However, the writer is grateful to Perri for emphasizing the very incomplete treatment given to this important problem in the paper. The curves shown on Figs. 9 and 10 represent the parameters involved in uncoupled sliding and rocking oscillations that were obtained mathematically be Arnold, Byeroft, and Warburton (5). By specifying conditions of horizontal translations without rotation, or rotation without translation, the boundary conditions are set up for the oscillator contact zone and introduced into the mathematical solution. Physically, this requires that the center of gravity of the oscillating mass must coincide with the line of action of the resisting elastic forces that, for the horizontal sliding case, requires that the mass be concentrated in a disk of zero thickness. In order to get some idea of the order of magnitude of the vibrations, the writer suggested that the amplitudes computed from the two uncoupled modes of vibration be superposed. This procedure is correct from the standpoint of mechanics, but may not represent more than a crude approximation to the actual dynamic behavior of a foundation. The differences between the frequencies determined for the uncoupled modes and the coupled frequencies may be estimated from the curves given by Jacobsen and Ayre (64) p. 337, or the lower of the two couple frequencies may be evaluated by the Southwell-Dunkerly procedure.

It should be noted that there are mistakes in the equations presented by Perri. The corrected equations are listed below.

$$I_y \theta = k_x a x - k_x a^2 \theta - k_t \theta + F_t e \cos(\omega t) \quad \ldots\ldots (24)$$

$$X_o = \frac{F_x\left(k_x a^2 + k_t + k_x a e - I_y \omega^2\right)}{\left(m\omega^2 - k_x\right)\left(I_y \omega^2 - k_x a^2 - k_t\right) - k_x^2 a^2} \quad \ldots\ldots(29a)$$

$$X_o = \frac{F_x\left(k_x a^2 + k_t + k_x a e - I_y \omega^2\right)}{m I_y \omega^4 - \left(I_y k_x + m a^2 k_x + m k_t\right)\omega^2 + k_x k_t} \quad \ldots\ldots(29b)$$

$$\theta_o = \frac{F_x\left(-m e \omega^2 + e k_x + a k_x\right)}{\left(m\omega^2 - k_x\right)\left(I_y \omega^2 - k_x a^2 - k_t\right) - k_x^2 a^2} \quad \ldots\ldots(30a)$$

$$\theta_o = \frac{F_x\left(-m e \omega^2 + e k_x + a k_x\right)}{m I_y \omega^4 - \left(I_y k_x + m a^2 k_x + m k_t\right)\omega^2 + k_x k_t} \quad \ldots\ldots(30b)$$

$$m I_y \omega^4 - \left(I_y k_x + m a^2 k_x + m k_t\right)\omega^2 + k_x k_t = 0 \quad \ldots\ldots(33)$$

$$\left(\frac{\omega}{\Omega_\theta}\right)^4 - \left(\eta + \eta \frac{a^2}{p_y^2} + 1\right)\left(\frac{\omega}{\Omega_\theta}\right)^2 + \eta = 0 \quad \ldots\ldots(39)$$

$$\left(\frac{\omega}{\Omega_\theta}\right)^2 = \frac{1}{2}\left\{\left[\eta\left(1 + \frac{a^2}{p_y^2}\right) + 1\right] \pm \sqrt{\left[\eta\left(1 + \frac{a^2}{p_y^2}\right) + 1\right]^2 - 4\eta}\right\} \quad \ldots\ldots(40a)$$

$$\frac{\omega}{\Omega_\theta} = \frac{1}{\sqrt{2}}\sqrt{\left[\eta\left(1 + \frac{a^2}{p_y^2}\right) + 1\right] \pm \sqrt{\left[\eta\left(1 + \frac{a^2}{p_y^2}\right) + 1\right]^2 - 4\eta}} \quad \ldots\ldots(40b)$$

$$\Omega_c = \Omega_\theta \frac{1}{\sqrt{2}}\sqrt{\left[\eta\left(1 + \frac{a^2}{p_y^2}\right) + 1\right] \pm \sqrt{\left[\eta\left(1 + \frac{a^2}{p_y^2}\right) + 1\right]^2 - 4\eta}} \quad \ldots\ldots(40c)$$

Fig. 12 was included for use in estimating the maximum stiffness that could be obtained by the use of point bearing piles that rest on an infinitely rigid stratum. This is an upper limit that can be reached only theoretically. Actually, the pile tip will move, and Eremin notes that the effect of surrounding piles should help stiffen the bearing layer that would, in turn, reduce the pile tip motion.

Hardin has presented some interesting data on the relations between confining pressure and the shear modulus of Ottawa sand, as influenced by changes in void ratio. The effect of change in void ratio is quite significant. He also observed that the modulus varied with about the 1/2 power of the confining pressure, which means that for this material the shear wave velocity varied with about the 1/4 power of the confining pressure. This is quite reasonable in view of the deviations from the theoretical slope of 1/6 found by Duffy and Mindlin (12) for longitudinal wave propagation in bars made up of uniform steel spheres. In the range between 1000 psf and 2000 psf, and for the first mode of vibration with the (1,0,0) orientation, their test data indicates that the longitudinal wave velocity varies with confining pressure according to the 1/5 power for high tolerance balls (1/8 $\pm$ 0.000010 in. diameter) and the 1/3.9 power for low tolerance balls (1/8 $\pm$ 0.000050 in. diameter). Actually it is remarkable that the test results for Ottawa sand correspond so well to those obtained from a granular medium composed of but slightly imperfect spheres.

Smoots, Stickel, and Fischer have brought up several interesting points. Of course, the use of a homogeneous, isotropic, elastic medium to represent a mass of soil represents a drastic simplification, and the approximations involved in this substitution must be re-evaluated for each different use of the theoretical results. In connection with the vibrations of foundations, the elastic waves represent a non-destructuve method of evaluating the stiffness of the soil in and adjacent to a constuction site.

They mention the observed effects of ground water on the compression wave and note that the shear wave seems to be little affected by the water table. The theoretical studies by Zwikker and Kosten (67) and Biot (68) on the elastic wave propagation in saturated porous materials have shown the influence of saturation on the shear and compression waves. The shear wave is uncoupled from the compression waves and is influenced only by the added mass of the fluid, whereas the compression waves in the fluid and in the soil structure are coupled and depend on both the stiffness and mass of each component. Hardin (69) has combined the characteristics of a granular medium with the theories of Zwikker and Kosten and of Biot and found that for saturated materials the shear wave velocity varied with the 1/6 power of the confining pressure as it does for the granular material in the dry condition. Consequently, the velocity of the shear wave as determined from seismic tests, or from steady state vibrations, should permit evaluations of the shear modulus of the soil that can be used in the theories for the dynamic behavior of foundations.

Smoots, Stickel, and Fischer have made computations for the resonant frequency of the oscillator described in Example A by several methods. Tschebotarioff's method utilizes the single degree of freedom undamped mass theory and a typical value for sandy clay soils. No determination of the amplitude of oscillation can be made by this method. Toriumi's approach to the problem is essentially the same as Reissner's (2) in that he assumes a uniform distribution of pressure over the circular loading area and a constant force type of oscillator. Apparently Toriumi has an error in his evaluation of the function f_2, that would affect the answers obtained from his curves. Because Toriumi's method is based on the assumption of a constant force oscillator instead of a rotating mass oscillator as used in Example A, it should be expected that his method would give lower values of resonant frequency.

The test conducted at the Kwajalein site represents valuable field data that is needed for a better evaluation of the theoretical procedures. Use of a shear

modulus of 1075 psi as obtained by Pauw's method would, of course, give a computed resonant frequency that was lower than the test value. A consideration of the curves on Fig. 16 and the average static contact pressure at the base of the footing indicate that the shear modulus could not have been as low as 1075

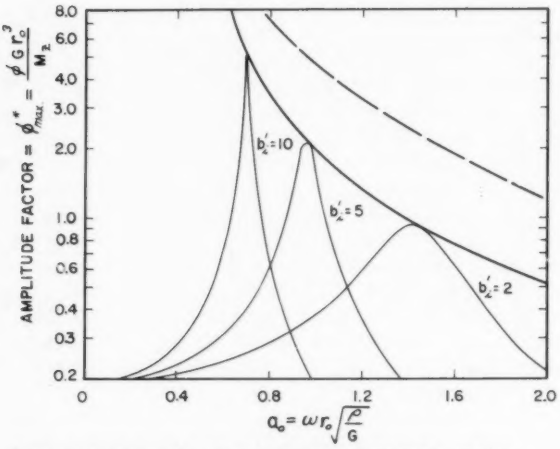

(a) AMPLITUDE FACTOR VS. FREQUENCY FACTOR RELATIONS

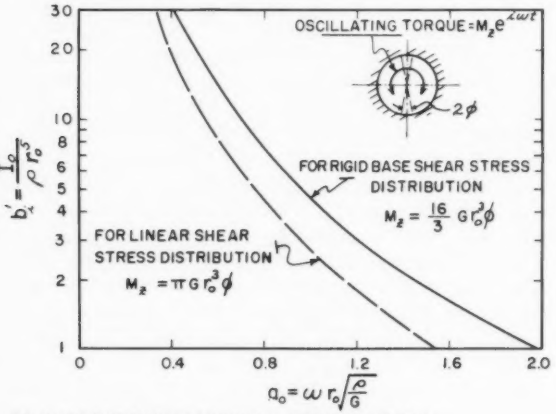

(b) MASS RATIO VS. FREQUENCY FACTOR RELATIONS

FIG. 22.—CHARACTERISTICS OF TORSIONAL OSCILLATION FOR AN OSCILLATOR RESTING ON A SEMI-INFINITE ELASTIC MEDIUM

psi in the region directly below the base. Consequently, the resonant frequency computed on the basis of this shear modulus is unduly low. The measured amplitude of 0.0022 in. is appreciably lower than that given by use of Fig. 8(b). It is unfortunate that more test data is not available from this site, because

the results from just one test are not sufficient to evaluate the effectiveness of a theoretical procedure.

The motion of the radar dish can also impart torsional oscillations to the foundation that may develop resonant vibrations. Solutions for this problem have been developed by Reissner (70) for the case of shear stresses varying linearly with radius, and by Reissner and Sagoic (71) for a rigid circular base. Fig. 22 gives the curves from which the maximum amplitude and resonant frequency can be computed. Because the torsional oscillation is an uncoupled mode of vibration, these motions can be considered separately.

Smoots, Stickel, and Fischer have also included an interesting list of practical uses for the data described in the paper and in the discussions. Further study, both analytical and experimental, should be conducted on each of these topics, as well as on the subject of instrumentation for this particular range of frequencies and amplitude of motion.

Wilson and Miller have contributed valuable test data concerning the effect of confining pressure on the compression wave velocity, and on the compression modulus and shear modulus of elasticity for several granular soils. Generally, the compression modulus varies with about the 1/3 power of the confining pressure. The two materials that deviated markedly from this behavior were designated as (SC) clayey gravelly sand and (SM) silty gravelly sand.

The resonant column procedure for determining the elastic wave velocities in soils was used by Hardin and by Wilson and Miller. In this test, a column of soil is subjected to a confining pressure then set into resonant oscillation to determine the wave velocity. As the confining pressure is increased, the void ratio of the material decreases in accordance with its compressibility. For sands, the void ratio decrease is relatively insignificant within the range of confining pressures shown on Figs. 6 or 18, but it is of importance for softer materials. Hardin's curves indicate that a considerable increase in slope might occur as a consequence of the decrease of void ratio. On the other hand, for a saturated fine grained material, it takes some time for an increase in increment of confining pressure to result in the corresponding change in effective stress in the soil. If the dynamic measurements are taken before consolidation is complete, the wave velocity corresponds to some pressure which is lower than the confining pressure, and a flatter slope will be produced on the confining pressure versus wave velocity diagram. Tests carried out by J. R. Hall, Jr., A. M. ASCE, in the writer's laboratory have shown this effect for Vicksburg loess. For a confining pressure increase from 360 psf to 1320 psf, the computed shear modulus increased from 4100 psi to 5470 psi after 20 min, and to 6670 psi after 20 hr. The corresponding increases in the exponent corresponding to the relation in Eq. 44 was from 0.22 to 0.37 as a consequence of the additional time the confining pressure was applied. There also appears to be some influence of the maximum pressure applied, on the preconsolidation pressure, as the confining pressure is reduced.

Additional experimental work is required to establish the confining pressure-time-wave velocity relations for silts and clays and for granular materials containing relatively small amounts of these fine-grained particles. It appears from the test data for samples C-1 and NJ-1, given by Wilson and Miller, that relatively small amounts of the fine-grained soil particles exert a considerable influence on the dynamic behavior of a clayey or silty gravelly sand.

The writer again wishes to express his appreciation to the discussers for contributing much valuable information. It is hoped that efforts to obtain field performance data, similar to that described by Smoots, Stickel, and Fischer,

will become a recognized part of the design procedure for dynamically loaded foundations. It is also expected that testing programs similar to those described by Hardin, and by Wilson and Miller will soon provide information on the behavior of soils containing a significant amount of fine-grained particles.

ADDITIONAL BIBLIOGRAPHY

64. "Engineering Vibrations," by L. S. Jacobsen and R. S. Ayre, McGraw-Hill Book Co., Inc., New York, 1958.

65. "Dimensional Analysis in Soil Mechanics," by H. Lundgren, Acta Polytechnica, Civil Engineering and Building Construction Series, Vol. 4, No. 10, 1957.

66. "Principles of Soil Mechanics - A Summary of Experimental Studies of Sand and Clay," by K. Terzaghi. Engineering News Record, 1925.

67. "Sound Absorbing Material," by C. Zwikker and C. W. Kosten, Elsevier Press, New York.

68. "Theory of Propagation of Elastic Waves in a Fluid-Saturated Porous Solid. I. Low Frequency Range," by M. A. Biot, Journal of the Acoustical Society of America, Vol. 28, 1956, p. 168.

69. "Study of Elastic Wave Propagation and Damping in Granular Materials," by Bobby Ott Hardin, thesis presented to the University of Florida in Gainesville, Fla., in August, 1961, in partial fulfillment of the requirements for the degree of Doctor of Philosophy.

70. "Freie und erzwungene Torsionsschwingungen des elastischen Halbraumes," by E. Reissner; Ingenieur Archiv, Vol. VIII, No. 4, p. 229.

71. "Forced Torsional Oscillations of an Elastic Half-Space," Part I by E. Reissner and H. F. Sagoci; Part II by H. F. Sagoci Journal of Applied Physics, Vol. 15, No. 9, p. 652.

Errata.—p. 3, line 1 - "text" instead of "test"; p. 11, - ordinate of Fig. 7(a) should be "$A^{(2)}_{max.}$" instead of "$A^{(1)}_{max.}$"; p. 17, - 8 lines from bottom, should be "has led" instead of "was led"; p. 27, - lines 1 and 2 should be "1.04" instead of "1.07"; line 2 should be "2.45" instead of "2.52"; lines 3 and 6 should be "1.20" instead of "1.19"; p. 27, - bottom line should read

$$I_o = \frac{W_o}{3g}\left(h^2 + a^2\right) + \frac{W_{mach}}{g}\,(14)^2 = 3.6 \times 10^6 \text{ ft-lb sec}^2;$$

p. 28, - lines 2, 5, and 15 should be "13.3" instead of "13.4"; line 4 should be "2.9" instead of "2.3"; line 6 should be "Fig. 9" instead of "Fig. 10" and should be "0.87" instead of "0.97"; lines 6 and 12 should be "3.0" instead of "2.5"; lines 8 and 10 should be "218" instead of "240"; and line 8 should be "3.63" instead of "4.02", p. 33, under reference 18, J. W. Clawson.

SEEPAGE REQUIREMENTS OF FILTERS AND PERVIOUS BASES[a]

Closure by Harry R. Cedergren

HARRY R. CEDERGREN,[24] M. ASCE.—W. J. Turnbull, F. ASCE pointed to a tendency, presumably more prevalent in past years than at present, for engineers to call for drainage blankets, but not to rely on them to function. One dominating factor that may be largely responsible for this attitude is the fact that filter design has been almost entirely on a qualitative basis, and designers have had no way of knowing in advance of construction if filters of proposed dimensions and materials would be capable of doing the drainage job expected of them. The approach suggested in the paper relates the physical dimensions and permeability of filter layers and pervious bases to the permeability of the soil from which water is being drained.

Possibly the manner in which permeability is defined has contributed to the willingness of many engineers to allow relatively low permeability aggregates to be used for filters. The coefficient of permeability actually relates to flow under a hydraulic gradient of unity. The flow potential in a given layer is proportional to the coefficient of permeability times the available gradient. In much highway drainage, for example, the available hydraulic gradient is only approximately 5%, or 5 ft in 100. The seepage potential under a gradient of 0.05 is only one-twentieth of that under a hydraulic gradient of unity. This point is amplified by Fig. 11. Line 1-1 represents the slope of a pavement, which also is the maximum gradient that can exist in the drainage layer without a head build-up that will produce uplift of the pavement. Line 2-2 represents a hydraulic gradient of unity. For this gradient to exist under a pavement there would need to be available a head of 100 ft for every 100 ft of seepage distance. A graded aggregate that would drain readily under this steep gradient might be rather slow-draining under conditions that actually can exist under pavements. The writer expects that much general thinking about the seepage capabilities of drainage aggregates is based on a gradient of 100 ft in 100 ft rather than the small gradients that can exist in the field.

E. S. Barber, M. ASCE, has shown by an approximate formula that the capacity of horizontal drainage layers to transmit water to the sides varies inversely with the square of the width of the layer. He shows that a foundation layer at Idlewild Airport with a width of 5,000 ft and an available head of 10 ft would be capable of transmitting seepage at a rate of less than 2 in. per yr. The soil has a permeability of 100 ft per day. His computations demonstrate the need for considering boundary conditions in the design of drainage systems.

Barber also presents curves (Fig. 10) showing that the kind and quantity of "fines" present in graded aggregates can have a major influence on permeabil-

---

[a] October 1960, by Harry R. Cedergren (Proc. Paper 2623).

[24] Senior Materials and Research Engr., Calif. Div. of Highways, Sacramento, Calif.

ity. For example, 10% of silica fines reduced the permeability of a graded aggregate to about one one-hundredth of the original value, whereas 10% of clay fines reduced the permeability to one ten-thousandth of the original value. Only 2% of silica fines reduced the seepage potential to less than $\frac{1}{2}$% and 2% of clay lowered the water-removing potential to about one-thirtieth!

Barber's curves lend considerable support to the hypothesis that realistic quality (and permeability) standards for filter aggregates are urgently needed.

In the face of this kind of evidence (which substantiates general information that has been available for many years), it is amazing that clay-bound subbases are still considered by some engineers to be "pervious." Simple computations such as those made by Barber can demonstrate in a few moments the inadequacy of such layers to serve effectively for subgrade drainage.

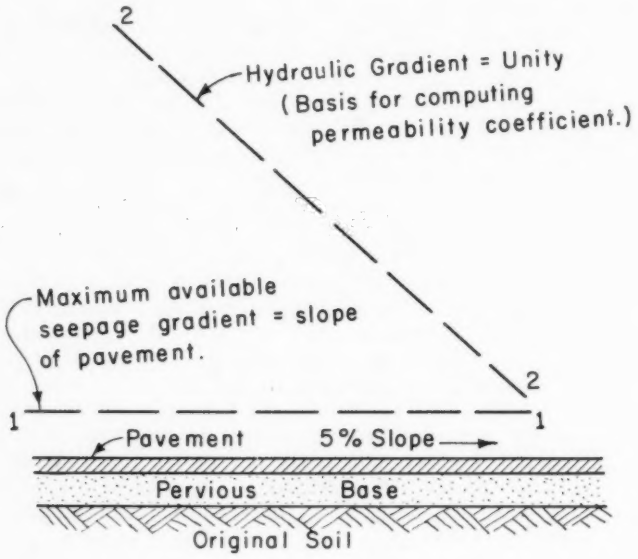

FIG. 11.—RELATIVELY SMALL GRADIENTS AVAILABLE TO INDUCE SEEPAGE IN PERVIOUS BASES FOR HIGHWAY PAVEMENTS

H. J. Gibbs, M. ASCE, referred to extensive filter studies by the U. S. Bureau of Reclamation, in which maximum flow is a principle basis for establishing limiting gradations of filter materials. The criteria that he furnished are a welcome addition to the paper. He says, "It was believed that when very broad limitations were allowed that an acceptable gradation could be misconstrued such that flow would be restricted and possibly be no better than the material protected." This statement emphasizes one of the main points of the paper. Under the low gradients that can exist in pavement drainage layers, the rate of escape of seepage can be unbelievably slow with aggregates that would be entirely adequate for filters for dams. A big difference can be attrib-

uted to the direction in which water flows through the filter. Flow across the narrow dimension of the filter (as in most dam filters) can occur much more readily than flow along the length of the filter (as in many highway filters). When this difference is taken into consideration, flow restriction is substantially worsened in pavement drainage. As suggested by Gibbs, determination of the permeability of filter materials is an important part of filter tests. When filters are required to function under low gradients, knowledge of the permeabilities of available aggregates is essential to the development of adequate, economical designs.

The writer wishes to thank Messrs. Turnbull, Barber, and Gibbs for their discussions.

Filters and pervious bases are serving an important function in the performance of many engineering works. In the past, most filter design (in terms of water-removing capabilities) has been entirely qualitative. While there have been a great many successes, there have been some failures. A rational approach to filter design, with consideration being given to water-removing capacity in relation to permeability and boundary conditions, can provide some assurance that filter designs will at least be "in the right county."

Errata.—Page 16, line 24, word "at" should be replaced with "to"; page 19, line 7, word "orientation" has transposed letters; page 20, line 29, word "had" should be replaced with "has"; page 21, line 26, word "not" should be eliminated, line 29, "$1\frac{1}{2}$:1 to 6:1" should read "$\frac{1}{2}$:1 to 6:1," footnote 11 word "Mechanics" has transposed letters; page 25, line 22, "this aquifer" should be replaced by "an underlying aquifer"; page 30, line 9, word "gradients" should be replaced with "gradings"; page 31, line 8, word "of" should be replaced with "or," line 25, numeral "140" should be "180" and "0.15 ft" should be "0.11 ft"; page 32, line 7, "0.7 ft per min" should be "0.07 ft per min," 5th line above bottom, word "record" should be "second"; and page 33, line 1, "looking" should be "locking."

TUTTLE CREEK DAM OF ROLLED SHALE AND DREDGED SAND[a]

Discussion by Stafford C. Happ

STAFFORD C. HAPP.[13]—The authors have ably shown that Tuttle Creek Dam is an interesting example of careful embankment use of dredged fill and broken shale and limestone. They have also reflected justifiable pride in the handling of foundation and rock fill problems, but their concern with the problems may obscure the fact that success in fitting design and construction methods to the existing conditions also justifies the geologic forecasts which contributed to site selection and planning. This analysis is devoted to the geologic factors, based on the writer's participation during planning and first-stage construction phases.

Favorable geologic features, as the authors have noted, included long Creek limestone at a suitable elevation and location for the outlet works foundation, and Sallyards limestone at suitable elevation. These provide a favorable surface for placement of spillway concrete, with incidental removal from the foundation of the weak Legion shale, in a topographic saddle leading to a relatively long tributary valley which provides added safety against excessive spillway erosion. In addition to these obvious advantages, even the presence of Neva limestone within the spillway cut was considered favorable, relative to alternate sites in similar geologic terrane, because it insured exposure to observation and would facilitate any necessary remedial treatment. The authors suggest that calyx observation holes should be included at future projects where similar conditions are suspected. Calyx holes were judged unnecessary during the Tuttle Creek investigations, and it seems doubtful whether they would have resulted in any appreciable change in plans, or saving in costs.

Weakness of the lower part of the Neva Limestone was recognized early in the investigation, and was the subject of a special study by S. S. Philbrick, Pittsburg District geologist who was called to consult on the Tuttle Creek site because of his experience with similar foundation materials. It was concluded, however, that any necessary remedial treatment of the lower Neva would be at least compensated by favorable features of the site. Later decision to classify all of the Neva as rock fill for embankment purposes was supported by studies indicating that deficiencies could, if necessary, be made up by quarrying Cottonwood limestone along its outcrop upstream from the dam, at greater but not prohibitive cost. Thus a computed risk was accepted, offering some prospect of significant economy, and protected by assurance of an acceptable alternative. Perhaps later disappointment with the Neva reflects some natural tendency toward wishful thinking, one decision had been made to try to use it all as rock fill.

---

[a] December, 1960, by K. S. Lane and R. G. Fehrman (Proc. Paper 2681).

[13] U. S. Atomic Energy Comm., Grand Junction Operation Office, Grand Junction, Colo.

Prospective economy was a major factor in the original proposal for berms-on-shale in the spillway side slopes. There seemed no point in excavating more shale than necessary, especially since laying back the shale slope would expedite erosion of the overlying limestone. At that time, however, knowledge of similar procedure was limited to a deep railway cut in eastern Ohio where the berm was placed on shale at base of a vertical face in sandstone, but with a thin limestone only a few feet beneath the top of shale. There, as Philbrick has reminded the writer, "The berm was preserved by the limestone and the primary criticism of the berm on shale, which is its rapid weathering or lack of durability, was overcome." Hence, unless additional experience came to attention later, the Tuttle Creek berm design was essentially experimental, and reports of future stability and maintenance experience should be helpful indications as to the desirability of similar practices elsewhere. Seepage is to be expected from the base of the Cottonwood limestone, providing a rigorous test of erosion resistance.

The outlet conduit foundation involved a problem illustrative of those frequently associated with minor geologic features. At the top was the thickest (approximately 1 ft) and firmest bed of the Long Creek limestone, essentially at the elevation desired for base of the conduit concrete. Preliminary drilling showed a weathered rind 1 in. or 2 in. thick at the top of this bed, with secondary carbonate cementation, and also deeper weathering along vertical joints. Thus there was some concern about risk of leakage and uplift pressure along possible open solution channels, and foundation cleanup specifications stressed exposure of firm limestone in order to reveal any open channels along the joints.

Removal of the weathered rind required use of jackhammer and rock spade, with which it was easier to excavate the entire top bed than to chip off only 1 in. or 2 in. of badly weathered limestone. Furthermore, weathering discoloration extended downward for several feet along many joints, although there were no open channels. In these circumstances, there was some tendency simply to remove all discolored limestone, but this would have weakened the foundation by isolating pillars between the joints, and would have required excessive concrete for replacement. Thus the easy distinction by color had to be ignored, and reliance put on close and discriminating inspection to assure sufficient exposure of joints to reveal any open channels, yet avoid over-excavation of rock which was firm although slightly weathered and discolored.

Reduction in riprap thickness on the flat 1 on 13 berm (as described in the paper) seems reasonable in principle, but what are appropriate criteria for determining the thickness needed? Presumably 18 in. may not exceed the dimensions of some of the individual pieces. There is a scarcity of published data on riprap design and experience, and it should be of interest if the authors could give a summary of the governing criteria.

The data on density of dredged sand fill seems clouded by the restriction of sampling to "reasonably uniform non-stratified material," and citation of only the "more reliable" results. It would be helpful to know why stratified samples were excluded, the range of values actually obtained, the proportion of measurements excluded as "less reliable," and reasons for such exclusions.

Concerning protection of shale surfaces against slaking and crumbling befor concrete placement, the authors say "slaking. . . was handled. . . by keeping them moist or by spraying with a bituminous shale sealer." Some possible difficulties had been foreseen, during the planning stage, in keeping steep shale

surfaces moist without causing erosion or slumping, and more details on just how this was accomplished would be of interest.

A principle of possible wide significance is suggested by the statement that the "old channel deposit" clay was "similar to the terrace clay." The latter is presumably a deposit of Pleistocene age, whereas the "channel fill" is much younger, occupying a depression or swale followed by intermittent tributary drainage across the present-day river flood plain, and normally boggy so that adequate sampling was difficult. Presumably there should have been much more opportunity, as there certainly was much more time, for consolidation of the terrace clay. Lack of any difference in physical characteristics would suggest that age differences in tens of thousands of years and soil loads of tens of feet are unimportant in consolidation of alluvial clays. This one case of course would not be taken as full proof of such a principle, but it would be desirable to have more details on the evidence of similarity between the two clay deposits.

Weathering was the most critical geologic factor in the Tuttle Creek foundation conditions, marked by lightening of colors and limonitic stains, solution of limestone, and softening, cracking and crumbling of both limestone and shale. Weathering of limestones seems to be almost unpredictably erratic. Relative abundance of different clay minerals, or other impurities, is a suspected factor, but lacks verification as a general controlling factor. Possibly the relatively rapid and extensive weathering of the lower Neva limestone reflects greater abundance or a more susceptible type of clay content, but pre-construction drilling results suggested that the more extreme Neva weathering might be related to local absence, by erosion, of the higher Cottonwood limestone. The Cottonwood is a principal aquifer, and Neva weathering may have been retarded in areas where overlying Cottonwood served as a horizontal drain to intercept downward-percolating waters. This hypothesis might be confirmed or disproved by additional information developed during construction, regarding the relations between areal extent of severe Neva weathering and of overlying Cottonwood limestone.

Weathering of shale (or mudstone, claystone, or siltstone) seems to progress relatively uniformly, although there were apparent differences among different kinds of shale at Tuttle Creek. A large amount of laboratory test data were accumulated, and it would be desirable to make this more widely available by publication, especially if it could be correlated with observations on behavior in construction. Limited studies of some of the Tuttle Creek shales were made by Ada Swineford, of the Kansas Geological Survey, indicating a predominance of illite which is considered among the more stable clay minerals. Hence extrapolation of data on strength and stability of these shales should be subject to confirmation of similar mineralogy. Rate of disintegration and weakening of shales in artificial embankments is obviously important in the long-term stability of structures such as Tuttle Creek Dam, yet there is little factual data to support design based on reasonable assumptions. It would seem desirable to undertake investigation by sampling and testing embankments of various ages, known to have been built from various shales of various clay-mineral compositions. Embankments of canals and related dams should provide examples a century or more old, and there is an abundance of highway as well as dam embankments of lesser age. Philbrick has called attention to nearby Kansas highway fills constructed from shales similar to those at Tuttle Creek. The whole field of weathering effects, relative to construction problems, should be worthy of society-sponsored investigations.

NEW METHOD OF CONSOLIDATION-COEFFICIENT EVALUATION[a]

Discussion by William Daniel Finn, B. V. Rangantham, and I. da Silveira

WILLIAM DANIEL FINN,[13] A. M. ASCE.—The author is to be commended for his significant contribution to the theory of consolidation. His ingenuity in applying the results of other fields to soil mechanics merits admiration.

The writer has some slight reservations about the establishment of the initial dial reading by the requirement that "consistent equal values of the co-efficient of consolidation result from a comparison of compressions at different values of N." Such a requirement is necessary to satisfy the assumptions of the theory. The initial dial reading, however, has an independent objective existence; its value is indifferent to any set of thought processes brought to bear on the consolidation problem. The corrected initial reading coupled with the assumptions of the consolidation theory may result in the closest fit to available consolidation data, but doubts may be reasonably entertained that it is the real initial dial reading.

As an extension of Scott's work, an analysis of three-dimensional consolidation with axial symmetry is presented herein. Examples of this type are (a) consolidation of a triaxial specimen in which radial and vertical consolidation may take place and (b) consolidation in the field where vertical sand drains are used to accelerate the consolidation process. It is assumed that layers exist which permit vertical consolidation.

The equation describing such consolidation is

$$\frac{\partial u}{\partial t} = C_v \frac{\partial^2 u}{\partial Z^2} + C_r\left(\frac{\partial^2 u}{\partial r^2} + \frac{1}{r}\frac{\partial u}{\partial r}\right) \quad \ldots\ldots\ldots (20)$$

in which u is the excess over hydrostatic water pressure, t denotes time, C_v represents the co-efficient of consolidation for drainage in the Z or vertical direction, r denotes radial distance from the Z-axis and C_r is the co-efficient for radial consolidation.

The equation may be split into two parts

$$\frac{\partial u}{\partial t} = C_v \frac{\partial^2 u}{\partial Z^2} \quad \ldots\ldots\ldots\ldots\ldots\ldots (21)$$

and

$$\frac{\partial u}{\partial t} = C_r\left[\frac{\partial^2 u}{\partial r^2} + \frac{1}{r}\frac{\partial u}{\partial r}\right] \quad \ldots\ldots\ldots\ldots\ldots (22)$$

---

[a] February, 1961, by Ronald F. Scott (Proc. Paper 2746).

[13] Asst. Prof. Civ. Engrg., Univ. of British Columbia, Vancouver, Canada.

Each part may be solved separately with appropriate boundary conditions. Solutions are to be found in the paper. The corresponding percentage consolidation for each case may then be found.

The partial results can be combined to give the total U% consolidation at time t according to the formula.[14,15]

$$100 - U\% = \left(100 - U_V\%\right)\left(100 - U_r\%\right)\left(1/100\right) \quad \ldots\ldots\ldots (23)$$

in which U% is the combined percentage consolidation, U_V% the percentage consolidation due to vertical drainage and U_r% the percentage consolidation due to radial drainage.

Then, as in the paper,

$$\frac{U(T)}{U(NT)} = \frac{V_t}{V_{Nt}} \quad \ldots\ldots\ldots\ldots\ldots\ldots (24)$$

However, now $U(T) = f\left(T_r, T_V\right)$ in which T_r is the time factor for radial consolidation and T_V the time factor for vertical consolidation. The compression ratio is also $= g\left(C_V, C_r\right)$. Thus two values of the compression ratio theoretically suffices for the solution of C_V and C_r since they are assumed constant.

Since the equation was solved by parts, it is preferable to determine C_r and C_V independently as in the paper and ultimately compute U by Eq. 23.

A third possibility is to compute a single average consolidation co-efficient for the problem. The consolidation may, for example, be assumed to be entirely due to vertical drainage. If Eq. 24 is then used, an equivalent vertical consolidation co-efficient is obtained. In like manner, an equivalent radial co-efficient may be determined. Either of these co-efficients may then be used to characterize the consolidation problem. The latter approach is analogous to transforming an anisotropically permeable section to one of uniform permeability.

B. V. RANGANATHAM[16].—The valuable paper by the author on a new method of consolidation-coefficient evaluation represents the only one of its kind which endeavors to probe into what happens within the loading interval because nothing but the average value can be computed by the use of the hitherto known methods. This, though a significant contribution to our knowledge, seems to suffer from the want of giving uniquely averaged value which is the result needed by the practicing engineer.

This can best be demonstrated with reference to a laboratory time curve for a typical load increment (taking care to choose one with little initial compression to eliminate correction) on a saturated black cotton soil. The computation of C_V, the coefficient of consolidation, was conducted in accordance with the example worked out in the paper, but for a number of combinations of initial time and N-values. Table 4 and Table 5 were prepared from such computed values. The coefficient of consolidation is plotted against N-values giving a family of curves (Fig. 2(a)) which are described by the values of initial time written adjacent to them. From the same results, another family of curves of

---

14 "Simple Two and Three Dimensional Cases in The Theory of Consolidation of Soils," by N. Carillo, Journal of Mathmatics and Physics, Vol. 201.

15 "Hawaii's Experience with Vertical Sand Drains," by K. B. Hirashima, Bulletin 90, HRB, 1954.

16 Lecturer in Soil Mechanics, Indian Inst. of Science, Bangalore, India.

TABLE 4.—COMPRESSION DIAL READING[a]

Time, in minutes (1)	Compression dial reading (in. x 10^{-4})	
	Black cotton clay ordinary type (2)	Black cotton clay impervious type (3)
0	2948	2846
0.25	2892	2834
1.0	2728	2822
2.25	2619	2810
4.0	2534	2798
6.25	2481	2786
9.0	2454	2774
12.25	2439	2762
16.0	2430	2750
25.0	2420	2725
36.0	2415	2701
49.0	2410	2676
64.0	2407	2654
81.0	2405	2630
100.0	2403	2609
121.0	2401	2587
144.0		2567
169.0		2549
196.0		2531
225.0		2515
243.0		2506
299.0		2482
467.0		2442
561.0		2430

[a] Pressure = 2 tons per sq ft.

TABLE 5.—COMPUTED[a] VALUES OF C_V

(a) Black cotton clay ordinary type						(b) Black cotton clay impervious type				
N-Value	Initial time, in minutes					N-Value	Initial time, in minutes			
	4.0	6.25	9.0	12.25	16.0		36.0	64.0	100	196
1.56					54.7	1.53				1.55
1.77			71.5			1.56		2.12		
1.96		82.3				1.78	3.17			
2.04				59.3		1.96			1.92	
2.25	87.4				48.9	2.25		2.11		
2.56			78.4			2.38				1.47
2.94				55.7		2.78	2.38			
4.0	82.5				42.7	2.86				1.34
5.22				49.8		2.99			1.74	
5.76		70.2				3.06		2.04		
7.11			57.7			4.00	2.17			
7.56					39.8	4.67		1.81	1.62	
9.0	76.5					5.44	2.16			
9.88				46.9		5.61			1.56	
10.24		65.4				7.30		1.70		
13.44			54.4			8.31	1.86			
16.0	73.4					8.77		1.69		
19.36		64.3				15.58	1.70			
30.25	71.8									

[a] C_V, in sq in. per min x 10^{-4}.

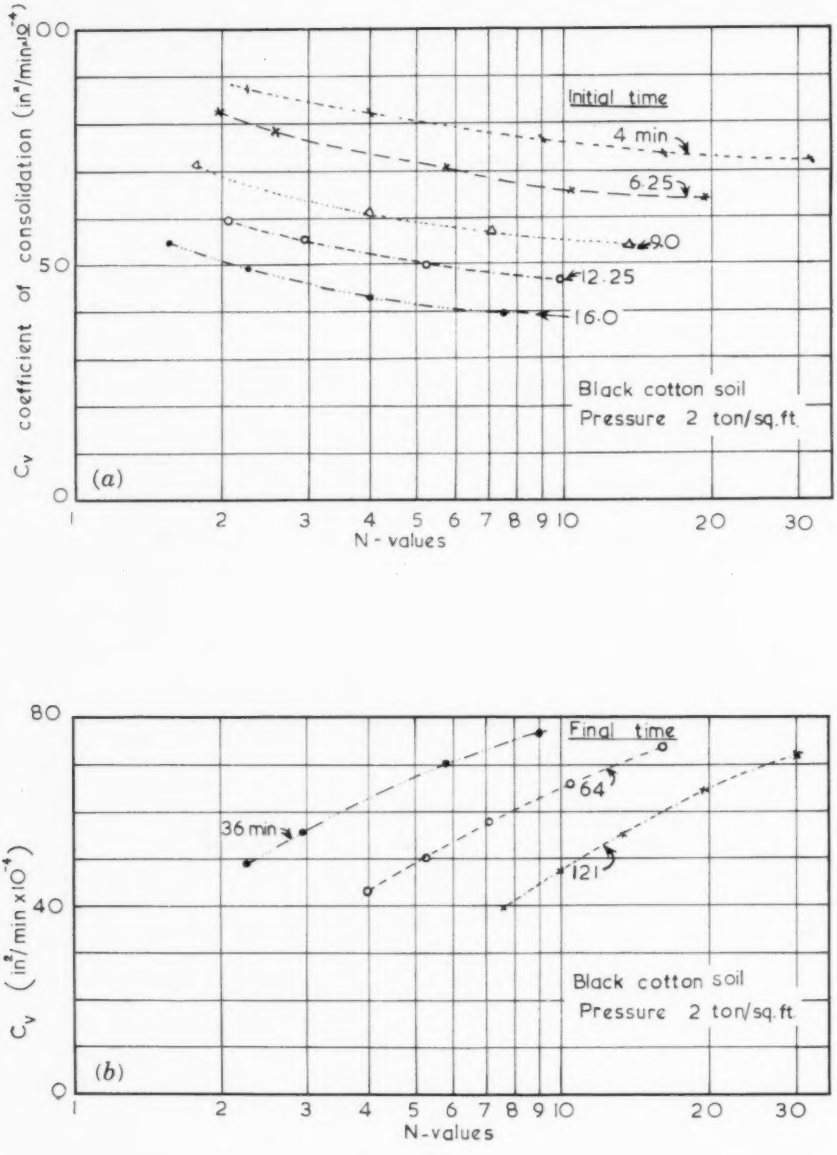

FIG. 2.—COEFFICIENT OF CONSOLIDATION VERSUS N-VALUES

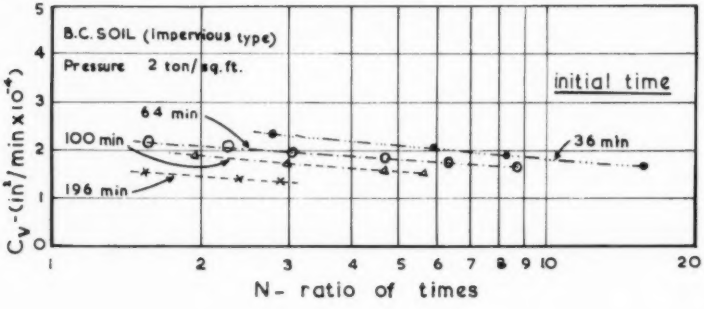
B.C. SOIL (impervious type)
Pressure 2 ton/sq.ft.
initial time
64 min
100 min
196 min
36 min
Cv-(in²/min x 10⁻⁴)
N- ratio of times

FIG. 3

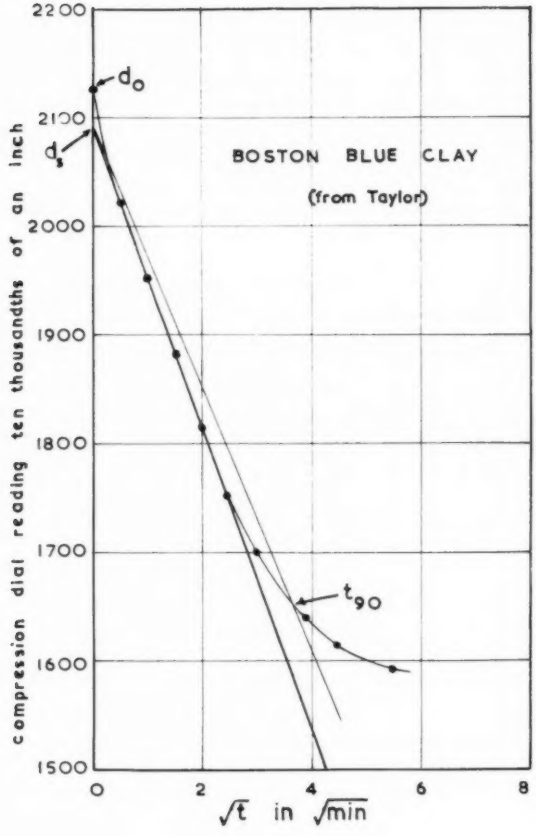
BOSTON BLUE CLAY
(from Taylor)
d0
ds
t90
compression dial reading ten thousandths of an inch
√t in √min

FIG. 4(a)

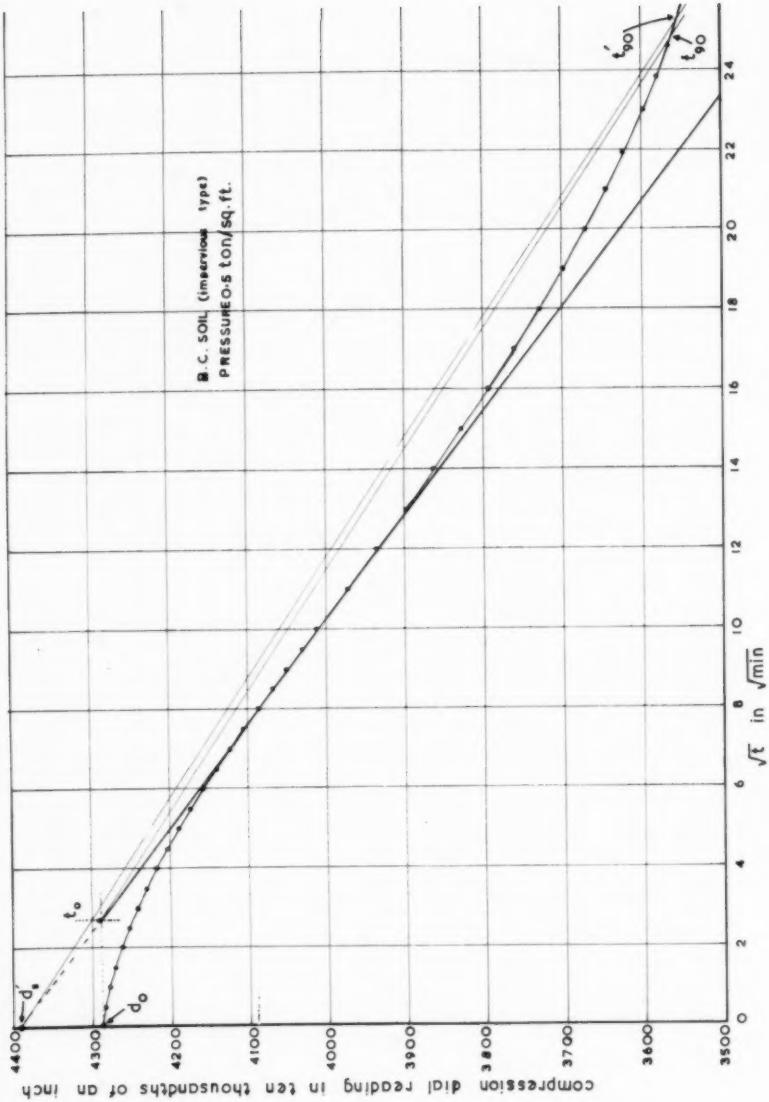
B.C. SOIL (impervious type)
PRESSURE 0·5 TON/SQ. FT.
compression dial reading in ten thousandths of an inch
4400
4300
4200
4100
4000
3900
3800
3700
3600
3500
0
2
4
6
8
10
12
14
16
18
20
22
24
√t in √min
d'o
do
to
t'90
t90

FIG. 4(b)

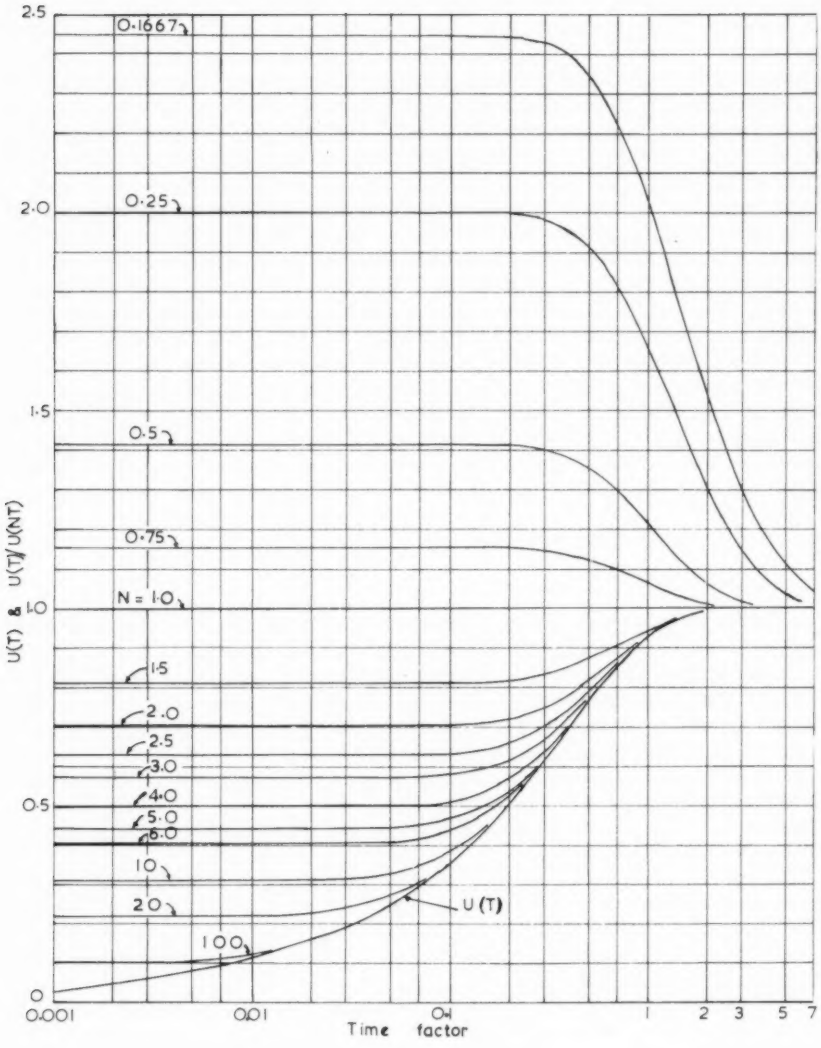
2·5
2·0
1·5
1·0
0·5
0
U(T) & U(T)/U(NT)
0·1667
0·25
0·5
0·75
N = 1·0
1·5
2·0
2·5
3·0
4·0
5·0
6·0
10
20
100
U (T)
0·001
0·01
0·1
1
2
3
5
7
Time factor

FIG. 5

C_v versus N which are described by the values of final time written adjacent to them is also produced (Fig. 2(b)). From these figures it can easily be discerned that the coefficient of consolidation so computed varies with the choice of values of initial time, final time and their ratio. The extent of variation is well more than 100%. This entire process was repeated with a typical laboratory curve for a more impervious type of black cotton soil and the final result reproduced in Fig. 3. Thus it can be further inferred that there is no unique variation either. Although it is not possible to get the average coefficient of consolidation by this method, these results are by no means intended to imply or even remotely suggest any fallacy in the procedure. On the contrary they only bring out the effect of the hitherto vaguely comprehended variable, secondary compression.

Fig. 4(a) and (b) show laboratory compression curves for two different soils, chosen to demonstrate the other practical difficulty in having to properly correct the zero reading. For the case reported in Fig. 4(b), uncorrected or improperly corrected zero reading gives absurd values for compression ratios. These two aspects, taken together, will demonstrate the necessity for obtaining a continuous record particularly in the early stages of compression.

From a general study of the family of curves produced in Fig. 1, it seems worthwhile examining rather more closely in the range for time factor between 0 and 0.1. Since U is an exponential function of T, it is considered befitting to use logarithmic plotting. The salient features are self-explanatory from the results of this further investigation reproduced in Fig. 5. This among other things is meant to indicate that N need not be limited only to values greater than unity and also to confirm that $\lim_{T \to o} \frac{U(T)}{U(NT)} = \sqrt{\frac{1}{N}}$.

I. Da SILVEIRA,[17] M. ASCE.—The method suggested in the paper is not a simple procedure for evaluation of the coefficient of consolidation, but it permits the identification of the degree of consolidation corresponding to certain dial reading obtained during the test. The complete consolidation curve can be obtained from three dial readings in substitution to the normal series of measurements as standard procedure of consolidation tests.

Such results are naturally possible of criticisms, because it is a typical extrapolation procedure.

However, many other advantages must be recognized in the ideas of the author by the analysis of his work.

The possibilities of the method for the early stage of consolidation, where the parabolic form, $U = 2\sqrt{T/n}$, was used, can be successfully overcome by using other formulas for determining the ratio $r = U(T)/U(NT)$. It is a matter of more accurated numerical values and of scale in plotting the results when preparing the graph (Fig. 1).

Then an advantage in time can be obtained in comparison with the actual possibilities, that a required degree of consolidation U(NT) corresponds to a time factor 0.2 or up and 50% of consolidation.

The correction of the zero reading can be obtained also by using Eq. 9 if the ratio (r) is well-determined, thus $d_s = (d_t - d_{NT}r)/(1 - r)$.

---

[17] Cons. Engrg., Com. Solos e Fundacões, Rio de Janeiro, Brazil.

This procedure is more general than those using the parabolic form, assumed as good approach for consolidation law at its early stages.

It corresponds to the case of radial drainage, mentioned in the paper, which Eq. 13 was suggested with this type of test by the writer[18,19] and presented as a mathematical problem of Soil Mechanics, also by R. E. Gibson and P. Lumb.[20]

Since some discrepancies between test results and numerical values obtained with this formula were emphasized, the writer re-examined the problem in Northwestern Tech. (1956-57) and checked the formula recently for the condition of equal strain with appreciable accuracy. A consolidation curve was obtained by plotting U_r against the ratio $(T_r/T_r - 50\%)$.[21]

This procedure has been successful for comparing different consolidation curves in its shape, and fixing a basic numerical time factor (T - 50%), for each case.

Any information about test results of radial drainage is greatly wanted.

---

[18] Teoria e utilidade do Ensaio de Consolidacão de argilas com drenagem radial externa, by I. da Silveira, Rev. do Clube de Engenharia, no. 165, Rio de Janeiro, 1950.

[19] Consolidation of a Cylindrical Clay Sample with External Flow of Water, by I. da Silveira, Proceedings, 3rd Internatl. Conf. of Soil Mechanics and Foundation Engrg., Vol. 1, Session 1 to 13, Zurich, 1953.

[20] Numerical Solution of Some Problems in the Consolidation of Clay, by R. E. Gibson and P. Lumb, Proceedings, British Inst. of Civil Engineers, Paper 5877, London, 1953.

[21] Discussion by I. da Silveira of "Procedure for Rapid Consolidation Test," by Hsuan-Loh Su, Proceedings, ASCE, Vol. 85, No. SM3, February, 1959.

GROUTING OF GRANULAR MATERIALS[a]

Discussion by Judson P. Elston

JUDSON P. ELSTON,[28] F. ASCE.—The paper is a contribution toward more intelligent and exhaustive thinking processes prior to moving ahead on a foundation treatment program by grouting methods.

The statement that ". . . grouting has been handled almost as an art, as opposed to the science it should much more nearly be," no doubt was deliberately intended to be provocative in the hope of drawing comment from the engineering profession.

The principle contribution, that this paper makes toward advancing the "art," or science, of grouting is to emphasize the need of designers for extensive, intelligent and thorough investigation and exploration of proposed foundations. The next logical step is to assess and evaluate the data received, not only through the facilities of laboratory procedures, but through the studies and judgment of highly qualified geologists, and soils and foundation engineers. In this specialized type of work it has always seemed that the orderly sequence of intelligent engineering deductions were most effectively furthered and brought to a successful conclusion by on-the-site testing under actual field conditions in the material or rock itself to be treated. In many of the writer's experiences this was carried one step further, or without a division line between design and construction, into the actual construction work or contract itself and continued to make itself felt throughout the work.

Soils mechanics is considered to be a science by most of the engineering profession, and yet some of our most famous authorities in this field have adopted a personal and somewhat "artistic," in their own words, approach to extremely difficult problems and with great success. Geology has been considered a science for many years, and yet some of our foremost engineering geologists have achieved notable success by novel, individual, and ingenious theories, predictions and practices later proven sound as exploration and construction developed.

The authors imply in the paragraph under "Objectives" that the only materials to be used for grouting clays are ". . . cement, or combinations of cement and other solids that will form layers or bulbs of hardened material."

It is extremely difficult to believe that, either in the laboratory or in the field, clays in place can be grouted (that is penetrated and saturated) by any materials, solids or otherwise. It would be indeed interesting to have described the field applications and test cores or pits in which combinations of undisturbed in-place sands, clays, and silts were consolidated.

---

[a] April, 1961, by J. C. King and E. W. Bush (Proc. Paper 2791).
[28] Civ. Engr., Rock Island Dist., Corps of Engrs., Rock Island, Ill.

The statements are made that the way to a choice of grouting materials is determined by effective pore size and assumption that all sand grains in nature are spherical.

The implication seems to be from the statement, "In other words, if the diameter of grouting particles is not over 1/5 x 1/3 = 1/15 of the particle diameter of the materials to be grouted, the grout will pass freely through the void system," that inasmuch as this formula was derived from some laboratory source, presumably, it should apply to similar materials found in place in nature. As to the uses of fly ash versus clays the writer feels, that obsolute volumes - when used with cements - being approximately the same, the size and variations in size of openings and comparative costs should be the controlling criteria assuming, naturally, that the fly ash can meet ASTM standards.

It is also the writer's opinion that "bleeding" is of no particular importance in pressure grouting underground as contrasted with the problem it often creates in concrete or pre-packing operations with cements and graded aggregates.

The authors delve rather extensively into "Grouting Materials and their Limitations." It would be interesting to know the costs and availability in local markets of Portland blast furnace slag cement in this country. It is assumed that they refer entirely to laboratory procedures or to carefully controlled and separated sand sizes where they state," . . . whereas for sand careful choice of the clay and cement enable one to extend the usefulness of cement as the solidifying agent at least one extra sieve size, as shown in Fig. 4 and Table 1."

The authors' comments and conclusions on bentonites and chemicals will not be discussed except to say that they, in the writer's opinion, have an extremely limited use under certain, at times rare, foundation conditions. The assumption is taken that the sodium silicate grouts are considered useful materials in conjunction with clays for the grouting of fine sands. The writer's experience in the last 25 yr does not include what he would consider successful grouting of fine sands with sodium silicate or clays, together or separately. As to compressive strengths shown in Fig. 6 and 7, were these derived from laboratory cylinders or from 6-in. cores recovered from field grouted areas?

The question also arises as to whether the statements contained in the last paragraph under "Chemicals" has been proven under in-service field operation or is largely a matter of conjecture from laboratory experiments and long-time tests. The writer's work has led him to the conclusion that the most reliable and valuable control criteria are derived in the field under existing conditions immediately prior to commencing the task of formulating and constructing, the strengthening foundation or impervious barrier or combination of both, as may be desired.

The writer finds himself forced to disagree that soft fine-grained satruated soils, that cannot be practically grouted by true chemicals such as chrome-lignins or AM - 9, can be grouted with cement and cement-sand grouts.

Such a theory would seem to imply that sands or solids can be grouted by other sands or solids with relatively the same void ratio, give or take one or two sieve sizes. It is of course quite true that in some instances sufficient pressure will permit injection through rupturing causing displacement. Whether the "take" is low or high in soils under pressure does not necessarily seem an indication that displacement is not as much in the vertical direction as in the horizontal direction.

GROUTING TO PREVENT VIBRATION OF MACHINERY FOUNDATIONS[a]

Discussion by I. Alpan and Judson P. Elston

I. ALPAN,[5] M. ASCE.—In order to appreciate the value of Gnaedinger's contribution, it may be appropriate to quote G. P. Tschebotarioff[6]: "It is most desirable to obtain a large number of complete records of foundation performance both where vibratory trouble occurred and where no such trouble was registered," because " . . . the progress of our knowledge in this field is dependent upon the systematic collection and analysis of records . . . concerning the performance of full scale structures."

It is evident that such a procedure must eventually lead to, or validate, a hypothesis concerning the operation of the structure under consideration, culminating in the possibility of predicting its behavior.

With such an object in view the paper under discussion offers an excellent opportunity of examining certain aspects of the problem of resonance in machine foundations.

The paper lists five factors that influence the natural frequency of a soil-foundation system. It is to be regretted that in the subsequent description of the troublesome machines these factors are not dealt with more fully. In particular, the weight of the machines and their foundations as well as the shape and magnitude of the contact areas would be of interest.

It can be shown[7] that, under certain simplifying assumptions, the resonant frequency of a machine-foundation-soil system can be expressed by the following relation:

$$f_n = C \frac{V_R \sqrt{\gamma}}{\sqrt{W_v}} \sqrt{\sqrt{A}} \quad \ldots\ldots\ldots\ldots\ldots (1)$$

in which f_n is the resonant frequency in cycles per unit of time; C denotes a coefficient dependent on the Poisson ratio of the soil and the shape of the foundation contact area; V_R is the propagation velocity of Rayleigh waves in the soil; γ represents the unit weight of the soil; A is the contact area of the foundation; and W_v is the weight of machine and foundation.

A typical value of V_R for dense sands would be 200 m per sec. Thus, Eq. 1 could be checked as to its accuracy in predicting resonant frequencies.

---

[a] April, 1961, by John P. Gnaedinger (Proc. Paper 2793).

[5] Senior Lecturer, Israel Inst. of Tech., Haifa, Israel.

[6] "Performance Records of Engine Foundations," by G. P. Tschebotarioff, ASTM Special Tech. Publication No. 156, 1953.

[7] "Machine Foundations and Resonance," by I. Alpan, Geotechnique, Vol. 11, 1961 (to be published).

It is stated in the paper that ". . . it is probable that the spring constant will increase with increased amplitude of vibration . . . ."

If the spring constant is defined by:

$$k = \frac{\Delta F}{\Delta X} = \frac{\text{Force}}{\text{Displacement}} \quad \ldots\ldots\ldots\ldots\ldots\ldots (2)$$

the prior statement quoted implies a "hard" (overlinear) spring. This contradicts the experimental findings of H. Lorenz[8,9] who established soils to have "soft" (sublinear) spring characteristics as shown in Fig. 6.

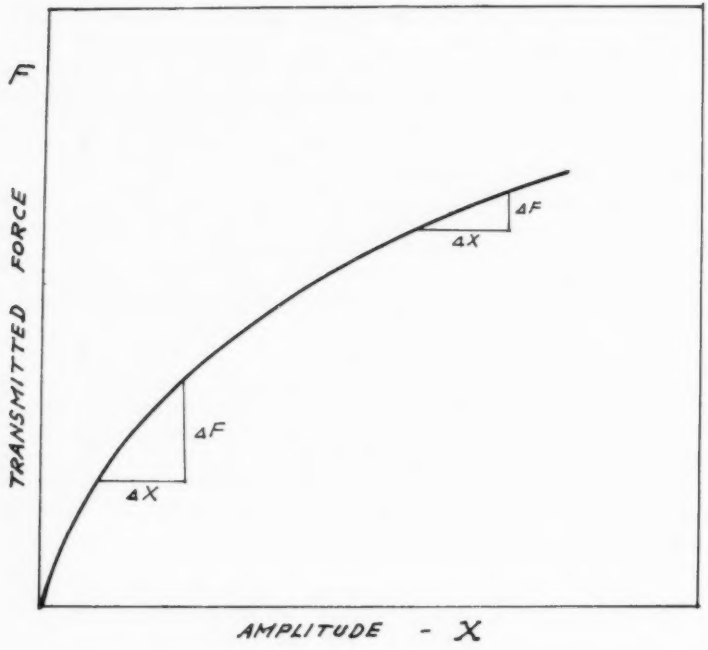

FIG. 6.—AMPLITUDE VERSUS TRANSMITTED FORCE

This characteristic of the "soil spring" might explain the smaller than anticipated increase in natural frequency after grouting underneath the Expander foundation: instead of the computed ratio 558/300 = 1.86, only 402/300 = 1.34 was found.

The amplitude-frequency curves of the compressors show an increase in the natural frequency after grouting. This tendency could have been predicted from Eq. 1 because γ and, consequently, V_R, would have increased because of grouting

8 "Der Baugrund als Federung und Dämpfung schwingender Körper," by H. Lorenz, Der Bauingenieur, Vol. 25, J., Heft 10, 1950.

9 "Elasticity and Damping Effects of Oscillating Bodies on Soil," by H. Lorenz, ASTM Special Tech. Publication No. 156, 1953.

The same curves show the peak amplitudes at the new resonance frequencies to be smaller than those at the original resonance frequencies. It is the writer's contention that resonant amplitudes tend to increase with their corresponding frequencies.

From the phase diagram at resonance of a simplified dynamic model the following relation can be deduced:[7]

$$X_n = \frac{m_o r}{c} (2 \pi f_n) \quad \ldots\ldots\ldots\ldots\ldots (3)$$

in which X_n is the amplitude at resonance; f_n represents the resonant frequency; m_o is the eccentric rotating mass, r denotes the radius of rotation; and c is the damping "constant."

In the model the unbalanced force varies with the square of the frequency.

It appears from Eq. 3 that the amplitude may be expected to increase with the resonant frequency unless the damping is similarly increased.

In the case under consideration, the process of grouting had the effect of increasing the density of the foundation soil; existing evidence shows[10] that densification increases the elastic modulus, the amplitude, and the wave propagation velocity of a soil but reduces its damping characteristic.

In Figs. 2 and 3 the final resonant frequencies are shown to have been computed. It should be of great interest to have details of the method used.

JUDSON P. ELSTON,[11] F. ASCE.—The writer is acquainted with the large quantity of foundation work by grouting methods going on in the Western Hemisphere, as well as in other parts of the world. And there is a tremendous amount of work with baffling problems as yet largely unsolved coming up in the immediate future in the treatment of soil and soil-rock foundations by grouting or other foundation treatment methods. Unfortunately, in most cases novel and ingenious job or field solutions are not brought to the attention of the engineering profession, except through hearsay, but are lost in prosaic job histories and semi-confidential project completion reports.

It is noted in the Introduction, "Into that clay was pumped 34 cu yd of a cement and cement-sand grout." Clark is discussing only the thick residual clays derived from disintegration and decomposition of the limestone itself. However, the author gives no mechanical analyses of the thick residual clay. The writer assumes that the author is referring to uncompacted material that has sluffed from its natural position resulting in large cracks and openings. Perhaps Clark would be kind enough to clarify this question. It is possible with sufficient pressures to rupture, heave, and displace soils or stratified sedimentary rocks and then proceed to fill up, by grouting, the zones of weakness. Clark does mention a ". . .gravelly pervious zone from 0 ft to 20 ft thick . . . ." It is assumed that he may have had this specific material in mind when he referred to thick residual clays.

The pattern of grout hole and sequence of grouting shown in Fig. 4 is similar to one experimented with by the writer in 1956 on the St. Lawrence Power Project. A circular pattern was used, grouting from the center out. The quantities of grout were controlled by varying mixes and pressures and stopping

---

10 "Ingenieur-Geologie," by L. Bendel, Vol. I, p. 457, Springer Verlag, Wien, 1949.

11 Civ. Engr., Rock Island Dist., Corps of Engrs., Rock Island, Ill.

all grouting in the pattern after heavy mixes under pressure eventually returned from all periphery holes.

A somewhat related principle was utilized in a circular pattern test grout program in 1959 on the Niagara Power Project to determine the need for grouting; hole spacings; depths and grout acceptances. This particular pattern and the procedures used permitted the writer to determine grout travel in 4 unconnected and unrelated zone depths containing separately connected and disconnected cavities, seams and water-bearing openings. Information that was of inestimable value was found as to spacing of holes; packer settings, mixes, pressures and helped to evaluate the cost of sealing off several miles of foundation prior to award of contracts.

The writer takes exception to cement-sand mixes of; 1 bag cement: 2.22 cu ft sand; 0.8 cu ft water (commonly known in the trade as a "brick mortar or dry pack mix"). The writer's faith in funnel viscometers is thus severely strained at such times when required to convert into large scale (volume) field mixes some of the results of these laboratory instruments. There is no question whatsoever as to the value of laboratory work, indoors and out, but in most instances the judicial interpretation based largely on varied experience in this type of work is lacking. All of which comes back to an opinion, held by most of those intimately acquainted with grouting, that the secret to success of the construction phase of this work lies with the abilities and experiences of those entrusted with the responsibility to complete the work in the field. In this respect, as stated before, Clark not only had a difficult problem, but solved it in a very satisfactory manner.

RESEARCH IN FOUNDATION GROUTING WITH CEMENT[a]

Discussion by Judson P. Elston

JUDSON P. ELSTON,[4] F. ASCE.—Kennedy's paper is an outstanding contribution in the field of research with cement grouts and represents painstaking, thorough, meticulous effort to compile in one paper this voluminous subject.

However, the writer finds words in the introductory paragraph that he is not in agreement with. The words "grout mortar" are commonly known and used in concrete and building construction. To many people grout mortar may even bring to mind a picture of the sanded lime mortars used in brick construction. In fact, the writer feels the word "mortar" should be barred from the vocabulary commonly used by people in the drilling and grouting business.

This minor criticism does not reflect or imply other than whole hearted admiration and respect for the contribution that Kennedy has made to the engineering profession, and especially to the "art," or science, of grouting. The writer believes it will become a classic description and compilation of the advances made in the field of laboratory research on cement grouts for foundations.

---

[a] April, 1961, by T. B. Kennedy (Proc. Paper 2794).

[4] Civ. Engr., Rock Island Dist., Corps of Engrs., Rock Island, Ill.

INVESTIGATION OF SAND-CEMENT GROUTS[a]

Discussion by Judson P. Elston

JUDSON P. ELSTON,[2] F. ASCE.—The writer is personally acquainted with Polatty, having worked with him professionally, and has very high respect for his abilities. The paper reflects an intensive, thorough program of laboratory testing with sand-cement grouts.

Polatty is aware of the writer's thinking on the use of sanded mixes in the field, and his reluctance and hesitation, at times, to consider seriously the use of such mixes except when filling large open cavities and seams. The writer is of the opinion that all attempts to use sands in clay, silt or sand filled openings are doomed to failure, or only partial success at best.

It is the writer's wish that the Corps of Engineers could embark on a program of field testing under known conditions of clean cavities and seams versus partially or completely filled cavities and seams with sands, silts, and clays proceeding then to use the methods and procedures so well described by the author.

---

[a] April, 1961, by James M. Polatty (Proc. Paper 2795).

[2] Civ. Engr., Rock Island Dist., Corps of Engrs., Rock Island, Ill.

PROCEEDINGS PAPERS

The technical papers published in the past year are identified by number below. Technical-division sponsorship is indicated by an abbreviation at the end of each Paper Number, the symbols referring to: Air Transport (AT), City Planning (CP), Construction (CO), Engineering Mechanics (EM), Highway (HW), Hydraulics (HY), Irrigation and Drainage (IR), Pipeline (PL), Power (PO), Sanitary Engineering (SA), Soil Mechanics and Foundations (SM), Structural (ST), Surveying and Mapping (SU), and Waterways and Harbors (WW), divisions. Papers sponsored by the Department of Conditions of Practice are identified by the symbols (PP). For titles and order coupons, refer to the appropriate issue of "Civil Engineering." Beginning with Volume 82 (January 1956) papers were published in Journals of the various Technical Divisions. To locate papers in the Journals, the symbols after the paper number are followed by a numeral designating the issue of a particular Journal in which the paper appeared. For example, Paper 2703 is identified as 2703(ST1) which indicates that the paper is contained in the first issue of the Journal of the Structural Division during 1961.

VOLUME 86 (1960)

AUGUST: 2564(SM4), 2565(EM4), 2566(ST8), 2567(EM4), 2568(PO4), 2569(PO4), 2570(HY8), 2571(EM4), 2572(EM4), 2573(EM4), 2574(SM4), 2575(EM4), 2576(EM4), 2577(HY8), 2578(EM4), 2579(PO4), 2580 (EM4), 2581(ST8), 2582(ST8), 2583(EM4)[c], 2584(PO4)[c], 2585(ST8)[c], 2586(SM4)[c], 2587(HY8)[c].

SEPTEMBER: 2588(IR3), 2589(IR3), 2590(WW3), 2591(IR3), 2592(HW3), 2593(IR3), 2594(IR3), 2595(IR3), 2596 (HW3), 2597(WW3), 2598(IR3), 2599(WW3), 2600(WW3), 2601(WW3), 2602(WW3), 2603(WW3), 2604(HW3), 2605(SA5), 2606(WW3), 2607(SA5), 2608(ST9), 2609(SA5)[c], 2610(IR3), 2611(WW3)[c], 2612(ST9)[c], 2613(IR3)[c], 2614(HW3)[c].

OCTOBER: 2615(EM5), 2616(EM5), 2617(ST10), 2618(SM5), 2619(EM5), 2620(EM5), 2621(ST10), 2622(EM5), 2623(SM5), 2624(EM5), 2625(SM5), 2626(SM5), 2627(EM5), 2628(EM5), 2629(ST10), 2630(ST10), 2631(PO5)[c], 2632(EM5)[c], 2633(ST10), 2634(ST10), 2635(ST10)[c], 2636(SM5)[c].

NOVEMBER: 2637(ST11), 2638(ST11), 2639(CO3), 2640(ST11), 2641(SA6), 2642(WW4), 2643(ST11), 2644(HY9), 2645(ST11), 2646(HY9), 2647(WW4), 2648(WW4), 2649(WW4), 2650(ST11), 2651(CO3), 2652(HY9), 2653(HY9), 2654(ST11), 2655(HY9), 2656(HY9), 2657(SA6), 2658(WW4), 2659(WW4)[c], 2660(SA6), 2661(CO3), 2662(CO3), 2663(SA6), 2664(CO3)[c], 2665(HY9)[c], 2666(SA6)[c], 2667(ST11)[c].

DECEMBER: 2668(ST12), 2669(IR4), 2670(SM6), 2671(IR4), 2672(IR4), 2673(IR4), 2674(ST12), 2675 (EM6), 2676(IR4), 2677(HW4), 2678(ST12), 2679(EM6), 2680(ST12), 2681(SM6), 2682(IR4), 2683(SM6), 2684(SM6), 2685(IR4), 2686(EM6), 2687(EM6), 2688(EM6), 2689(EM6), 2690(EM6), 2691(EM6)[c], 2692 (ST12), 2693(ST12), 2694(HW4)[c], 2695(IR4)[c], 2696(SM6)[c], 2697(ST12)[c].

VOLUME 87 (1961)

JANUARY: 2698(PP1), 2699(PP1), 2700(HY1), 2701(SA1), 2702(SU1), 2703(ST1), 2704(ST1), 2705(SU1), 2706 (HY1), 2707(HY1), 2708(HY1), 2709(PO1), 2710(HY1), 2711(HY1), 2712(ST1), 2713(HY1), 2714(PO1), 2715 (ST1), 2716(HY1), 2717(SA1), 2718(SA1), 2719(SU1)[c], 2720(SA1)[c], 2721(ST1), 2722(PP1)[c], 2733(PO1)[c], 2724 (HY1)[c], 2725(ST1)[c].

FEBRUARY: 2726(WW1), 2727(EM1), 2728(EM1), 2729(WW1), 2730(WW1), 2731(EM1), 2732(SM1), 2733(WW1), 2734(SM1), 2735(EM1), 2736(EM1), 2737(PL1), 2738(PL1), 2739(PL1), 2740(PL1), 2741(EM1), 2742(ST2), 2743(EM1), 2744(WW1), 2745(WW1), 2746(SM1), 2747(WW1), 2748(EM1), 2749(WW1), 2750(WW1)[c], 2751 (EM1)[c], 2752(SM1)[c], 2753(PL1)[c], 2754(ST2)[c], 2755(PL1).

MARCH: 2756(HY2), 2757(IR1), 2758(AT1), 2759(CO1), 2760(HY2), 2761(IR1), 2762(IR1), 2763(HY2), 2764 (ST3), 2765(HY2), 2766(HW1), 2767(SA2), 2768(CO1), 2769(IR1), 2770(HY2), 2771(SA2), 2772(HY2), 2773 (CO1), 2774(AT1), 2775(IR1), 2776(HY2), 2777(HY2), 2778(SA2), 2779(ST3), 2780(HY2), 2781(HY2)[c], 2782 (HW1)[c], 2783(SA2)[c], 2784(CO1), 2785(CO1)[c], 2786(IR1)[c], 2787(ST3)[c], 2788(AT1)[c], 2789(HW1).

APRIL: 2790(EM2), 2791(SM2), 2792(SM2), 2793(SM2), 2794(SM2), 2795(SM2), 2796(SM2), 2797(SM2), 2798 (EM2), 2799(EM2), 2800(EM2), 2801(EM2), 2802(ST4), 2803(EM2)[c], 2804(SM2)[c], 2805(ST4)[c].

MAY: 2806(SA3), 2807(WW2), 2808(HY3), 2809(WW2), 2810(HY3), 2811(WW2), 2812(HY3), 2813(WW2), 2814(HY3), 2815(WW2), 2816(HY3), 2817(HY3), 2818(SA3), 2819(WW2), 2820(SA3), 2821(WW2), 2822 (WW2)[c], 2823(HY3), 2824(SA3), 2825(HY3), 2826(SA3)[c], 2827(HY3)[c].

JUNE: 2828(SM3), 2829(EM3), 2830(EM3), 2831(IR2), 2832(SM3), 2833(HW2), 2834(IR2), 2835(EM3), 2836 (IR2), 2837(IR2), 2838(SM3), 2839(SM3)[c], 2840(IR2)[c], 2841(HW2)[c], 2842(EM3)[c], 2843(ST5), 2844(ST5), 2845 (ST5), 2846(ST5)[c].

JULY: 2847(PO2), 2848(SU2), 2849(HY4), 2850(PO2), 2851(HY4), 2852(PO2), 2853(SU2), 2854(HY4), 2855 (PO2), 2856(PO2), 2857(PO2), 2858(SA4), 2859(SU2), 2860(SA4), 2861(PO2), 2862(SA4), 2863(HY4), 2864 (HY4), 2865(HY4), 2866(HY4), 2867(HY4), 2868(PO2)[c], 2869(SA4)[c], 2870(SU2)[c], 2871(HY4), 2872(HY4)[c], 2873(SU2), 2874(SA4).

AUGUST: 2875(WW3), 2876(WW3), 2877(WW3), 2878(SM4), 2879(ST6), 2880(EM4), 2881(SM4), 2882(EM4), 2883(WW3), 2884(EM4), 2885(SM4), 2886(WW3), 2887(EM4), 2888(WW3), 2889(AT2), 2890(AT2), 2891 (AT2), 2892(AT2), 2893(AT2), 2894(AT2), 2895(AT2), 2896(AT2), 2897(AT2), 2898(AT2), 2899(AT2), 2900 (AT2), 2901(AT2), 2902(SM4), 2903(ST6), 2904(ST6), 2905(SM4), 2906(ST6), 2907(EM4), 2908(ST6), 2909 (EM4), 2910(ST6), 2911(EM4), 2912(SM4), 2913(ST6), 2914(WW3)[c], 2915(ST6)[c], 2916(EM4)[c], 2917(SM4)[c].

c. Discussion of several papers, grouped by divisions.

AMERICAN SOCIETY OF CIVIL ENGINEERS

OFFICERS FOR 1961

PRESIDENT

GLENN W. HOLCOMB

VICE-PRESIDENTS

Term expires October 1961:
CHARLES B. MOLINEAUX
LAWRENCE A. ELSENER

Term expires October 1962:
DONALD H. MATTERN
WILLIAM J. HEDLEY

DIRECTORS

Term expires October 1961:
THOMAS J. FRATAR
EARL F. O'BRIEN
DANIEL B. VENTRES
CHARLES W. BRITZIUS
WAYNE G. O'HARRA
FRED H. RHODES, JR.
N. T. VEATCH

Term expires October 1962:
ELMER K. TIMBY
SAMUEL S. BAXTER
THOMAS M. NILES
TRENT R. DAMES
WOODROW W. BAKER
BERNHARD DORNBLATT

Term expires October 1963:
ROGER H. GILMAN
HENRY W. BUCK
EARLE T. ANDREWS
C. MERRILL BARBER
JOHN D. WATSON
HARMER E. DAVIS

PAST PRESIDENTS

Members of the Board

FRANCIS S. FRIEL
FRANK A. MARSTON

EXECUTIVE SECRETARY

WILLIAM H. WISELY

TREASURER

E. LAWRENCE CHANDLER

ASSISTANT SECRETARY

DON P. REYNOLDS

ASSISTANT TREASURER

LOUIS R. HOWSON

PROCEEDINGS OF THE SOCIETY

HAROLD T. LARSEN
Manager of Technical Publications

PAUL A. PARISI
Editor of Technical Publications

MARVIN L. SCHECHTER
Associate Editor of Technical Publications

IRVIN J. SCHWARTZ
Assistant Editor of Technical Publications

COMMITTEE ON PUBLICATIONS

THOMAS M. NILES, *Chairman*

WAYNE G. O'HARRA, *Vice-Chairman*

BERNHARD DORNBLATT
HENRY W. BUCK
JOHN D. WATSON
HARMER E. DAVIS